Doctoral Dissertation
Doctoral Program in Energy Engineering (38th Cycle)

Sustainable approaches for the Land-Energy nexus through Energy System Optimization Models

Daniele Mosso
* * * * * *

Supervisors
Prof. Laura Savoldi., Supervisor

Politecnico di Torino
October 31, 2025

I hereby declare that the contents and organisation of this dissertation constitute my own original work and does not compromise in any way the rights of third parties, including those relating to the security of personal data.

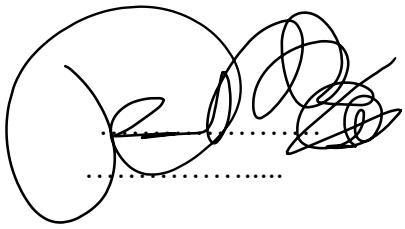

Daniele Mosso
Turin, October 31, 2025

Summary

Integrating sustainable development and climate change mitigation, into decision-making processes is one of the most pressing challenges for current policy frameworks. The energy sector has relied on modelling tools to understand system complexity and to design cost-efficient and environmentally effective policies. As a result, economic (least-cost optimization) and environmental (emission reduction) dimensions have long been at the core of energy system planning. However, these two dimensions alone are not sufficient. The growing of the sustainability agenda requires modelling approaches that incorporate additional dimensions—social, security-related, and cross-sectoral. Despite this need, Energy system optimization models (ESOMs), which for decades served as robust planning tools, remain limited in their ability to account for sustainability indicators and the so-called "nexus" of interlinked systems: climate, water, land use, and energy. In particular, the land-use sector is often mis-represented in current models, leading to biased conclusion about its role. This nexus is increasingly relevant considering new challenges such as the large-scale deployment of renewables and the impacts of climate change directly interact with agriculture, forestry and other land uses (AFOLU).

The scientific literature has highlighted two main research gaps. A first one is related to the necessity of developing sustainability metrics able to link energy system results with globally recognized sustainability objectives. Such metrics should extend beyond environmental impacts to also capture social and energy security aspects and should move beyond the subjectivity of current weighting schemes by introducing a methodology capable of identifying persistent critical indicators across different weight configurations. The second is related to the need for deeper integration of nexus elements, with particular emphasis on those aspects that represent critical bottlenecks depending on the regional context. In Mediterranean and European settings, the availability of land for energy purposes and the decline in agricultural yields due to climate change are particularly relevant. These constraints must be explicitly considered, especially since the land-use sector is often expected to provide significant ecosystem services for climate mitigation.

The objective of this thesis is therefore dual. The first objective is to provide a sustainability metric capable of overcoming the limitations of current approaches.

The complementary objective is to enhance the representation of AFOLU sector within energy system. The thesis develops and applies a novel sustainability metric to the Italian power sector, demonstrating that land use and energy system reliability emerge as critical dimensions. Building on this insight, the thesis expands the modelling of the AFOLU sector within energy system frameworks. To test the robustness and reproducibility of the proposed methodology, two implementations were developed: one in the TIMES model for Sweden and one in the TEMOA model for Italy. In Sweden, the integration of AFOLU revealed that negative emissions from forests can, in some scenarios, reduce the mitigation effort required from other sectors. In Italy, by contrast, the analysis showed that while land use is highly emphasized in national plans, the sector is often unable to generate the assumed negative emissions—sometimes not even offsetting its own positive emissions. This highlights the risk of overestimating AFOLU contribution in energy planning and the need for more balanced and realistic assumptions.

Graphical summary

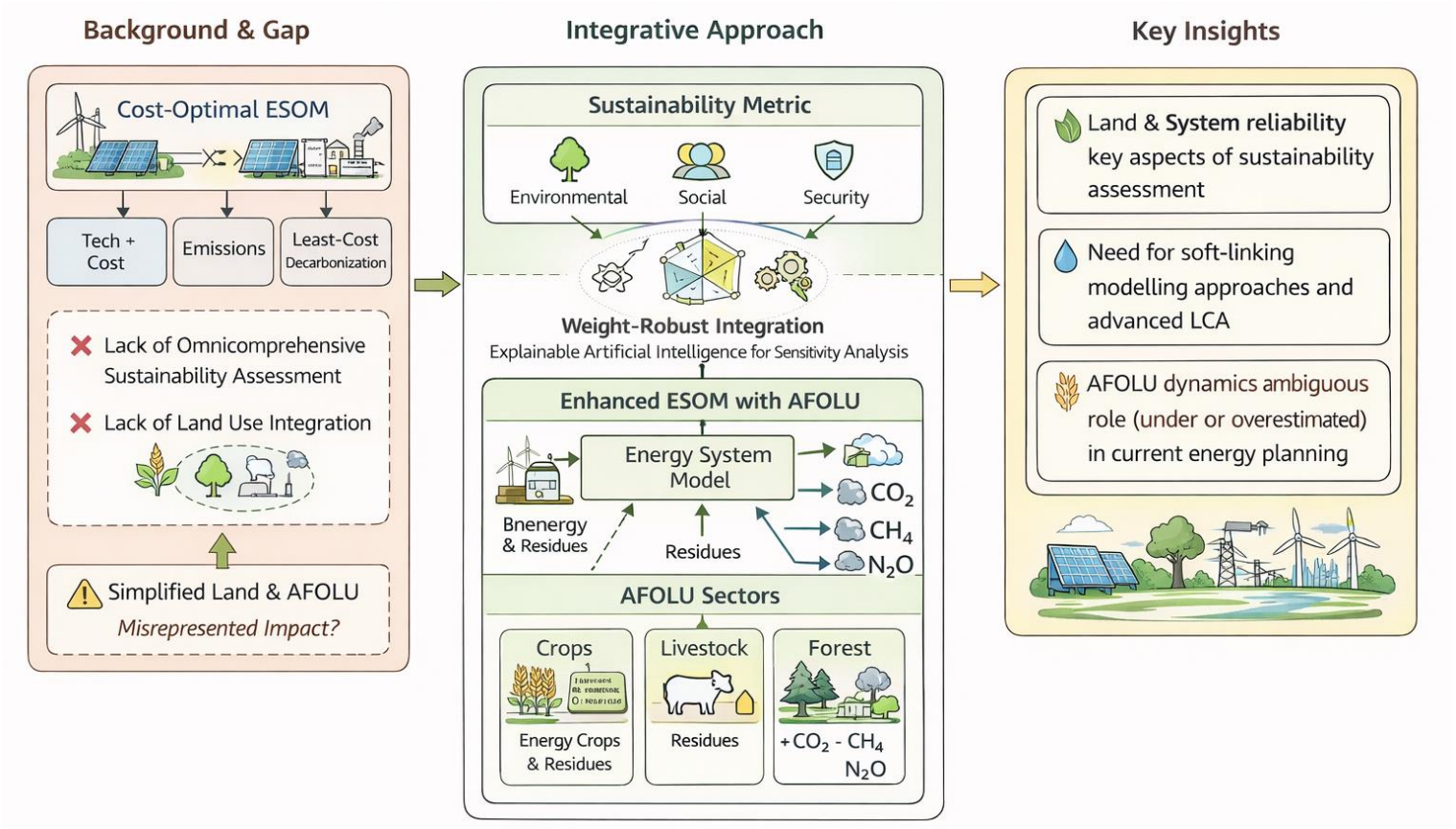

Acknowledgment

“As I reach the end of this journey, I would like to dedicate this thesis to all those who have supported and enriched me throughout this period…My father and Debora for their consistent support in everyday life, particularly during challenging times. I also thank my mother for her presence during important moments. I also thank my friends—Fede, Cixy, Matte, Toti, and many others—for making this path lighter and life more enjoyable. My sincere appreciation goes to all the MAHTEP colleagues, and especially to Laura for her exemplary work ethic and determination to do things well, to Matteo for his presence in the group and his honest exchange, Dani, Gianvito and Alessio... and “last but not least” to Eleonora for sharing both the frustrations and the growth that accompanied this journey.”.

Contents

1. Introduction & Literature Review 1
1.1. Climate Change and Sustainable development Goals 1
1.2. Energy System Optimization Models 7
1.3. Review of approaches for sustainable energy modelling 11
1.4. Identified research gaps 13
1.5. Aim of the work 16
1. Approach 1 – Ex post sustainability assessment 19
1.1. Introduction 19
1.2. Sustainability indicators definition 20
1.2.1. MCDA Framework for scenario evaluation 33
1.2.2. Post-mining analysis 36
1.3. Results 37
1.3.1. Electricity mix and carbon emissions 37
1.3.2. Sustainability index 39
1.3.3. Post-mining analysis 40
2. Approach 2:Introduction of land-use potential in ESOMs 43
2.1. Introduction 43
2.2. Methodology 44
2.2.1. Land eligibility 45
2.2.2. Potential assessment 46
2.2.3. Data aggregation 53
2.2.4. Case study: The Pantelleria Island 55
2.2.5. Model Integration 61
2.3. Results 62
3. Approach 3– A Framework for AFOLU integration in ESOMs 65
3.1. Introduction 65
3.2. Methodology 66
3.2.1. Model structure 66
3.3. A multi-context and multi scenario analysis: Insights from Sweden and Italy 92
3.3.1. Swedish case-study and scenario 92
3.3.2. Swedish results 99
3.3.3. Italian case study and scenario 105
3.3.4. Italian results 108

3. Discussion, Conclusion and Perspectives 114
3.1. Ex-post sustainability assessment 114
3.2. Integration of land-use in ESOMs 118
3.3. AFOLU 121
References 129
Appendix A: The TEMOA Modelling Framework 150
Appendix A.1: The TEMOA-Italy 155
Appendix A.2: The TEMOA-Pantelleria 160

List of Figures

Figure 1. General structure of an energy system optimization modeling framework. 7
Figure 2. General layout of an ESOM process. 8
Figure 3. Workflow of the methodology. 19
Figure 4. Data flows of the MCDA process. 33
Figure 5. CO2 emissions reduction for TEMOA-Italy Reference and Decarbonization scenarios (a) and Electricity consumption increase (b). 37
Figure 6. Evolution of the electricity production by source obtained in the TEMOA-Italy a) Reference scenario and b) Decarbonization scenarios. 38
Figure 7. Sustainability score profiles for Reference (a) and Decarbonization (b) scenarios considering all the 10'000 combinations (grey lines) with evidence of the SI profile associated to an equal weight of the indicators (blue dashed line). 39
Figure 8. Analysis of the SI profile magnitude (a, b) and of the profile trend (c, d) for the Reference (a, c) and Decarbonization (b, d) scenarios, respectively. Dashed lines represent the centroid of the three identified profiles and the red green -blue areas around them are the associated standard deviations. 41
Figure 9. Feature importance for Magnitude (a, b) and Trend (c, d) classification analysis in both Reference (a, c) and Decarbonization (b, d) scenarios. 42
Figure 10 - Workflow of the data aggregation phase, from raw data to TEMOA-Pantelleria characterization 54
Figure 11. Visualization of the Pantelleria island and its placement in the Strait of Sicily 55
Figure 12. Land Eligibility analysis for the Pantelleria Island. (a),(b) and (c) represent the constraint for photovoltaic installations while (d) ,(e) and (f) are the ones for wind. (a),(d) are antrhopic exclusion. (b) and (e) are constaint due to natural habitat and landscape heritage laws. (c) and (f) represent limitation associated to environmental reasons. 56
Figure 13. Photovoltaic Capacity factor by season, Day and Peak time slices 57
Figure 14. Wind capacity factor by timeslice and height. Average value, standard deviation, minimun and maximum values. 58
Figure 15 - Results of clustering with different algorithms. (a) HDBSCAN (b) K-Means and (c) DBSCAN 59
Figure 16. Traditiona average (a) and cluster discretized (b) TEMOA Pantelleria VRES characterization , timeslice capacity factors 60
Figure 17. Power sector capacity and activity for traditional modelling instance and land specific modeling isntance . . Subplot (a) - (b) represents the traditional TEMOA modeling instance, while (c)-(d) the land explicit one in the low land price case, (e)-(f) the intermediate price case and (g)-(h) the highest price case. 63
Figure 18. Land occupation (a) and Total cost for land rent (b) in the highest (dashed) and lowes land price scenarios 64
Figure 19. AFOLU sector and its interaction with TIMES 66
Figure 20. AFOLU Reference Energy System (RES) illustrating the flow of primary commodities (land, water) through transformation processes (e.g., livestock, manure management, crop production, and forestry) to final commodities (energy carriers, food, and materials). Key pathways include resource allocation, species-specific options, and GHG emissions accounting for CO_2, CH_4, and N_2O. 67
Figure 21. Generic AFOLU process 69
Figure 22. Livestock modelling 73
Figure 23. Crop representation 76
Figure 24. Pastures representation 77
Figure 25. Forest model 79
Figure 26. Forest and HWP Reference system 81
Figure 27. AFOLU sub-energy products supply chain for the energy system. 91
Figure 28. Overview of Swedish AFOLU sector emissions. Global Swedish emissions at 2022 (a) and AFOLU emission by source (b). 93

Figure 29. Driver Projections for the modelled years. GDP and Population are shown starting from 2019 to 2050. 97
Figure 30. Scenario tree for the three decarbonization pathways of the AFOLU sector. 98
Figure 31. Total Final Energy Consumption (TFEC) by consumed commodity in TIMES-SE with (darker) and without (lighter) AFOLU module. 99
Figure 32. Electricity production mix with (darker) and without(lighter) AFOLU module 100
Figure 33. Emissions by gas type in TIMES-SE with (darker) and without (lighter) AFOLU model. 101
Figure 34. Crop production by type in the 18 different TIMES-SE Scenarios. 102
Figure 35. Livestock production by type. 102
Figure 36. AFOLU emission by type of GHG (a) and by source (b). BY is on the right side of the plot while the 2050 configurations of the analyzed scenarios are on the left. 103
Figure 37. Water (a) and land (b) use by AFOLU sector at the base year (first column) and last year (2050) for the 18 analyzed scenarios. 105
Figure 38. Italian GHG emissions by sector (a) and agriculture emissions by source (b) [238]. 106
Figure 39. Scenario tree. 107
Figure 40. Sectoral greenhouse gas emissions (a) and total primary energy supply by source (b) across BAU and PNIEC scenario for TEMOA-Italy energy system. 108
Figure 41. Evolution of electricity generation capacity (a) and actual generation output (b) across BAU and PNIEC scenario for TEMOA-Italy power sector. 109
Figure 42. Changes in agricultural production, livestock systems, and land use under baseline and alternative scenarios to 2050. (a) Crop production is shown in million tons (Mt), disaggregated by cultivation system: open-field, organic, greenhouse, and aquaponic. (b) Livestock numbers are reported in thousand heads (k heads), distinguishing between farming-based and grazing-based systems.(c) Forest and pastureland areas are shown in thousand hectares (kha), highlighting shifts in land allocation between natural and managed ecosystems. 110
Figure 43. Positive AFOLU emission trend (a) and 2020-2050 positive emission change by source (b). 111
Figure 44. Negative emission technologies contribution in 2050 for net zero emission scenarios. 112
Figure 45. Land Use by cropping and renewable deployment in 2020 and 2050 for different mitigation scenarios 113

List of Tables

Table 1. Review of current literature on Sustainability Assessment in the energy field. 5
Table 2. Overview of decarbonization strategy by SDG area and sustainability dimension. T represent Trade-offs while S represent Synergies. Where both appears, it means that the action create positive and negative effects together. 6
Table 3. Main parameters for the characterization of energy technologies in ESOMs. 10
Table 4. Comparison between soft and hard linking modeling options.....15
Table 5. Examples of different well-established nexus modeling approaches. 15
Table 6. LCA data sources (categorized by reference power plant and origin database) for the technologies involved in this study.....21
Table 7. Power sector technologies characterization for LCA Environmental Footprint indicators at the base year. 23
Table 8. Italian primary fossil fuel supply in 2021 distinguishing between supplier country and national production.[117] 24
Table 9. Global supply chain share in 2020 by country and by supply chain step for solar PV and wind turbines.[119].....25
Table 10. Political Stability Index (PSI) by country.[123] 27
Table 11. Power sector technologies characterization for security indicators at the base year. 29
Table 12. Human Development Index by country.[124] 30
Table 13. Accident-related fatality rates/GWh. 31
Table 14. Power sector technologies characterization for Equity indicators at the base year. 32
Table 15. Description of sustainability dimensions and indicators. 33
Table 16. Accuracy, Recall and Precision of the four classifiers developed for the Reference and Decarbonization scenarios. 41
Table 17. Review of the main land eligibility analysis found in literature.....45
Table 18. Constraint expression for Land Eligibility analysis. Exclusion rule for distance are derived from Italian regulation [151] 46
Table 19. Data sources for general and technology specific resource assessment. Characterization by spatial and temporal coverage and resolution. 48
Table 20. Main characteristics of the wind turbine models used for the producibility calculation. For each turbine, data are obtained by the online wind-turbine-model repository [183] 51
Table 21. Performance of the three different clusterign algorithms 59
Table 22. Cluster characterization 60
Table 23 - Demand components 70
Table 24 - Data entry for livestock sector.....71
Table 25. Data entry for crop sector 74
Table 26 - Data entry for livestock sector.....77
Table 27. Data entry for livestock sector 79
Table 28. HWP carbon content.....83
Table 29. HWP Decay constant k 84
Table 30. Sustainable agricultural practices 85
Table 31. Crop mitigation options parameters for greenhouse and aquaponic. Comparison with open field values for yield (CAP2ACT) and water consumption ratio.....86
Table 32. Costs for afforestation and maintenance.....87
Table 33. Mitigation options abatement potential for different manure management options 88
Table 34. Cost for Manure Abatement Options. 90
Table 35. Lumped parameters of bioenergy chain.....92

Table 36. Overview of the AFOLU technologies and their main model parameters, input and outputs..95
Table 37. Crop yield variation projection in 2050 under pessimistic and optimistic hypothesis according to FABLE Swedish report [220]. 98
Table 38. Limitation and potential impacts of simplifying assumptions for the AFOLU module. 125

Nomenclature

Acronym	Description
AFOLU	Agriculture, Forestry, and Other Land Use
AP	Acidification Potential
AS	Activity Share
BECCS	Bioenergy with Carbon Capture and Storage
CAP2ACT	Capacity-to-Activity Ratio
CCS	Carbon Capture and Storage
CHPR	Combined Heat to Power Ratio
CLEW	Climate, Land, Energy, Water
CF	Capacity Factor
EP	Eutrophication Potential
ER	Emission Reduction
ESOM	Energy System Optimization Model
ETSAP	Energy Technology Systems Analysis Program
FAO	Food and Agriculture Organization
FO	Flow Output
FSC	Forest Stewardship Council
GHG	Greenhouse Gas
GLOBIOM	Global Biosphere Management Model
GR	Growth Rate
GWP	Global Warming Potential
HWP	Harvested Wood Products
IAEA	International Atomic Energy Agency
IAM	Integrated Assessment Model
IEA	International Energy Agency
IND	Indicator set (e.g., GWP, AP, …)
LCA	Life Cycle Assessment
LCI	Life Cycle Inventory
LCIA	Life Cycle Impact Assessment
LT	Lifetime
LU	Land Use
MAgPIE	Model of Agricultural Production and its Impact on the Environment
MAVT	Multi-Attribute Value Theory
MCDA	Multi-Criteria Decision Analysis
MOO	Multi-Objective Optimization
NExST	Nexus Solutions Tool
NEEDS	New Energy Externalities Development for Sustainability

NGHGI	National Greenhouse Gas Inventory
NPV	Net Present Value
PEFC	Programme for the Endorsement of Forest Certification
PSI	Political Stability Index
PWR	Pressurized Water Reactor
RES	Reference Energy System
SDG	Sustainable Development Goals
SS / SI	Overall Sustainability Score (or Sustainability Index)
TEMOA	Tools for Energy Model Optimization and Analysis
TFEC	Total Final Energy Consumption
TIMES	The Integrated MARKAL-EFOM System
TPES	Total Primary Energy Supply
TSI	Technology Sustainability Index
TSS	Technology Sustainability Score
W	Weight (associated with a sustainability dimension or indicator)
WEC	World Energy Council
WU	Water Use

Chapter 1

1. Introduction & Literature Review

1.1. Climate Change and Sustainable development Goals

Climate change (CC) is now the biggest and most pressing environmental and socioeconomic challenge on the planet [1]. Growing scientific evidence shows that human activity, and particular the massive use of fossil fuels, has led to an unprecedented increase in atmospheric concentrations of greenhouse gases (GHGs). Carbon dioxide concentrations reached values above 415 ppm in 2022, compared to around 280 ppm in the pre-industrial era [1]. This alteration of the Earth's radiative budget has already produced an average increase in global temperature of about 1.1 °C compared to pre-industrial levels, with tangible impacts on every continent [1]. The effects of global warming are not limited to the average increase in temperature but include an increased frequency and intensity of extreme weather events, such as heat waves, droughts, torrential rainfall and hurricanes([2], [3]). The IPCC AR6 (2023) [1] report highlights how, without rapid reductions in emissions, there will be an exponential increase in climate risks, with more severe impacts in already vulnerable regions, such as sub-Saharan Africa, South Asia and small island states. However, Europe is not without threats either: recent events such as the heatwaves in 2022 or the floods in Germany and Belgium in 2021 clearly show the vulnerability of industrialized societies[4]. Faced with this situation, the scientific community has identified a critical threshold not to be exceeded: keeping the temperature increase well below 2 °C, ideally aiming for 1.5 °C [5]. This target, highlighted in the 2015 Paris Agreement [5], represents the international framework within which states have committed to drastically reducing their GHG emissions. The IPCC estimates that meeting the 1.5°C target requires net-zero global emissions by mid-century, with reductions of the order of 80–95% compared to 1990 levels [5].

Reducing emissions while preserving the same delivery of any goods implies a systemic transformation of the global economy, unprecedented in scale and speed [6]. Universal access to reliable, sustainable and affordable energy is a necessary condition for poverty reduction, economic growth and social justice, while the decarbonization of energy systems is crucial to reducing emissions [7]. However, despite regulatory and technological advances, current trends show a significant "emission gap": according to UNEP 2024 Emission Gap Report [8], even adding up national commitments (NDCs), the world is on a warming trajectory of between 2.4 and 2.8 °C by 2100. The recent experience of the COVID-19 pandemic has provided a practical demonstration of the difficulties inherent in structural emission reductions: In 2020, the sharp slowdown in economic activities led to a reduction in energy consumption of 4% and CO_2

emissions of 6.3% on a global scale, the sharpest drop in decades. However, already in 2021 emissions rebounded strongly, approaching pre-crisis levels. This episode has highlighted how contingent and forced reductions cannot replace structural policies and profound transformations of the energy and production system [8].

In this scenario, the European Union has taken a leadership role [9]: with the 2019 European Green Deal [10], the Commission presented an integrated strategy to transform Europe into the first climate-neutral continent by 2050. The Green Deal is based on a systemic approach that combines climate objectives with measures for sustainable economic growth, technological innovation, biodiversity protection and social justice. At the heart of the strategy is the energy transition, based on a sharp increase in the share of renewables, improving energy efficiency, reducing dependence on fossil fuels and innovation in emerging sectors such as green hydrogen and CO_2 capture and storage (CCS) technologies [11]. To support this trajectory, in 2021 the EU launched the "Fit for 55" legislative package, which provides for a net reduction in emissions of 55% by 2030 compared to 1990 levels [11]. The package includes a revision of the Emissions Trading System (EU ETS), new energy efficiency standards for buildings and transport, and binding targets for renewable energy. In addition to these measures, there is the REPowerEU plan, drawn up in response to the 2022 energy crisis and the war in Ukraine, with the aim of accelerating energy independence from fossil gas and further increasing the share of renewables [12].

These strategies place the EU among the most advanced global actors in the fight against climate change [13]. Despite these significant efforts and the undoubted centrality of decarbonization, the question whether these efforts are also beneficial (or are causing a damage) to other non-climate domains, compromising the sustainable development, is arising [13]. Sustainability is a multidimensional concept that goes beyond the mere reduction of emissions. Glavik et.al, in 2007 [14] provided an overview of the different meaning and implications of the arising sustainability trend in the field of environmental management. They observed that sustainable systems introduce interconnections between environmental protection, economic performance and societal welfare, guided by a political will, and ethical and ecological imperatives. Therefore, sustainability approaches are aimed at integrating at least three interdependent dimensions: environmental, economic and social [15]. To address complex global challenges, the United Nations 2030 Agenda, approved in 2015, introduced the 17 Sustainable Development Goals (SDGs) as a global framework for human and economic development [16]. Among them, SDG 7 ("Affordable and Clean Energy") and SDG 13 ("Climate Action") place energy at the heart of the climate challenge [13]. A truly sustainable energy system, therefore, must not only reduce emissions, but also ensure social fairness, economic stability and security of supply. This complex interrelationship between goals is often referred to as the "energy trilemma– decarbonization, acceptability and security [17]. Several authors have proposed trilemma-coherent energy strategies. Already in the 1993 at the United Nations Global Energy, Environment and Economic development the intricate relationship between energy, environment and development had been pointed out [18]. In particular, the focus had been places on short- and long-term conflict between those three components, dividing between developing and developed countries [18]. Later in 2014, Liu et. [19]al developed and reviewed an energy trilemma index and the transition to sustainable energy in

the top ten CO_2-emitting countries in the world, using fixed asset investment and energy use as moderators from 1990 to 2016. They found out that trilemma in the world energy sector, and the transition to sustainable energy simultaneously enhances economic growth and environmental quality in the long run. Kang et. al [20] analyzed the relationship between energy trilemma (ET) and economic growth in 109 countries between 2000 and 2020 across income levels and regions suggesting that a balanced environmental policy reflecting various aspects of ET is required and can contribute to the economic growth. However, the intricate nature of planning sustainable development paths in this domain presents substantial obstacles. First, a clear definition of sustainability is difficult to establish due to its multifaced and dynamic nature [21]. The existing literature extensively discusses sustainability, and although specific aspects may vary, there is a consensus on its broad scope. The existence of an environmental dimension is recognized, in relation to global warming, deforestation, air, land, and water pollution [22], [23], as well as an economic dimension accounting for profitability and affordability of energy [24], [25]. In addition, there is increasing attention at the technical capacity of the system to provide energy [26] and its security, both in the short term (grid security) and in the long term (geopolitical trades) conditions [27]. Finally, an emerging paradigm in several analyzed studies is the social sustainability, referred to as the effect of energy in society, comprehensive of aspects as acceptability and social impact [28] , [29]. The sustainability ingredients commonly considered in the sustainability assessments are summarized in Table 1. Several selected studies [30], [31] have sought to incorporate indicators within the Social and Economic dimensions to address the capability of the energy system and grid to ensure a secure supply (internal factors), as well as concerns related to the safety of the energy supply chain (external factors). These considerations have further gained significance due to recent events such as the Ukrainian war [32], [33] and material crises [33], which have independently highlighted the importance of energy security. As a result, it is crucial to explicitly include this dimension, previously hidden in other categories, and allocate specific attention to it to achieve a comprehensive sustainability assessment. Also, an Economic and the Technical dimensions is to be considered. At European level, Moreno et. al [13] used a multi-model integrated assessment framework with nine different climate policy models to analyze the relationship between decarbonization pathways and the SDGs, with a focus on the European Union. The key findings indicate that while ambitious climate action creates synergies by improving health and agricultural productivity and reducing inequality, it also presents trade-offs. As it can be understood, the relationship between decarbonization practices and sustainability is a complex topic which has to be carefully evaluated. Since each energy transition implies actions, these last can have impacts both on the carbon emission as well as other sustainability aspects. In Table 2, different energy transition operations and their impact area are highlighted, with the aim of giving a clearer picture of the different positive and negative linkages. The positive ones are usually called “Synergies” and the negative ones “Trade-offs”.

A first point concerns the competition for biophysical resources, particularly land and water [34]. Measures such as bioenergy expansion, afforestation, and hydropower illustrate the inherent limits of natural systems. In 1997, Dale [35] analyzed in detail the bidimensional relationship between land, climate and energy, highlighting how induced land used by humans can be a stressor to climate and ecosystems, but also how it can be affected negatively by climate and environmental stressor. Land and water use for energy competes directly with food

production (SDG 2: Zero Hunger) and biodiversity conservation (SDG 15: Life on Land). Modelling studies have demonstrated that large-scale deployment of bioenergy crops could raise global food prices by 10–30% under certain mitigation scenarios, intensifying poverty (SDG 1) and inequality (SDG 10) [36]. These measures also raise security concerns by fueling "land grabbing" and contributing to international disputes over transboundary water resources (SDG 16: Peace, Justice, and Strong Institutions) [37]. Nevertheless, in the late 2008, Omar et.al [38] pointed out that even with modest assumptions about the availability of land, comprehensive fuel-wood farming programs offer significant energy, economic and environmental benefits [38]. A second set of trade-offs arises around distributional justice and the social acceptance of policies [39]. Instruments such as carbon taxes, fossil phase-outs, and mandatory housing renovations deliver strong environmental outcomes by reducing emissions (SDG 13: Climate Action) and improving air quality (SDG 3: Good Health and Well-Being) - [40], [41]. However, their regressive socio-economic impacts—including higher cost of living, concentrated job losses, and displacement of vulnerable groups —represent major barriers to sustained implementation [42]. Without compensatory measures such as carbon dividends or just transition funds, low-income households bear a disproportionate share of the costs [42]. A third theme concerns emergent dependencies and new vulnerabilities created by the transition to low-carbon technologies [43]. Critical minerals such as lithium, cobalt, and rare earths, which are required for batteries and renewable technologies, generate significant environmental degradation (SDG 6: Clean Water and Sanitation; SDG 15: Life on Land) and pose social risks such as labor exploitation (SDG 8: Decent Work and Economic Growth). Security risks arise from the geopolitical dependencies embedded in mineral supply chains, reproducing vulnerabilities akin to fossil fuel dependence but in a new form [44]. The role of governance and scale is also decisive in shaping outcomes [45]. Decentralised renewables, sustainable mobility systems, and ecosystem restoration projects are among the measures that consistently show synergies across environmental, social, and security dimensions [46]. They reduce emissions, deliver local social benefits such as improved health, reduced energy poverty, and empowerment of women (SDG 5), and enhance community resilience to shocks[47]. Yet the extent to which these synergies are realized depends heavily on governance processes [48]. Poorly managed siting of wind and solar farms or afforestation projects can lead to procedural injustice, where local communities are excluded from decision-making [49]. This reproduces patterns of inequality and generates local opposition, delaying deployment and undermining long-term security benefits [50]. To analyze the above-mentioned aspects, several tools has been developed. Among all of them, Integrated Assessment Models (IAMs) and particularly their sub-category Energy System Optimization Models (ESOMs) have shown potential for their ability to capture multiple sectors and the capacity to merge energy-environmental-economic dimension together [51].

Table 1. Review of current literature on Sustainability Assessment in the energy field.

Economic	Environmental	Technical	Social	Security	Year	Source
v	*v*		*v*		1997	[52]
v	*v*		*v*		1999	[53]
v	*v*	*v*	*v*		2007	[14]
v	*v*	*v*	*v*		2009	[54]
v	*v*	*v*	*v*		2012	[55]
v	*v*	*v*	*v*		2014	[19]
v	*v*	*v*	*v*		2014	[56]
	v	*v*	*v*		2015	[57]
v	*v*			*v*	2016	[58]
v	*v*	*v*	*v*		2017	[59]
v	*v*				2019	[60]
v	*v*	*v*	*v*		2019	[30]
v	*v*	*v*			2020	[61]
v	*v*	*v*			2021	[31]
v	*v*			*v*	2022	[62]
v	*v*	*v*		*v*	2022	[63]
v	*v*	*v*	*v*		2022	[64]
v	*v*	*v*		*v*	2023	[65]
v	*v*	*v*		*v*	2023	[66]
v	*v*		*v*	*v*	2024	[44]
v	*v*	*v*	*v*	*v*	2024	[13]
v	*v*	*v*			2025	[67]

Table 2. Overview of decarbonization strategy by SDG area and sustainability dimension. T represent Trade-offs while S represent Synergies. Where both appears, it means that the action create positive and negative effects together.

Decarbonization Strategy	Impacted SDG(s)	Environmental	Social	Security	Source
Large-scale Biofuel Production	2, 7, 10, 15	T	T	T	[34][36]
Phasing out Fossil Fuels	3, 8, 10, 11	S	S	S	[68]
Carbon Pricing / Subsidy Removal	1, 10, 16	S	T	T	[39]
Utility-Scale Solar/Wind Farms	7, 8, 15, 16	T/S	T	S	[69]
Mining for "Transition Minerals"	6, 8, 12, 16	T	T	T/S	[43]
Large-scale Hydropower Dams	2, 6, 10, 16	T	T	T	[70]
Decentralized Solar (Off-grid)	1, 5, 7, 8	S	S	S	[45], [71]
Sustainable Urban Transport	3, 5, 10, 11	S	S	S/T	[72], [73]
Nature-Based Solutions (NbS)	6, 11, 15, 16	S	S	T	[70]
Aggressive Electric Vehicle (EV) Mandates	10, 11, 1	–	T	–	[74]
"Green" Building Mandates & Retrofitting	1, 10, 11	S	T	–	[40]
Tree planting for carbon credits (“green grabbing”)	1, 2, 10	S	T	T	[37]

1.2. Energy System Optimization Models

Energy system models were first developed following the 1973 oil crisis, as they represented the only structured instruments able to analyze resource dependency in connection with economic development [75]. Over the decades, these models have expanded, initially targeting the links between energy and the environment and later embedding the costs of climate mitigation and environmental externalities [76]. Bottom-up frameworks are characterized by their granular representation of energy sectors and interlinkages, making them especially appropriate for assessing how individual technologies affect the long-term evolution of the system [77]. Within this context, ESOMs are designed to compute the optimal configuration of an energy system, subject to an objective function, typically across medium- to long-term horizons. In most cases, this objective corresponds to minimizing the total cost of the system across the planning horizon [78]. The horizon is normally divided into time-steps, which capture groups of hours or representative periods within a month or season for operational resolution, and into optimisation years for investment decisions, usually extending 5 to 30 years into the future [78]. The typical ESOM structure is shown in Figure 1, relying on a technology-rich dataset covering both supply and demand sectors.

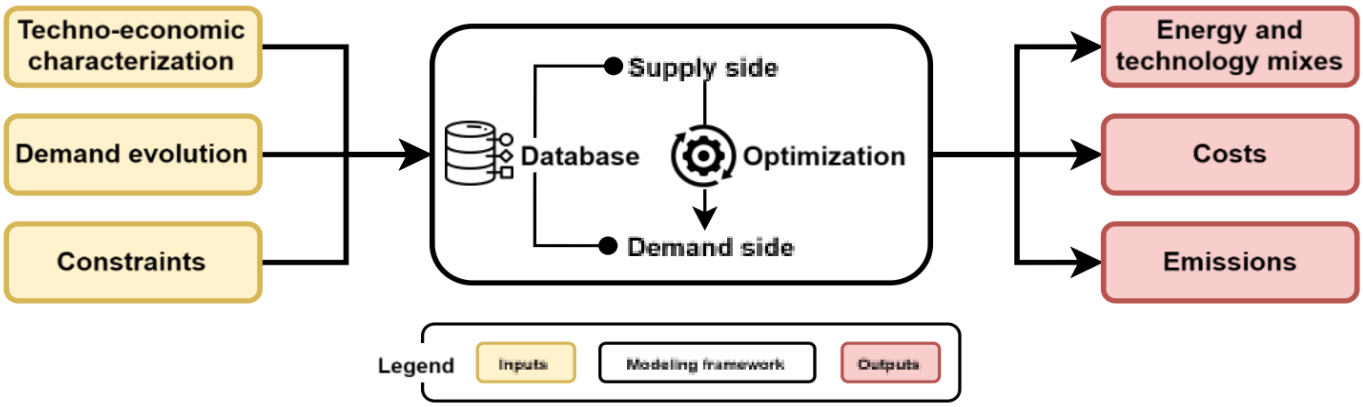

Figure 1. General structure of an energy system optimization modeling framework.

During optimisation the system identifies the least-cost match, with decision variables including new technology capacities and their activities (or production levels) [79]. Generally, a linear problem is formulated. This problem involves minimizing the objective function, which represents the total cost of the energy system (denoted as C_{tot}). The total cost, calculated in Equation (1), depends on the discount factor (DiscountFactor, representing the discounted value to the beginning of the time horizon of a unitary payment) and the cost values of individual technologies chosen in the optimal technology mix. Three key parameters in technology modeling play a crucial role in computing the objective function: investment cost (C_{invest} [M€/cap.]), fixed operation and maintenance (O&M) cost (C_{fixed} [M€/cap.]), and variable O&M cost ($C_{variable}$ [M€/cap.]). While investment cost and fixed O&M cost are linked to a technology's installed capacity, variable O&M cost is tied to the total flow of output (FO) commodities. $LA_{r,t,v}$ is used to annualize a technology's investment cost, determined by the process-specific loan length and discount rate. The objective function is the following:

$$
\begin{aligned}
C_{tot} = C_{loans} + C_{fixed} + C_{variable} = \\
= \sum_{r,t,v} \big(& CostInvest_{r,t,v} \cdot LA_{r,t,v} \cdot DiscountFactor \\
& \cdot Cap_{r,t,v} \big) \\
+ \sum_{r,p,t,v} & \big(CostFixed_{r,p,t,v} \cdot DiscountFactor \cdot Cap_{r,t,v} \big) \\
+ \sum_{r,p,t,v} & \Bigg(CostVariable_{r,p,t,v} \cdot DiscountFactor \\
& \cdot \sum_{s,d,i,o} FO_{r,p,s,d,i,t,v,o} \Bigg)
\end{aligned}
\tag{1}
$$

Inputs consist of techno-economic parameters of technologies, trajectories of final energy demands, and scenario constraints (e.g., emission reduction targets). Outputs can be used to analyze energy and technology portfolios, system costs, and emissions, or extended to provide indicators on environmental, security, or social dimensions [80]. On the supply side, the model usually represents upstream processes, including resource extraction, conversion, and imports, as well as their use in producing electricity, heat, or hydrogen [79]. On the demand side, it covers end-use sectors such as agriculture, buildings, industry, and transport [79]. These components are linked through the reference energy system, a detailed network representation whose three building blocks [79] are illustrated in Figure 2:

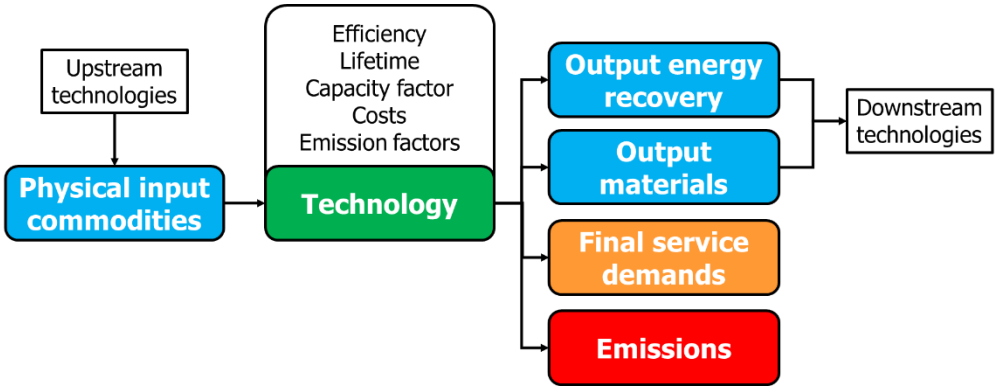

Figure 2. General layout of an ESOM process.

- **Technologies (or processes):** these are systems converting one commodity into another. They include resource supply processes such as mining or imports; transformation processes such as refineries, power stations, or hydrogen plants; and end-use devices such as boilers or vehicles [79]. They are described by techno-economic parameters including costs, efficiency, capacity factors, lifetimes, and emission intensities.
- **Commodities:** these encompass physical, demand, and emissions commodities. Physical commodities include fuels (fossil, bio-based, uranium), carriers (electricity, heat, hydrogen), and materials (e.g., iron and steel feedstocks, chemical precursors). Demand commodities refer to final service requirements such as energy use or mobility (e.g., passenger-kilometres). Emission commodities represent greenhouse gases or other pollutants.
- **Commodity flows:** these specify the links between commodities and technologies, such as between a power plant and electricity supply, or between a boiler and heat provision.

Technologies are usually described according to a limited set of technical and economic parameters (techno-economic characterization) to allow the definition of specific energy production/consumption levels, economic features and environmental performances, all concurring to the determination of the optimal objective function [81], as reported in Table 3. Note that a more extensive set of parameters is available in complex ESOMs like, for instance, TIMES [82], to provide descriptions of very specific techno-economic features (e.g., the maximum non-operational time before the transition to next-stand-by condition, or the ramp-up/ramp-down cost per unit of load change) which are uncommonly used. Constraints are also fundamental in the ESOM formulation [83] and can be defined by the user to model:

- the real life mechanisms of technological substitution. For instance, old capacity at the end of its operational lifetime should be substituted avoiding abrupt investment in new capacity [81] through, e.g., minimum/maximum capacity constraints or limiting growth rates;
- physical and operational real-world phenomena through, e.g., minimum/maximum activity (production) constraints;
- trajectories to limit GHG emissions in future scenarios.

Although constraints are widely adopted for the definition of the different energy scenarios, it is commonly suggested not to adopt many restrictive constraints to avoid “railroading” the model, which should instead respond to its optimization paradigm [81]. Indeed, constraints should be used just to replicate either real life constraints on technological adoption and evolution, or the availability of resources, thus not to force model results to obtain the desired outcomes. As a common approach in forecasting models, technological substitution throughout the considered time horizon is taken into account distinguishing between two kinds of technologies [84]:

- Base year technologies, used to model the demand and the energy use at the beginning of the time horizon. The base year demand is calculated by combining energy statistics concerning total energy consumption with dummy efficiency values and coefficients associated to the generic technologies for which an existing capacity is there. In this way, base year energy consumption is allocated to the existing capacity (see Table 3) of a specific technology.

- New technologies, used to model the energy use throughout the model time horizon, are added to the existing fleet of base year technologies from the second time-step on.

Table 3. Main parameters for the characterization of energy technologies in ESOMs.

Type of parameter	Definition	Description
Technical	Efficiency	Input-to-output transformation parameter
	Capacity factor	Utilization factor to define the available capacity fraction during a specific time slice
	Technical lifetime	Operational lifetime
	Capacity to activity	Conversion factor to be used in case capacity units differ from activity units
	Existing capacity	Capacity installed prior to the beginning of the time periods set for the optimization
Economic	Investment cost	Total cost of investment in new capacity
	Annual fixed operation and maintenance cost	-
	Variable operation and maintenance cost	-
	Technology-specific discount rate (optional)	Interest rate on investment for a specific technology
Environmental	Emission activity	Emission rate for the specific technology

Commodities are essential as they represent the inputs and outputs of the technologies. They can be labeled as physical, emission, or demand commodities [83]. Physical commodities can be transformed by technologies to obtain either other physical or emission or demand commodities. They represent energy-intensive materials (e.g. clinker or alumina), fuels (e.g. gasoline or gas oil) or other energy carriers (e.g. electricity or hydrogen). Emission commodities are mainly produced as outputs from technologies involving combustion of fossil fuels or take into account other process-related emissions (e.g. CO_2 emissions from calcination in clinker production): usually, CO_2 is the main emission commodity taken into account for the definition of energy scenarios as it is considered the main climate-altering agent [85], but any ESOM user may decide whether to also include other emission commodities like, e.g., methane CH_4 or nitrogen dioxide NO_2 for both accounting purposes and the definition of emission targets related to other commodities than CO_2 alone. Demand commodities are either given pre-assigned values or may be elastic to the computed price. In the former case, demand levels must be satisfied at each step of the time scale. Demand commodities generally represent energy services supplied by energy-intensive processes: they may represent several needs ranging, for instance, from the heated surface in a residential building to the quantity of produced steel or the driven distance by a car in a year. Commodity flows are represented according to the way commodities are used and produced by the technologies of the RES, so that the assigned commodity-specific efficiencies connect commodities and technologies to define the whole chain from extraction of natural resources to the final service demands.

1.3. Review of approaches for sustainable energy modelling

In the currently existing literature, alternative approaches exist allowing the integration of sustainability-related aspects within energy models. Attempts have been performed in the direction of a direct integration of sustainability paradigms in the optimization strategy (endogenous integrations), or by conducting sustainability assessments on the outcomes of energy models (ex-post analysis) [86]. Endogenous integrations can be realized by integrating sustainability variables in the energy model, subsequently performing a traditional economic optimization, a Multi-Objective Optimization (MOO), or an impact monetization [87]. In the MOO, one or more target functions related to the sustainability aspects are integrated directly within the ESOM instance and optimized together with the traditional economic objective function. The different objectives can be integrated in the same formulation (weighted sum method [88]) generating a single solution, or computed separately, obtaining in both cases a Pareto front to estimates trade-offs between different objectives [89]. In [90], for instance, integrated social (job creation, human health, diversification) and environmental (water and land use, acidification, and global warming) criteria are considered in an ESOM together with the economic objective function in a weighted sum approach, analyzing scenarios for the Iranian power system up to 2050. The main limitation consists in the fact that the final solution is a compromise between the different objectives, strongly depending on their weighting (exogenously assigned). Moreover, the complexity of the model leads to a high computational cost. In the impact monetization, economic damages of the different impacts considered in the analysis are quantified and subsequently integrated in the economic objective function of the model [76]. Monetization of impacts is well-established in the context of power models, such as the NEEDS [87] and the ExternE [91] European frameworks. Advantages are related to the adaptability of this method to already-existing modeling frameworks by a simple reformulation of the objective function, without the necessity to develop new and complex optimization tools [92]. The main disadvantages concern the uncertainties related to the monetization process, particularly social and security impacts.

Among all the methodologies previously described, a new one has found remarkable potential in providing solutions that are both sustainable and economically viable. Recent quantitative studies have revealed that integrated "nexus" approaches, which consider the deep interdependencies between climate, land, energy, and water (CLEW), can uncover critical synergies and detecting damaging trade-offs [51] between energy, environment and the broader economy. The combined optimization of the various sectors together, like the energy and the agricultural one or the water and the food, often leads to better outcomes than mono-sectoral optimization [93]. Concerning nexus, a review by Liu et al. (2018) [94], which synthesized insights from nearly 400 papers, pointed to several key gaps regarding both methodologies and empirical nexus evidence. Primarily, the review found that no studies at the time had explicitly quantified the contributions of nexus approaches toward meeting the SDGs. The disconnection between the technical outputs of nexus models and the globally accepted benchmarks for sustainable development has been identified as a major gap. Indeed, a more recent review by

Khan et al. (2022) [95] reinforces this point, recommending that the SDGs must be treated as an essential framework for the adoption of nexus methodologies into practice. This suggests clear research need for post-processing integration of SDG-related metrics. Nevertheless, ex-post analyses, in which ESOMs results are integrated with LCA impacts databases to establish the energy system footprint, are already available in literature. Among them, [86] developed an ex-post LCA analysis of results by the JRC-EU TIMES model [96] and estimated the environmental impact indicators across 18 categories in scenarios that achieve 80–95% CO2 emission reduction by 2050. A relevant outcome is the qualitative evaluation of the analyzed policies for each impact class. This may serve as a tool for policymakers in establishing the pros and cons of a strategy, but still lacks a unique quantitative method to identify the best alternative among a wide set of impact classes. Also, the authors of [97] analyzed with a quantitative decision-making tool twenty European energy scenarios characterized by different degrees of decarbonization for twelve LCA environmental impact classes, concluding that there is a co-benefit between emission reduction and mitigation of environmental impacts. A consistent limitation of that study is related to the adoption of the LCA parameters as unique sustainability paradigm since the latter should not be restricted to the environmental component only [16].

Moreover, beyond the thematic inclusion of sustainability goals, the technical challenge on how to properly integrate the different systems of the nexus in the model remains a central question. The development of any CLEW model requires making fundamental choices regarding its core paradigm, with the most significant being the choice between hard-linking and soft-linking of model components. Hard-linked models integrate all sectoral components into a single, unified computational platform, whereas soft-linked models couple separate, often more specialized, models that exchange information iteratively. The implications of this choice are substantial, as summarized in Table 4. Moreover, to illustrate how these theoretical choices and other core features manifest in practice, Table 5 summarizes the key characteristics of several prominent models and frameworks analyzed in the literature. As visible, for example NEST [98] achieves high technical detail in its water component by soft linking with the CWatM Python model, but this comes at the cost of a complex, iterative process. [98] Its linkage to SDGs, while valuable, fail to capture the full dimensions of the sustainability, leading to a environmental only focused evaluation of the nexus. Moreover, the role of weight for the SDG metric is totally neglected, biasing results towards the original weight configuration. Another model, WHAT-IF [99] avoids this complexity through a hard-linked structure but, in doing so, sacrifices the fidelity of its hydrological component. Its single-objective function, focused on maximizing economic surplus, is a classic example of a paradigm that overlooks broader sustainability dimensions. When talking about hard-linked models with an economic paradigm, it's impossible not to fall into GCAM [100] . In GCAM's logit formulation, market options are ranked by a merit order approach, using some proxy parameters (e.g., cost for the energy system or profit for the land system). The model does not assume a single optimal choice captures the entire market; instead, it acknowledges that unmodeled factors like relevant nexus between sectors can lead to a global suboptimal solution. A key limitation of this merit-order-based simulation is its inability to account for nexus trade-offs. For instance, a scenario requiring a higher cost in the energy sector to secure greater savings in the food sector would be overlooked because the model simulates sectoral behavior rather than performing an

integrated optimization. Despite this, GCAM's simulation-based approach is appropriate for its global scale. At this level, simulation is more suitable than optimization because planning is not globally aggregated but conducted by regional entities. Therefore, simulation is valuable for identifying potential critical situations on a global scale, where optimization / planning has limited practical utility. As Howells et. al pointed out in early 2000 [101], for a national or local application that aim at being policy relevant, a proper CLEW integration framework should include at least those nexus components (climate, land, energy and water) for which a strong interlinkage is present. Compared to water, land has more direct and multifaceted linkages with energy systems, especially in Mediterranean regions. There are three main reasons for prioritizing land use:

- AFOLU sectors are standalone contributors to both energy consumption and greenhouse gas emissions. As such, they appear explicitly in national GHG inventories and require mitigation actions like those of the energy sector [102].
- AFOLU can act as a carbon sink, contributing negative emissions through practices like afforestation and land-use change, which are crucial for achieving net-zero targets [102].
- The land sector is also a direct provider of energy commodities, such as biofuels and biomass, making it an integral component of energy planning [102].

Given these strong interlinkages, and the relative scarcity of hydropower potential in many Mediterranean countries [103], land use emerges as a more critical constraint than water.

1.4. Identified research gaps

Two main areas of intervention emerge at the intersection between sustainability assessment and energy system modelling. The first area of intervention does not concern the structure of the energy model itself but rather how the results are interpreted and communicated. As discussed, energy models typically provide highly technical outputs (e.g., system cost, installed capacity, emissions) that do not directly correspond to the sustainability goals they are intended to support. This creates a disconnect between modelling outputs and policy-relevant insights. As stated in Section 1.3, a useful decision-making tool, able to link the decarbonization targets of the energy models with their implications in terms of sustainability, should rely on a comprehensive metric, encompassing a comprehensive range of aspects [104]. In the analyzed frameworks, two existing aspects were recurrent when dealing with sustainability metrics:

- Incompleteness: Existing metrics tend to focus exclusively on environmental dimensions, typically using LCA methodologies [67]. However, sustainability is inherently multidimensional, and must also encompass social and security-related impacts [44]. These dimensions must be assessed not only through environmental life cycle impacts but also through a life-cycle perspective on social and

geopolitical aspects, for instance by examining the supply chains of key energy technologies [105]. Evans et.al [106] has already raised in 2007 the limitation of an environmental centric approach, developing a framework for the evaluation of the best technologies in terms of several sustainability dimensions.

- Subjectivity of weighting schemes: Most multicriteria metrics rely on arbitrary or expert-assigned weights to combine indicators[107]. This introduces a high level of subjectivity and limits the generalizability of the results. In 2009, Wang et. al [108] had already highlighted the benefit of incorporating stakeholder preference and variation thank to weighting schemes [108]. The thesis proposes to decouple the metric from a fixed weighting scheme and instead perform a sensitivity analysis across a wide range of plausible weights, like the Stochastic Multicriteria Acceptability Analysis [109]approach. This approach allows for the identification of indicators that consistently appear as problematic or beneficial, regardless of stakeholder preference, and thus represent critical dimensions of the energy system.

The second area of intervention, focus on energy model core structure by embedding the nexus components that are more neglected and more relevant for the energy system, thus, AFOLU. While there have been significant improvements in AFOLU assessment techniques and model development, there is still ongoing work to refine the process. Several key methodological challenges present opportunities for improvement.

- Global Analysis and Spatial Considerations: Understanding land-use systems globally is crucial for various reasons. The impacts of LULUCF often extend globally, and activities in one region can affect outcomes beyond its borders, environmentally or economically [110].
- Depicting Land Diversity and Product Variability**:** A crucial aspect of global land use assessment is representing land diversity accurately. From a modelling perspective, this is a complex task, especially for economically focused models that may overlook variations in land quality. Most models do not consider soil composition as a parameter, which can impact model choices, leading to the installation of crops on unsuitable terrain [110].
- Challenges with Data Availability**:** One primary obstacle to progress in this field is the availability of data. A nuanced understanding of LULUCF relies on accessible data, influencing the spatial breakdown of land-use categories, socio-economic statistics, and types of land use [110].

Table 4. Comparison between soft and hard linking modeling options.

Feature	Hard Linking (Unified)	Soft Linking (Separate)
Model Structure	WEF interactions are endogenously integrated within a single framework.	Allows for the use of more advanced, technically superior, and specialized modules for each sector.
Primary Advantage	Is superior for performing holistic, simultaneous optimization of the entire system.	Offers flexibility and facilitates collaboration between different communities of modelers.
Primary Disadvantage	Can lead to a loss of detail and accuracy for complex components, such as detailed simulative models.	Often incurs a higher computational cost due to the need for iteration or the use of emulators.

Table 5. Examples of different well-established nexus modeling approaches.

Model	Linking	Key Feature /Objective	Primary Limitation
NEST	Soft-Linking	Iteratively links a detailed hydrological simulation (CWatM) with an economic optimization scheme (MESSAGEix-GLOBIOM).	High computational cost ; relies on a land-use
WHAT-IF	Hard-Linking	Maximizes the sum of consumer and producer surplus within a single, integrated framework.	Hydrology module is a simplified translation of external models, leading to a loss of technical detail and accuracy.
GCAM	Hard-Linking	Simulates market evolution based on myopic "recursive dynamics," where agents respond to current prices.	"Merit order" logic fails to identify optimal nexus trade-offs that an optimization model would uncover.
SIMON	Soft-Linking	Acts as a broker to couple existing models, using transformation functions to resolve scale and unit mismatches.	A novel framework designed to

1.5. Aim of the work

This thesis pursues two interconnected objectives to advance the field of sustainability assessment for energy systems. First, it addresses the methodological gaps identified in 1.4. through the development of a more comprehensive evaluation metric. A metric alone, however, is insufficient; its effectiveness is fundamentally limited by the completeness of the model. This leads to the second objective: to improve the underlying model by incorporating a more robust representation of the energy-land nexus. This research will therefore focus specifically on enhancing the modeling of land use, an endeavor that will proceed in two phases.

Initially, the thesis explores the land requirements of the energy sector, specifically how land is consumed by various electricity generation technologies. This is used to assess whether land availability constitutes a bottleneck for the decarbonization of the power sector. However, this approach reveals several limitations. Evaluating land use without representing the AFOLU sector itself introduces strong biases. Land is treated as a passive constraint, rather than as a dynamic commodity actively consumed and managed by multiple sectors. To address this, the thesis integrates a dedicated AFOLU module into an open-source ESOM framework. This allows for the explicit modelling of agricultural and forestry activities, land use change, and mitigation options such as improved manure management, crop practices, and carbon sequestration. Once the AFOLU sector is fully incorporated, the initial analysis on land requirements for electricity generation is repeated, now accounting for land competition between energy and agriculture. Through this multi-step modelling strategy, the thesis moves from simple land footprint accounting to a comprehensive and integrated land use representation, enabling more realistic assessments of decarbonization pathways. This enriched modelling structure provides a platform for future research on nexus interactions and helps bridge the gap between energy transition planning and broader sustainability agendas. In summary, the three core contributions of this work are:

- The design of a holistic sustainability metric that captures environmental, social, and security dimensions, and includes a sensitivity analysis of indicator weighting to reveal critical system properties.
- The spatially explicit integration of land use constraints and energy infrastructure siting into an energy system optimization model, with application to real-world case studies.
- The development and implementation of a detailed AFOLU module in ESOMs, enabling the modelling of mitigation options in agriculture and forestry and the realistic allocation of land between competing sectors.

Together, these contributions respond to the urgent need for modelling tools that are both technically robust and policy relevant, supporting integrated planning across the SDG framework and helping decision-makers navigate the complex trade-offs of sustainable decarbonization. This option provides a more detailed and formal description, suitable for a thesis introduction.

The methodological framework of this dissertation is organized into three distinct chapters, each corresponding to one of the three primary research gaps identified in the literature review. These chapters, respectively titled Approach 1, Approach 2, and Approach 3 are substantially informed by the publications that constitute the foundational basis of this work. The first methodological chapter, Approach 1, is dedicated to an *ex-post* analysis of sustainability conducted on the energy model. The second chapter, Approach 2, advances this inquiry by endogenously integrating sustainability considerations, specifically by accounting for the land consumption of variable renewable energy sources within the energy models. The final methodological chapter, Approach 3, addresses the integration of the AFOLU sector into energy system models. A consistent structure is maintained across these three chapters. Each begins with a presentation of the case study, referencing the literature from which it is inspired. This is followed by a comprehensive methodological section and a detailed presentation of the results. Concluding this research, a final chapter provides an extended discussion of the results obtained, analyzing their significance both in terms of empirical evidence and the generalizable knowledge that can be extracted. An overview of the logical pathway underlying the manuscript is provided in Figure 3.

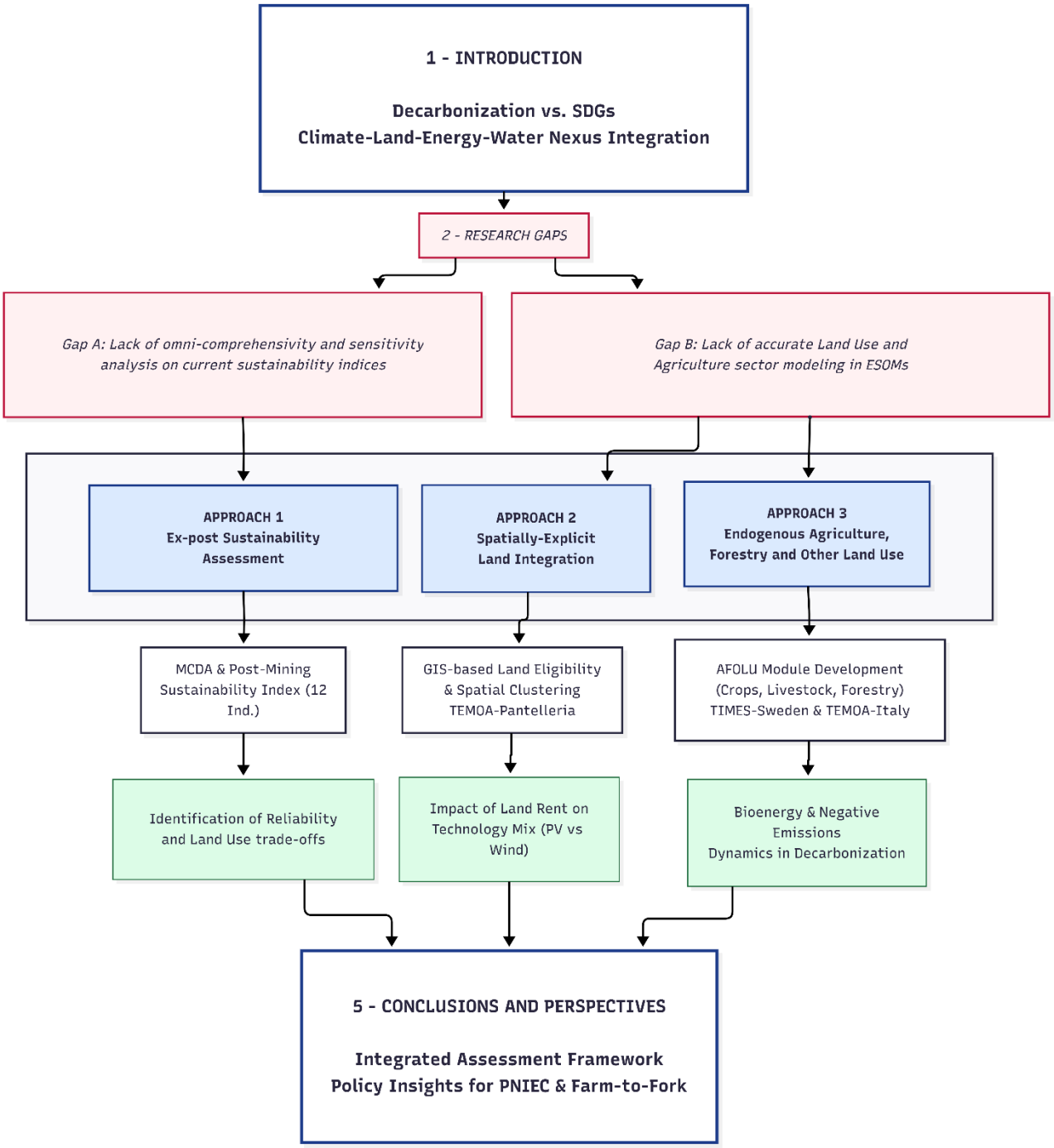

Figure 3. Overview of the logical workflow underlying the manuscript.

Approach 1 – Ex post sustainability assessment

Following the discussion about the limitations of ex-post sustainability assessment available in literature, especially in relation to comprehensiveness of SDG aspects and subjectivity in the evaluation scheme, this chapter propose a solution to the identified research gap. This section is inspired by Mosso et. al [80]

1.1. Introduction

This section introduces the methodological framework for the development and the interpretation of the proposed sustainability index. According to Figure 4. The initial phase involves the selection of a suitable case study to evaluate their sustainability performance. To obtain those decarbonization trends, the TEMOA-Italy energy system optimization model has been used, under the declared national policies. Both the selected model and the scenario under analysis are detailed in appendix. Once a case study has been defined, it's necessary to identify a relevant set of indicators to analyze it. Therefore, according to existing literature, 12 sustainability indicators are identified pertaining to three thematic areas: environment, security and social. Those indicators are then combined in a mathematical framework which is used to derive a single sustainability index depending on the assigned weights. Since of the main limitation of previous work was related to the subjectivity of the weights, an extensive sensitivity is applied whose results are studied with a post-mining framework.

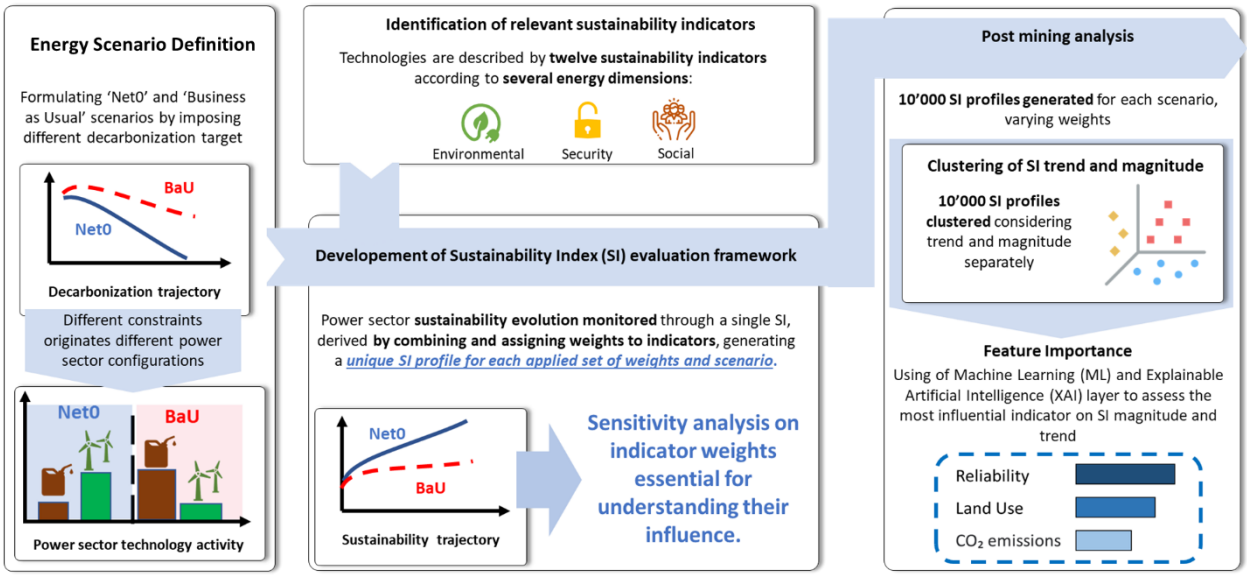

Figure 4. Workflow of the methodology.

1.2. Sustainability indicators definition

To adequately address the extensive scope of each sustainability dimension, a comprehensive set of indicators are needed to accurately describe the associated problems. Since an energy system is a systemic concept that encompasses various energy processes and commodities, it is then crucial for the metric to establish a hierarchical structure [111], where indicators and technologies are linked and constitutes the starting point. Therefore, each power sector technology has been characterized in terms of each included indicator, according to these general dimensions.

For the **environmental** dimension, the selected parameters affect different areas of the environment. The *Global Warming Potential* (GWP), *Acidification* and *Eutrophication Potentials* (AP, EP) are linked to the provoked damage, and they mainly depend on emissions from fossil-based plants. On the other side, *water consumption* and *land use* refer to the natural resources consumed by the power sector technologies. To preserve the comprehensive cradle-to grave approach of the metric in the accounting of these five elements, the Life cycle assessment (LCA) assessment framework is used [112]. That is a standardized method defined by the ISO 14040 series [113] and widely used for evaluating the environmental impact of technologies. The ISO 14040 series ensures reproducibility and transparency in LCA studies, although direct comparability between ISO-compliant studies may not be guaranteed [112]. To mitigate this uncertainty issue, LCA indicators are derived from the UNECE Report "Integrated Life Cycle Assessment of Electricity Sources" [114] , which represent the most recent and significative effort in creating a comprehensive power sector LCA database at a European level. In LCA analyses, the primary goal is to assess and quantify the environmental impact associated with a specific technological process, encompassing its entire life cycle from extraction of raw materials to disposal. This entails establishing a comprehensive linkage between the overall impact of the production process and expressing the analysis as a ratio between the total impact and the output quantity of the process. By doing so, it becomes possible to derive impact factors for each indicator identified by f_I^{LCA}. Each factor represents the impact (I) associated to the production of an electricity unit (MWh) [115] . The overall impact values of the different phases (I_n) for a reference power technology are summed creating the overall Life Cycle Impact (each impact is characterized by a different Unit of Measurement (UoM_I). Then, the overall impact is divided by the total electricity produced by the reference power plant (MWh) creating an average impact for each unit of produced electricity $\left[\frac{UoM_I}{MWh}\right]$. By considering an electricity production technology characterized by *N* life cycle stages, the LCA unitary impact factor f_I^{LCA} for a generic impact *I* is calculated as in the Equation (2).

$$f_I^{LCA}\left[\frac{UoM_I}{MWh}\right] = \frac{\sum_{n=1}^{N} I_n \ [UoM_I]}{Life\ cycle\ electricity\ production\ [MWh]} \tag{2}$$

However, there is an issue related to the regional variability of the LCA impacts parameters. UNECE [114] analyzed the vast majority of LCA impact from power plants, dividing the values for 12 world regions. Considering the relative difference between the European data and the rest of the world region (computed for each impact and for each technology included in the study), is possible to observe a delta around 50%, with peaks reaching 200%. Therefore, data must be selected as local as possible when performing an LCA Analysis, otherwise the introduced uncertainty is very high. In this work, the European data of the UNECE report has been assumed valid for the Italian case study due the absence of more detailed sources. Moreover, due to the lack of biomass and geothermal in the main source, data are completed with the NEEDS database, elaborated with the ReCiPe [115] method in the OpenLCA [116] software. Unfortunately, spatial aggregation for the biomass and geothermal was present only at global level, introducing further uncertainties in the analysis. Beyond the spatial aggregation, there is an issue of technological aggregation when performing LCA analysis. The discretization for the type of power plants usually presents in ESOMs, and in TEMOA-Italy, is not always reproducible in the LCA database, where the discretization is generally lower. Therefore, simplifying assumptions are needed to group plants together. The way technologies are matched to LCA database ones, specifying the spatial and technological aggregation, is shown in Table 6.

Table 6. LCA data sources (categorized by reference power plant and origin database) for the technologies involved in this study.

Technology	Reference Power Plant	Source	Reference Zone
Coal steam turbine	Hard coal, IGCC, without CCS	UNECE	EU
Oil steam turbine	Generic, oil-fired power plant	UNECE	EU
Gas turbine < 300 MW	Natural gas CC, without CCS	UNECE	EU
Gas turbine < 80 MW with steam	Natural gas CC, without CCS	UNECE	EU
Gas Combined cycle< 3000 MW	Natural gas CC, without CCS	UNECE	EU
Biogas Agro-Zoo	Biofuel CHP	NEEDS+ReCiPe	Global
Biogas Waste	Biofuel CHP	NEEDS+ReCiPe	Global
Bioliquid plant	Biofuel CHP	NEEDS+ReCiPe	Global
Biomass plant	Biofuel CHP	NEEDS+ReCiPe	Global
CSP	CSP, trough	UNECE	EU
PV roof plant	Photovoltaic, polycrystalline silicon, roof-mounted	UNECE	EU
PV ground plant	Photovoltaic, polycrystalline silicon, ground-mounted	UNECE	EU
On-shore wind farm	Wind, onshore	UNECE	EU
Off-shore wind farm	Wind, offshore, gravity-based foundation	UNECE	EU
Off-shore deep water wind farm	Wind, offshore, steel foundation	UNECE	EU
Mini hydro	Hydro, 660MW	UNECE	EU
Mini hydro >1 MW	Hydro, 660MW	UNECE	EU
Geothermal plant – high enthalpy	Flash steam power plant	NEEDS+ReCiPe	Global
Geothermal plant – low enthalpy	Flash steam power plant	NEEDS+ReCiPe	Global

As it can be observed from Table 6, the most significant case is the one of biomass, where a single plant is used to describe four different technologies- in TEMOA-Italy. Concerning the regionality, European data coming from UNECE are the majority, even if global data are found for biomass plants and geothermal plants. In conclusion, biomass plants constitute the highest source of uncertainty, also due to the complexity of modelling the various feedstock-agricultural practices-conversion-technology combinations [114].

An overview of the indicators of the LCA Environmental Footprint dimension for power sector processes is provided in Table 7. The table summarizes the environmental impacts of various energy generation technologies using five indicators: Global Warming Potential (GWP), Acidification Potential (AP), Eutrophication Potential (EP), Land Use, and Water Use. Conventional sources like coal and oil steam turbines have the highest environmental impact, emitting significant GHGs and pollutants while requiring relatively less land and water. Gas turbines perform better in terms of emissions and resource use. Biogas, bioliquid, and biomass plants offer sustainable alternatives by utilizing organic materials, resulting in lower environmental impacts compared to coal and oil steam turbines. Renewable energy technologies, including solar, wind, and hydro, exhibit favorable environmental indicators. In particular, solar power has low emissions and water use, while wind farms perform well in terms of emissions and land and water use. Hydroelectric power has higher emissions due to reservoir methane, but minimal acidification and eutrophication potential if compared with the other technologies. Finally geothermal plants show low emissions and land use, but higher acidification and eutrophication potential.

The security of an energy system encompasses several aspects [117]: among these, there is a stable and uninterrupted supply by the energy infrastructures, including the power sector [118]. In this regard, ESOMs usually rely on a poor representation of the power system, not considering the dispatchability issues of VRES if not in a rough manner [88]. Therefore, it is not guaranteed that a feasible ESOM scenario also provides feasible and well-performing solutions when simulated on dispatch models [119]. Therefore, the indicators in this dimension must necessarily involve the reliability issue, here expressed by the technology's capacity factor, in accordance with existing literature [30] [107]. Considering the long-term side, a secure energy infrastructure also depends on the import availability, with possible disruptions to be mitigated [118]. The spread of VRES and more in general clean energy technologies is beneficial for energy security, since it decreases the fossil fuel import reliance that many countries have been experiencing until today: however, the expected massive penetration of renewables could lead to new import dependencies, that must be strategically faced before they overcome the above-mentioned energy security benefits [120]. Clean energy technologies (e.g., batteries, solar panels, wind turbines) present high geographical concentration in some countries (mainly China [121]) along the whole value chain, from raw material extraction to technology assembly, increasing the risk of possible value chain bottlenecks [122]. Therefore, this analysis has been narrowed down to technologies that pose concerns for energy security: fossil fuel plants, photovoltaic, and wind energy, as corroborated by the literature [122], [123][122], [123]. This selection is predicated on the fact that both fossil and renewable technologies involve the import of "critical" commodities. Although other plants also entail

dependencies (e.g., steel, cement, foreign components), there is no supporting evidence justifying the inclusion of these materials as critical. Therefore, the assumption is that other technologies and electricity imports do not pose security concerns. In this regard, for energy carriers and critical materials (both considered critical commodities for the security of supply) three indicators are considered: the volume shortage risk, the import dependence, and the geopolitical stability. The rationale behind this choice is to quantify both the quantity of import (import dependence) and its quality (volume shortage risk, representing the diversification of the mix), and geopolitical stability, that quantify reliability of energy partners.

Table 7. Power sector technologies characterization for LCA Environmental Footprint indicators at the base year.

LCA Footprint indicator	GWP [a] $\left[\frac{kg_{CO_2,EQ}}{MWh}\right]$	AP [b] $\left[\frac{g_{SO_2,EQ}}{MWh}\right]$	EP [c] $\left[\frac{g_{PO_4,EQ}}{MWh}\right]$	Land Use $\left[\frac{m^2}{MWh}\right]$	Water Use $\left[\frac{m^3}{MWh}\right]$
Coal steam turbine	849.0	430.2	424.0	0.3	1.7
Oil steam turbine	693.6	627.5	128.7	0.3	1.9
Gas turbine < 80 MW	433.7	966.7	19.7	0.2	1.2
Gas turbine < 300 MW	433.7	966.7	19.7	0.2	1.2
Gas Combined cycle< 3000 MW	433.7	966.7	19.7	0.2	1.2
Biogas Agro-Zoo	212.0	853.1	138.5	0.1	1.5
Biogas Waste	212.0	853.1	138.5	0.1	1.5
Bioliquid plant	212.0	853.1	138.5	0.1	1.5
Biomass plant	212.0	853.1	138.5	0.1	1.5
CSP	42.0	528.4	13.8	10.1	0.34
PV roof plant	34.8	528.4	39.3	5.6	0.63
PV ground plant	36.7	528.4	28.4	10.1	0.58
On-shore wind farm	12.4	60.9	6.7	1.4	0.18
Off-shore wind farm	13.3	50.1	6.9	1.4	0.16
Off-shore deep water wind farm	14.2	50.1	6.8	1.4	0.16
Mini hydro	147.0	0.2	12.6	10.1	0.37
Hydro >1 MW	147.0	0.2	12.6	10.1	0.37
Geothermal plant – high enthalpy	41.0	189.7	25.1	2.5	1.4
Geothermal plant – low enthalpy	41.0	189.7	25.1	2.5	1.4

[a] Global Warming Potential (GWP) factor for equivalent carbon dioxide emissions each MWh of electricity produced

[b] Acidification Potential (AP) factor for equivalent sulfur dioxide emissions each MWh of electricity produced

[c] Eutrophication Potential (EP) factor for equivalent sulfur phosphate emissions each MWh of electricity produced

Data for these indicators are quantified and gathered differently. The reliability indicator is directly obtained from the capacity factor values available in the TEMOA-Italy database: hence, there are not concerns regarding spatial and technological aggregation when considering this indicator. Since the model includes capacity factor data for all the modelled years and for all the technologies, it is not necessary to assume future variation for the capacity factor. Instead, the remaining security indicators are obtained from external sources, since TEMOA-Italy only provides, among the results, the total amount of imported energy commodities. The fuels considered in the analysis are oil, coal, and natural gas, while it is worth pointing out that

their import is not solely related to the power sector consumption, since other sectors (chemical in particular) strongly rely on these fuels. Moreover, in the model version used for this study there is no explicit distinction between import countries. Data for fuel import by country are taken from the Italian fossil fuels national statistics ([124], [125]) and reported in Table 8. For each fossil fuel, its import dependence is the sum over all the supplier countries.

Table 8. Italian primary fossil fuel supply in 2021 distinguishing between supplier country and national production.[124]

Country	Coal	Oil	Natural Gas
Africa	2%	31%	30%
Asia	2%	25%	10%
Europa	10%	6%	3%
Middle East	22%	24%	16%
North America	5%	3%	2%
Russia	52%	10%	39%
Latin America	3%	1%	0%
National Production	0%	0%	5%

Table 8 shows that Africa is the largest supplier of oil, followed by Asia and the Middle East. Russia supplies to Italy most of the coal and natural gas. For natural gas, Russia is followed by Africa and the Middle East. Latin America is the smallest exporter of all three commodities. Among the major exporters, the Middle East has an almost constant presence in all the three fossil fuels, while Russia and Africa are unbalanced with respect to oil and coal, respectively. For the materials, the current version of the model does not account for the required amount in the case of technology installation. Moreover, concerns about security of supply arise along the whole clean energy technology supply chain, as described in the JRC report [122], that distinguishes the following steps: raw material extraction, material processing, manufacturing of the technology components, and system assembly. The indicators related to the security of supply are formulated for all these steps, considering only solar photovoltaic systems (i.e., solar PV) and wind turbines, since they are the only technologies included in the TEMOA-Italy power sector (indeed, batteries are not modelled) for which the JRC report has highlighted relevant potential bottlenecks. The global supply share in 2020 by country and supply chain step from [122] is summarized in Table 9.

.

Table 9. Global supply chain share in 2020 by country and by supply chain step for solar PV and wind turbines.[126]

Technology	Country	Raw Materials	Processed Materials	Components	Assemblies
Solar PV	EU27	6%	5%	0%	1%
	Rest of Europe	3%	0%	0%	0%
	China	53%	50%	89%	70%
	Japan	4%	0%	0%	0%
	Russia	5%	0%	0%	0%
	US	7%	0%	0%	0%
	Africa	13%	0%	0%	0%
	Rest of Asia	3%	0%	1%	8%
	Latin America	4%	0%	0%	0%
	Others	3%	38%	9%	21%
Wind turbines	EU27	0%	12%	20%	58%
	Rest of Europe	1%	0%	0%	0%
	China	54%	41%	56%	23%
	Japan	1%	6%	0%	0%
	Russia	0%	0%	0%	0%
	US	3%	9%	11%	0%
	Africa	2%	0%	0%	0%
	Rest of Asia	6%	0%	2%	0%
	Latin America	29%	0%	0%	0%
	Others	3%	32%	11%	19%

In Table 9 the diversification of the wind and photovoltaic supply chain is reported. It is imperative to acknowledge that the dataset under consideration pertains to the comprehensive global supply dynamics, as opposed to being exclusive to the supply specifically destined for the European region. Notably, there exists a current dearth of available data pertaining to the supply directed towards Europe [123]. Underlying this analysis is the assumption that the global supply data can reasonably serve as a surrogate for European imports, predicated upon the notion that if Europe engages in importation, the aggregate composition of its imports will inherently mirror the broader landscape of global supply patterns. This hypothesis is very relevant because it constitutes the basis for the calculation of three security indicators: Import dependence, Political Stability Index and Volume shortage. Moreover, it the next section, also the Human Development Index is calculated under this assumption. It's possible to observe a higher diversification in the wind turbine supply chain than in the solar PV one. Wind turbine raw material extraction mainly happens in China and Latin America. Then, the next processing steps are mainly owned again by China, then Europe and Other countries (plus a little in the US), respectively. For the photovoltaic systems, despite a small diversification for the raw material phase, all the other steps are mainly concentrated in China. It must be remarked that, in absence of analysis conducted at an Italian level, European data are assumed to be valid for Italy also considering the small role played by all the EU27 countries in this market.

Data of Table 8 and Table 9 represent the present situation and, since the model does not account for changes on supplier countries, all the assumptions about the future evolution of these data must be exogenous. Therefore, it is assumed to keep these values constant for all the time horizons. – For fossil fuel extraction the situation is not expected to change dramatically (due to the physical location of the natural resources), while for the solar PV and wind technology supply chain, no possible evolution was found in literature (even if some mitigation solution to the diversification problem has started being discussed [123]). Once the geographical concentration data above discussed are collected, the Import dependence and the Volume shortage indicators are computed. For each fossil fuel, the import dependence value from Table 8 (summing up over all the importer countries) is directly associated to the technology consuming it (e.g., import dependence of natural gas is associated to all the natural gas-based power production technologies). For the renewable technologies where 4 values are present (one for each supply chain phase), the worst one is chosen to account for possible bottlenecks risks

Both for critical materials and energy commodities, the Volume Shortage Risk, is quantified applying the "N-1" criteria [127], representing the remaining percentage of supply if a failure of the biggest supplier happens. The math for this index is reported in Equation (3):

$$N-1=\sum_{i=1}^{N_{importer\ countries}} \%\ of\ tot.imp.fuel-\left(\%\ imp.fuel_{\ largest\ supplier}\right) \quad (3)$$

Concerning the Volume shortage indicator (see Equation (3)), it is obtained by considering all the suppliers (import and domestic supply) and subtracting the maximum value, obtaining as a final amount the percentage of fuel or renewable technology available if there is a shortage from the largest supplier. Concerning renewable technologies, the worst values of Table 8 and Table 9 are taken. Final technology values for both the indicators are reported in Table 11. The security of supply depends also on geopolitical factors [118]: in this perspective, the supplier countries can be characterized in terms of reliability as a trading partner. This have been already done both for fuels [118] and raw materials [123], [128], considering geopolitical stability indexes that account for several governance dimensions. The one chosen for the analysis is the Political Stability Index (PSI) [129], which measures perceptions of the likelihood that the government will be destabilized or overthrown by unconstitutional or violent means, including politically motivated violence and terrorism. Its measure is usually performed at a country level, while commodities are supplied by a mix of countries. Therefore, is necessary to pass from a country-defined to a commodity-defined PSI value. At this point, importer countries are characterized by their import share (for each critical commodity) and their PSI. Then, an average PSI for each energy commodity or material supply chain is derived, starting from the PSI of the supplier countries and their weights in the import share. This is done through a weighted average process as in Equation (4):

$$PSI_{commodity} = \sum_{i=1}^{N_{importer\ countries}} PSI_{country(i)} * import\ share_{country(i)} \quad (4)$$

The final PSI is reported in Table 10 .

Table 10. Political Stability Index (PSI) by country.[130]

Country	Political Stability Index (PSI)
EU27	0.76
Rest of Europe	0.21
China	-0.48
Japan	1.03
Russia	-0.65
USA	0.42
Africa	-0.69
Rest of Asia	-0.39
Latin America	-0.23
Others	0.86

As it is possible to notice in Table 10 the highest PSI occur for the western countries such as Japan, Europe 27 and USA. The tier 2 countries are the other European nations, the Latin America, and the Rest of Asia. Finally, the less trustable countries in terms of political stability are Africa, Russia, and China, that also plays a major role in the international trade. Conclusively, reports all the supply chain indicators. The fossil fuel supply chain security refers to the imported fuels: then, security issues can be reflected at the technology level since technologies consume these fuels to produce their outputs, referred to as technology activity (e.g., the activity of a power plant is the produced electric energy). On the contrary, the technology supply chain security directly refers to the installation phase of the technologies. In both cases, these indicators are associated with the activity of the technologies, leading to two limitations. First, for the fuels, the indicators measured for the imported, and then consumed fuels, are directly associated to the technology, without passing through its efficiency. Indeed, mixing upstream data (fuel import) and production (activity) is not possible, because the scenario evaluation must be performed on a normalized basis, in this case obtained by the activity share (which values are always between 0 and 1). Second, the technology supply chain security issues are reflected in the technology operation phase (activity share), instead of the installation phase (capacity share). Theoretically, fossil fuel powered plants involve a security issue if the commodity is consumed, and this is someway proportional to the activity. For renewable plants, the security issue related to materials happens only in the installation phase, quantified in the model by the new installed capacity. Again, due to the need of evaluating the scenario on a common basis, security issue of renewable plants is assumed proportional to activity. Both these limitations are considered necessary to consistently include the security dimension in the sustainability metric, in which all the indicators are associated to the activity of a technology.

Table 11. Power sector technologies characterization for security indicators at the base year.

Security indicator	**Import Dependence**	**Volume shortage risk**	**Geopolitical Stability**
Descriptive parameter	***Imported supply (%)***	***N-1 residual supply (%)***	***Political Stability Index [-]***
Coal steam turbine	100.0%	47.2%	-0.20
Oil steam turbine	100.0%	77.0%	-1.10
Gas turbine < 300 MW	95.0%	60.0%	-0.59
Gas turbine < 80 MW with steam	95.0%	60.0%	-0.59
Gas Combined cycle < 3000 MW	95.0%	60.0%	-0.59
Biogas Agro-Zoo	0.0%	100.0%	0.76
Biogas Waste	0.0%	100.0%	0.76
Bioliquid plant	0.0%	100.0%	0.76
Biomass plant	0.0%	100.0%	0.76
CSP	0.0%	100.0%	0.76
PV roof plant	96.0%	34.5%	-0.16
PV ground plant	96.0%	34.5%	-0.16
On-shore wind farm	76.5%	56.5%	0.12
Off-shore wind farm	76.5%	56.5%	0.12
Off-shore deep water wind farm	76.5%	56.5%	0.12
Mini hydro	0.0%	100.0%	0.76
Mini hydro >1 MW	0.0%	100.0%	0.76
Geothermal plant – high enthalpy	0.0%	100.0%	0.76
Geothermal plant – low enthalpy	0.0%	100.0%	0.76

Lastly, for the Social dimension, intended as the ability of an energy system to provide safe, clean, and affordable electricity [17], the choice of the indicators should reflect the wideness of this definition. Indeed, three sub-aspects are selected. The Quality of labor indicator refers to the unsustainability associated with poor labor conditions in the countries supplying the primary commodities required for energy systems. Specifically, this indicator addresses the labor conditions related to fossil fuels and critical materials, which are predominantly extracted in less developed countries. Considering that the case study focuses on Italy, the countries from which Italy imports these commodities were considered. The Quality of labor is assumed to be proportional to the Human Development Index (HDI) of the countries associated with the supplier country. As Italy is a developed country, the quality of internal jobs was not considered as a concern. The HDI values associated with a particular technology are linked to the specific commodity required by that technology. Data for the technology supply chain phase are already known from Table 8 and Table 9. For the HDI, it is a summary measure of average achievement in key dimensions of human development for a certain country. HDI is generally expressed in a 0-1 scale where the closer the value to 1, the higher the country achievements in terms of human development. For the sake of this study, as it happens for the PSI, the HDI is translated from the one of the supplier countries to the one of energy material/commodities. HDI of supplier countries is reported in Table 12:

Table 12. Human Development Index by country.[131]

Country	Human Development Index (HDI)
EU27	0.94
Italy	0.89
Rest of Europe	0.89
China	0.77
Japan	0.93
Russia	0.82
USA	0.92
Africa	0.55
Rest of Asia	0.63
Latin America	0.75
Others	0.71

According to Table 12, Europe, Japan, and USA are the most developed countries according to this index, while Africa and Rest of Asia lie at the bottom of this ranking. The conversion between country values to technology-specific value is done by performing a weighted average of the HDI of countries for their supply chain phase shares (single value for fossil and worst value for PV and Wind, as before). The result is an HDI defined for each material and fossil fuels, that can be subsequently associated to the technologies consuming that specific commodity.

Then, human health impacts are accounted for through the Human Health Damage (HDD) indicators. This is a LCA end-point kind [115] (different from the environmental ones, which are midpoint) because it directly relates the electricity production of a plant to the human health implications, expressed in Disability Adjusted Lifetime Years (DALY), the impact assessment unit for overall disease burden, expressed as the number of years lost due to ill-health, disability, or early death [132]. Data for HHD are again derived from the UNECE Report [114] as for the LCA and, together with them, they are reported in Table 7. Within LCA HHD indicator lies the fatalities one. It represents the complement of the human health damage. If HDD accounts for the predictable deaths or damages to human health linked to normal power plants operations, fatalities account for accidental events (deaths) caused by electricity production. Finally, fatalities derived by power plants hazards are added because they represent another kind of damage to human, not related to hill but to unpredictable hazards happening over the whole life cycle of the plant, even if evidence is not clear on the proportion of fatalities that occur during construction versus during operation (in developed countries) [30]. Source values are taken from [133], a well-established reference in literature. The inclusion of HHD, quality of labor, and fatalities is in line with many of the sampled work, where internal factors like fatalities and pollution were considered (e.g., [30], [62], [63]) together with external issues as human rights and labor conditions [30]. Data for fatalities are derived from the IPCC study on renewable energies and climate change mitigation [134] and are reported in Table 13. As happens for the LCA parameters the technological discretization of the study is different from the model one, therefore a connection between databases is performed.

Table 13. Accident-related fatality rates/GWh.

Technology	Specifications (Country / Sub-tech)	[Fatalities / GWyr]
Coal	OECD	1.2E-01
	EU 27	1.4E-01
	non-OECD w/o China	5.7E-01
	China	5.9E+00
Oil	OECD	9.3E-02
	EU 27	9.9E-02
	non-OECD	9.3E-01
Natural Gas	OECD	7.2E-02
	EU 27	6.8E-02
	non-OECD	1.2E-01
Hydro	OECD	2.7E-03
	EU 27	8.5E-02
	non-OECD	7.0E+00
	non-OECD	9.4E-01
PV	Cristalline Silicon	2.5E-04
Wind Onshore	DE	1.9E-03
Wind Offshore	UK	6.4E-03
Biomass	CHP Biogas	1.5E-02
Geothermal	EGS	1.7E-03

In Table 13 accident fatality rates for one GWh of electricity are reported for different power sector technologies. The IPCC study provides a statistical analysis conducted on different countries, highlighting for each technology the rate of fatalities, providing, when possible, some specifications about the type of plants used for the study and the countries. Accident-related fatalities range from 2,5E-04 (PV min) to 7,0E+00 (hydro-max. The maximum IPCC hydropower value represents nations out of the Organization for Economic Co-operation and Development, while the minimum values are found for OECD countries and nations of the European Union. This is a general pattern in the table, even if the hydropower case is the most visible, also due to the three order of magnitude variation. The IPCC does not explain the large difference between these values compared to other technologies.

Table 14. Power sector technologies characterization for Equity indicators at the base year.

Equity Indicator	Fatalities $\left[\frac{\text{Deaths}}{\text{MWh}}\right]$	Quality of Labor *Human Development Index*	Human Health Damage [a] $\left[\frac{\text{DALY}}{\text{MWh}}\right]$
Coal steam turbine	0.14	0.85	1.9
Oil steam turbine	0.09	0.83	1.0
Gas turbine < 300 MW	1.08	0.78	0.5
Gas turbine < 80 MW with steam	1.08	0.78	1.1
Gas Combined cycle< 3000 MW	1.12	0.78	0.5
Biogas Agro-Zoo	0.15	0.94	2.0
Biogas Waste	0.15	0.94	2.0
Bioliquid plant	0.15	0.94	2.0
Biomass plant	0.15	0.94	2.0
CSP	0.02	0.94	0.2
PV roof plant	0.02	0.76	1.9
PV ground plant	0.02	0.76	1.9
On-shore wind farm	0.19	0.80	0.0
Off-shore wind farm	1.04	0.80	0.0
Off-shore deep water wind farm	1.04	0.80	0.0
Mini hydro	1.25	0.94	0.0
Mini hydro >1 MW	1.25	0.94	0.0
Geothermal plant – high enthalpy	0.17	0.94	0.0
Geothermal plant – low enthalpy	0.17	0.94	0.0

It is also important to notice that the unit of measurement of indicators differs and some amounts are directly proportional to sustainability (e.g., Capacity factor for *reliability*), while others are in opposition (e.g., emissions, resource consumption). We categorize our indicators into two groups: 'The Lower the Better' (TLTB), where the lowest value signifies maximum sustainability (scored as 1), and the highest denotes minimum sustainability (scored as 0), and 'The Higher the Better' (THTB) indicators, which present the opposite scenario. The sustainability indicators and their related dimensions are summarized in Table 15.

Table 15. Description of sustainability dimensions and indicators.

Sustainability Dimension	Sustainability indicator	Measure	Normalization
Environmental	Global Warming Potential (GWP)*	$\frac{Kg_{CO_2,EQ}}{MWh}$	TLTB
	Acidification Potential (AP)	$\frac{g_{SO_2,EQ}}{MWh}$	
	Eutrophication Potential (EP)	$\frac{g_{PO_4,EQ}}{MWh}$	
	Land Use	$\frac{m^2}{MWh}$	
	Water Use	$\frac{m^3}{MWh}$	
Security	Reliability	Capacity factor (%)	THTB
	Import Dependence	% of imported commodity	TLTB
	Volume shortage Risk	N-1 residual supply (%)	THTB
	Political Stability Index	Political Stability Index [-]	THTB
Social	Human Health Damage	$\frac{DALY}{MWh}$	TLTB
	Fatalities	$\frac{Deaths}{MWh}$	TLTB
	Quality of Labor	Human Development Index	THTB

1.2.1. MCDA Framework for scenario evaluation

The optimal technology mix derived for the power sector by the results of the adopted ESOM and the indicators from data inventory are combined in a proper framework to obtain a separate SI for each scenario. The process can be divided into three phases: database creation, normalization and weighting, and sustainability evaluation of energy scenarios. An overview of the dataflows is provided in Figure 5.

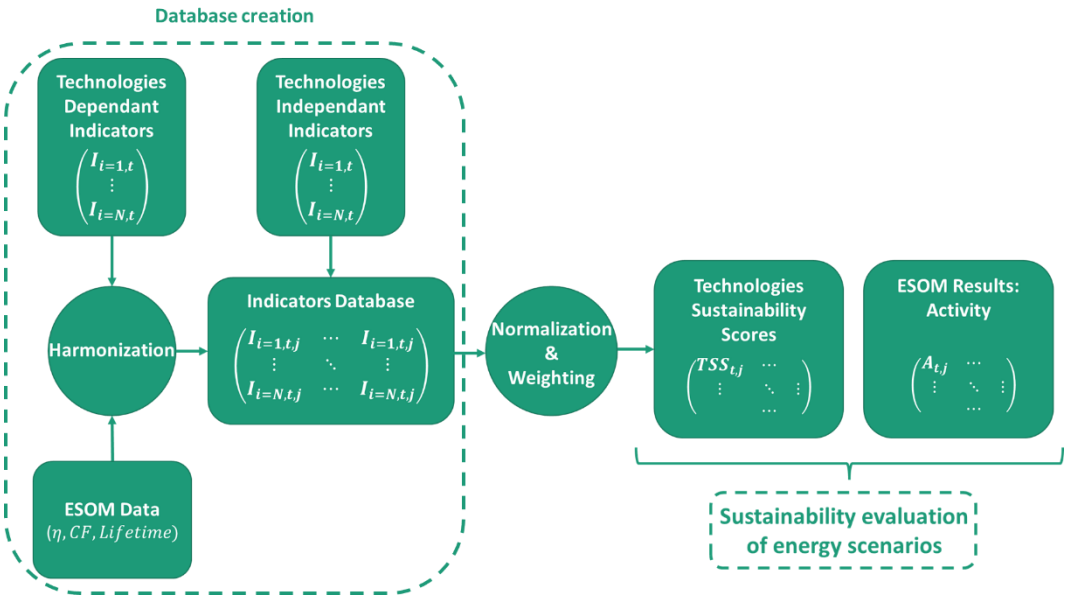

Figure 5. Data flows of the MCDA process.

Database creation

The aim of the first phase is to create a dataset with twelve indicators for each technology and milestone year in ESOM. The impact values for sustainability indicators are collected not only at the ESOM base year, but throughout the entire time horizon of the model. While parameters independent of technological improvement are assumed constant over the years, those related to specific technological parameters derived from ESOM data, namely efficiency (η), lifetime (LT), or capacity factor (CF), are calculated to consider the reduction in impact caused by improved technological performance over time. Improvements in technical parameters generally cause a reduction in overall LCA impacts. This process is called harmonization and adds a dynamic component to the LCA dataset. If the life cycle-based impacts are primarily due to the operation of the plants (as in the case of fossil power plants or biomass power plants), then a change in efficiency has a significant impact. On the other hand, if the impact is primarily due to the construction of the plants (as in the case of PV and wind and non-emitting technologies), then capacity factor and lifetime are the most influential parameters. To account for this temporal variation, the LCA parameters vary according to the average growth rate of the technological drivers as in Equation (3a) for the fossil and biomass efficiency, in Equation (3b) for CF and lifetime for the other technologies.

$$\overline{GR}_{t,j} = \begin{cases} \dfrac{\eta_{t,j} - \eta_{t,BY}}{\eta_{t,BY}} & \text{(5a)} \\ \vdots & \\ \dfrac{CF_{t,j} - CF_{t,BY}}{CF_{t,BY}} + \dfrac{LT_{t,j} - LT_{t,BY}}{LT_{t,BY}} & \text{(3b)} \end{cases}$$

For each technology, the average variation of the three technical parameters at year *j* with respect to the base year ($j = BY$) is used to reduce the LCA Impacts according to Equation (6).

$$LCA\ Footprint\ indicator_{t,j} = LCA\ Footprint\ indicator_{t,BY} \cdot \left(1 - \overline{GR}_{t,j}\right) \quad (6)$$

The final dataset is composed of a set of parameters $I_{t,j,i}$ of twelve indicators, where both activity and parameters are defined for each technology and year.

Normalization and weighting

The second step involve converting the different technology indicators ($I_{i,t,j}$) to a single value. Each indicator i in year j is first normalized for each technology t using a common scale of [0-1] with reference to the best and the worst indicator for the same indicator category, as in Equation (7).

$$I_{i,t,j}^{NORM} = \frac{I_{i,t,j} - \text{worst}\left(I_{i,t,j}\right)}{\text{best}\left(I_{i,t,j}\right) - \text{worst}\left(I_{i,t,j}\right)} \quad (7)$$

For each indicator, the technology with the most sustainable value takes 1 and the worst 0, while the others are interpolated between this range. As explained in Table 15, we utilize two distinct normalization approaches for our indicators: traditional normalization, where the highest value is assigned a score of 1, and the lowest receives 0, and reverse normalization. Several normalization techniques are available [111] , but we have found (not shown) that the min-max scaling is the one causing less distortion on data distribution. Moreover, some indicators already in a 0-100% scale (import dependency, volume shortage, reliability) do not require this process, but just a translation in the range 0-1. After this step a new dataset of indicators I^{NORM} for each sustainability indicator (*i*) is obtained for each milestone year in the model. The overall yearly sustainability performance of a technology ($TSS_{t,j}$) is obtained by hierarchical weighted sum of its qualitative set of indicators, that allows moving to a single SI value. Since there may be different configurations according to how different indicators are relevant for the scope of the analysis, each indicator must be associated to a weight (the sum of all the weights always has to be equal to one).Weights are identified by the term w_i in Equation (8), and assigned to each indicator (*i*). Technology sustainability score (*TSS*) is the weighted sum of all the indicators.

$$TSS_{t,j} = \sum_{i=1}^{12} I_{i,j}^{NORM} \cdot w_i \,, \qquad where \sum_{i=1}^{11} w_i = 1 \tag{8}$$

Sustainability evaluation of energy scenarios

When all the power sector technologies are characterized by a yearly overall sustainability evaluation, it is possible to compute a global score (SS_j) evaluating the sustainability of the technology miv under analysis. This is done by allowing each technology to influence the final score according to its contribution to the electricity production share used in Equation (9), where the electricity production share (activity share *AS*) is identified by the term $AS_{t,j}$ and represents, as an outcome of the scenario, the contribution of the produced electricity by the technology *t* (or process) in the final electricity mix for the year *j*. AS is an output of the ESOM, computed according to a specific scenario.

$$SS_j = \sum_{t=1}^{N_{tech}} TSS_{t,j} * AS_{t,j} \tag{9}$$

This framework allows the direct visualization of the power system performance in terms of sustainability through a trendline. One sustainability profile, associated to a specific set of weights, is obtained as output for each analyzed scenario.

1.2.2. Post-mining analysis

To assess the impact that different sets of weights have on the SI profile in a specific scenario, a sensitivity analysis is performed. In this regard, for each scenario, the weights of the twelve indicators used for the evaluation of the SI are sampled generating many combinations with the only constraint that their sum should be always equal to 1. As expected, each set of weights produces a unique SI profile that, over the reference time horizon of the scenario, is characterized by its own magnitude (e.g., low, medium, high) and trend (e.g., increasing, decreasing, stable). The main objective of this analysis is then to extract from the considered scenarios recurring patterns that describe the relationship between indicator weighs and the characteristics (trend and magnitude) of 10.000 SI profiles obtained after the weight sampling. To do so, magnitude and trend are treated separately according to the following methodological steps:

a. **Clustering analysis of the SI profiles**: In a selected scenario, this analysis aims at identifying reference groups of SI profiles among the 10.000 ones obtained after the sampling of indicator weights. At the end of this analysis each SI profile is tagged with the label of the cluster in which it has been grouped in using a hierarchical clustering algorithm with the Euclidean distance used as a similarity metric and the Ward.D2 as linkage method [135]. The optimal number of clusters is determined by means of well-known quality metrics such as Davis-Bouldin [136] and Silhouette index [137];

b. **Development of a classification model**: At this stage an estimation model based on a machine learning decision-tree algorithm is developed to classify a SI profile in one of the pre-determined classes evaluated through the clustering analysis. The considered model inputs are the weights of the 12 indicators used to calculate the sustainability index while the estimated output variable is the cluster label. The developed model is a random forest based on the ensemble of 500 decision trees trained on different parts of the available dataset imposing a minimum size of terminal nodes equal to 10. The classification accuracy of the model is assessed training the classifier on the randomly sampled 70% of the dataset and testing it on the remaining 30%.

c. **Analysis of the feature importance**: This step exploits an explainable artificial intelligence (XAI) technique to explain and interpret the developed classification model to infer which indicators have the highest influence on a specific feature of the SI profile (i.e., magnitude or trend). Specifically, the importance of an input variable (i.e., one of the 12 indicators used to evaluate the SI) is assessed according to the increase in the model classification error after permuting the variable. A variable is than considered as "important" if the shuffling of its values significantly increases the model error, because in this case the model relied on that variable for the classification. On the other hand, a variable is considered "unimportant" if shuffling its values, the model error is not remarkably affected, because in this case the model did not exploit that variable for the classification. In this study the increasing of the model classification error is measured in terms of Cross-Entropy, as reported in [138].

To separately analyze the SI profile properties, the above-described process is applied to not normalized profiles to characterize the magnitude of the profiles and to normalized profiles to better highlight differences in terms of their trends. To analyze the trend, all the considered 10.000 SI profiles of a scenario are normalized with respect to their maximum value then emphasizing the shape attributes of the profiles more than the magnitude ones. Eventually, the sensitivity analysis for both magnitude and trend of the SI profiles is carried out for different scenarios to understand if the discovered relations are or are not characterized by traits of generalizability.

1.3. Results

The outcomes resulting from the application of the methodology are here presented. The section is structured as follows. First, the energy scenarios in terms of electricity production and emissions are discussed. In particular, the scenarios are explained with a specific focus on the technological change in the power sector required by the decarbonization policy and its implications in terms of sustainability. Next, the outcomes for the SI calculation are presented highlighting the role of the SI as a tool to compare energy scenario and providing an example of readability and interpretation. Finally, the post-mining analysis is performed, gaining a deeper understanding on the effect and impact of alternative selection of the weight values.

1.3.1. Electricity mix and carbon emissions

The applied constraints result in different electricity production and carbon emission trajectories between scenarios. Thanks to Figure 6a is possible to appreciate how the emissions reduction (evaluated with respect to the period 2007-2010) performed by the Reference scenario (thanks to efficiency improvements) is incomplete if compared to net-zero targets.

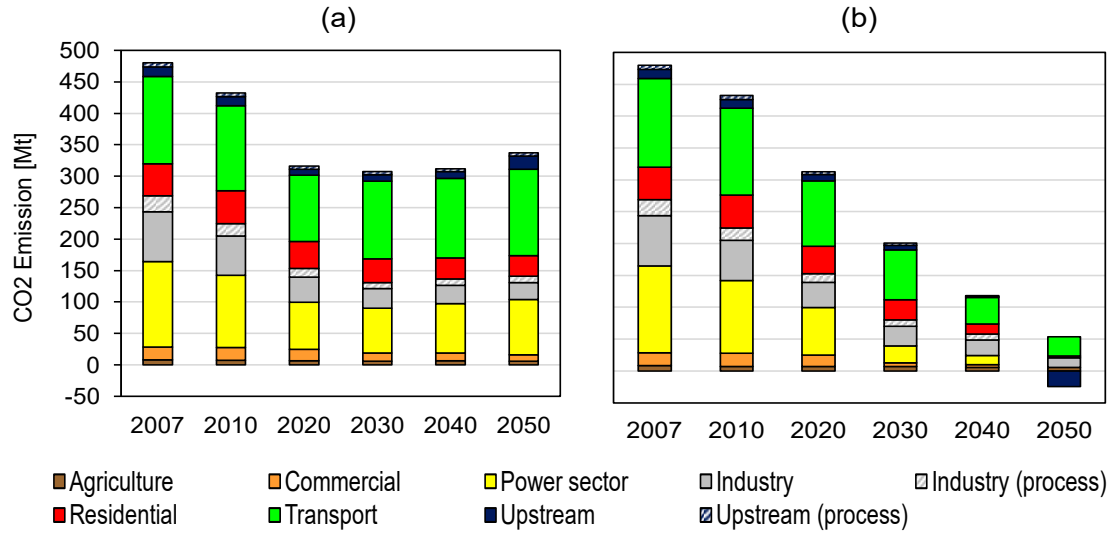

Figure 6. CO2 emissions reduction for TEMOA-Italy Reference and Decarbonization scenarios (a) and Electricity consumption increase (b).

Indeed, the reduction of carbon emissions only reaches around 30% in 2050. Differently, the Decarbonization scenario (Figure 6b) puts in place a transition to an almost carbon-neutral condition: in 2050, with a ~94% emissions reduction with respect to base year. It is also evident how the main emission sources are the transport and the power sector (in the Reference 2050). In absence of constraints (Figure 6a) the emissions from the two sectors are quite constant. On the contrary, in the Decarbonization (Figure 6b), the final emissions reach negative values (-24,5 Mt CO_2) thanks to the direct air capture and the biomass with CCS. Moreover, both the transport and the power sector experience a deep emission reduction driven by the constraints. This means a higher electrification of transports and renewable share in the power sector. The higher decarbonization effort in the Decarbonization scenario requires a 30% increase in electricity consumption with respect to the base year (see Figure 7), while the Reference one presents an almost stationary trend. Considering the electricity production sources, the Reference scenario (Figure 7a) does not significantly change its energy mix across the time, relying mainly on natural gas, import and renewables, respectively. Differently, the strong Decarbonization targets mainly leads to a transition towards solar and wind (Figure 7b).

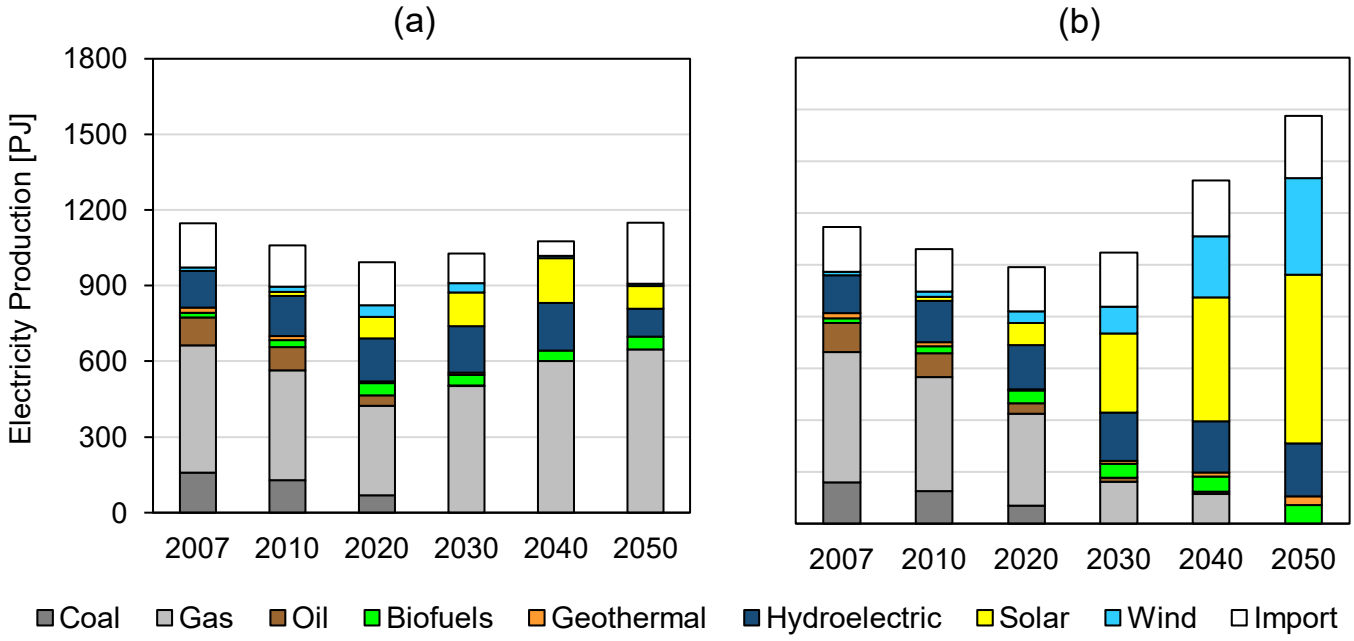

Figure 7. Evolution of the electricity production by source obtained in the TEMOA-Italy a) Reference scenario and b) Decarbonization scenarios.

Diving into details, Figure 7 shows that after 2030 the differences between the two scenarios start being sharper. If in the Reference the gas dominates the electricity production with a significant increase (around 30% from 2030 to 2050), in the Decarbonization renewables take the scene. From 2030 to 2050, photovoltaic and wind experience a sharp rise in production, around 120 % and 300% respectively.

1.3.2. Sustainability index

Once all the necessary data are acquired, the sustainability index calculation is applied. Since the sustainability index calculation is affected by the assigned sets of weights, 10000 combinations of indicator weights are tested, by making all the weights vary between minimum and maximum values of 0 and 1, respectively, and keeping their overall sum equal to 1. The implications of using different sets of weights are reflected in the technology sustainability evaluations that, applied to scenarios activity, define 10000 different SI profiles. To preserve interpretability, only the case with an equal weight configuration is shown, with the other profiles laying in the background of the plot. In Figure 8 the SI for both Reference and Decarbonization scenarios is plotted. This visualization highlights the role of the sustainability index as a tool to quantitively compare scenarios across a user-specified indicator ranking. With the specific weight configurations applied, the Decarbonization scenario demonstrates a slightly superior performance when compared to the Reference scenario. Notably, the former exhibits a progressively increasing trend in contrast to the relatively flat to slightly decreasing trajectory of the latter, resulting in an approximately 10% relative difference by the year 2050. Despite the case-specific outcome, what must be noticed is the wide spectrum of profiles (grey lines) covered by the SI when changing the set of weights. Indeed, according to the assigned set of weights, the SI can range from 0.1 to 1 in magnitude while assuming different trends. A level of explanation based on artificial intelligence techniques is used to determine whether and how the magnitude and trend of SI are affected by the single indicators, trying to find patterns allowing for extraction of general knowledge.

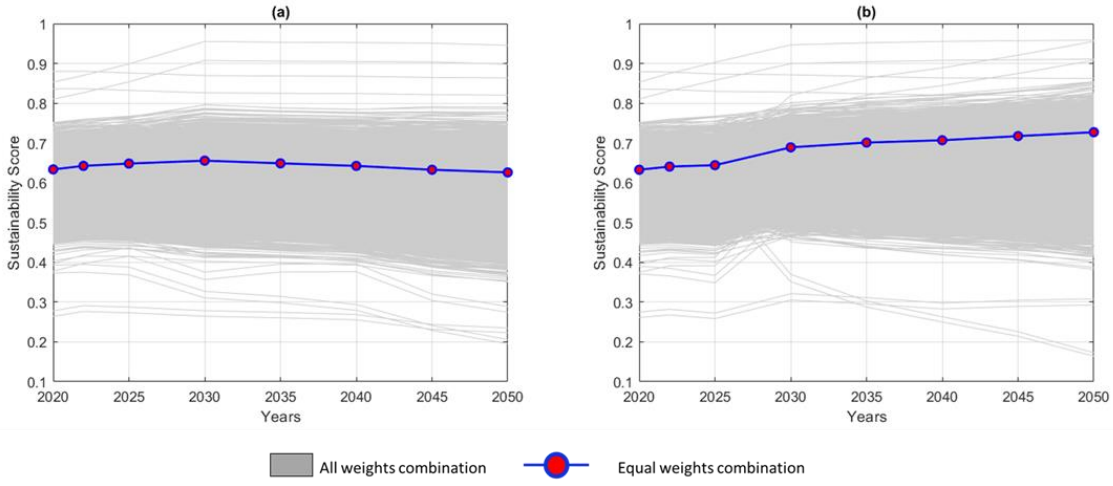

Figure 8. Sustainability score profiles for Reference (a) and Decarbonization (b) scenarios considering all the 10'000 combinations (grey lines) with evidence of the SI profile associated to an equal weight of the indicators (blue dashed line).

1.3.3. Post-mining analysis

The aim of the post mining analysis is the assessment of the influence that indicator weights have on the sustainability index. After having obtained 10,000 SI profile samples, they are analyzed considering their magnitude and their trend separately but repeating the same steps in analyzing both. The first step of the post-mining analysis is clustering the SI profiles, which makes possible to extract reference qualitative groups for magnitude (e.g., Low, Medium, High) and trend (e.g., increasing or decreasing over time). The clustering phase results are not to be intended as final outcomes, but functional to the generation of them. Indeed, after the identification of the reference clusters of SI profiles, the classification models are developed with the aim to extract the relationships between the indicator weights and the features of the SI profile itself. This last step facilitates the identification of patterns that substantially influence the variations of the SI.

Clustering analysis

Cluster profiles obtained are reported in Figure 9, showing the clustering results obtained for both the Reference and Decarbonization scenarios. In particular Figure 9 (a) and Figure 9 (c) show the obtained reference clusters of SI profiles if not normalized (to characterise the magnitude) and when normalized (to characterize the trend), respectively, for the Reference scenario. Similarly in Figure 9 (b) and Figure 9 (d) the clustering results pertaining the Decarbonization scenario are shown. It is possible to notice that the four indipendent clustering analyses converged on a optimal number of SI profile groups equal to three, with the only exception of Figure 9(d), with four optimal groups. The SI magnitude of both scenarios is generally included in the range between 0.4 and 0.8, with slightly higher values for the Decarbonization scenario. For what concerns the trend patterns extracted from both scenarios, it is possible to identify three main behaviors for the Reference scenario and four for the Decarbonization one. Specifically, regardless to the magnitude level, the SI profiles can decrease over time (as for the Reference scenario), can be stable on the first period of the scenario and then decrease (cluster 4 in Figure 9 (d)), or can increase (during the first part of the scenario and then remain stable, as cluster 1 in Figure 9 (d) , or increase like cluster 2 in Figure 10(d)).

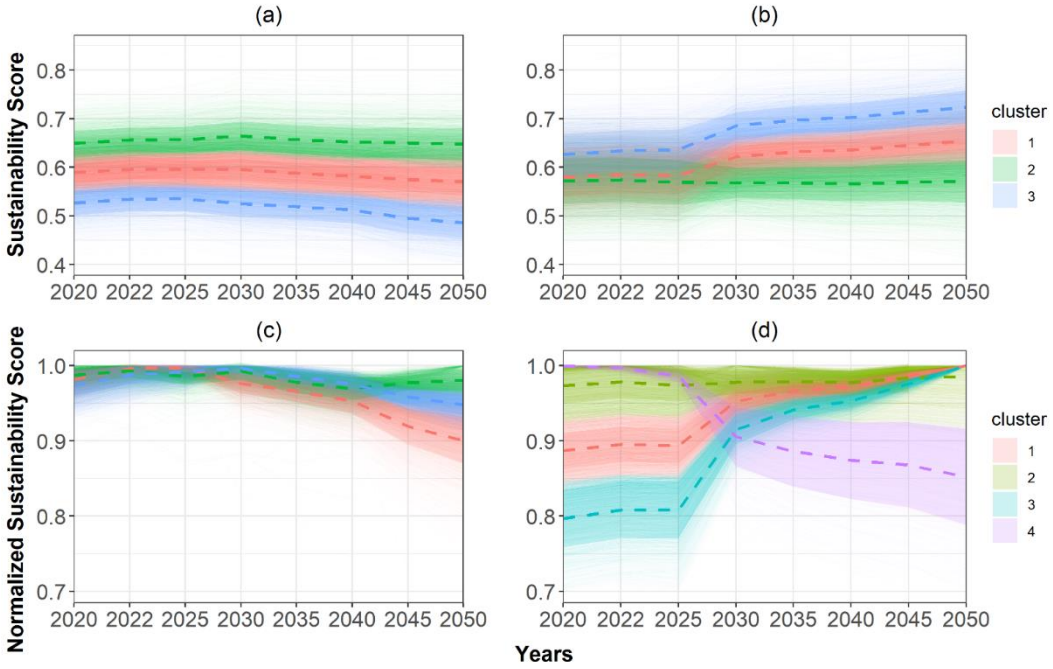

Figure 9. Analysis of the SI profile magnitude (a, b) and of the profile trend (c, d) for the Reference (a, c) and Decarbonization (b, d) scenarios, respectively. Dashed lines represent the centroid of the three identified profiles and the red green -blue areas around them are the associated standard deviations.

Classification models and feature importance

To extract the relationships that exist between the indicator weights and the features of the SI profile itself (i.e., magnitude and trend), two classification models for each scenario are applied. The four models achieved very good accuracy values (85 ~ 90%) demonstrating their capability in capturing all the important dependencies between a certain level of magnitude or trend of an SI profile and the associated indicator weights. Table 16 reports the results obtained for each classifier in terms of accuracy achieved in the testing phase, calculated as defined in [139].

Table 16. Accuracy, Recall and Precision of the four classifiers developed for the Reference and Decarbonization scenarios.

Scenario	SI Profile Feature	Accuracy
Reference	Magnitude	87.6%
Reference	Trend	85.3%
Decarbonization	Magnitude	86.9%
Decarbonization	Trend	83.8%

The final step of the analysis aims at describing what the classification model learnt from the data generated with the sampling of indicator weights. To this purpose an explanation layer is defined on top of the classification model to assess the importance of each input variable in the characterization of SI profile magnitude and trend. Since the importance of an input variable is measured according to the increase of the model prediction error when its values are shuffled. Table 16 Each bar chart included in Figure 10

Figure 10 reports the input variables in descending order according to their importance. The bar height is associated to the average increase of the model Cross-Entropy among 10 permutations, while the vertical dashed lines represent the baseline Cross-Entropy value for each model. The higher the Cross-Entropy loss after permutations, the higher is the importance of the input variable. The first interesting result is that in both analyses (magnitude and trend), the most important features are the same across scenarios. For magnitude these are Import Dependence, EP, and quality of labor, while for trend Reliability the Land Use, Fatalities, and AP ones. This fact can be read as a general validity of the most important indicators among the scenarios, at least for those analyzed in this work. Delving into the details of the magnitude plots, the Reference scenario results appear to be strongly influenced by environmental indicators related to plants operations (AP, EP) and geopolitical issues related to fossil fuels (quality of labor and Import dependence). For the Decarbonization scenario results, the model predicts reliability as a pivotal issue due to a strong renewable penetration. Furthermore, the Eutrophication fostered by solar panels construction [140] and the Import dependency issues previously discussed also gain their relative importance. The second noteworthy finding pertains to the role of Reliability and the Land Use indicators in predicting the trend of the Sustainability Index. Indeed, Reliability and Land Use weights assume a primary role in affecting the model accuracy, with a dominant role of the former in both scenarios. This second consideration suggests that Reliability and Land Use have a high impact on its increasing or decreasing trend over time. With the Reliability playing a pivotal role in both magnitude and trend of the Decarbonization. The importance attributed to these features highlights two major technological challenges, already mentioned in actual literature, associated with the energy transition [141].

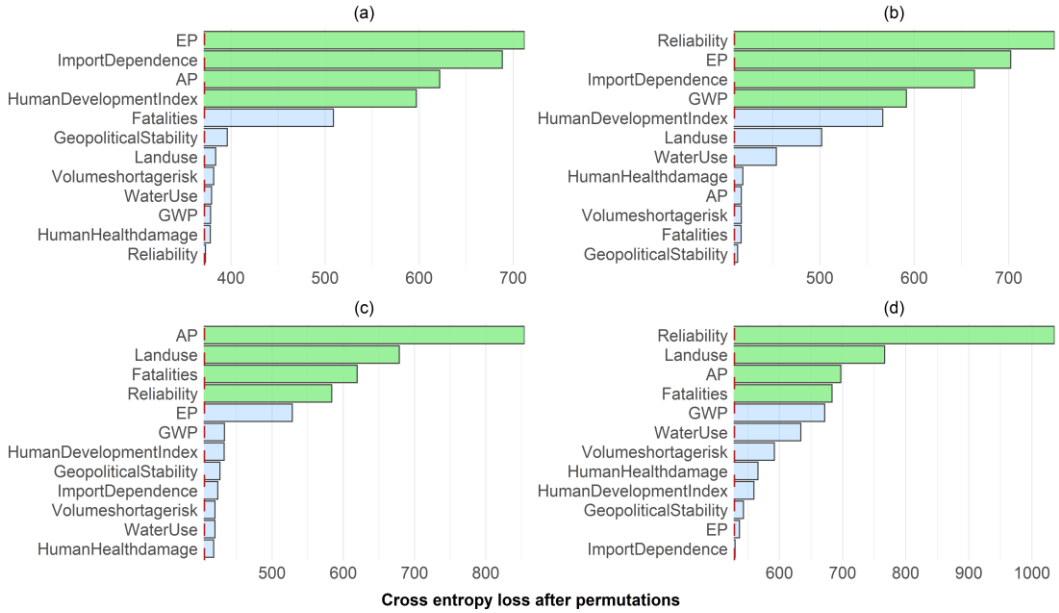

Figure 10. Feature importance for Magnitude (a, b) and Trend (c, d) classification analysis in both Reference (a, c) and Decarbonization (b, d) scenarios.

Approach 2– Introduction of land-use potential in ESOMs

Introduction

In Section 1.4, the limitations of ESOMs in integrating nexus components have been discussed, with particular attention to the land-use dimension. Among the various nexus aspects, land use is considered particularly relevant for the Mediterranean context due to its geographical, environmental, and socio-economic characteristics. The preliminary approach adopted in this work has confirmed that land use, even when considered in a post-processing manner, represents a significant source of uncertainty in the evaluation of decarbonization policies. This highlights the need to test the hypothesis that land use can have a substantial impact on the outcomes of energy system models, thereby providing a justification for its direct integration into ESOM frameworks.

The objective of this study is therefore to serve as a bridge between previous work—based primarily on ex-post analysis of model outputs—and the full integration of land-use sectors within energy system models. To this end, a generic methodology is developed and applied to a case study of the island of Pantelleria, using a small-scale model. This localized focus is intended to amplify the effects of spatial scale, enabling a clearer assessment of land-use dynamics in a constrained system. Depending on the robustness and significance of the results, the approach may then be extended to broader contexts.

2.2. Methodology

This section details the Geospatial Information Systems (GIS) and sources used in the analysis are briefly described. The coupling of land use data in energy models is divided in three main steps: the data gathering of renewable resource potential and land availability, the definition of a proper case study and the incorporation of and the incorporation into the selected modelling instance. Our research required a light and flexible modeling framework for rapid prototyping and analysis. For these reasons, The TEMOA framework has been selected. Its open-source Python and Pyomo implementation makes it an ideal tool for testing and customization without proprietary software limitations. To ensure the credibility of our results, it's important that TEMOA's structure is analogous to widely used models (e.g., MARKAL/TIMES, MESSAGE) and that it has been formally validated against the TIMES framework [142]. For a detailed technical overview of TEMOA, please refer to the Appendix.

In this analysis, two macro categories of data are being used, and namely simple spatial data and spatiotemporal time series. Spatial data are represented as a list of numbers using a particular coordinate system. For example, the objects of an electronic map are represented using spatial data (roads, buildings, windspeed by location), represented as points and shapes with a specified position. In this analysis, spatial data are both the constraints used to perform the land eligibility analysis and, in general, all the spatial properties that are fixed during time (e.g., cost of land rent). The superimposition of the different thematic layer (e.g., administrative, or physical constrains) allow to draw the final land eligibility map. These kinds of data are fixed among all the scenario periods; therefore, they are applied once and does not change during time. On the contrary, spatiotemporal time series, related to the resource potential for both photovoltaic and wind, is time dependent. A geo-referenced time series keeps the whole history of the evolving object over a period [143]. Typical examples include the monitoring of crop health over years [144], and meteorological time-series [145]. For the manipulation of both types of data, the use of Geographic Information System(s) (GIS) is mandatory. GIS is a specialized tool designed for the organization and management of diverse datasets associated with geographic or spatial coordinates, utilizing a specific map projection system [23]. In our research, we employ the QGIS software [24] for handling, analyzing, and visualizing spatial information. GIS technology plays a pivotal role in spatial energy planning, as it enables the amalgamation of data pertaining to renewable energy resources, regulatory guidelines, and natural constraints.

2.2.1. Land eligibility

Existing literature extensively discusses eligibility criteria, and although specific aspects may vary, there is a consensus on its broad scope. Thanks to a review of the main analysis about this topic (as summarized in **Error! Reference source not found.**), it becomes evident that s everal consistent exclusion components are commonly considered. These include economic factors, administrative and technical considerations, and social aspects. Thus, it is expected that a study aligned with the existing body of knowledge should incorporate these elements as essential components when assessing the eligibility of land for renewable installations.

Table 17. Review of the main land eligibility analysis found in literature

Administrative	Technical	Economic	Social	Year	Source
v	*v*			2014	[146]
v	*v*	*v*	*v*	2018	[147]
v	*v*	*v*		2020	[148]
v	*v*	*v*	*v*	2020	[149]
v	*v*	*v*	*v*	2021	[150]
v	*v*			2022	[151]
v	*v*	*v*	*v*	2022	[152]
v	*v*	*v*	*v*	2023	[153]

It is evident from Table 17 that all the pertinent research concurs on the existence of two primary clusters, pertaining to administrative and technical constraints. Administrative limitations typically encompass regions where the establishment of new facilities is prohibited for various reasons, including natural protected areas [154], proximity to historical sites [155], and residential agglomerations [156]. On the other hand, technical constraints are predominantly linked to challenges in constructing or operating new facilities due to factors such as terrain and soil conditions [157], or adverse weather patterns (e.g., low wind speeds, shadowing effects from hills and mountains). Additionally, these factors may also exert an influence on economic constraints, as there are overlaps between technical and economic characteristics, including criteria such as wind speed thresholds and slope thresholds. As underscored by McKenna et al. [152], there is a pressing need within the literature for the validation of studies related to land eligibility. Furthermore, there appears to be a notable absence of social and political considerations in the existing analyses. Consequently, the adopted criteria and their associated clusters are reported in Table 18.

Table 18. Constraint expression for Land Eligibility analysis. Exclusion rule for distance are derived from Italian regulation [158]

Area	Constraint	Exlcusion rule	Source
Environmental / Technical	Wind Speed	below 4.5 m/s	RSE [159]
	Irradiance	below 3.0 kWh/m2 day	UMEP ERA 5 [160]
	Slope	≥15%	TinItaly [161]
	Permanent crops	Inside	CLC [157]
	Water bodies	Inside	-
	Rocks	Inside	-
	Coast	Inside	-
Administrative/Habitat	Natural Habitats	Inside	Natura 2000 [162]
	Bird Areas	Inside	-
	Biospheres	Inside	WDPA [155]
	Protected Landscape	1000 m	-
	Reserves	Inside	-
	Parks	Inside	-
	Monuments	1000 m	-
	Hydrological risk	Inside	GeoPortale []
Anthropic	Road distance	100 m	OpenStreetMap [156]
	Urban settlement	200 m	-
	Industrial sites	200 m	-
	Airport	1500 m (Wind Only)	-
	Recreational Areas	200 m	-

In accordance with Table 18, land availability is constrained by environmental/technical criteria, thereby rendering the construction phase of the plant unfeasible due to adverse soil conditions and distance from the grid. Similarly, operational convenience for the plant is compromised due to low resource availability. Data pertaining to resource availability are distinctly derived for wind and photovoltaic sources and are more comprehensively discussed in the resource assessment phase. Information concerning crop types and soil conditions is obtained from the Corine Land Cover source [157], a widely recognized reference in the literature, corroborated by GLAES [147].

2.2.2. Potential assessment

The way solar and wind resource are assessed should be in line with the most recent and well-established existing literature. As highlighted by McKenna et.al [152] in the above-mentioned review, the technical potential assessment requires a standardization of the analysis and the tools. This is justified by the need of reproducibility and data availability. To accomplish these requirements solar and wind technical potentials are estimated using the calculation methodology of Elkameen et. al [163]. Technical potential is estimated starting

from solar irradiance and wind speed data and, after some passages, obtaining capacity factor for the different sites. The detailed steps are described in the specific photovoltaic and wind assessment sections, respectively. The starting point is the choice of the data sources for the potential assessment. This practice must be in line with the needs of the analysis (e.g., extension of the area under study, temporal horizon, model resolution) [164]. Therefore, after having fixed the methodological steps, a detailed analysis of all the possible data sources for both wind and photovoltaic has been conducted. Solar radiation and wind speed can be estimated in two different ways [152], trough database already providing the energy potential at a certain resolution, or trough detailed model considering slope, aspects, shadowing effects and roughness of the terrain that calculate the potential. Concerning the former, the analysis is conducted both considering large global databases and national specific ones. The results are summarized in Table 19, presenting a classification of the main database for solar and wind technical potential assessment. Sources are characterized according to data typology, cover and resolution. For these last two items, data are differentiated also by temporal and spatial attributes. Sources belong to the following classes:

Table 19. Data sources for general and technology specific resource assessment. Characterization by spatial and temporal coverage and resolution.

Tech	Data typology	Database names	Coverage		Resolution	
			Spatial	Temporal	Spatial	Temporal
General	Observation	HadISD [165], Tall Tower Database [166]	Global	Historical, 20-50 years	Site specific	5 min - 1 hr
	Reanalysis	MERRA-2 [167], ERA5 [168]	Global	Historical, 40-70 years	30-60 km	1-6 hr
	Climate models	CMIP5 [169],EUROCORDEX [170]	Global	Historical and future, 80-250 years	10-300 km	Hr- Montly
Solar	Atlas	GSA [171], SolarGIS [172]	Global	Historical	90 m	0.5-1 hr
	Reanalysis	HelioClim-3 [173]	Global	Historical and real time	3 km	15 min - 1 hr
Wind	Reanalysis	NEWA [174], DOWA [175], RSE[176]	Regional (EU)	Historical, 11-30 years	1,5-3 km	0.5-1 hr
	Atlas	GWA [177]	Global	Historical average	50-200 m	N/A
	Reanalysis	WINDographer [178], Mesonet [179]	USA	Historical	3 km	Hourly

Observation: The observational approach entails the acquisition of empirical data from weather stations and measurement devices, providing invaluable insights into contemporary weather patterns, wind speed observations [166], and solar radiation measurements [165].

Reanalysis: The reanalysis methodology integrates numerical weather prediction models with observed datasets, yielding comprehensive datasets encompassing various meteorological parameters [152]. Examples include ERA5 [168] and MERRA2 [167], which serve as reputable sources for historical climate data assessment in wind resource studies, while similar data sources exist for solar energy assessments [173].

Climate models: Climate models from initiatives like the Climate Model Intercomparison Project (CMIP) and CORDEX simulate future climate conditions, facilitating the assessment of wind and solar resource variability in response to long-term climate changes ([169], [170]). These models are instrumental in understanding the potential impacts of climate change on renewable energy resources.

Atlas: Wind and solar atlases, exemplified by the New European Wind Atlas (NEWA) and the Global Wind Atlas (GWA), offer high-resolution spatial information regarding energy potentials in specified regions ([174], [177]). These atlases play a crucial role in renewable energy planning and development by providing detailed assessments of wind and solar resources.

Most of the database are made available at a Global level, even if one exception is found for New European Wind Atlas (NEWA) with a European focus. In terms of temporal coverage, Atlas are the most limited since they only provide historical average or single year data. For both Observation and Reanalysis, the timeframe is wider (from the 10 to the 70 past years). Finally, Climate models are the only ones capable of providing future projections, even if there are non-negligible errors in models forecasts [152]. The limitation inherent to databases, whether they are global or local in scope, is their inherent inability to accommodate site-specific factors that exert a discernible influence on energy potential. In regions characterized by intricate topographical features, such as fluctuations in elevation, surface orientation (including slope and aspect), and the presence of shadows, pronounced local gradients in energy distribution become manifest ([180], [181]). Consequently, it becomes imperative to employ models capable of incorporating local considerations into energy estimations. In this context, the availability of hourly time series at a microscale resolution (~ 1.5 km) made available by RSE represent a pivotal step, and this has motivated the selection of it as source for wind potential of this analysis. It is worth noting, however, that the sources of solar data under examination do not inherently furnish specific microscale considerations. Consequently, the utilization of comprehensive models becomes indispensable for accounting for these intricacies. Existing literature offers a variety of potential approaches. Notably, the "r.sun" algorithm, a development within the GRASS-GIS framework [182], stands out as a robust contender, as it calculates solar radiation at an hourly resolution when supplied with a Digital Elevation Model (DEM) corresponding to the target region. Additionally, ArcGIS [183] provides a Solar Radiation Toolbox [184], which operates in a similar fashion to r.sun and has undergone calibration and validation through international research endeavors [185]. The advantage of r.sun is the number of users it has already reached, and so, the number of calibration and validations this tool has undergone [186]. Therefore, for solar potential assessment, r.sun was selected, applying the methodology described in the work of Gasparovic et.al. [187].

Photovoltaic Potential Assessment

To assess the yearly potential conversion capacity of a photovoltaic (PV) power facility, denoted as AEP_{PV}, within a specific grid cell denoted as $'i'$ we employed Equation (1) [163]. This calculation hinges on both the available solar resources and the specifications of the solar modules in use. Additionally, we determined the capacity factor, CF_{PV}, for PV systems within grid cell $'i'$ using Equation (2) [163]. This factor signifies the actual electrical output that a PV power plant could generate at its designated location over a given time frame when compared to its theoretical maximum potential output, assuming uninterrupted operation. This capacity factor calculation considers technology-specific parameters and the accessibility of location-specific resources, thus enabling performance comparisons across different sites before the installation of PV systems.

$$AEP_{PV,i} = GHI_i * \eta_{PV} * PR * A_{PV,i} \quad (10)$$

$$CF_{PV,i} = \frac{AEP_{PV,i}}{P_{PV,rated} * T} \quad (11)$$

In equations (10) and (11):

- GHI_i represents the average global horizontal irradiation (kWh/m2/time).
- $A_{PV,i}$indicates the area within grid cell 'i' suitable for PV implementation (km2).
- η_{PV} represents the efficiency of the PV module in converting sunlight to electricity, with an assumed value of 21 % [163].
- PR denotes the performance ratio for the solar module, set at 0.85 [163]. This ratio accounts for the disparity between performance under standard test conditions and the actual system output, factoring in losses due to conduction and thermal effects.
- T signifies the total number of hours in a year, equivalent to 8760.
- $P_{PV,rated}$ represents the power density or of the solar PV system. For this study, we employed a value of 32 MW/km2 for a fixed-tilt utility-scale solar system using mono-crystalline silicon cells, which is the most common in actual market [188].

The GHI is derived from r.sun starting from a Digital Elevation Model (DEM) with a 10 m resolution. Subsequently, the original irradiance has been corrected for atmospheric attenuation based on the clear sky coefficient (k_{cs}) as in Equation (13) [163].

$$GHI' = GHI * k_{cs} \quad (12)$$

TEMOA time slices are categorized into seasons, each comprising day, night and peak periods. As there is no sunlight during the night, the capacity factor (CF) is uniformly assumed to be zero for all seasons. Consequently, our focus narrows down to determining the seasonal CF values for two distinct periods: day and peak. This entails computing eight capacity values. For each of these, we have applied Equations (1) and (2), substituting the term "GHI" with the solar radiation received during the validity period of the capacity factor and the term "T" with the hours specific to that period. Aggregated solar radiation for the specific “T” period is obtain starting from the hourly irradiance (W/m^2) and integrating all along the period T. A detailed explanation of this phase is provided in Appendix NN. Moreover, r.sun requires specifying a reference year on which the calculation is performed. Since the aim is to compare different lands under the same atmospheric conditions, yearly variability of solar irradiance is neglected, and 2020 values are assumed constant. Another remarkable hypothesis is related to the division between day and peak production. As specified above, within a season, a day might have various times of interest. For instance, the peak electrical load might occur midday in the summer, and a secondary peak might happen in the evening. This division should be accounted when evaluating the photovoltaic potential, since the mismatch between producibility potential and demand is one of the main problems with VRES [189].

Wind Potential Assessment

The RSE AEOLIAN Platform provides wind speed data at heights of 50. 75, 100. 125, and 150 meters above sea level [176]. These values correspond to the most representative hub heights for both onshore currently installed wind turbines and future potential installations on both land and at sea. As was done for solar potential calculation, the goal is to obtain capacity factor values for each time-slice of the model. This primarily involves translating hourly wind speed data into site-specific energy production. The site-specific energy production calculation is achieved by combining the historical time series (or probability density function) of wind speeds at the hub height of the wind turbine with the power curve of the specific wind turbine of interest, also expressed as a function of wind speed at the hub height. Theoretically, to calculate site-specific energy production, one should use many power curves and compute a representative average. However, due to difficulties in obtaining a representative set for data availability issues, the site-specific energy production analysis was conducted using a single wind turbine model for each hub height. We considered the three lower hub heights: 50. 75, and 100 meters asl, along with three commercially available wind turbine models accessible online. Table 20 provides the main characteristics of the three wind turbines used for the calculation at the considered hub heights:

Table 20. Main characteristics of the wind turbine models used for the producibility calculation. For each turbine, data are obtained by the online wind-turbine-model repository [190]

Reference [m]	WTG model	Nominal Power [MW]	Rotor Diameter [m]	Hub Height [m]
50 m	Riva Calzoni 500.54	0.5	54	50
75 m	Leitwind LTW90- 950	0.95	90	80
100 m	Vestas V117 3450	3,45	117	91
125m	NREL_6MW_RTW	6	128	119

Table 20 presents key specifications of WTG models at varying hub heights, ranging from 50 to 125 meters. Notably, it reveals the increasing nominal power and rotor diameter as hub height elevates, which is essential information for optimizing wind energy production at different altitudes. It also must be noticed that wind reference and hub heights differ. Therefore, there is an error introduced by the wind speed at the data level with respect to the real height at which the wind turbine is installed. Nevertheless, considering the power law at which wind speed variation is subjected [191], it has been checked (not shown) that the producibility errors is always below 5%. After obtaining hourly site-specific energy production at different heights, in line with TEMOA time-slices, the capacity factor for time-slice 'i' for turbine 't' was calculated as in Equation (13):

$$CF_{t,i} = \frac{PS}{P_{nomimal,t} * T} \quad (13)$$

where the term PS [MWh] represent the integral of the hourly production function during the time-slice temporal horizon T [h] of the turbine "t", characterized by $P_{nomimal,t}$ [MW].

Cost of land

The potential assessment phase determines the operational yield of the plant. Nevertheless, when seeking to differentiate various land types for capacity expansion plans, technical potential is not the only influencing parameter. According to International Renewable Energy Agency (IRENA) 2021 report [192], renewable installations levelized costs of electricity (LCOE) is mainly determined by: capacity factors, investments costs, operations & maintenance (O&M) and auxiliary costs. Since the purpose of spatially explicit energy planning is to consider geographic aspects capable of influencing ESOM outcomes [193], is necessary to identify which of the above-mentioned voices are spatial-dependent. For capacity factors, this aspect has already been addressed. Coming to costs, when faced with the decision between lands of equal potential, the cost of the land (by rent or acquisition) and the expenses associated with its connection to grid infrastructure become pivotal factors [192].

The cost of land is assumed to be equal to the agricultural land price. Agricultural land rents refer to the price of renting one hectare of agricultural land without buildings or plantations for one year. This data is derived from a Eurostat analysis [194] dated 2021 with a spatial scope of the whole European territory and a spatial resolution of country regions. The arable land prices for the Italian regions span from 0.0216 to 0.1714 M€/km^2. A significant variation is observed between the maximum and the minimum value, being the former around 10 times the latter. This is justified by the great diversity of the Italian territory. This choice is driven by the overarching methodological and demonstrative objectives of this analysis, which aims to illustrate the implications of the new land use module component. To achieve this, we have opted to utilize this range of land price values for the purpose of conducting a sensitivity analysis within the model. This approach is designed to assess, specifically within the context of our case study, the extent to which the additional components influence the outcomes of the model. For the cost of connection, there are some concerns that comes with its accounting. First, according to Italian Energy Transmission Authority (TERNA) [195], the specific point of connection (that determines the distance) is not known a priori, and strongly depend on design specific considerations. According to plant size and desired output voltage, the connection can be performed at a grid-level or at the primary cabin [195]. This introduces the first uncertainty in this cost estimation. Then, ESOMs generally do provide aggregated capacity for all the plants belonging to the same category [196], therefore it in not known how the aggregated capacity is discretized, with uncertainties also in the size term. Lastly, the detailed IRENA cost analysis of wind power technology [197] do not specify the distance from grid as a pivotal factor in determining the connection cost. Given the design-specific nature of grid connection costs and the challenges in estimating them accurately, we have chosen not to include them as a factor in our analysis.

2.2.3. Data aggregation

At this stage of the analysis, the data pertaining to wind potential, solar potential, and the costs are presented as rasters with varying spatial resolutions, rendering them incompatible with the structure of ESOMs [198]. Notably, the TEMOA model requires a data format that is not geospatially explicit. As any other traditional energy system optimization model, TEMOA present an aggregated description of the system, where the spatial features of technology (e.g., land occupied) and costs (land rent according to soil occupancy) is not present. Therefore, it is necessary to pass the information of having geographically dependent technological and terrain features, in such a way that it do not to make the model computationally intractable. The aggregation of data based on spatial attributes (e.g., location and location-dependent costs) and technological attributes (notably, spatially explicit capacity factors) [164] has been then addressed through a spatial and technological aggregation scheme, to transform the numerous rasters into interpretable inputs for the model. Spatial aggregation entails the amalgamation of contiguous regions with similar characteristics, thus reducing the spatial resolution and intricacy of the ESOM data. Simultaneously, technological aggregation involves the grouping of similar technologies, such as the consolidation of wind turbines with comparable time series data [164]. Within this framework, an established methodology, as presented by Stolten et al. [164], offers a structured workflow for transitioning from multiple variable renewable energy sources (VRES) data to a limited number of aggregated technologies, each associated with a respective land cluster, representing the total available land area suitable for the installation of the corresponding technology. This framework is shown in Figure 11, aim of this phase is to translate raw data (rasters or shapefile at different resolution) into model interpretable amount. This step can be further divided in two sub operations: The data aggregation and the model adaptation. In the technological aggregation phase, photovoltaic and wind technologies are categorized based on their capacity factors (CF) and cost characteristics. This categorization results in aggregated technology clusters, such as Agg_PV_X and Agg_WIND_Y, each with its own distinct capacity factor and associated cost. Spatial aggregation, on the other hand, condenses geographical information into discrete land clusters. Each cluster, represented by a land type such as Land X or Land Y, is defined by its area and the cost of land use. These spatial clusters form the basis for the physical constraints within the model, dictating the potential for technology deployment across different geographical areas. Finally, in the model adaptation phase, TEMOA original code is modified to account for land availability and for linking specific technologies at their belonging cluster

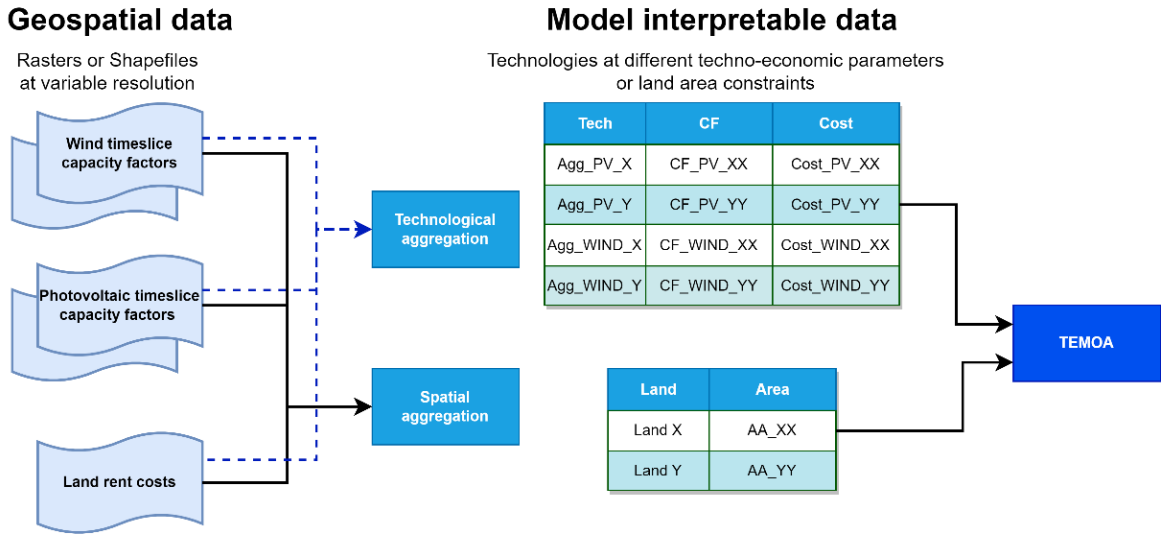

Figure 11. Workflow of the data aggregation phase, from raw data to TEMOA-Pantelleria characterization

In the aggregation of data into clusters characterized by analogous attributes [164] (in this case, costs, and renewable energy potential) a rigorous data handling approach, as well as the application of advanced statistical techniques, becomes imperative. Data aggregation necessitates meticulous data preparation. Notably, one significant challenge in data preparation arises from the divergence in spatial resolutions among the various datasets. Additionally, a critical issue emerges when attempting to overlay the different layers involved in the analysis – is the lack of correct intersection of boundaries between them. This issue, also named the partition problem [199], is created by the mismatched spatial resolutions and boundaries and presents a formidable hurdle in the aggregation process. To solve this issue, a uniform mesh is created, in which data at different resolution and intersection should be aggregated. The clustering of the geospatial cells among the selected attributes is performed with multiple algorithms, to determine which one show the best performance according to data structure The three tested algorithms are the HDBSCAN [200], The Kmeans [201] and the DBSCAN [202]. HDBSCAN, a hierarchical density-based algorithm, is adept at identifying clusters of varied density without the need for pre-specifying the number of clusters. Its approach is particularly suitable for geospatial data, which often exhibits heterogeneous density distributions due to the irregular spatial distribution of renewable energy resources. In contrast, Kmeans—simple and efficient—a centroid-based algorithm, meaning that objects in the data are clustered by being assigned to the nearest centroid. However, a major pitfall of K-Means is its lack of detecting outliers, or noisy data points, which leads them to be classified incorrectly. Furthermore, K-Means has an intrinsic preference for globular clusters and does not work very well on data comprised of arbitrarily shaped clusters. DBSCAN stands as a middle ground between the rigidity of Kmeans and the flexibility of HDBSCAN. By designating core points within high-density regions and expanding clusters from these cores, DBSCAN excels in discovering clusters with arbitrary shapes, an attribute of high value when dealing with spatially complex landscapes. Moreover, its ability to treat outliers as noise renders it less sensitive to anomalies, thereby enhancing the robustness of the clustering process. For the clustering algorithms

requiring the computation of the distance matrix, a spatial sampling procedure is performed [203] , clustering only the smallest subset of data. Then, nearest neighbor [204] method is used to predict the cluster affiliation for the non-sampled particles. The silhouette score [205]— ranging from -1 to 1— has been used as a quantitative measure of cluster cohesion and separation. A high silhouette score indicates a clustering configuration where inter-cluster distances are maximized and intra-cluster distances are minimized, reflecting distinct and well-separated clusters that are integral for spatial analysis. Complementarily, the computational time and memory usage are critical metrics for assessing the scalability of these methods. They provide insight into the algorithms' operational efficiency and practicality for large-scale applications, where rapid processing and memory management are essential

2.2.4. Case study: The Pantelleria Island

The Island of Pantelleria was selected as a case study, thanks to its properties of territorial diversity [206], the numerous data sources at regional [207] level. In Figure 12, the island of Pantelleria is shown, centrally positioned within the Strait of Sicily. Specifically, Pantelleria is situated at 36.785° latitude and 11.992° longitude, a geographical coordinate that underscores its pivotal location within the Strait of Sicily. This geographical circumstance yields meteorological conditions of paramount significance, rendering Pantelleria an exceptionally auspicious site for the harnessing of Variable Renewable Energy Sources (VRES). Pantelleria presents a consistently elevated level of solar radiation throughout the year, amounting to approximately 2000 kWh/m2. This abundance of solar irradiance is instrumental in the island's clean energy transition agenda, affording substantial potential for solar energy generation. Additionally, the island experiences a substantial and dependable prevalence of wind, predominantly originating from the northwest, with wind speeds averaging around 7 meters per second at an elevation of 25 meters above sea level. All these climatic factors, in conjunction

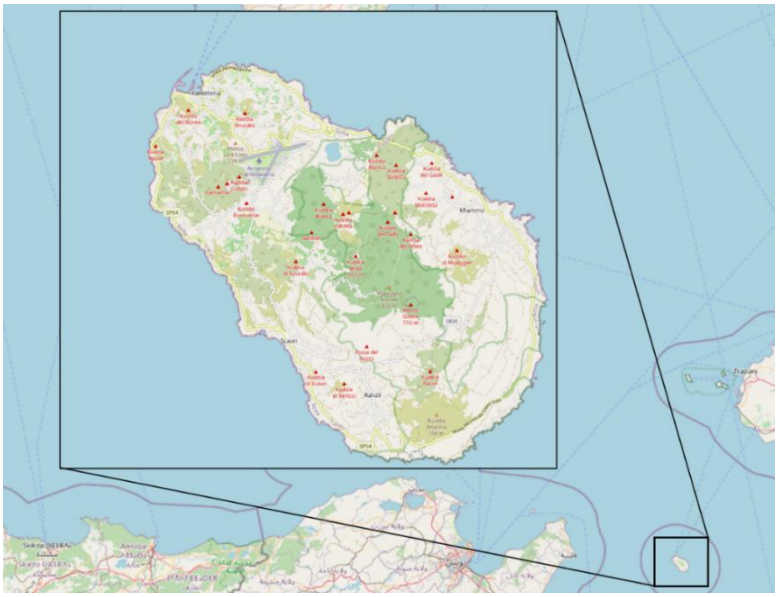

Figure 12. Visualization of the Pantelleria island and its placement in the Strait of Sicily

with the strategic location, pose Pantelleria at the forefront of sustainable energy exploration and underscores its critical role in advancing clean energy initiatives [206], making it as a compelling case study in the pursuit of land and energy sustainability. Concerning the modelling framework, the TEMOA-Pantelleria energy models is described in Appendix. Here, only the phases of the land and technological characterization are reported.

Land eligibility

The land eligibility assessment previously described has been applied to the Pantelleria Island. Administrative and habitat constraints, predominantly driven by natural preservation objectives, are derived from Natura 2000 [162] and the World Database of Protected Areas (WDPA) [155]. Natura 2000 serves as the principal instrument of European Union policy for biodiversity conservation, while WDPA stands as the most exhaustive global database encompassing marine and terrestrial protected areas. Lastly, for anthropic limitations, data are extracted from OpenStreetMap (OSM) [156], an open-access global database characterized by public participation during data collection. In Figure 13 the different limitation categories, for both wind and photovoltaic technologies, are reported. For the solar resource, its land availability is mainly eroded by anthropic and environmental limitations (~ 15 % and ~31% of unavailable land respectively), while there is no specific constraint due to natural habitat and historical heritage.

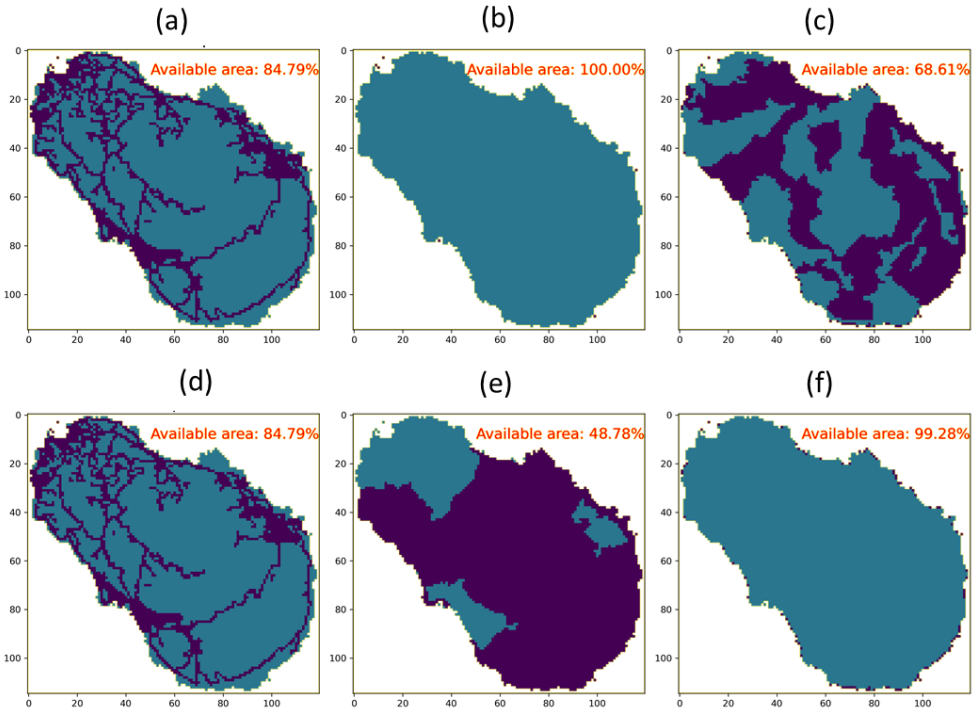

Figure 13. Land Eligibility analysis for the Pantelleria Island. (a),(b) and (c) represent the constraint for photovoltaic installations while (d) ,(e) and (f) are the ones for wind. (a), (d) are anthropic exclusion. (b) and (e) are constraints due to natural habitat and landscape heritage laws. (c) and (f) represent limitation associated to environmental reasons.

Considering overlapping of categories, the final available area results in ~ 35 %. Differently, for wind, the main limitations are the habitat one (~ 51 % of land made unavailable due to Natura 2000 [162]) and again, the anthropic one. This result in an overall ~10% of available land.

Potential assessment

As previously described, the energy yield of both solar and wind technologies is calculated at a particle level for all the island territory and then aggregated. Following the same order of the methodology, seasonal daily and peak capacity factors under the assumption before described are reported in Figure 14.

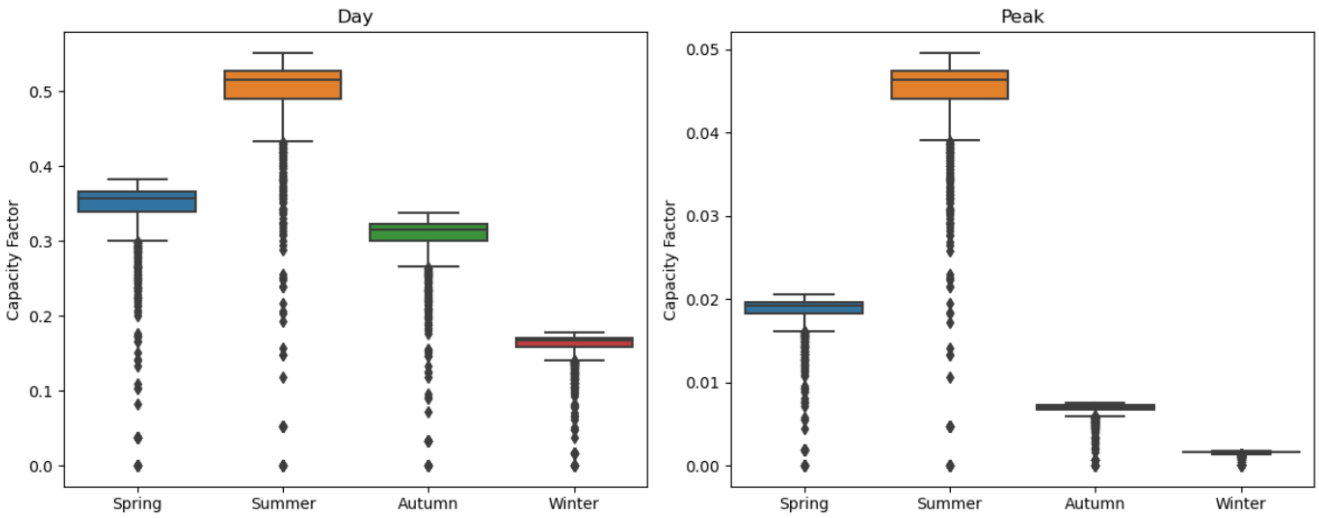

Figure 14. Photovoltaic Capacity factor by season, Day and Peak time slices

The presented box plots reveal that Spring and Summer exhibit higher median capacity factors compared to Autumn and Winter, indicative of a stronger solar potential during these warmer seasons (36 % and 52% with respect to 31% and 17%). These periods also display broader capacity factor ranges, likely influenced by intermittent cloud cover or variations in solar incidence angles. Notably, Summer stands out with occasional exceptionally high-capacity factors, attributed to optimal sun angles and longer daylight hours. In contrast, the Winter season demonstrates a compact interquartile range (IQR) and lower median, reflective of shorter days and lower sun angles. Lower-end outliers in Winter may indicate days with minimal solar irradiance due to adverse weather conditions. The "Peak" period capacity factors also follow a seasonal trend, with Spring and Summer consistently outperforming Autumn and Winter. However, "Peak" distributions are narrower across all seasons compared to "Day" distributions, highlighting the reduced susceptibility of peak sunlight hours to diurnal and weather-induced fluctuations.

For wind, the same analysis is carried out, and the results of this process are shown in Figure 14. In this figure, two different kinds of pattern are observable. The analysis reveals distinct seasonal and daily patterns in wind turbine capacity factors. Across all turbine heights, winter consistently displays approximately 20-25% higher capacity factors compared to summer, notably

pronounced during nighttime slices. In comparison to summer, autumn showcases marginally elevated capacity factors, approximately 10-15% higher, especially evident during day and night periods. The impact of turbine height is observable with a consistent increase in capacity factors across all seasons, with higher heights indicating approximately 15-20% better performance. Moreover, the variability within each season and time slice remains relatively consistent, with night periods displaying notably wider ranges than day. Outliers, though sporadic, suggest instances of extreme deviations in capacity factors.

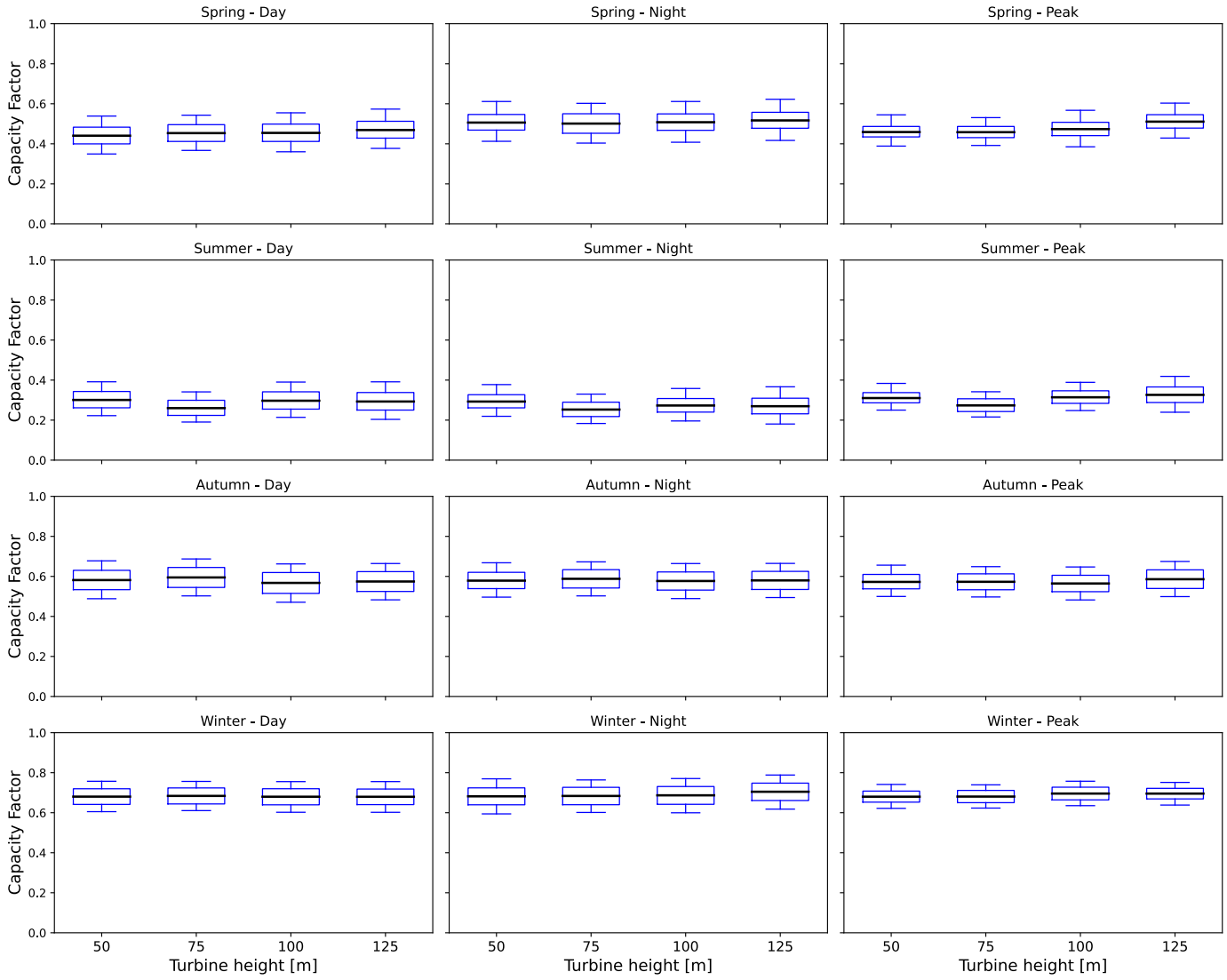

Figure 15. Wind capacity factor by timeslice and height. Average value, standard deviation, minimun and maximum values.

Then, following the methodological steps, Pantelleria energy data are aggregated into clusters following different techniques and evaluating the best one. As appreciable in Table 21, Kmeans and DBSCAN outperform HDBSCAN in terms of silhouette score and memory usage, with Kmeans standing out as the best one in all the three metrics under analysis.

Table 21. Performance of the three different clusterign algorithms

Method	Silhouette Score	Time (seconds)	Memory (MB)
HDBSCAN	0.527	1,729	2,246
Kmeans	0.827	0.369	0.224
DBSCAN	0.807	2,940	0.810

The outstanding performance of k-means can be justified by the absence of outliers. Indeed, for both cost and renewable energy potential, the minimum value is zero where no installation is possible, and maximum values are constrained in a very similar range for all the data. (There is no drastic resource variability along the Pantelleria Island). Therefore, also considering the possibility of selecting clusters a-priori, Kmeans is selected for this analysis. Moreover, the underlying hypothesis of the Kmeans, that data must be globular and isotropic, is verified considering the high value of the silhouette score. Considering Figure 16is appreciable how HDBSCAN and DBSCAN are more flexible in terms of cluster shapes, which is evident from the varied shapes and sizes of clusters. KMeans, on the other hand, assumes the clusters are spherical, leading to more uniform and rounded clusters. In term of noise, HDBSCAN and DBSCAN can identify outliers inserting them in the (-1) cluster, even if very few elements are present in this category (checked, not shown). The final number of clusters is another pivotal parameter in this analysis. In Kmeans it is imposed at 5, while the other methods reach 11 (HDBSCAN) and 17 (DBSCAN) clusters. In this case, especially for DBSCAN, the clusters are very fragmented and some of them appear to contain few elements. In conclusion, since the aim is to identify macro-areas characterized by similar energy properties and to have a method as scalable as possible, the Kmeans still guarantee the best outcome. The refinement of geospatial data through clustering algorithms has yielded a comprehensive set of land and technological clusters, each distinctly characterized by both spatial and technological attributes. These clusters are delineated not only by their physical geography—encapsulated by land area and associated rental costs—but also by technological potential, specified through capacity factors for feasible renewable technologies like wind and photovoltaic systems.

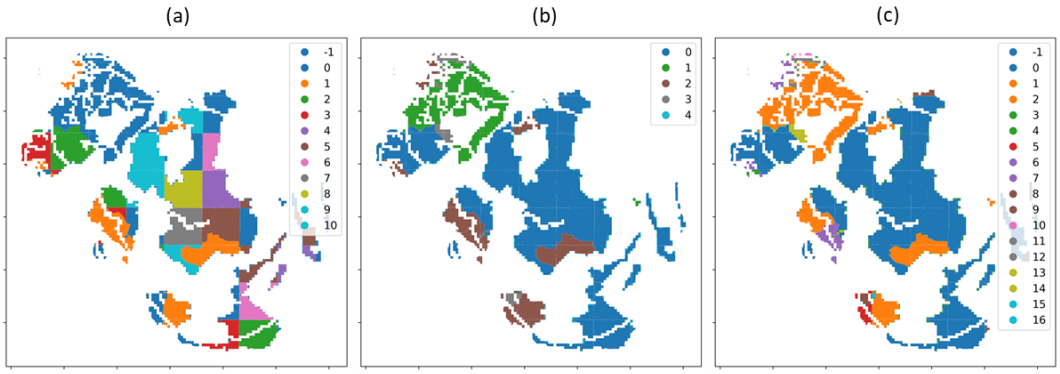

Figure 16. Results of clustering with different algorithms. (a) HDBSCAN (b) K-Means and (c) DBSCAN

The abovementioned process generates a technological characterization that differs from the original one presented in the Appendix, because it's no more relying on average data rather than site-specific data aggregated following a procedure that preserve the differences.

Therefore, this originates two model configuration that will be tested: an average parameter one and a site-specific parameter one. In Figure 17 those cluster discretized capacity factors are reported and compared with the average ones, to highlight the improvements brought by the cluster analysis carried out. In the land cluster description, the available area and the installable technologies on the cluster are highlighted (Table 22).

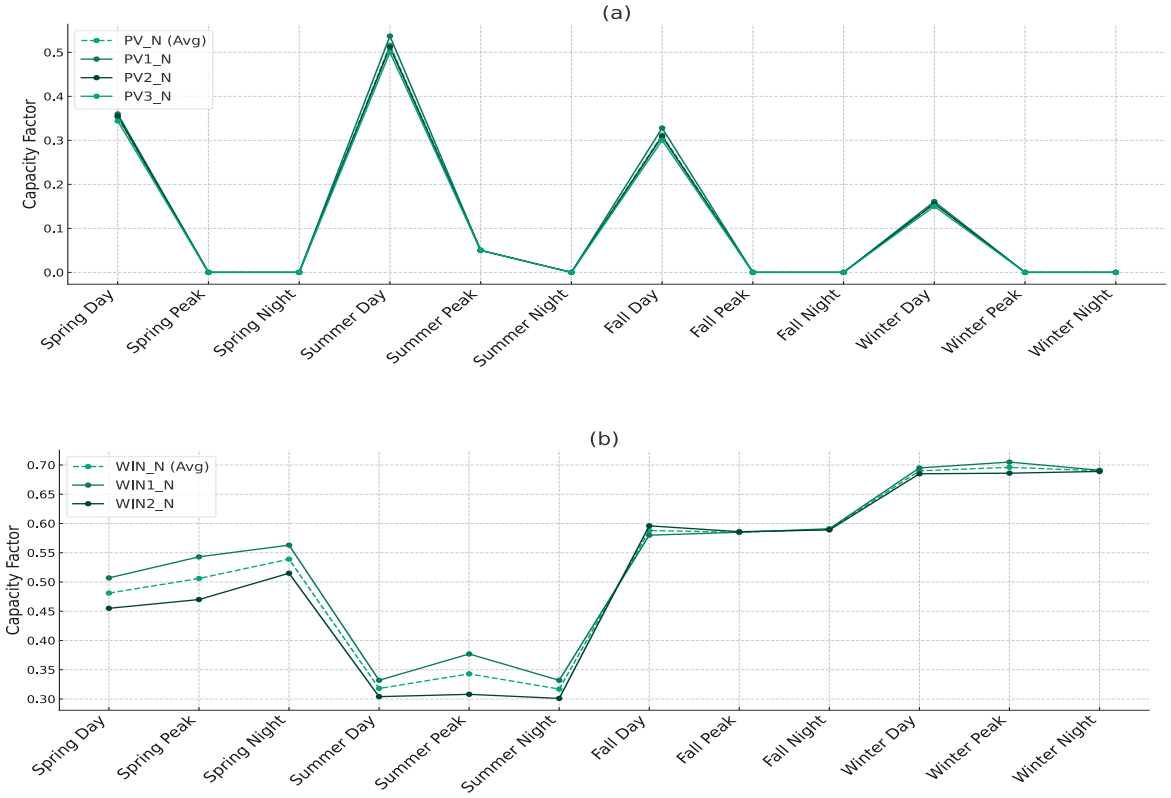

Figure 17. Traditional average (a) and cluster discretized (b) TEMOA Pantelleria VRES characterization, time slice capacity factors

As mentioned above, the limitations for the installation of specific technologies on certain clusters and the land price accounting in the objective function are present only in the TEMOA-Pantelleria land explicit configuration. Discretizing technologies based on their spatio-temporal attributes bring non-negligible advantages in terms of technological options for the model, which may cause a lower total cost of the system. Considering the relative difference between the old and the new technologies, is possible to observe values around 10% (Summer and Spring wind peak). Therefore, according to the sign of the difference, the model overestimate/underestimate the installed capacity of the same amount. Strongly influencing the cost.

Table 22. Cluster characterization

Land Cluster	Available area [km^2]	Installable technologies
LC_1	2,850	PV2_N
LC_2	0.457	WIN1_N, PV_1
LC_3	4,909	PV_1
LC_4	1,947	PV_ 3, WIN2_N

2.2.5. Model Integration

After the data aggregation procedure, a reduced set of land and technological items is made available for model integration. Each cluster (or item) is characterized by land attributes (the area of the cluster and the land rent cost) and technological attributes (the capacity factors for the different technologies installable on that land). Therefore, for each cluster, a corresponding land item (characterized by an area) exists, as well as a set of wind and PV technologies with specific capacity factors and costs, that can be installed only on that cluster. In this context, there are two optimization goals. The first is to install the renewable energy technologies on the "best" cluster, where "best" denotes the cluster identified by the ESOM following the least cost optimization. The second is to have a renewable energy installation development compatible with land limitations of the Pantelleria island. Therefore, the ESOM must be capable of using the inputs of the clustering phase (technological parameters for renewables, land price and area for land clusters) to determine the optimal deployment of technologies across different land clusters. To achieve this goal, is necessary to bring some modification to the TEMOA code:

- **Insert in TEMOA a new set that describe the land resource.** Traditional ESOM elements (mainly process and commodities) do not allow for a proper land representation. Indeed, it would be wrong to model the land consumed by plants installation as a commodity or a technology, for two main reasons. First, a commodity is something that is exchanged between processes as input or output. Here, the role of land is to host its associated technology (at certain conditions of capacity factor and cost) for the lifetime of this last. Second, the commodity consumption is related to the activity of a plant, passing through its efficiency (e.g., natural gas consumption proportional to combined cycle plant activity. In this case, land is consumed when new capacity is installed and becomes available as soon as the installed technology on that land dies. As depicted in Equation(14) and (15), the new TEMOA set is called $Land\ Cluster$ for which a $Land\ Area_l$ value is associated, describing the available area for the land cluster *"l"*.

$$Set = Land\ Cluster\ (LC) \tag{14}$$

$$Attribute = Land\ Cluster_l \tag{15}$$

- **Insert in the model a new parameter and new constraint, linking the capacity installation to land consumption.** Indeed, as shown in Equation *(16)*, the Land Use Intensity (LUI) parameter acts as a critical bridge linking the land clusters "LC_i" with the applicable technologies *"j"*. It quantifies the amount of land required for the installation of a unit of technology (e.g., megawatt of wind or solar power). The LUI parameter ensures that the

model's solutions are not just economically optimized but also spatially feasible. If an LUI is not defined for a specific technology within a given land cluster, it implies that the technology cannot be installed in that cluster, thereby introducing a direct spatial constraint into the optimization process.

$$LandArea_{LC_i} \geq \sum_{j=1}^{n} Capacity_{T_j} * LUI_{i,j} \quad (16)$$

According to the TEMOA optimization module, thanks to Equation *(16)* the model has several opportunities to consume land area to install photovoltaic or wind plants, but the convenience is determined by the capacity factor of the process. Therefore, TEMOA will first select the best technology, and then consume the area of the cluster associated to that technology, and this is made possible by the introduction of the LUI parameter. In this way, the useful output will be both the capacity installed and the geographical location of the plant, at least in terms of land cluster. The number of clusters determines the precision of that information.

2.3. Results

This section presents a comparative analysis of energy scenarios derived from two modeling approaches: one integrating the advanced land feature considerations previously described, and a conventional one. The objective is to test the hypotheses stated before about the advantages of spatially explicit energy planning.

Energy scenarios, referring to optimized technological mix in terms of activity and capacity, then generating emissions and costs, are here discussed. Since objective is to test how the land use module changes model outcome, the results are proposed for the two different model configurations. The land explicit one is tested with a parametric analysis on the land price, making this last vary between the minimum and the maximum possible values. Due to the power sector focused approach of this work, the main outcomes presented are the electricity generation (capacity and activity, Figure 18), the relative energy system cost differences and the land consumption for the land explicit modelling instance. Starting from the power sector configuration, in Figure 18 the capacity (MW) and the electricity generation (GWh) are presented. In all the configurations, differences in the outcomes are appreciable both in terms of absolute and relative amounts. Indeed, the scenarios differs for the total installed capacity and the generated electricity, but also in the way these amounts are obtained. First, it can be easily noticed (and confirmed by subsequent data analysis, not shown) that the traditional model and the low land price configuration do not present any differences, as expected, while the high land price instance has significative differences with respect to the previous two. This is symptom of a threshold phenomenon that change model outcomes under a certain land price value. Going into detail, the traditional TEMOA-Pantelleria (Figure 18 (a), (b)) and the low

land price instances (Figure 18 (c), (d)) present a higher installed capacity with respect to the intermediate and high land price configurations (Figure 18 (e) - (h)). In the first two cases, the capacity of energy technologies starts at just under 2 MW in 2020 and shows a more than threefold increase to approximately 7 MW by 2050. The technology mix remains relatively stable, with wind technologies dominating the share, followed by solar and biomass, this last mostly covering the base-load needs. Considering the activity, its level starts at around 15 GWh in 2020. increasing to nearly 23 GWh by 2050. This increase is justified by the increased electrification (mainly in the transport sector) caused by the decarbonization constraints at which the Island is subjected. The proportions of each technology within the activity profile change slightly over time, with "WIN1_N" gaining a larger share, indicative of not only increased capacity but also high utilization rates. The most valuable outcomes visible from Figure 18 are related to the differences in the photovoltaic installations and the overall power production between the two previously described configurations.

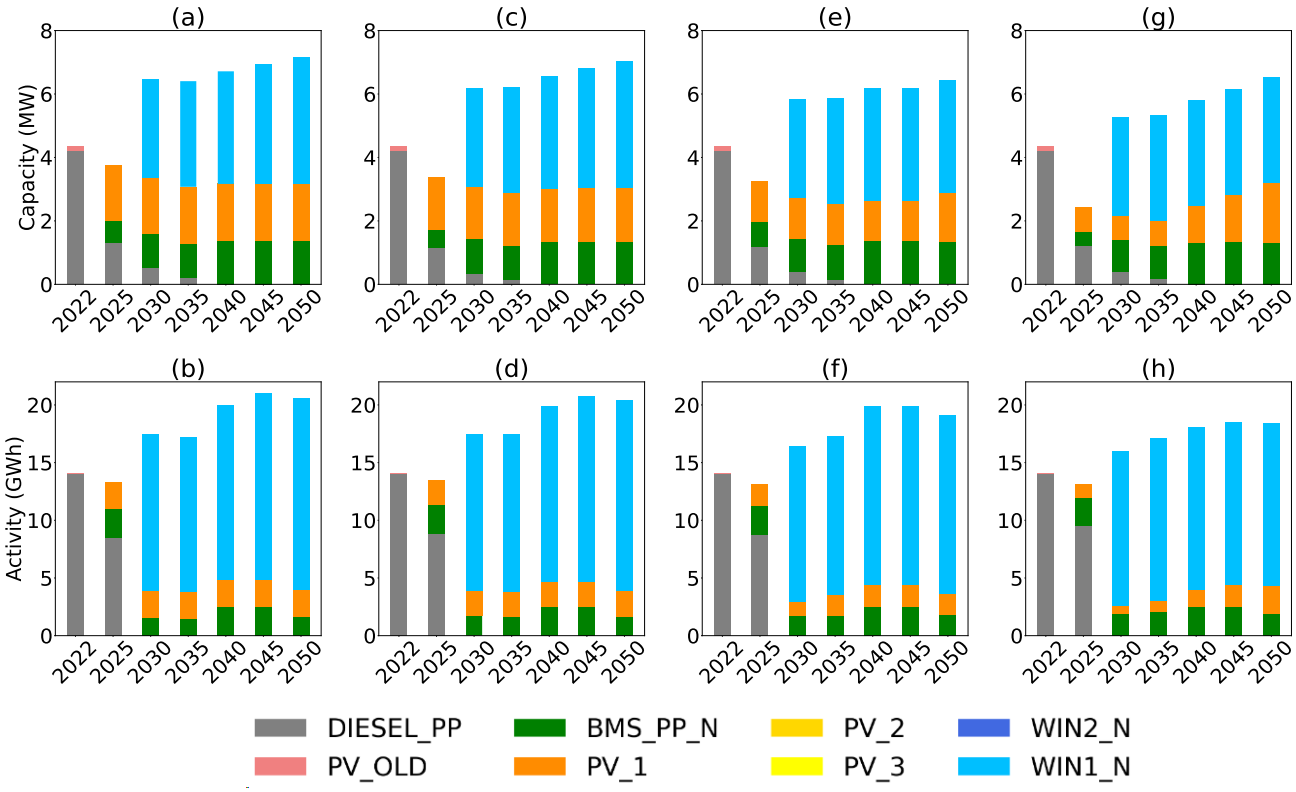

Figure 18. Power sector capacity and activity for traditional modelling instance and land specific modeling isntance . . Subplot (a) - (b) represents the traditional TEMOA modeling instance, while (c)-(d) the land explicit one in the low land price case, (e)-(f) the intermediate price case and (g)-(h) the highest price case.

In both the zero (or low) and in the high land price configurations, there is a growth in capacity over time, but the technology preferences differ. In the low/null land price case (a)/(c), there is a major reliance on solar technology (PV_1, the highest performing one), which suggests that larger, more land-intensive solar projects are feasible and economically viable due to lower land costs. Conversely, with a higher land price (e), there is a marked preference for wind systems, indicative of a strategy to maximize energy yield per unit of land area. In particular, the total difference in 2050 is of 1,2 MW of installed capacity and around 2.2 GWh

of electricity produced. With this consumption gap mainly driven by commercial and residential sectors. It must be specified that, in all the cases, the limitation caused by the land use constraint of Equation (*16*) is not influencing the model outcome. This happens because the necessary capacity for the Pantelleria power sector is not occupying any land cluster at its maximum. Indeed, the model select the highest performing technologies (WIN1_N, PV1_N) considering area the limitation of the cluster these are installed in. This consideration is supported by Figure 19, which highlights the land cluster occupation, and the land price costs in the two-model configuration. In Figure 19 (a) the difference in land occupation by cluster in the two model configurations are shown. In both cases, the land cluster "LC_3" is the most consumed due to the installation of the solar technology "PV1_N", reaching a maximum occupation of ~10% in low price and ~6% in low price in 2040. Even if the LC_3 is the one with the highest absolute occupation, the LC_2, due to its limited extension, is the one reaching the highest percentage of occupation. Indeed at 2040. due to the installation of WIN1_N, the LC_2 is occupied at 26% in both the configurations. These considerations are reflected in the cost, that notably show higher values for the high price configuration. In this configuration, land rent price start from 0.026 M€ at 2025, increasing and stabilizing around 0.07 M€ from 2040 to the last year. In the low-price instance, these costs are much lower, reaching a maximum of 0.014 M€ at 2040.

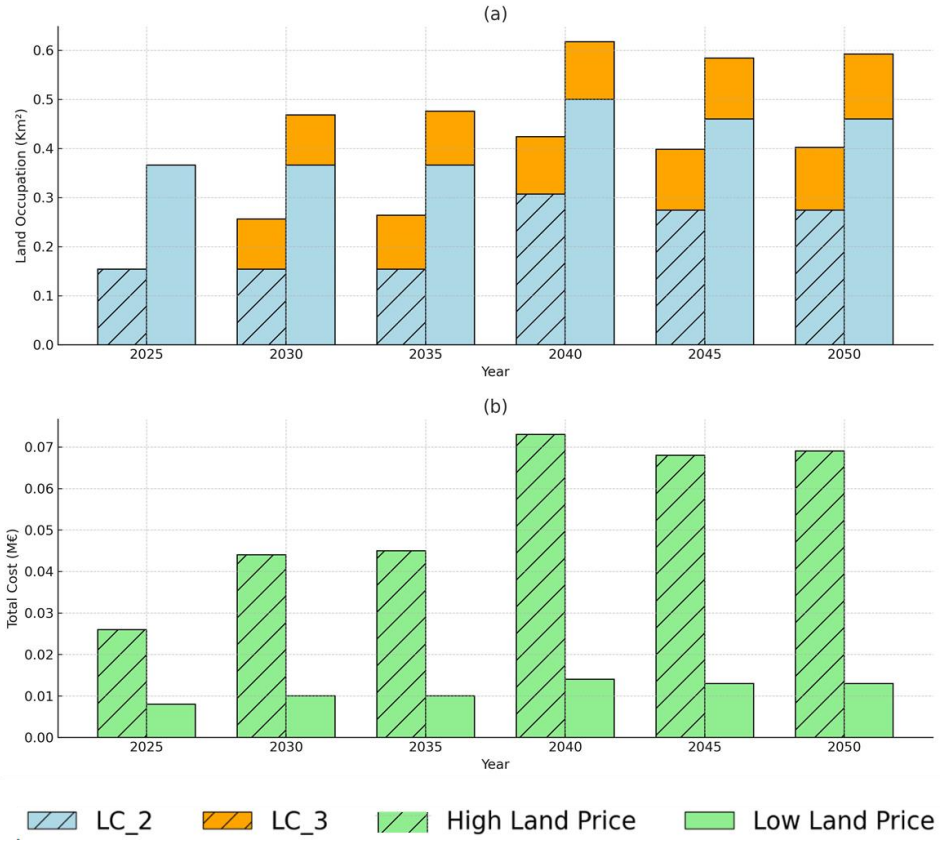

Figure 19. Land occupation (a) and Total cost for land rent (b) in the highest (dashed) and lowes land price scenarios

Approach 3– A Framework for AFOLU integration in ESOMs

3.1. Introduction

In the previous chapter, land use has been identified has e key-element both in influencing ex-post results analysis and in altering modelling outcome. Nevertheless, it's integration in energy modelling framework has always been scarce and limited to accounting for it's energy contribution, not accounting for the several implications this sector can have in mitigation pathways. Therefore, this section proposes a detailed modelling approach to the AFOLU sector and an evaluation of the economic, energy and environmental trade-offs caused by the presence of the sector. To demonstrate the usefulness, scalability and ease of use of the proposed solution, two different models' integrations are proposed. The former relies on the TIMES modelling framework and is applied to Sweden, while the latter uses TEMOA, and it's applied in Italy. Even if the two still rely on the same methodology, the application involves two different (but similar in nature) modelling frameworks and two European case studies which stands add the odds of the European borders. Sweden, characterized by cold climate, high presence of forest and small population and Italy, which has high population stressors and reduced forest coverage. Even the purpose of the analysis is different. The Swedish is more focused on the effects of climate change and the different hypothesis related to the AFOLU model. While the second, the Italian one, is more related to understand the policy perspective and possible energy implication of the AFOLU models. The general methodology is described below, then it follows the detailed description on Swedish and Italian case study respectively.

3.2. Methodology

Here, it follows a logical description of the integration of AFOLU into the ESOMs, together with the data requirements and technical assumptions made to facilitate the modelling. Next, the techno-economic representation of the AFOLU sector as well as the steps necessary to create a national modelling instance are detailed.

3.2.1. Model structure

The representation of the AFOLU sector in the model adopts a flow-based approach, consistent with the ESOMs framework. In this approach, the technical and economic attributes are standardized, ensuring a consistent classification of commodities, processes, and flows across the new AFOLU and the existing TIMES sectors. The conceptual structure of the agriculture module is illustrated in the flowchart shown in Figure 2. The complexity of the AFOLU system has been modelled in a simplified manner, focusing on three key elements: (1) its supply-side commodities, (2) its technological component and (3) its service demands, which include the required outputs for livestock, crops, forests, and pasture sectors. In this framework, the energy sector meets the energy needs of agriculture, while agriculture itself holds the potential to supply bioenergy commodities back to the energy sector.

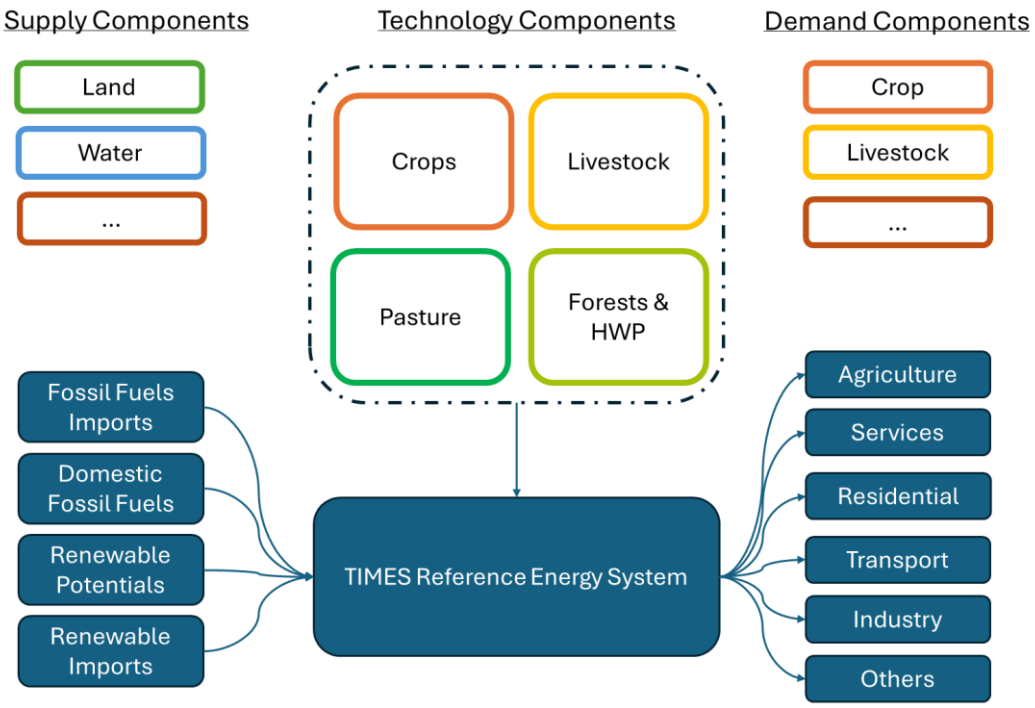

Figure 20. AFOLU sector and its interaction with TIMES

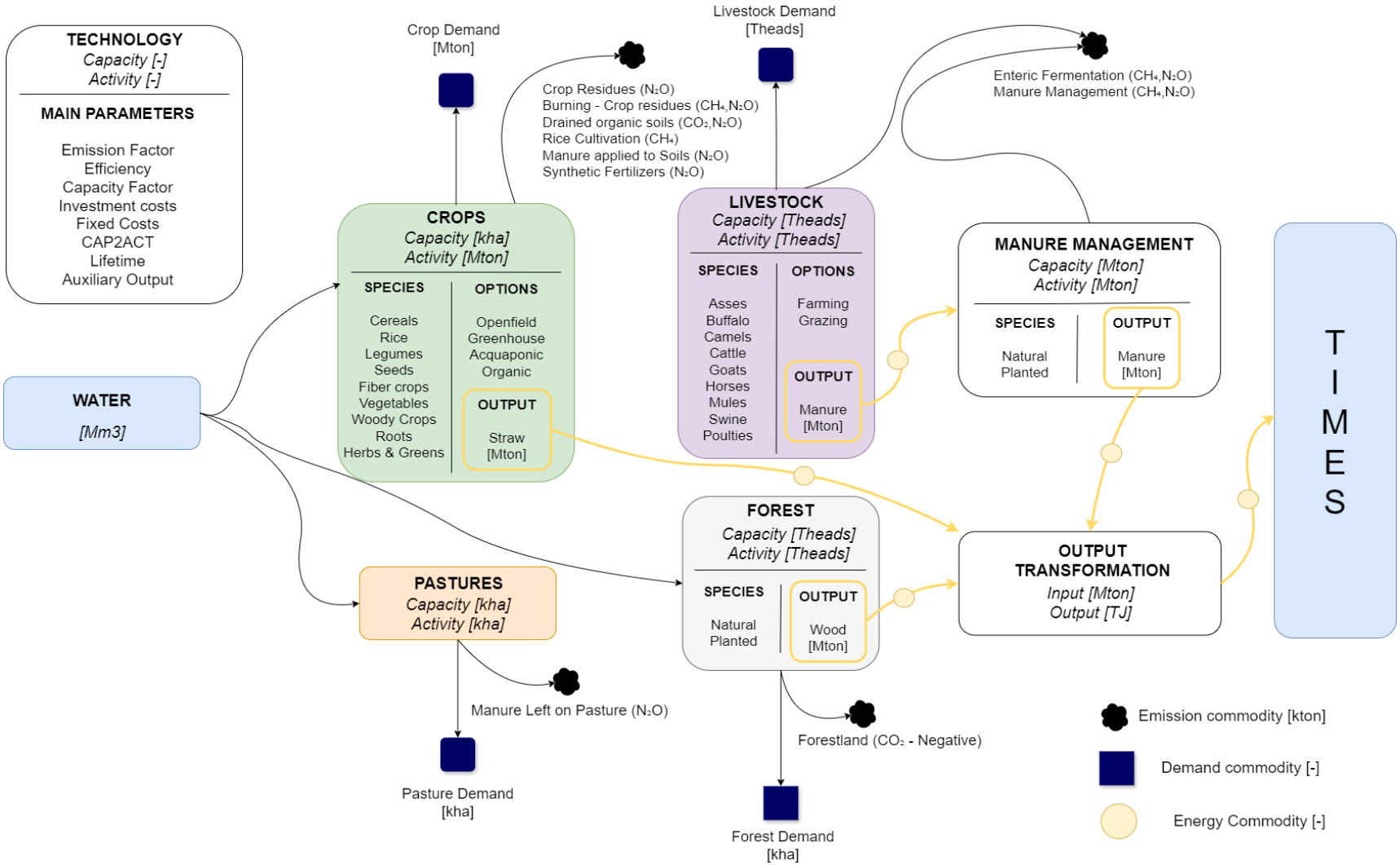

Figure 21. AFOLU Reference Energy System (RES) illustrating the flow of primary commodities (land, water) through transformation processes (e.g., livestock, manure management, crop production, and forestry) to final commodities (energy carriers, food, and materials). Key pathways include resource allocation, species-specific options, and GHG emissions accounting for CO_2, CH_4, and N_2O.

Its Reference Energy System can be conceptualized as a series of interconnected building blocks. The primary commodities layer encompasses resources extracted from natural systems, categorized as water mining that can serve different subsectors. Cropland supports the cultivation of diverse crop types, including cereals, rice, legumes, vegetables, and woody crops, employing various farming systems such as open-field agriculture, organic methods, greenhouse cultivation, and aquaponics. Livestock systems, supported by water resources, accommodate multiple species, from cattle and sheep to poultry, with outputs ranging from animal products (to demand side) to manure (to energy system). Pastureland facilitates both natural regeneration and managed grazing systems, while forestland provides timber, harvested wood products (HWPs), and contributes to ecosystem services like carbon sequestration. Additionally, organic residues, such as straw, and wood byproducts, can be redirected into energy production systems, such as anaerobic digesters and biomass plants, supporting circularity and resource efficiency. The final commodities layer illustrates the outputs that meet societal demands, including food (crops, livestock), fiber (forests, HWPs), and pasture-based resources. These are complemented by environmental outputs, particularly emissions. The framework tracks emissions across multiple processes, including livestock-related sources (manure management, enteric fermentation), cropland activities (fertilizer use, manure application), and forestry (carbon stock changes). By explicitly linking emissions, water and land use to production systems, the model enables the assessment of trade-offs between productivity and environmental impacts. The basis of all the AFOLU module lies in its process definition, represented as systems transforming natural resource inputs into outputs while generating emissions. Figure 22 illustrates the general structure of processes in the AFOLU module. Processes in this system consume natural resources, such as water, as a key input. But the way land and water consumption is accounted differs. Land is measured in thousands of hectares (kha) and represent the capacity of the land consuming technologies, while water is measured in million cubic meters (Mm^3) and is defined as a commodity. Each process is defined by two key parameters: its capacity-to-activity ratio (CAP2ACT), which links the available capacity to its maximum possible activity, and its efficiency (EFF), which measures how effectively inputs are converted into outputs. For crops, the capacity is expressed in terms of cultivated land (kha), and production is measured in tons. The CAP2ACT is used to connect these two quantities and represents the crop yield. For livestock, forests, and pastures, where capacity and activity are directly related, the CAP2ACT is simply set to 1. Efficiency is used to estimate water consumption. Emissions of CO_2, CH_4, and N_2O are calculated based on the activity of each process.

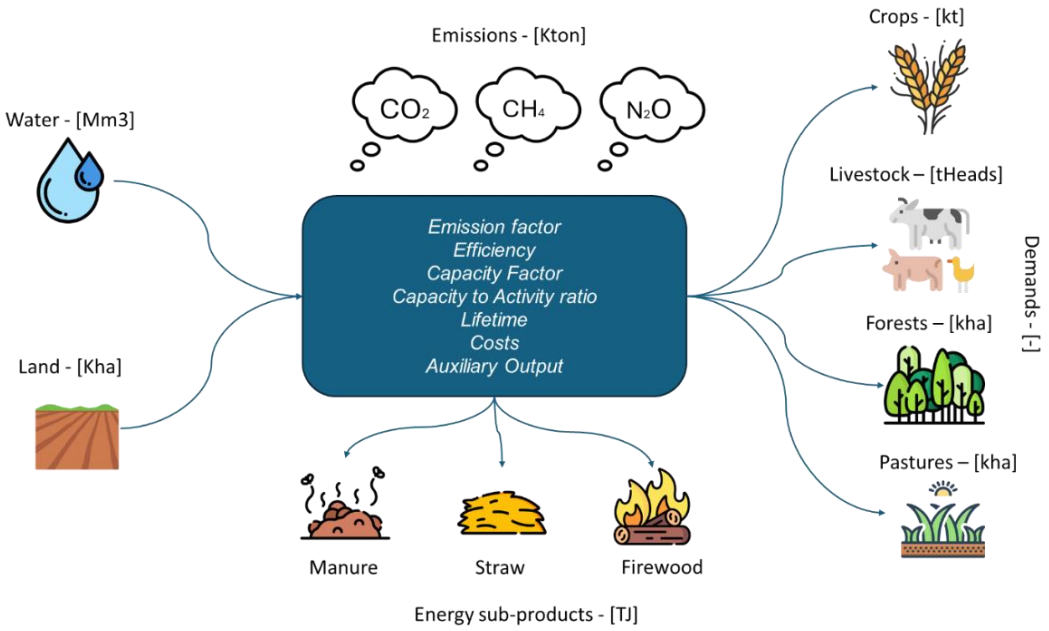

Figure 22. Generic AFOLU process

For crops, emissions are first distributed over the cultivated area and then related to production using yield data. Similarly, for livestock, forests, and pastures, emissions are calculated following specific steps based on available data. Process outputs are divided into two categories. The first includes main products, such as crop yields, livestock products, and forest goods, which satisfy specific demands. The second category includes byproducts like straw, manure, or wood, which have additional uses, such as serving as secondary resources in the energy system. Two types of processes are considered: those reflecting current practices (base-year processes) and alternative processes aimed at reducing emissions. Base-year processes are cost-free and modelled to reflect historical trends. Alternative processes, on the other hand, include data on investment, operation, and maintenance costs, as well as differences in resource use and emissions. Mitigation options for crops and livestock focus on reducing emissions, for example, by adopting different farming technologies or organic practices that eliminate the use of fertilizers. Forests, by their nature, act as a mitigation option by offsetting emissions from other sectors.

Demand components

As for all the ESOMs sectors, the AFOLU sector is driven by exogenous demands specified by a list of sectoral demands, actual values in the base year (calibration), and values for all milestone years (projections). In the proposed version of the model, as illustrated in Table 23, there are 13 demands for livestock,9 for crops, a generic one for pasture and forest area, and 4 different demands for forest byproducts.

Table 23 - Demand components

Sector	Process	Unit
Livestock	Asses Camels Cattle, dairy Cattle, non-dairy Goats Horses Mules and hinnies Sheep Buffalo Swine, breeding Swine, market Llamas Poultry	thousand - heads
Crops	Cereals Legumes Seeds Fiber crops Vegetables Roots Herbs and greens Woody crops Rice	kilo-tons
Pastures	Pasture	kilo-hectares
Forest	Generic Forest Sawn wood Other Industrial Roundwood Wood Panels Pulp and Paperboard	kilo-hectares tons

Supply component

Supply component are the demand technologies. As detailed in Figure 21 they belong to four categories. Livestock, Crops, Pasture and Forest, the same as the demand ones. Their description is reported here below considering their relevance in the overall emission balance.

Livestock

Livestock are the highest emissive sources in the AFOLU sector [208], specifically for their enteric fermentation and manure management (CH_4 and N_2O) emissive components. Moreover, there is increasing importance in the abatement option for this sector, especially the manure management emissions ones, which deserve a particular section in this chapter. For each

modelling instance, livestock must be characterized in terms of capacity and activity, emissions, and resource flow efficiencies, both as primary commodities input and final demands. For each nation and year, the data required to correctly model the livestock sector are reported in Table 24. Division is made by type of data and unit of measurement.

Table 24 - Data entry for livestock sector

Data	Unit of Measurement
Stocks	[An] - animals
Enteric fermentation by species (Emissions CH4)	[Kton]
Manure management by species (Emissions CH4)	[Kton]
Manure management by species (Emissions N2O)	[Kton]
Water requirements	[Mm3]

The data from FAOSTAT, both for stocks and total emissions, is given by species. To switch from total emissions as provided by FAO to an emission factor (as ESOM process requires) the overall emissions for each GHG are equally divided by livestock population. Therefore, for each GHG and for each livestock, the emission factor is derived as in Equation (21):

$$\mathrm{EF}_{\mathrm{livestock,nation,GHG_i}} = \frac{Total\ Emissions_{species,nation,GHG_i}\ [tons\ of\ GHG_i]}{population_{species,nation}\ [Heads]} \tag{17}$$

Similarly, the process must be repeated for water, to link the general water use data to the single livestock. Indeed, for each livestock, knowing its population, the total water consumption, and the water consumption factors from literature, the water consumption by species can be calculated in this way: First, estimated water consumption (EWC) calculated by multiplying water consumption factors (WCF) from literature, which are already contained in the model, but that can be changed, and the number of animals.

$$\mathrm{EWC}_{\mathrm{livestock,nation,GHG_i}} = WCF_{species}\left[\frac{liters}{Heads * year}\right] * population_{species,nation}\ [Heads] \tag{18}$$

Then, a calibration is performed between the estimated data and the total real water consumption by livestock, to provide accurate adjusted water consumption (AWC):

$$\mathrm{AWC}_{\mathrm{livestock,nation,GHG_i}} = \left[\frac{WCF_{species}\ \left[\frac{liters}{Heads * year}\right]}{Total\ WC_{estimated}\ [liters]}\right] * \left[\frac{Total\ WC_{real}}{population_{species,nation}\ [Heads]}\right] \quad (19)$$

The AWC, expressed as water consumed by unit of output, is imposed in the model as the process efficiency, creating a link between the input commodity (water) and the output one (livestock demand). Nevertheless, the livestock modelling goes beyond this since livestock also requires natural resources, particularly crops and other feeding materials, to meet their nutritional needs. In turn, livestock generate by-products such as manure, which can be utilized for biogas production within energy systems. The key distinction between livestock and other agricultural sub-sectors lies in the direct demand livestock impose on both crop production and pastureland, as they consume crops and graze on pastures. From a modelling perspective, this interaction should be represented as stocks of crops and pastureland supporting both farming and grazing livestock, which would result in indirect land use in both sectors. In TIMES, there should be intermediate technologies that transform crop and pasture sectoral output to livestock commodities. However, this interaction is only partially modelled, by linking the capacity of grassland to the one of the grazing livestock, imposing that they grow together. The crop dependencies, instead, is not accounted.

This omission stems from the underlying assumption that a portion of crop demand is allocated not for human consumption but for livestock feed. Since the model's primary objective is to account for emissions, water usage, and land use, it simplifies this relationship by embedding the indirect livestock component within the crop sector. This approach avoids creating additional interconnections that would complicate the model structure and increase data requirements. The drawback of this assumption is that it limits the model's ability to optimize and represent land use directly linked to livestock activities. Consequently, it is up to the modeler to develop scenario-specific assumptions regarding livestock, which can be reflected in adjustments to crop and pastureland use patterns in future projections. Furthermore, the direct land use by livestock differs from that of other agricultural sub-sectors. In the case of farmed livestock, land use is minimal because farming is treated as an industrial process. The land occupied by farming facilities is negligible compared to the extensive land required for feed crop production. Therefore, it is neglected. For grazing livestock, as previously mentioned, pasturelands are assumed to be designated for grazing. Both the land use and emissions associated with these activities are accounted for within the pastureland sub-sector. After the hypothesis statements and according to them, the generic livestock process is shown in Figure 23.

The generic livestock receives the commodity Agricultural Water (AGR_WTR), expressed in millions of cubic meters (Mm^3), as input. The water use efficiency of the livestock process is then translated into ESOM parameters. Water consumption is linked to the livestock

production process (Activity of the process, expressed in kilotons of livestock products) through the efficiency parameter. As with livestock production, water is treated as a flowing material exchanged between processes and modelled as a commodity. For livestock, the CAP2ACT is equal to 1, meaning that the unit of capacity and the unit of activity are the same (thousand head of livestock). In terms of outputs, livestock directly satisfies demand by producing livestock commodities. Additionally, manure is generated as a by-product. This waste stream is defined as an energy carrier because it can be used in manure digesters to produce biogas, which can then be fed into the energy system.

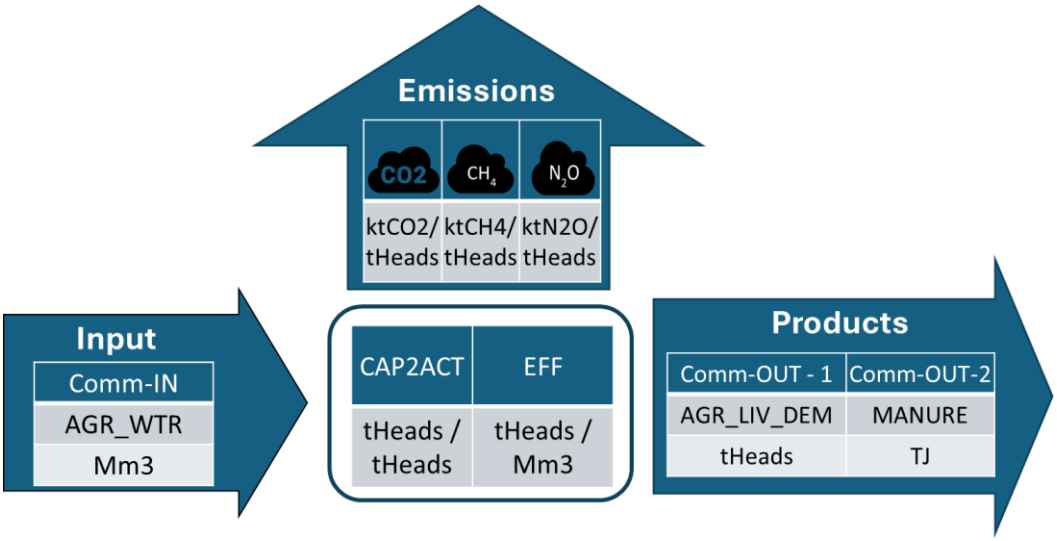

Figure 23. Livestock modelling

Crops

Crops represent the second most impacting component of the AFOLU sector in terms of emission, and the first in terms of direct water and land use [208]. Therefore, the level of detail in terms of modelling should reflect this relative importance. The model can account for land and water use by crop production, as well as their related emissions. According to actual (base year) and future (future years) demand projections, the AFOLU modules retrieve the necessary natural resources consumption and emissions flows, optimizing according to the best technological options. Always following the minimum cost pathways of the main model. For each nation and year, the data required to correctly model the crop sector are reported in Table 25. The elements of Table 25 can be sourced from various datasets. For OECD countries, the most precise and reliable data source is the UNFCCC database [209]. This provides robust, standardized data for countries within the OECD region. For all countries, particularly those outside the OECD area, the primary source of data is FAO-Stat [210], which offers comprehensive global coverage on agricultural and environmental metrics. The model accounts for all three emissions reported by the IPCC: CO_2, N_2O, and CH_4. To obtain emission factor for each crop process, is necessary to perform some hypothesis regarding the association from FAO category to crop technologies. In particular, the emissions are provided as total national

emissions of a certain GHG [kt], while the area data regarding crop cultivation are expressed in kilo hectares [kha].

Table 25. Data entry for crop sector

Data	Unit of Measurment
Area harvested by crop and year*	[kha]
Production by crop and year*	[Mton]
Emissions by year (N2O) - Crop Residues	[kton]
Emissions by year (CH4) - Burning - Crop residues	[kton]
Emissions by year (N2O) - Burning - Crop residues	[kton]
Emissions by year (N2O) - Synthetic Fertilizers	[kton]
Water requirements and Irrigation split percentage by crop and year	[Mm3 - % of irrigation by crop]

Therefore, the emission factors for each crop (expressed in [kt_GHG/kha]) are obtained as follow: First, the overall emissions are firstly summed up between IPCC categories, obtaining a single overall emissions amount for each nation and GHG, as in Equation (20):

$$Total\ Emissions_{nation,GHG_i} = \sum_{j=1}^{n} TE_j \qquad (20)$$

$$where\ i = CO_2, CH4\ and\ N_2O\ and\ j = Rice\ Cultivation, \dots, Other$$

Then, the overall emissions for each GHG are equally divided by crops according to their area. Therefore, for each GHG and for each crop, the emission factor is derived as in Equation (21):

$$\mathrm{EF}_{\mathrm{crop,nation,GHG_i}} = \frac{Total\ Emissions_{nation,GHG_i}\ [tons\ of\ GHG_i]}{cultivated\ cropland_{crop}\ [Kha]} \qquad (21)$$

Given the impossibility of directly relating the emission to a specific type of crop, the simplification of introduced here assign a share on emissions proportional to the cultivated cropland. Nevertheless, since the emissions factor should be linked to the activity of the process to be computed, the final emissions factor is divided by the crop yield as in Equation (22):

$$\mathrm{EF}_{\mathrm{crop,nation,GHG_i}}\left[\frac{tons_{GHG}}{tons_{crop}}\right] = \frac{\mathrm{EF}_{\mathrm{crop,nation,GHG_i}}\left[\frac{tons_{GHG}}{Kha}\right]}{crop\ yield_{crop}\left[\frac{tons\_crop}{Kha}\right]} \qquad (22)$$

Similarly, the process must be repeated for water, to link the general water use data to the single crop, passing to the percentage of irrigation by crops. For each crop, knowing its area and the irrigation share, the total irrigated area is calculated as in Equation (23):

$$Irrigated\ area\ [ha] = Irrigation\ share\ [\%] * Crop\ area\ [ha] \qquad (23)$$

In the same way, knowing the total irrigation water withdrawal and the irrigation share, the water consumption for each crop is calculated as in Equation (24):

$$\begin{aligned} &Crop\ Irrigation\ Consumption\ \ [Mm^3] \\ &= Irrigation\ share\ [\%] * Total\ agricultural\ water\ withdrawal\ [Mm^3] \end{aligned} \qquad (24)$$

Then, the specific water consumption by crop is derived from Equation (25), by dividing the two above-mentioned components and the crop yield by FAO data:

$$\begin{aligned} &Crop\ water\ consumption\left[\frac{Mm^3}{ton}\right] \\ &= \left(\frac{Crop\ Irrigation\ Consumption\ \ [Mm^3]}{Irrigated\ area\ [ha]}\right) * \frac{1}{Crop\ yield\ \left[\frac{ton}{Mm^3}\right]} \end{aligned} \qquad (25)$$

Crop directly consumes water and land natural resources, satisfying their related demand and producing residues that can feed bioenergy plants. The generic crop process receives as input the commodity Agricultural Water in Millions of cubic meters (Mm3). Through the process efficiency, the water is transformed into crop demand commodity, while the land accounted as the capacity of the process.

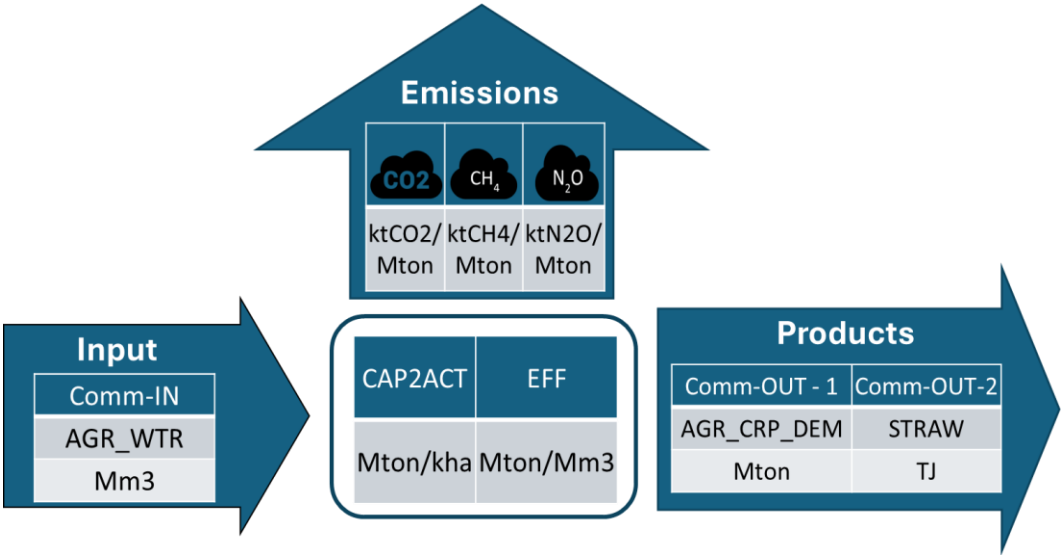

Figure 24. Crop representation

In particular, the land use efficiency, or crop yield, is transferred in the model thanks to the Capacity to Activity (CAP2ACT) parameter. This serves to link the capacity of the crop (kilo-hectares of cultivated area) to the production required. Similarly, the amount of water consumed is linked to the crop production (Activity of the process, expressed in kilotons) thanks to the efficiency parameter. In this way the water, which is a flowing material exchanged between process, is treated as a commodity. Conversely land, which is the fixed base on which the crop process takes place, is treated as a capacity. In terms of output, the crop directly feed its related demand by producing the commodity as a primary output. In addition, the waste of the crop (if present) is also defined as an energy carrier due to its possible use in biomass electricity plants. Therefore, while the efficiency defines the ratio between the water and the demand commodity, the output commodity parameter is used to link the crop production at the energy amount of waste obtained accordingly.

Pastures

Pastures represent a significant component of the AFOLU sector, particularly in terms of land use and emissions associated with grazing activities[208] . The modeling of pastures must consider their role in land occupation and emissions resulting from grazing livestock, including CO_2, CH_4, and N_2O. Effective modeling should capture the interactions between pasture use and livestock emissions, as well as the potential for carbon sequestration in managed pastures. For each nation and year, the data required to correctly model the pasture sector are reported in Table 26. Division is made by type of data, unit of measurement and related excel file on which the data must be filled.

Table 26 - Data entry for livestock sector

Data	Unit of Measurement
Land Under permanent pastures and meadows	[kha]
Manure applied on Pastures (Emissions CH4)	[kton]
Manure management by species (Emissions N2O)	[kton]
Water requirements	[Mm3]

Pasture directly consumes natural resources, specifically land and water, to satisfy demand, without involving any transformative processes or secondary outputs. According to Figure 25, the pasture process takes in the commodity Agricultural Water (AGR_WTR), measured in millions of cubic meters (Mm^3).

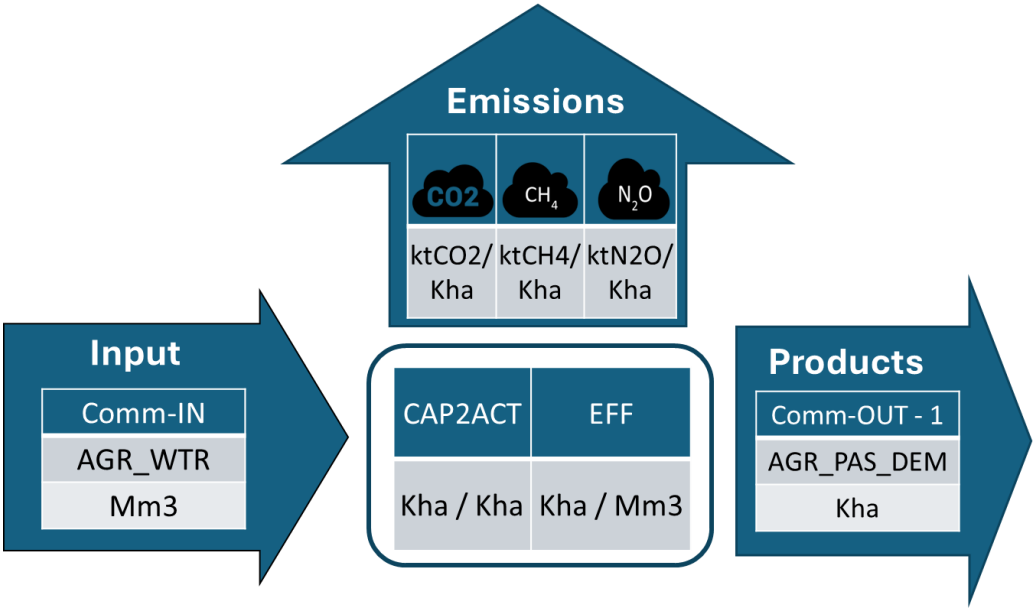

Figure 25. Pastures representation

However, unlike crops, pasture does not have a yield, as both its capacity and activity are expressed in kilo hectares, simply representing the total pasture area. The land use efficiency is inherent in the Capacity to Activity (CAP2ACT) parameter of TIMES [211], but since both capacity and activity are measured in kilo hectares, they are identical, directly reflecting the demand for pastureland. Water consumption is linked to the activity (pasture area) through an efficiency parameter, treating water as a flowing commodity between processes. However, pasture does not generate any waste or secondary output, making it a straightforward representation of land use for grazing, with no further connections to other sectors.

Emissions factor and water requirement for pasture, similarly to crops, are obtained as follow: The overall emissions are firstly summed up between IPCC categories, obtaining a single overall emissions amount for each nation and GHG, as in Equation (20):

$$Total\ Emissions_{nation,GHG_i} = \sum_{j=1}^{n} TE_j$$

$$where:$$

$$i = CO_2, CH4\ and\ N_2O\ and\ ; \tag{26}$$

$$j = Manure\ left\ on\ pastures$$

The emission factor is derived by dividing pastures overall emission by their area, as in Equation (21):

$$EF_{pastures,nation,GHG_i} = \frac{Total\ Emissions_{nation,GHG_i}\ [tons\ of\ GHG_i]}{pasture\ area\ [Kha]} \tag{27}$$

For pastures, knowing its area and the irrigation share, the total irrigated area is calculated as in equation:

$$Irrigated\ area\ [ha] = Irrigation\ share\ [\%] * Pasture\ area\ [ha] \tag{28}$$

In the same way, knowing the total irrigation water withdrawal and the irrigation share, the water consumption for each crop is calculated as in equation:

$$Pasture\ Irrigation\ Consumption\ \ [Mm^3]$$

$$= Irrigation\ share\ [\%] * Total\ agricultural\ water\ withdrawal\ [Mm^3] \tag{29}$$

Then, the specific water consumption by crop is derived from equation, by dividing the two above-mentioned components and the crop yield by FAO data:

$$Pasture\ water\ consumption\left[\frac{Mm^3}{ha}\right] = (\ \frac{Pasture\ Irrigation\ Consumption\ \ [Mm^3]}{Irrigated\ area\ [ha]}) \tag{30}$$

Forests and Harvested Wood Products

Forests are the most significant mitigation option in the AFOLU sector. At the same time, they are the largest source of carbon capture and carbon emission [208]. Concerning the latter,

deforestation due to land use change leads to net positive emissions, which the IPCC identifies as the highest impacting sources [212]. Therefore, forest modelling must account for their dual role in both negative emissions and land use change, particularly concerning CO_2 sequestration. Additionally, forests provide wood products that not only meet demand but also function as carbon sinks, known as harvested wood products (HWP), which will be discussed in the following chapter. For each nation and year, the data required to correctly model the forest sector are reported in Table 27.

Table 27. Data entry for livestock sector

Data	Unit of Measurement
Forestland	[kha]
Forestland (Emissions CO2)	[kton]
Net Forest emissions (Emissions CO2)	[kton]
Water requirements *Only in case of irrigated forest	[Mm3]
Forest production	[tons] or [m3]
Forest emission factors	[ktCO2/Kha]

Moreover, forests production and the emissions factors that must be obtained by literature, considering the specific forest species present in the selected geographic area. Since forests do not typically require irrigation, and as a result, the default technology in the model does not include water inputs and associated efficiency metrics. If irrigation is present in specific national instances, it is the responsibility of the modeler to introduce relevant technologies to account for this practice.

According to Figure 26, the forest produces two key outputs: a generic forest demand commodity, which can be modified to test the impacts of different afforestation and deforestation practices, and a generic wood product. The product, still expressed in kilo-hectares, serves as the source for Harvested Wood Products (HWPs), which fulfill national demands and act as a carbon sink.

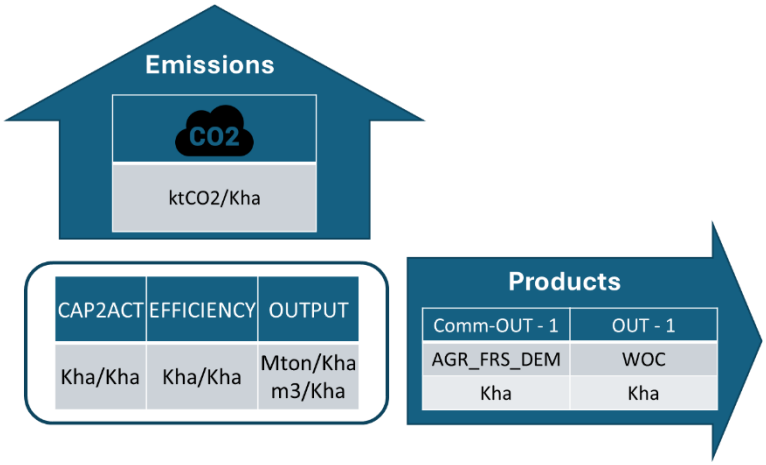

Figure 26. Forest model

Notably, the forest does not generate positive greenhouse gas (GHG) emissions. Instead, it functions as a carbon dioxide sink. The negative emissions factor should be calibrated based on the base year and projected for future years, considering the geographical and technological factors relevant to each case. The model distinguishes between two generic forest types: naturally regenerating forests and planted forests. Both types produce Wood Products (WOC) with unitary efficiency, meaning the WOP output is measured in the same units as the forest demand commodity, maintaining consistent values for clarity and simplicity. WOP is then converted into Wood Output Commodity (WOC), which is further transformed into different Harvested Wood Product (HWP) by-products to meet specific demands. These conversions take place in the HWP-related section of the model, as shown in Figure 27.

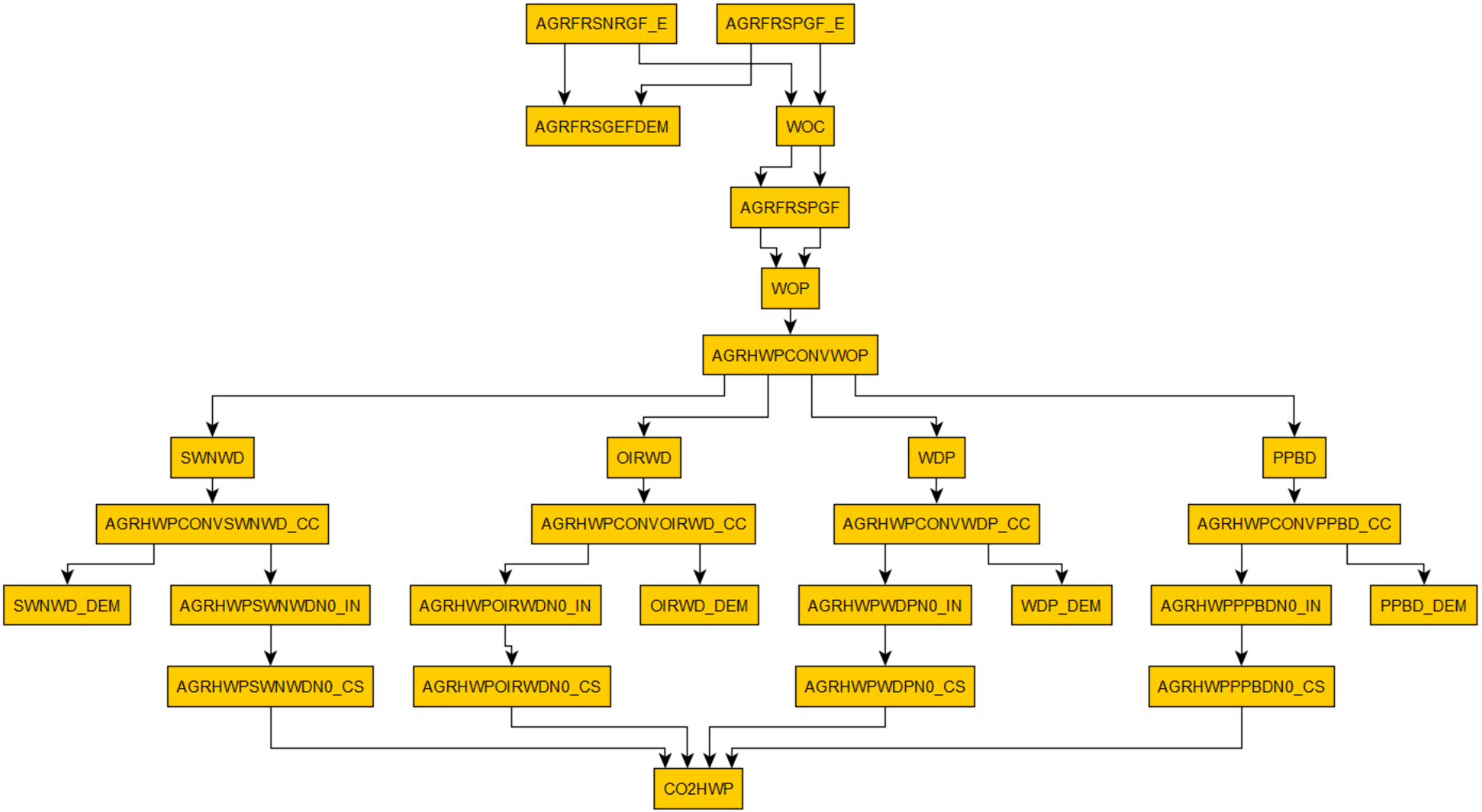

Figure 27. Forest and HWP Reference system

As visible from Figure 27 both planted and naturally regenerated forests meet their forestland demand while also producing wood output, referred to as WOC (Wood Output from Capacity), expressed in kilo hectares (kha). This represents the overall productive capacity of the forests. The next step involves converting this generic wood production (WOC) into Harvested Wood Products (HWP), based on specified production statistics. A key point to consider in this conversion is that the original unit of WOC is in kha, while HWP is measured in both cubic meters and tons. To bridge this gap, a conversion must be applied using an efficiency parameter that captures how much wood product (in terms of volume and mass) can be derived from a given area of forestland. This efficiency factor is a unique parameter that translates the forestland area into a combined figure representing both cubic meters and tons of harvested wood products. Consequently, the amount of forest production in Kha is converted into a single number that reflects the total quantity of HWP, expressed as a mix of volume (cubic meters) and weight (tons), as indicated by the following Equation (31):

$$\eta_{\text{WOC,WOP}} = \frac{\sum HWP_i\ (in\ m^3) + \sum HWP_j\ (in\ tons)}{Forestland\ area\ [Kha]} \tag{31}$$

This data manipulation is simply a numerical workaround to handle the original dataset, which contains products measured in different units. As a result, the total HWP production is represented as a single numerical value that mixes both cubic meters and tons. This combined figure allows for simplified processing, even though it doesn't distinguish between the two units. The total HWP production is calculated as shown in the following Equation (33):

$$\begin{aligned}&\text{Total HWP Production [sum of tons and m}^3\text{]}\\ &= \eta_{\text{WOC,WOP}} * Forestland\ area\ [Kha]\end{aligned} \tag{32}$$

Then, it's necessary to split this numerical amount in the different sub-products, this time considering the correct unit of measurement. In particular, the Agricultural Wood Product to HWP Conversion Technology (AGRHWPCONVWOP) has 4 different output factors, one for each HWP type, whose values is obtained as follow: Let W_i represent different wood products, where i represents each specific product. The total amount for each category C_j (e.g., Sawnwood, Other Industrial Roundwood) is the sum of all relevant wood products W_i in that category:

$$C_j = \sum_{i \in j} W_i \tag{33}$$

Then, the share S_j of category j in the total wood products can be calculated as:

$$S_j = \frac{C_j}{\sum C_j} \tag{34}$$

The share as in (34) is imputed as the TIMES parameter "Share-O~FX", which is calibrated at the base year and can be imposed for the future ones, allowing to test different HWP production scenarios to see their impact on emissions. Once each HWP reach its specific path, as from the centre to the bottom of Figure 27, the first step involves converting the product into its **tons of carbon equivalent**, based on its volume or mass. This ensures consistency with the IPCC guidelines for HWP accounting [213]. The conversion is performed by the technology **AGRHWPCONVXXXX_CC**, where "XXXX" corresponds to one of the generic wood product categories. The efficiency of this process is represented by the conversion factors provided by the IPCC. These factors, specific to the main wood product categories, are summarized in Table 28**.**

Table 28. HWP carbon content

Type	Value	Unit
Sawn wood	0.229	[tC/m3]
Other Industrial Roundwood	0.229	[tC/m3]
Wood Panels	0.269	[tC/m3]
Paper and paperboard	0.386	[tC/adt]

The amount of produced HWP by year, expressed in tons of carbon, is the starting point for the harvesting representation, that constitutes both source of carbon stock and negative emissions. The modelling of HWP carbon stock and its related capture effect is based on the IPCC modelling of that AFOLU subsector [213]. According to Tier 1 methodology, by knowing the annual production at the year i is possible to calculate the carbon stock at the next year $(i+1)$ and its loss δC:

$$C(i+1) = e^{-k} * C\ (i) + \left[\frac{(1-e^{-k}}{k}\right] * Inflow(i)$$
$$\delta C = C(i+1) - C(i) \tag{35}$$

Where $Inflow(i)$ is the production at the year i and k is the decay constant, which is different for each HWP. This can be derived from the IPCC documentation, and it is reported here in Table 29.

Table 29. HWP Decay constant k

Type	Value
Sawn wood	0.020
Other Industrial Roundwood	0.020
Wood Panels	0.028
Paper and paperboard	0.347

From Equation (35) demonstrates that carbon loss occurs in two distinct phases: during the inflow of carbon into storage and throughout the year while the carbon remains stored. The first phase of emissions is modelled using a traditional storage inflow efficiency, as shown in Equation (36) and computed for each wood product. This efficiency is represented by the process AGRHWPXXXX_IN, where 'XXXX' refers to the specific wood product. Consequently, these emissions are accounted for as part of the overall process efficiency.

$$\eta_{\text{inflow}} = \left[\frac{(1 - e^{-k}}{k}\right] \tag{36}$$

Then, the carbon stock loss which is reported by the IPCC as a negative emission [213], is modelled at the efficiency of the process AGRHWPXXXX_CS, where "XXXX" represents the generic HWP name. In this way, this emission loss is already discounted. As in Equation (37):

$$\eta_{\text{storage}} = \left[\frac{(1 - e^{-k}}{k}\right] \tag{37}$$

Land Based Mitigation Options

In the context of agricultural mitigation strategies, several key practices have been identified for their potential to significantly reduce greenhouse gas emissions and enhance sustainability in crop and grassland management. One of the major review in the field, mixing up to 300 scientific publications and policy papers, identified up to 60 different land-based adaptation and mitigation options [214]. The measures spans to different soil management techniques, bioenergy with carbon capture and more agricultural side measures to social measures: Like limited urban sprawl and sustainable tourism. Nevertheless, for the purpose of this analysis, only the options that can be modelled in a technological compatible way and that presents relevant implication in terms of emissions, land and energy are accounted for.

Therefore, here there are two kinds of options considered: different cropping techniques and sustainable agricultural practices. Considering the former, and according to FAO [215], the following table summarizes these mitigation options, including their descriptions, technical and economic potential, and specific notes on their effectiveness and application.

Table 30. Sustainable agricultural practices

Mitigation Option	Description	Technical Mitigation Potential
Soil Carbon Management	Practices to improve soil carbon in croplands and grasslands. Includes improved crop management, nutrient management, reduced tillage, residue retention, cover crops, organic matter application, improved rice management, biochar application, vegetation management, livestock management, and fire management.	Croplands: 1.9 (0.4–6.8) GtCO2 yr^{-1}; Grasslands: 1.0 (0.2–2.6) GtCO2 yr^{-1}
Biochar	Produced via pyrolysis and gasification; improves soil properties and persists for decades to thousands of years.	2.6 (0.2–6.6) GtCO2-eq yr^{-1}
Agroforestry	Integrates trees and shrubs with crops/livestock, increasing carbon accumulation in vegetation and soil.	Not specified
Crop Nutrient Management	Optimizes fertilizer application and combines various practices like crop rotations, cover crops, and manure application to reduce N2O emissions.	0.3 (0.06–0.7) GtCO2-eq yr^{-1}

However, for the current version of the model, these mitigation options are documented but not yet included. In existing literature, a lack of comprehensive techno-economic assessment is still lacking, as well as a regionalized dataset about the land suitability. To fully account for their impact and potential contributions to greenhouse gas reduction and sustainable agriculture, a more detailed review is requested. For the latter options, related to the different cropping techniques, here we mainly refer to aquaponics, greenhouse and organic cropping, which has shown potential in increasing crop yield, reducing land use, water use and emissions ([216], [217]). For these two options, in absence of more precise literature, factors have been assumed regarding the improved efficiency with respect to traditional cropping. In Table 33 those factors are summarized. These general factors are derived from a comparison based on the Jordan model for specific crops, which has been generalized as a hypothesis for all crops. This approach is intended to evaluate the theoretical effectiveness of the measure. Nonetheless, it remains the responsibility of modelers to collect data on region-specific factors and to exclude technologies for which aquaponic or greenhouse options are not feasible (e.g., for cereals, which generally require extensive open spaces).

Table 31. Crop mitigation options parameters for greenhouse and aquaponic. Comparison with open field values for yield (CAP2ACT) and water consumption ratio.

Parameter	Tech-type long	Value	Description
CAP2ACT Ratio	Open Field	1	Ratio to Open Field Yield, representing how much more t of the crop a greenhouse, aquaponic or other growing method are compared to Open Field
	Greenhouse	3	
	Aquaponics	6	
Water Ratio	Open Field	1.00	Ratio to Open Field Yield, representing how much more water consumption a greenhouse, aquaponic or other growing method are compared to Open Field
	Greenhouse	0.75	
	Aquaponics	0.50	

As reported in Table 31, two different options can substitute the traditional open-field cropping: greenhouses and aquaponics [212]. Both the different cropping technologies are modeled by applying correction factors to yield (CAP2ACT) and water use (EFF) ratios relative to traditional open-field systems. These factors ensure that production outputs, emissions, and natural resource consumption are adjusted proportionally – either directly or indirectly – reflecting the application of these corrections. Installation costs for these technologies, measured per hectare, can be generally implemented based on values reported in the literature, this according to the nation of interest. Conversely, organic cropping systems are derived directly from input data, mirroring the structure of open-field systems with two key distinctions: (1) yields are adjusted downward according to national projection and (2) emissions from nitrogen fertilization are excluded from the emissions factor calculation. Concerning the economics of the land-based mitigation options, is must be differentiated between the options that simply require land expansion (e.g., organic cropping) with respect to the ones that requires infrastructure (greenhouse, aquaponic) or land management (afforestation). Regardless of the specific case study, being it Sweden or Italy, two costs components are accounted for. All the land-intensive technologies are characterized by a fixed cost equal to the country specific cost of land rent by Eurostat [194]. This means that, for example, organic cropping that require additional land due to lower yield, will have higher fixed costs. Nevertheless, greenhouse and aquaponic cropping both require additional land and infrastructure. In the absence of a comprehensive database detailing average national or European-level costs for crop mitigation options (e.g., greenhouse systems), cost estimates have been sourced from specific European case studies [218]. Inside all the land – based mitigation option there is also the afforestation practice, which refers to planting trees that capture carbon during their lifespan. Again, afforestation represents a mix of land that must be occupied (fixed rent cost) plus forest installation (initial investment cost). General data at the European level for the cost of afforestation has been taken from [219] and are reported in Table 32.

Table 32. Costs for afforestation and maintenance.

Cost Category	Cost per unit (EUR)
Felling	
Regeneration felling	12.57 EUR / m^3
Thinning	25.13 EUR / m^3
All felling	16.09 EUR / m^3
Silvicultural Measures	
Clear-cut cleaning	187.13 EUR / hectare
Scarification	295.61 EUR / hectare
Planting (including plants)	676.19 EUR / hectare
Sowing	588.51 EUR / hectare
Precommercial thinning	328.21 EUR / hectare
Fertilization and liming	271.20 EUR / hectare
Total Initial Planting Cost*	**1,158.93 EUR / hectare**

Mitigation option for livestock's

This section details the different mitigation options available for the livestock sector. According to the 7th IPCC impact assessment report [208], it identifies in the livestock enteric fermentation and manure management emissions as the most impacting ones, especially in developed countries where no more deforestation is taking place. The estimated technical potential for both the option is 0.5-3.2 GtCO2eq [208]. Therefore, a proper modelling of the abatement option for this sector must be inserted.

Enteric Fermentation

Enteric fermentation, a process in ruminant animals like cattle, goats, sheep, and buffalo, is a significant source of methane emissions [220]. Mitigation strategies include direct measures targeting ruminal methanogenesis or improving production efficiency, classified into feeding practices, supplements (such as additives and vaccines), and livestock breeding or husbandry improvements[221]. Chemically synthesized inhibitors show promise, with mitigation potential between 16% and 70%, but challenges such as persistence, costs, and regulatory approval remain. Additionally, administering these inhibitors in pasture-based systems poses difficulties, and CH_4 vaccines are still under development [221]. While developed countries focus on direct technical options, developing nations emphasize improving production efficiency. The global technical potential for reducing methane emissions from enteric fermentation is estimated at 0.8 (0.2–1.2) GtCO2-eq per year, with 0.2 (0.1–0.3) GtCO2-eq per year available at costs below USD 100 per tCO2-eq [221]. Due to the low

technology readiness level (TRL) of the available options and the lack of comprehensive data, enteric fermentation is currently omitted from the modeled mitigation options.

Manure Management

Manure management measures target the mitigation of methane (CH_4) and nitrous oxide (N_2O) emissions from manure storage and deposition, addressing both direct and indirect sources, such as the conversion of ammonia and nitrate into N_2O. Integrating manure management with livestock and soil management practices enhances system resilience, sustainability, food security, and prevents land degradation, while also benefiting local environments. These measures have a global technical mitigation potential of 0.3 (0.1–0.5) GtCO2-eq per year, with 0.1 (0.09–0.1) GtCO2-eq per year available at costs up to USD 100 per tCO2-eq[221].

Country-specific strategies reveal various regionally tailored solutions. For example, small-scale anaerobic digestion, solid manure coverage, and daily manure spreading are prominent in Asia, the Developing Pacific, and Africa. Meanwhile, developed countries emphasize large-scale anaerobic digestion, tank/lagoon covers, improved manure application timing, nitrogen inhibitors for urine patches, soil-liquid separation, livestock nitrogen intake reduction, trailing shoe or injection slurry spreading, and acidification [221]. In this case, due to the higher applicability of manure management practices, the availability of relevant case studies, and their established presence in various regions, these manure mitigation options have been included in the modeled mitigation strategies. All the mitigation options described by FAO [222] are listed in Table 33.

Table 33. Mitigation options abatement potential for different manure management options

Mitigation Option	CH_4	N_2O
Dietary manipulation (reduced crude protein)	+71% (increase)	-30%
Daily/weekly manure removal	-55%	-41%
Chemical/biological scrubbers	N/A	+164% (biological scrubbers)
Anaerobic digestion	-29%	-23%
Acidification of manure	-74%	-17%
Covers during manure storage	-12%	500%
Biogas implementation in small-scale systems	-60% to -80%	N/A
Biofilters (for wet manure/slurry)	N/A	N/A

Since each livestock species is associated with two distinct emission factors—one for CH_4 and one for N_2O—the reduction in emissions varies across species. Applying the same percentage reduction to different livestock technologies leads to different overall emission factor reductions due to the inherent variation in species-specific emissions.The emission factor for a generic mitigation option j is and species i , accounting for the mitigation option reduction percentage MOR_j, is calculated as in Equation (38):

$$EF_{i,j} = EF_i * MOR_j \ [\%] \tag{38}$$

Regarding costs, local data should be sourced from relevant case studies in the literature, as there is considerable variability across regions. Typically, costs are reported as abatement costs, expressed in terms of [M€/ktCO_2eq]. To use these in a livestock-specific context, a conversion process is required to translate abatement costs into a cost per livestock unit. Since the investment cost is attributed to each livestock unit, it is necessary to convert the emissions reduction (in tons of CH_4 or N_2O) into a corresponding cost per livestock unit. This involves calculating the emissions reduction per unit of livestock and mitigation option ($ER_{i,j}$). Then, applying the abatement cost per ton of CO_2-equivalent emissions, ensuring that the cost aligns with the scale of emissions reductions for each livestock category. This can be obtained by applying Equation (39):

$$ER_{i,j}\left[\frac{Kton_{CO2}}{tHeads}\right] = \sum_{i=1}^{N_{GHG}} MOR_j[\%] * EF_i\left[\frac{Kton_{GHG}}{tHeads}\right] * \mu_{GHG}\left[\frac{Kton_{CO2}}{Kton_{GHG}}\right] \tag{39}$$

Known the emission reduction for each species and mitigation option, the final cost of abatement for livestock unit can be obtained as in Equation (40):

$$MAC_{i,j}\left[\frac{DKK}{tHeads}\right] = ER_{i,j}\left[\frac{Kton_{CO2}}{tHeads}\right] * MAC_j\left[\frac{DKK}{Kton_{CO2}}\right] \tag{40}$$

In this way, there exists different livestock technologies that, at a different cost, provide different abatement options, each one with its own reduction factor. A significant limitation of simplistic modeling approaches is their inability to accurately assess the cumulative impact of implementing multiple abatement technologies in sequence. For example, a model might not be able to calculate the combined effect of first using a manure storage cover and then applying slurry acidification. It is incorrect to simply sum the individual reduction percentages, as this would overestimate the total abatement. To overcome this limitation, a more robust methodology is required. The proposed approach models the manure management system as a sequential chain of operations. This conceptualizes the flow of manure through various

treatment stages, where each stage represents the application of a specific abatement technology. Within this framework, the first technology in the chain is applied to the total initial emission potential of the manure (for methane, CH4, and nitrous oxide, N2O). The reduction factor for any subsequent technology is then applied not to the original emission potential, but to the remaining potential that was left after the preceding intervention. The total reduction is the produttoria of the different emission reductions of the chain:

$$EF_{i,TOTAL} = \prod_{J=1}^{n} MOR_i \tag{41}$$

Data for the costs of the different abatement options has been sourced from [223] and are reported, including mixed options which has been calculated, are reported in Table 34

Table 34. Cost for Manure Abatement Options.

Method	Species	Cost [M€/ktCO2eq]
Acidification	Cattle, dairy	0.047
	Cattle, non-dairy	0.047
	Swine, breeding	0.065
	Swine, market	0.065
Daily_Weekly_Manure_Removal	Cattle, dairy	0.130
	Cattle, non-dairy	0.130
	Swine, breeding	0.006
	Swine, market	0.006
Manure_Storage_Covers	Cattle, dairy	0.013
	Cattle, non-dairy	0.013
	Swine, breeding	0.013
	Swine, market	0.013
Acidification + Daily_Weekly_Manure_Removal	Cattle, dairy	0.030
	Cattle, non-dairy	0.030
	Swine, breeding	0.039
	Swine, market	0.039
Acidification + Manure_Storage_Covers	Cattle, dairy	0.072
	Cattle, non-dairy	0.072
	Swine, breeding	0.010
	Swine, market	0.010
Daily_Weekly_Manure_Removal + Manure_Storage_Covers	Cattle, dairy	0.089
	Cattle, non-dairy	0.089
	Swine, breeding	0.035
	Swine, market	0.035
Acidification +	Cattle, dairy	0.063

Daily_Weekly_Manure_Removal + Manure_Storage_Covers		
	Cattle, non-dairy	0.063
	Swine, breeding	0.028
	Swine, market	0.028

Linkage with the energy sector

Beyond final products, most AFOLU technologies also generate secondary outputs. Forest systems provide harvested wood products (HWPs), while crops and livestock yield byproducts such as straw and manure. These residuals feed into an interconnected value chain illustrated in Figure 28. Crops and manure can be directed toward anaerobic digestion systems, with biogas either upgraded for grid injection or combusted directly for electricity generation. Alternatively, straw can be redirected to livestock feeding or soil conditioning, while untreated manure may be applied to fields, affecting nutrient cycles and emissions profiles. The inclusion of manure treatment pathways - ranging from acidification to covered storage—ensures accurate estimation of emissions from the manure management subcategory, a known hotspot for non-CO_2 GHGs.

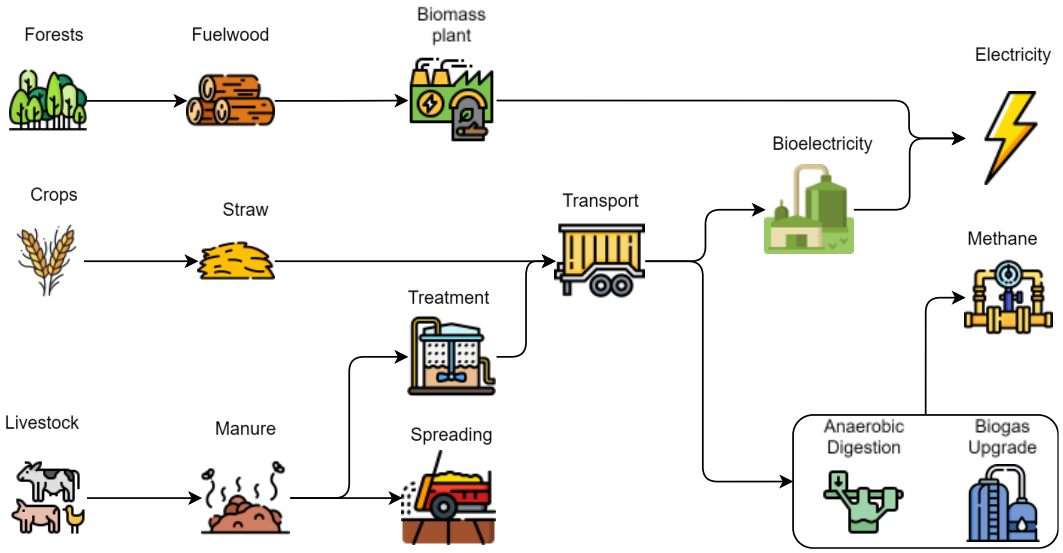

Figure 28. AFOLU sub-energy products supply chain for the energy system.

The economics of the bioenergy chain is derived from different sources all under the IEA BIOENERGY collaboration program [224] and are reported in Table 35.

Table 35. Lumped parameters of bioenergy chain

Technology	INPUT	OUTPUT	CAPEX (M€/GW)	FIX (M€/GWy)	VAR (M€/PJ)
Forest biomass plant	Fuelwood	Electricity	2560	150	
Anaerobic Digester	Manure, Straw	Biogas	3500	200	
Mixed biomass plant	Manure, Straw	Electricity	4500	150	
Manure transport	Manure	Manure			10
Biogas Upgrading	Biogas	Methane			132

3.3. A multi-context and multi scenario analysis: Insights from Sweden and Italy

The previously discussed AFOLU energy modelling framework has been tested on two different case studies: The TIMES-Sweden and the TEMOA-Italy energy models. The analysis are aimed at testing different aspects of the same modelling framework, accounting for the peculiarity of the different context and the different roles that AFOLU plays in the respective energy systems. The first presented is the TIMES-Sweden, on which the AFOLU model has been originally developed. This analysis is characterized by an increased effort in testing out the model strength and weaknesses and behaviours in general, since it was an early-stage work. Also, the framework on which the model is built is the consolidated TIMES model generator [225], in its Swedish instance. The second piece of work, elaborated in TEMOA – Italy [226], is more related to the testing on the policy and land use dynamics of Italy, taking into consideration that the model has been validated in the Swedish case study

3.3.1. Swedish case-study and scenario

Sweden, due to its strong commitments to decarbonization [227], represents a good testbed in view of the relevance of its AFOLU sector in achieving climate goals [228]. Although Sweden is one of the largest countries in Europe by area, only around 2.7 million hectares - approximately 6.5% of its total land area - is cultivated [227]. Agriculture in Sweden is influenced by the country diverse climate, with markedly different conditions in the northern and southern regions. Over half of Sweden's farms are engaged in animal production, which plays a central role in the agricultural sector. The dairy industry contributes roughly one-third of the sector added value, while poultry production has seen rapid growth, increasing by about 40% over the last decade [228]. In contrast, the number of dairy cows has been declining steadily. Sweden's stringent animal welfare legislation further characterizes its agricultural practices [229]. Swedish crop production is dominated by cereals such as barley, oats, and wheat, along with grassland, with cereals accounting for 40% of arable land use [230]. Forests dominate Sweden's landscape, covering about 70% of its land area. Approximately 75% of this forest land is actively managed, supporting the country's substantial forestry sector. Timber

supply has doubled since the 1920s, and reforestation efforts plant around 400 million seedlings annually, ensuring that 2–3 new trees replace every tree harvested. Sustainable management is guided by strict national regulations and certification schemes like FSC (Forest Stewardship Council) and PEFC (Program for the Endorsement of Forest Certification), balancing economic goals with biodiversity conservation and environmental protection ([231], [232]).

In terms of emissions, Sweden's emissions in 2020 were significantly influenced by the transport and agriculture sectors [233]. Transport emerged as the largest contributor, emitting 15.78 Mt CO_2-eq, followed by agriculture at 8.08 Mt CO_2-eq and land use change and forestry at -11.32 Mt CO_2-eq (which shows a net sequestration). Industry and energy sectors contributed comparatively lower emissions.

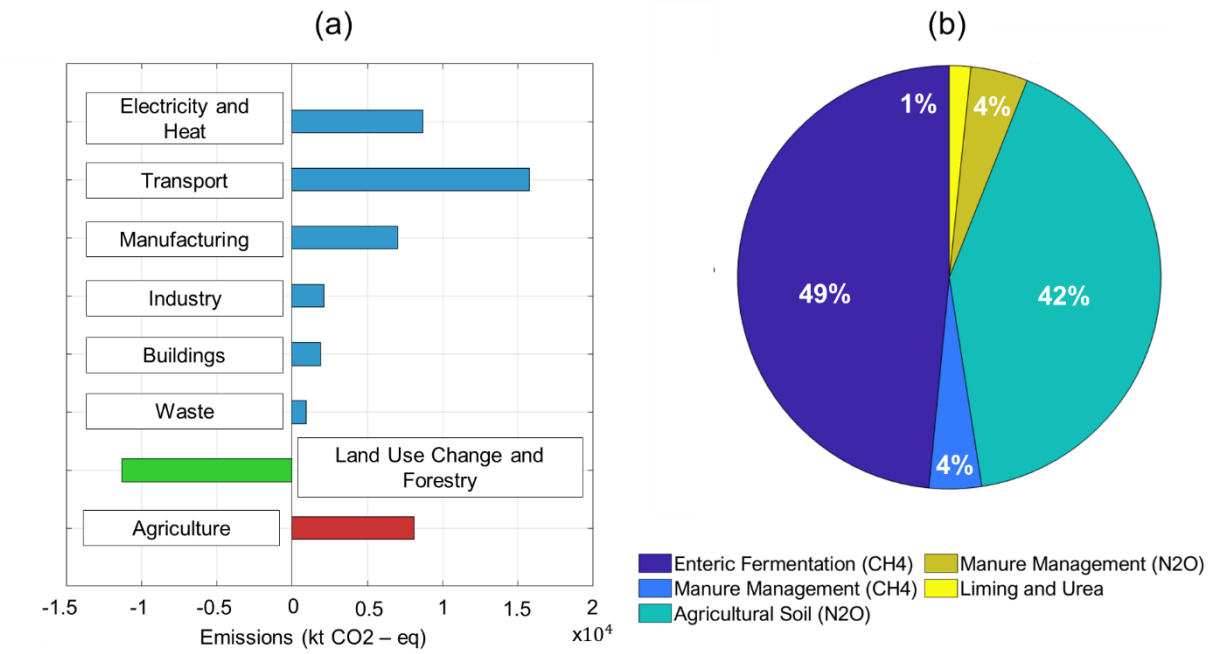

Figure 29. Overview of Swedish AFOLU sector emissions. Global Swedish emissions at 2022 (a) and AFOLU emission by source (b).

Emissions by sector in 2020 highlights the prominent role of agriculture as in Figure 29 (a), and the sink effect of land use change and forestry. As shown in Figure 29 (b), the breakdown of agricultural emissions reveals that CH_4 and N_2O together contribute significantly to the total agricultural emissions. Specifically, enteric fermentation (CH_4) is the largest contributor, followed by agricultural soil and manure management (N_2O). To study Sweden, the Swedish TIMES model has been used. The TIMES-SE model is a national instance of the TIMES framework developed by Energy Modelling Lab [234] in collaboration with IVL Swedish Environmental Research Institute [235]. It provides a detailed representation of Sweden's energy system, covering all major demand sectors - residential, commercial, industry, transport, agriculture, and electricity and heat production - and is now expanded to include the AFOLU (Agriculture, Forestry, and Other Land Use) sector. The model divides the country into the four official Swedish electricity bidding zones, thus allowing for geographically disaggregated analysis of regional energy balances. TIMES-SE is calibrated for the base year 2022, using official statistics from Eurostat, UN, and national energy agencies,

ensuring coherence with observed energy balances and sectoral activity levels. The electricity and district heating sectors are further refined using detailed data from major Swedish energy producers. A key strength of TIMES-SE is its temporal resolution: it features 8,760 hourly time slices, enabling robust modeling of variable renewable energy sources and electricity system dynamics. The optimization horizon spans from 2025 to 2050 in 5-year intervals. The model captures emissions of CO_2, CH_4, and N_2O, enabling analysis aligned with Sweden's climate goals and international commitments. Emission accounting is linked to both fossil fuel combustion and non-energy processes in sectors like agriculture and land use. Prices for emissions (e.g., EU ETS allowances) and renewable energy certificates can be included as policy inputs. TIMES-SE is actively used and maintained by IVL for policy-relevant scenario analysis[236]. In this framework, the recent extension to include the AFOLU module broadens the system boundary and enables integrated assessments of mitigation options across land-based and energy sectors. In Table 36 the primary processes for the AFOLU sector are presented, excluding those with less than 10% of the total capacity in the base year (BY). The processes are categorized into four distinct subsectors: Crops, Livestock, Pasture, and Forests. For the sake of conciseness, Harvested Wood Products (HWP) and mitigation options have been excluded. The first column represents the generic output satisfying the demand, while the second pertains to the auxiliary output. Auxiliary outputs representing straw or manure are available for all crops, whereas for livestock they are provided only for cattle, pigs, and poultry—where collection of manure is more common. Forests yield wood production, a fraction of which is allocated to biomass production according to FAO statistics on wood products [230]. Pasture grass is not assumed to be used as an energy source because it is typically consumed by grazing animals. Livestock processes differentiate between farming and grazing, with grazing assumed to be approximately 50% more intensive in terms of water consumption (estimate). In terms of emissions, crops, livestock, and pastures do not directly emit CO2; instead, they primarily emit CH4 and N2O. Consequently, the CO2 column is empty for these subsectors, while forests display negative CO2 emissions due to absorption. Conversely, CH4 and N2O emission factors per unit output (UO) represent the main emissions for crops, livestock, and pastures, with crops exhibiting the higher values. Finally, cost data are provided for the various technological options to foster competition. For land-intensive sectors—namely crops, pasture, and forests—a fixed annual cost equal to the average land rental cost in Sweden by Eurostat is assigned [237]. For livestock processes involving manure production, a transportation cost proportional to the amount of manure—derived by the Danish Ministry of Agriculture and applied to Sweden—is included [238]. Additionally, forest investment costs for new forest installations in Sweden are incorporated [239].

Table 36. Overview of the AFOLU technologies and their main model parameters, input and outputs.

Technology Description	Input	Output	Auxiliary Output	CAP2ACT [Mt/kha]	EFF [UO/Mm3]	OUTPUT [TJ/UO]	EF (CO2) [ktCO2/UO]	EF (CH4) [ktCH4/UO]	EF (N2O) [ktN2O/UO]	FIX [M€/CI*y]	VAR [M€/UO]	INV [M€/UO]
Crops Open Field Cereals Existing	WTRAFO	AFOCRPCERDEM	CERSTR	6.11E-04	-	7.79E-03	-	6.85E-01	1.87E+01	2.00E-01	-	-
Crops Open Field Legumes Existing	WTRAFO	AFOCRPLEGDEM	LEGWSB	3.32E-04	7.21E-03	1.33E-03	-	1.26E+00	3.43E+01	2.00E-01	-	-
Crops Open Field Seeds Existing	WTRAFO	AFOCRPSEEDEM	SEEWSB	3.36E-04	5.73E-03	6.71E-04	-	1.25E+00	3.40E+01	2.00E-01	-	-
Crops Open Field Vegetables Existing	WTRAFO	AFOCRPVEGDEM	VEGWSB	4.51E-03	5.78E-03	4.51E-03	-	9.27E-02	2.53E+00	2.00E-01	-	-
Crops Open Field Roots Existing	WTRAFO	AFOCRPROODEM	ROOWSB	5.25E-03	1.72E-02	5.25E-03	-	7.96E-02	2.17E+00	2.00E-01	-	-
Livestock Grass Cattle, dairy Existing	WTRAFO	AFOLIVCADDEM	CADMNR	-	5.62E+01	1.09E+01	-	1.38E-01	1.03E-03	-	3.86E-02	-
Livestock Grass Cattle, non-dairy Existing	WTRAFO	AFOLIVCANDEM	CANMNR	-	8.99E+01	4.00E+00	-	6.30E-02	4.03E-04	-	1.82E-02	-
Livestock Grass Goats Existing	WTRAFO	AFOLIVGOADEM	-	-	4.49E+02	-	-	5.13E-03	8.33E-06	-	-	-
Livestock Grass Sheep Existing	WTRAFO	AFOLIVSHPDEM	-	-	8.99E+02	-	-	8.19E-03	1.91E-05	-	-	-
Livestock Grass Swine, breeding Existing	WTRAFO	AFOLIVSWBDEM	SWBMNR	-	1.87E+02	1.46E+00	-	1.05E-02	2.41E-04	-	3.20E-03	-
Livestock Grass Swine, market Existing	WTRAFO	AFOLIVSWMDEM	SWMMNR	-	4.99E+02	8.49E-01	-	7.50E-03	7.41E-05	-	3.20E-03	-
Livestock Grass Poultry Existing	WTRAFO	AFOLIVPOUDEM	POUMNR	-	1.20E+04	4.00E+00	-	0.00E+00	0.00E+00	-	2.20E-04	-
Livestock Farm Cattle, dairy Existing	WTRAFO	AFOLIVCADDEM	CADMNR	-	3.75E+01	1.09E+01	-	1.38E-01	1.03E-03	-	3.86E-02	-
Livestock Farm Cattle, non-dairy Existing	WTRAFO	AFOLIVCANDEM	CANMNR	-	5.99E+01	4.00E+00	-	6.30E-02	4.03E-04	-	1.82E-02	-
Livestock Farm Goats Existing	WTRAFO	AFOLIVGOADEM	-	-	3.00E+02	-	-	5.13E-03	8.33E-06	-	-	-
Livestock Farm Sheep Existing	WTRAFO	AFOLIVSHPDEM	-	-	5.99E+02	-	-	8.19E-03	1.91E-05	-	-	-
Livestock Farm Swine, breeding Existing	WTRAFO	AFOLIVSWBDEM	SWBMNR	-	1.25E+02	1.46E+00	-	1.05E-02	2.41E-04	-	3.20E-03	-
Livestock Farm Swine, market Existing	WTRAFO	AFOLIVSWMDEM	SWMMNR	-	3.33E+02	8.49E-01	-	7.50E-03	7.41E-05	-	3.20E-03	-
Livestock Farm Poultry Existing	WTRAFO	AFOLIVPOUDEM	POUMNR	-	8.01E+03	4.00E+00	-	0.00E+00	0.00E+00	-	2.20E-04	-
Pasture Naturally regenerating Generic pasture Existing	WTRAFO	AFOPASGEPDEM	-	-	3.83E+01	-	-	-	7.35E-04	-	-	-
Upstream Forest Naturally regenerating Generic forest Existing	-	FRSNATGEF	-	-	-	-	-	-	-	2.00E-01	-	-
Upstream Forest Planted Generic forest Existing	-	FRSPLAGEF	-	-	-	-	-	-	-	-	-	-
Forest Naturally regenerating Generic forest Existing	FRSNATGEF	AFOFRSGEFDEM	WDPR	-	1.00E+00	5.27E+02	-5.83E-01	-	-	2.00E-01	-	1.42E+00
Forest Planted Generic forest Existing	FRSPLAGEF	AFOFRSGEFDEM	WDPR	-	1.00E+00	5.27E+02	-5.83E-01	-	-	2.00E-01	-	1.42E+00

Three scenarios' narratives were developed to explore the future of AFOLU systems and, due to the methodological focus of this work, to verify the model functionalities. Numerical value and the hypothesis are built on the assumptions outlined in the FABLE 2023 Sweden report [227]. Within these scenarios, key variables such as the target level for organic cropland, afforestation rates, and emission factors for crops and their yields are varied. Additionally, the scenarios incorporate different global energy system emissions constraints, enabling an assessment of the role of AFOLU in contributing to national mitigation pathways and evaluating its potential for providing a net positive contribution to climate change mitigation.

To ensure comparability, the scenarios in this study adopt a structure consistent with those developed in prior research with similar objectives [228]. Three primary scenarios were analyzed to evaluate the model under varying constraints and decarbonization targets. As shown in Figure 31, each scenario includes two sub-branches based on agricultural land expansion limits, and for each of these sub-branches, three additional sub-scenarios are defined based on crop yield sensitivity analysis, resulting in a total of 18 scenarios. The Baseline scenario assumes no emission constraints and maintains the status quo. Organic agricultural land expansion is limited to a target of 30% by 2050. Two sub-branches are explored:

- Free agricultural land expansion, where there are no constraints on land use changes.
- Constrained agricultural land expansion, where organic agricultural land is limited to a maximum of 50% by 2050.

The Intermediate scenario builds on the Baseline scenario, maintaining the same 30% organic target by 2050 but introducing a net-zero emissions constraint that accounts for the role of forests in carbon sequestration. As in the Baseline, this scenario also includes the same two sub-branches: free and constrained agricultural land expansion. The Sustainable scenario represents the most transformative pathway. Organic agricultural land expansion reaches 50% by 2050, and a stringent negative emissions target is imposed, requiring forests to offset all residual agricultural emissions The main assumptions behind the projections of future parameters in TIMES-SE – including macroeconomic drivers and AFOLU-specific trends – are harmonized across all scenarios. AFOLU projections are based on a common set of socio-economic drivers (e.g., population, land availability), and all scenarios are designed as exploratory policy relevant trajectories reflecting different levels of mitigation ambition. While the AFOLU sector is modeled using identical demand drivers across scenarios, differences emerge from the implementation of specific constraints or policy targets (e.g., emission reduction, organic farming expansion, afforestation), which represent distinct visions of governance.

Sectoral demand can grow proportional to Population (as it happens for residential and AFOLU) or with GDP (for commercial, industry and transport). The drivers evolution for the TIMES-SE demands are provided in Figure 30. In terms of absolute value, Swedish population is expected to start from 10.4 billion in 2022 and reaching 12.4 billion in 2050. In line with the FABLE Swedish report hypothesis for the baseline scenario [228]. The GDP has been derived

according to OECD long term forecast national projection for Sweden [240]. Starting at 532.2 billion $ at 2019 and reaching 986.4 billion $ at 2050.

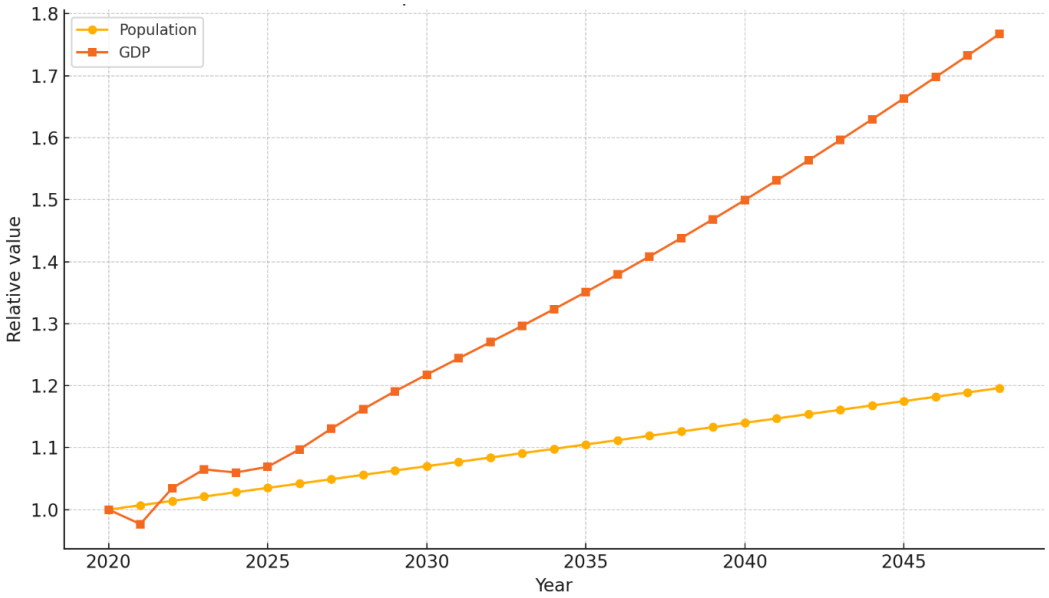

Figure 30. Driver Projections for the modelled years. GDP and Population are shown starting from 2019 to 2050.

While FAO remains a primary reference, it does not provide complete datasets - particularly with regard to costs and crop yield projections. Therefore, additional sources are integrated to support the scenario narrative, especially for yield trends. Depending on the narrative, both optimistic and pessimistic assumptions can be adopted to reflect different future developments. In the absence of a comprehensive database detailing average national or European-level costs for crop mitigation options (e.g., greenhouse systems), cost estimates have been sourced from specific European case studies, such as aquaponics systems [218].

The three narrative scenarios are also divided into two sub-branches for agricultural land expansion: free and constrained. For each of these six final scenarios (two sub-branches per primary scenario), a sensitivity analysis on crop yield improvements is conducted, resulting in three sub-scenarios:

- **No improvement (sub-scenario 1):** Assumes no changes to current cropping practices or fertilizer use, with crop yields remaining constant.
- **Base improvement (sub-scenario 2):** Assumes yield increases driven by enhanced fertilizer use, following FABLE 2023 base (pessimistic) projections. Emissions increase proportionally with crop yield improvements.
- **Optimistic improvement (sub-scenario 3):** Assumes higher yield improvements aligned with FABLE 2023 optimistic projections, with emissions scaling proportionally to yield changes.

Data on crop yield reductions for organic farming and future yield projections for both open-field and organic systems have been taken from the FABLE report for Sweden [228]. These sources ensure consistency and comparability across studies. To maintain clarity, crop

yield projection and organic reduction are systematically reported in Table 37. Table 37 provides both general yield reduction between open field and organic at the base year, as well as the 2050 crop yield increase assumptions, due to forecasted improvements of agricultural techniques and, for open field, of fertilizer efficiency. It's observable how, for optimistic assumptions, there's a threshold value for both, indicating a limit for enhanced agricultural techniques to provide a contribution. In terms of crop yield reduction, not all the crop present data. Therefore, for these ones no organic crop variation has been modelled.

Table 37. Crop yield variation projection in 2050 under pessimistic and optimistic hypothesis according to FABLE Swedish report [227].

Crop	Organic vs. conventional yield reduction	Pessimistic		Optimistic	
		Conventional	Organic	Conventional	Organic
Cereals	48.6%	40%	27%	55%	55%
Legumes	30.8%	38%	22%	54%	54%
Woody crops		23%		47%	
Roots	62.9%	34%	34%	51%	51%
Seeds	68.0%	28%	50%	48%	48%
Vegetables		39%		59%	

In total, the framework includes 18 scenarios: 6 final scenarios (2 sub-branches for each of the 3 primary scenarios) multiplied by 3 crop yield sensitivity sub-scenarios.

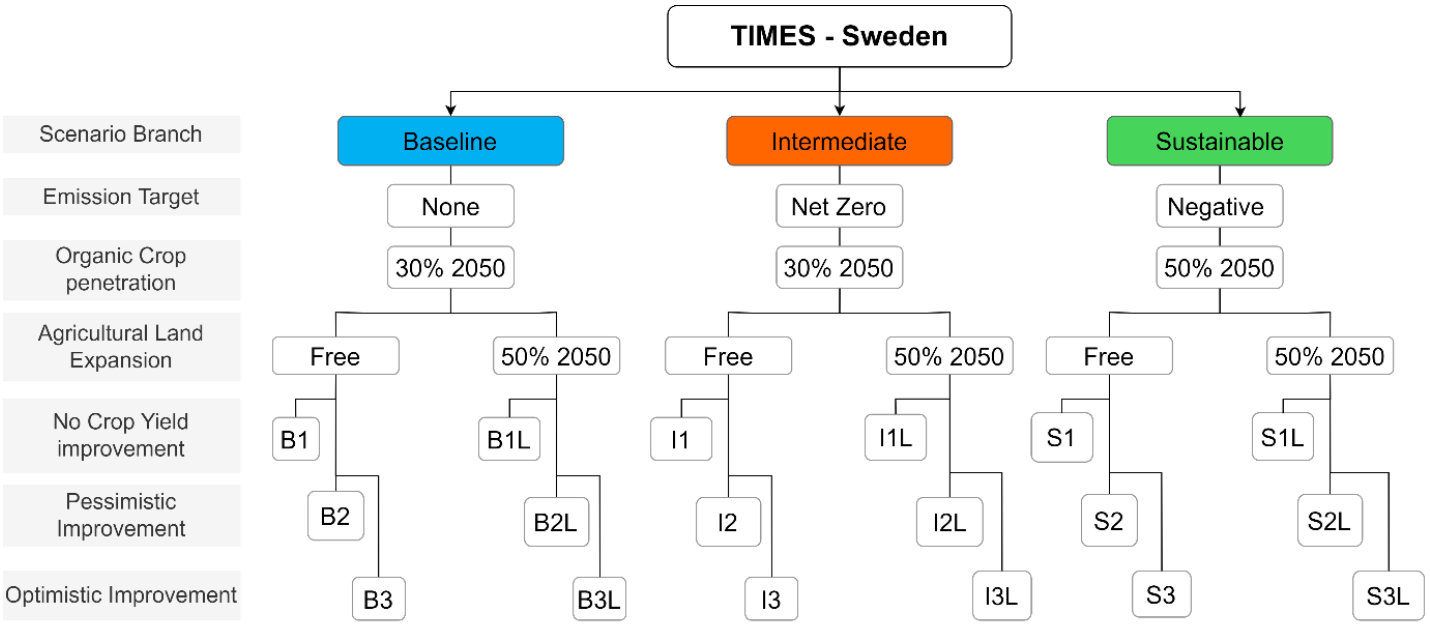

Figure 31. Scenario tree for the three decarbonization pathways of the AFOLU sector.

3.3.2. Swedish results

This section describes results of running scenarios of Figure 31. It starts with the results peculiar of the energy system such as the Total Primary Energy Supply (TPES), the power production by source, and global emissions. Then, role of the AFOLU sector is detailed, respectively focusing on the technology, resource use and emission dynamics internal to the sector.

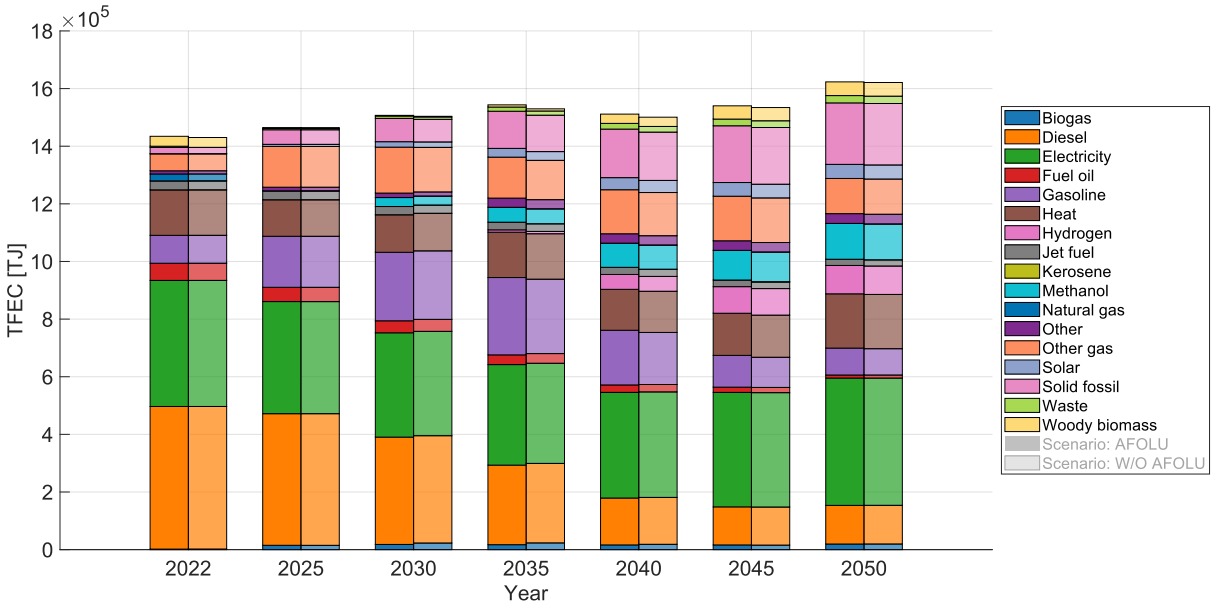

Figure 32. Total Final Energy Consumption (TFEC) by consumed commodity in TIMES-SE with (darker) and without (lighter) AFOLU module.

For the global energy system results, it should reflect the expected impact of the AFOLU module where relevant, while ensuring that its introduction does not produce unintended effects outside its designated domain. As illustrated in Figure 32, which presents the Total Final Energy Consumption (TFEC) by sector, there is a clear similarity between the two bars: the lighter bars (without AFOLU) and the darker ones (with AFOLU). This consistency confirms that the AFOLU module functions as intended, without altering broader system dynamics. By looking at results is clear that the Swedish energy system exhibits a strong reliance on diesel and electricity, which together account for approximately 64% of total final energy consumption. Over time, diesel gradually declines, primarily in favor of electricity and gasoline, a shift that is largely driven by structural changes within the transport sector (not shown). A particularly relevant aspect concerns biogas utilization. While its source changes - being exclusively an imported commodity without AFOLU and partially derived from domestic AFOLU bio-production in the second case - its overall penetration in the energy system remains largely unchanged. This stagnation can be attributed to the low competitiveness of biogas

plants, limiting it to 0.13 TJ in 2022 and then slightly decreasing. In the same way, the electricity production by source of do not present significant alteration between its two instances. Indeed, the electricity production mix of Figure 32 where in both the cases the energy mix is initially dominated by hydroelectric, nuclear, and wind power. However, as the system evolves, a substantial shift towards a fully renewable energy mix becomes evident. By 2050, hydroelectric, wind, and solar power are projected to constitute approximately 21%, 33%, and 42% of total electricity generation, respectively. This transition results in the complete phase-out of nuclear power, marking a decisive shift toward a decarbonized electricity sector. Simultaneously, the total electricity production increase of around 5% from 2022 to 2050, driven by transformations in transport, industry, and commercial sectors.

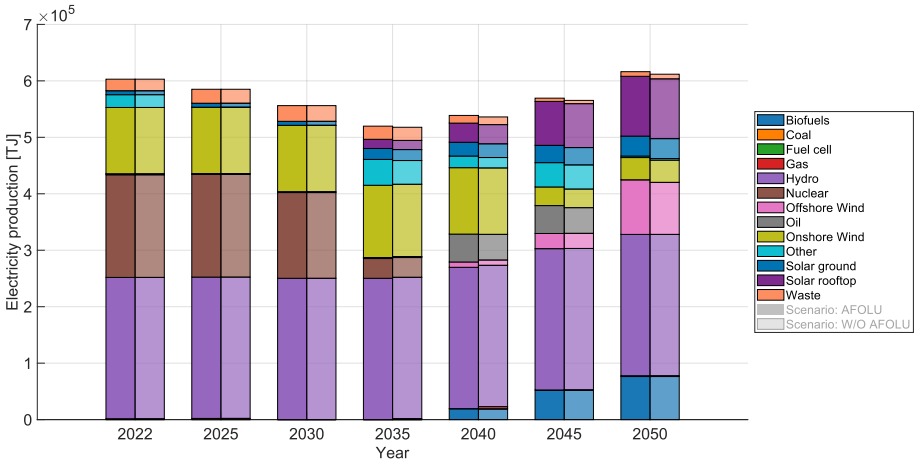

Figure 33. Electricity production mix with (darker) and without(lighter) AFOLU module

This increasing demand is met entirely by renewable sources, reinforcing the alignment of the energy system with long-term sustainability objectives. The observed electrification trend, particularly in transport and industrial applications, is further corroborated by a deeper analysis of sectoral results (not shown), which highlight a systematic transition away from fossil fuel dependence. The global greenhouse gas (GHG) emissions trends in the base scenario are illustrated in Figure 34, comparing the system with and without AFOLU. The inclusion of the AFOLU module in leads to an overall higher GHG emissions profile due to the additional accounting of emissions from the AFOLU sector. This confirms that the module introduces relevant emissions without altering sectors outside of its scope. In 2022 total GHG emissions are around 60’000 (without AFOLU) and 68’000 (with AFOLU) kt CO_2-equivalent, with $GHGCO_2$ (violet area) representing the dominant source, followed by other non-CO_2 gases such as Over time, emissions first increase and then decrease in both cases, reaching approximately the original value of 2022 at 2050. At those data it has to be added the contribution of forest that are equal in both cases (-17’000 kt CO_2-equivalent) not shown to preserve plot interpretability. However, the AFOLU presence introduces additional emissions from the AFOLU sector, which are absent in the original version, The CO_2 sink (CO2NSINK, orange area) related to HWP. A key takeaway is that the AFOLU sector adds both sources and sinks of emissions, leading to a net increase in total GHG emissions when fully accounted for. Importantly, non-AFOLU emission categories—such as $GHGCO_2$ from energy and transport—

remain largely unchanged between the two cases, demonstrating that the AFOLU module does not interfere with the emissions trajectory of other sectors. Taken together, the analysis of these three key energy system trends - total final energy consumption, emissions, and electricity production - demonstrates that the introduction of the AFOLU module does not introduce unintended distortions in the broader energy system. Instead, its effects remain confined to its designated domain, ensuring that the overall model maintains internal consistency and correctly reflects expected energy transition dynamics. GHGCH_4 and GHGN_2O.

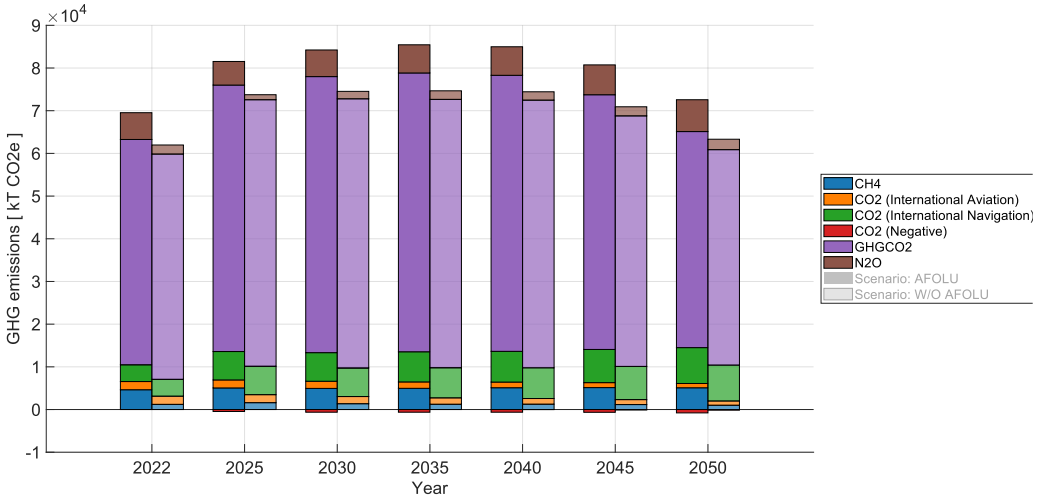

Figure 34. Emissions by gas type in TIMES-SE with (darker) and without (lighter) AFOLU model.

Concerning AFOLU, crops and livestock production sector is presented in Figure 35 and Figure 36 respectively. Figure 35 illustrates crop production by type across 18 scenarios, compared to the base year (first column). In all scenarios, crop production in 2050 slightly increases to meet projected demand, with almost negligible variation. Two distinct scenario clusters emerge based on organic cropping penetration. The first one includes all the base scenario plus I2 and I2L. Here, due to the economic advantage of conventional cropping methods over organic farming, organic crops account for only 8% to 13% of total production, adhering to the minimum organic cropping area constraints, which impose a 30% (notice that the constraint is on area and not on production). The second cluster comprises scenarios with partial organic adoption. In these cases, the model favors organic crops when decarbonization is required, assuming constant or optimistic yield scenarios without significant land-use restrictions. Here, a production going from 5.2 to 7.7 Kt of organic crop in 2050 is observed. However, under intermediate yield assumptions, the model shifts preference to open-field cropping, emphasizing the environmental-economic trade-offs and the critical role of yield. At the same time, both aquaponic and greenhouse do not find space, mainly for economic reason.

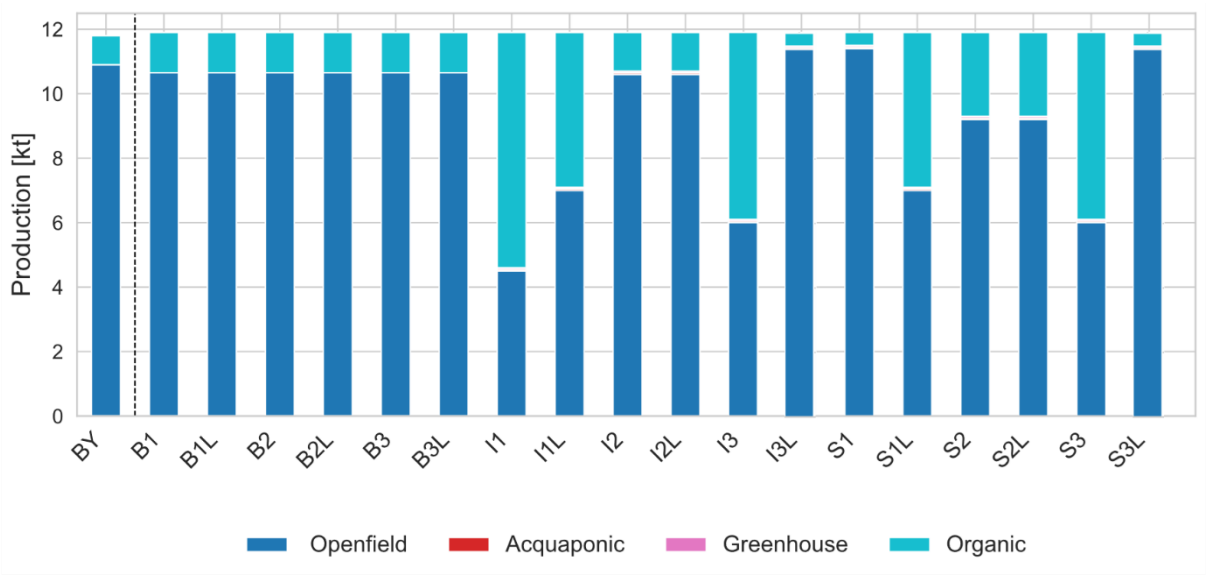

Figure 35. Crop production by type in the 18 different TIMES-SE Scenarios.

Then, Figure 36 illustrates livestock production by type (anaerobic digestion, livestock farm, and livestock grazing) for the base year (2022) and two selected scenarios (B1 and S1) in 2050.

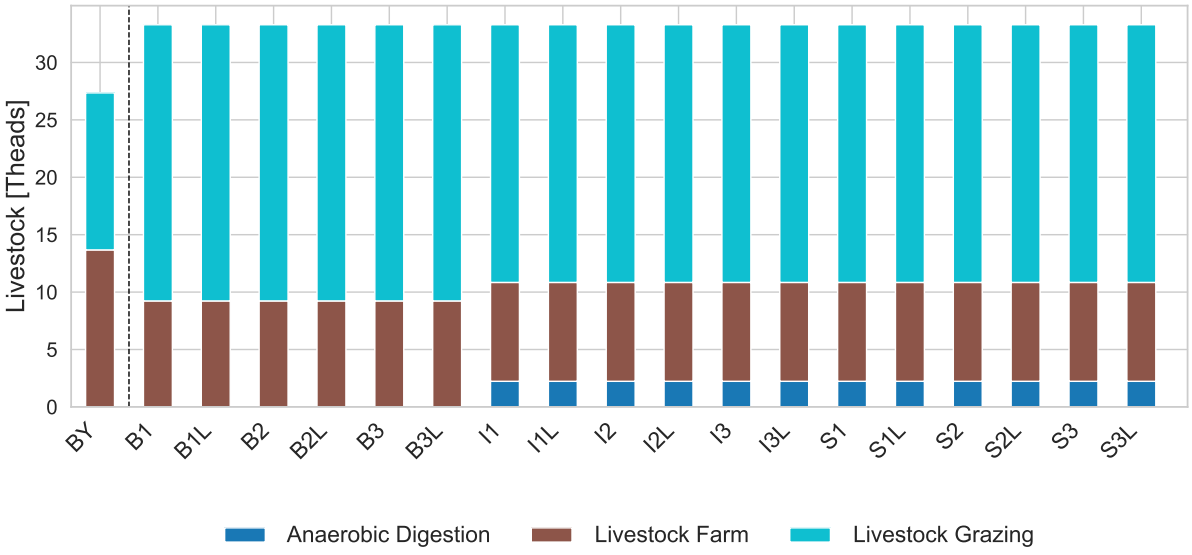

Figure 36. Livestock production by type.

Again, the total production slightly changes and remain quite stable, following the drivers of population projection. In both scenarios, livestock grazing dominate production, accounting from the 67% (Intermediate and Sustainable) to 74% (Base) of the total production at 2050. Anaerobic digestion emerges as a minor contributor in 2050, appearing only in scenario S1, suggesting the potential for diversification in livestock production methods under specific scenario conditions. The consistency in values across the 18 scenarios is reflected in the similarity between B1 and S1, which represents the general behavior of all analyzed cases.

For the environmental impact assessment of the AFOLU sector, result starts with emissions, in Figure 37 two different representations of the same amount are presented. Figure 37a represents the overall AFOLU emissions at the base year and at 2050, for all the 18 scenarios analyzed, divided by type of GHG. Figure 37b collects the emissions by source.

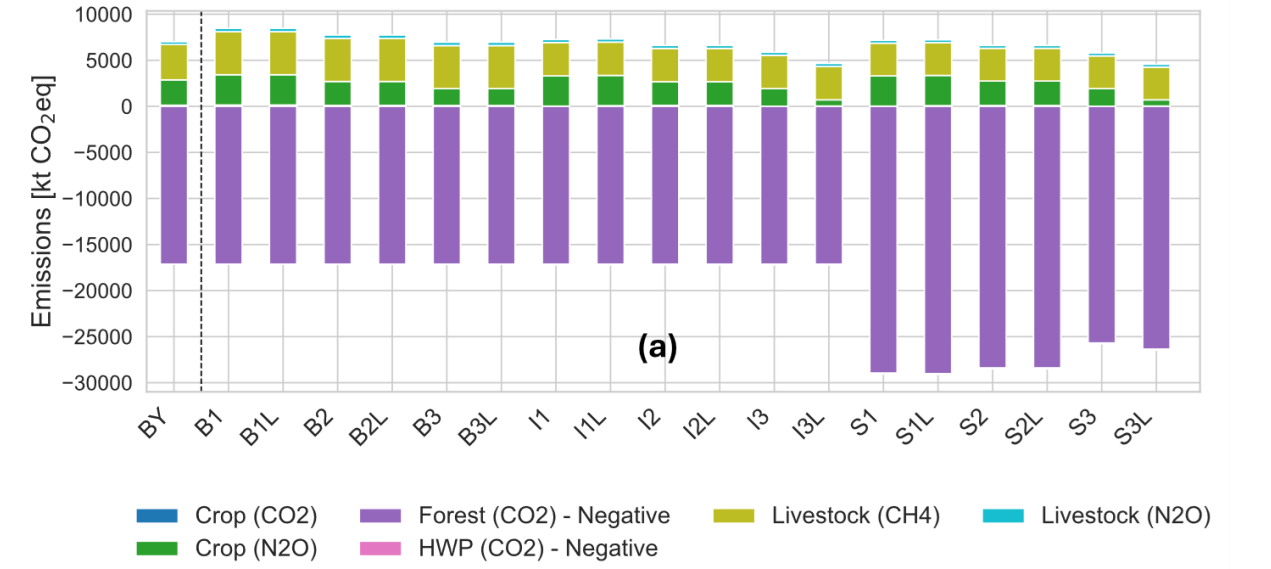

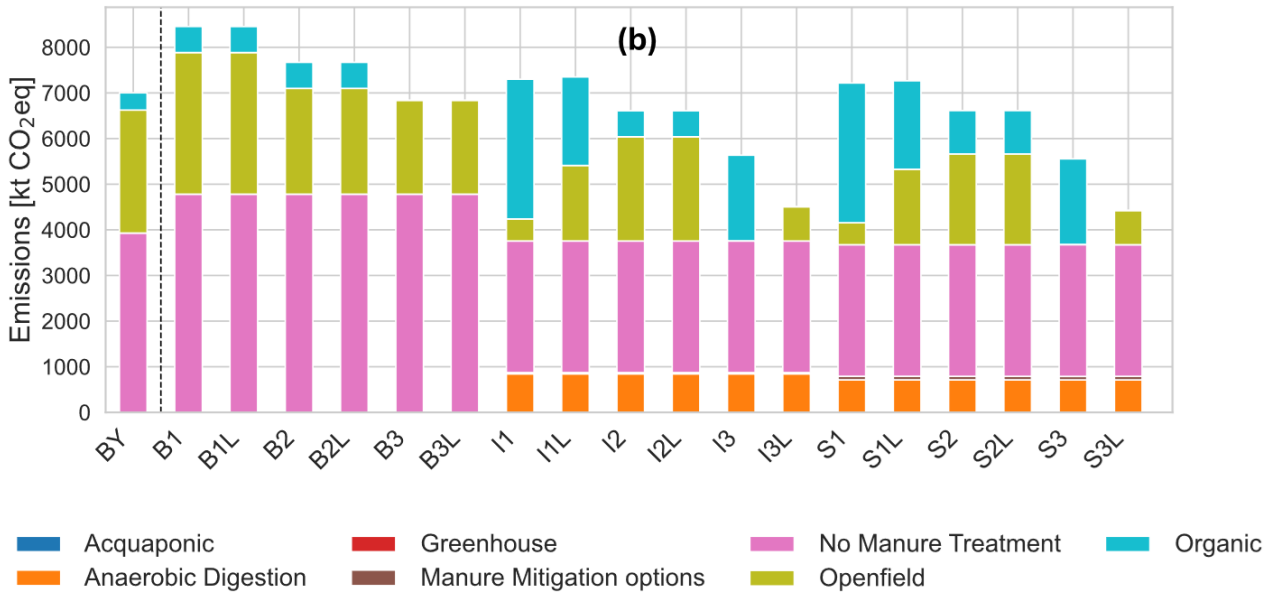

Figure 37. AFOLU emission by type of GHG (a) and by source (b). BY is on the right side of the plot while the 2050 configurations of the analyzed scenarios are on the left.

Methane emissions from livestock, driven primarily by enteric fermentation (GHGCH4LIV), and nitrous oxide emissions from crops (GHGCRPN2O), resulting from the application of organic and inorganic fertilizers, emerge in Figure 37a as the dominant contributors. Across the scenarios, a general trend of emissions reduction is evident as the system transitions from the baseline to more sustainable scenarios. Initial net emissions (~8,500 $ktCO_2eq$ in the baseline scenario) decline, reaching approximately ~3,700 $ktCO_2eq$ in the intermediate scenario (I3). Simultaneously, forest carbon sequestration compensates for these emissions, with net absorption increasing from -17’000 $ktCO_2eq$ in the baseline to as much as

-29’000 $ktCO_2eq$ in the sustainable scenarios. Among scenarios governed by the same decarbonization constraints, significant shifts in emissions patterns are primarily driven by variations in crop yields and, to a lesser extent, by limitations on land expansion. Notably, in the I3 and S3 scenarios, characterized by maximal crop yields and an absence of constraints on organic cropping, emissions from crops are nearly negligible. Figure 37b illustrates a significant shift in emissions contributions among various sources across the investigated time horizon. The emission peak is at approximately 3600 $ktCO_2eq$ in the baseline scenario (B1L) and decrease to nearly zero in the intermediate (I3) and sustainable (S3) scenarios. This reduction is counterbalanced by a substantial increase in emissions from organic cropping under certain conditions. For example, in decarbonized scenarios such as I1 and S1, where crop yields are static and land expansion is unconstrained, organic crops cover most agricultural land. This leads to a positive emissions contribution of approximately 3300 $ktCO_2eq$ - roughly 8% lower than the emissions associated with a fully open-field cropping solution for meeting the same demand. In contrast, emissions from anaerobic digestion and manure management, as well as their associated mitigation options, exhibit greater stability across scenarios. This indicates a lower propensity for change, despite the presence of both economic (least-cost optimization) and environmental (decarbonization constraints) pressures.

Key environmental variables in the AFOLU sector include water and land use, as shown in Figure 38a and Figure 38b, respectively. Regarding water consumption (Figure 38a), the total withdrawal is approximately 67 Mm^3, with 41% attributed to the livestock sector and the remainder to crops. In all baseline scenarios, water consumption patterns closely follow increasing demand, reflecting an unchanged technological mix and minimal deviation from the original usage patterns. A notable shift occurs in the intermediate and sustainable scenarios with the introduction of anaerobic digestion livestock technologies, linked to anaerobic digesters. This shift is driven by decarbonization constraints that promote biogas utilization, maximizing the share of livestock-related technologies within the broader energy system. Within this framework, three scenarios (I3, S1, and S3) emerge as outliers due to a common underlying phenomenon. Specifically, these scenarios exhibit a sharp increase in water usage by organic crops, reaching approximately 100 Mm^3. This trend aligns with the results in Figure 38b, highlighting that under decarbonization constraints and the absence of land expansion limitations, the model prioritizes organic cropping. For example, in Figure 38b is possible to observe that the full organic cropping penetration is selected by the model only in I3 and S3, where decarbonization and land expansion drivers create the basis for organic farming development. While organic crops have lower yields and emissions, they require significantly higher water and land use to produce the same output. Consequently, the scenarios with the lowest emissions peaks are associated with higher water and land usage by crops. Another notable trend is the overall reduction in water and land use as crop yields improve, particularly in the transition from scenario 1 to scenario 3. Furthermore, under land limitation constraints, the model shifts toward open-field cropping systems, which are characterized by higher yields and reduced land requirements.

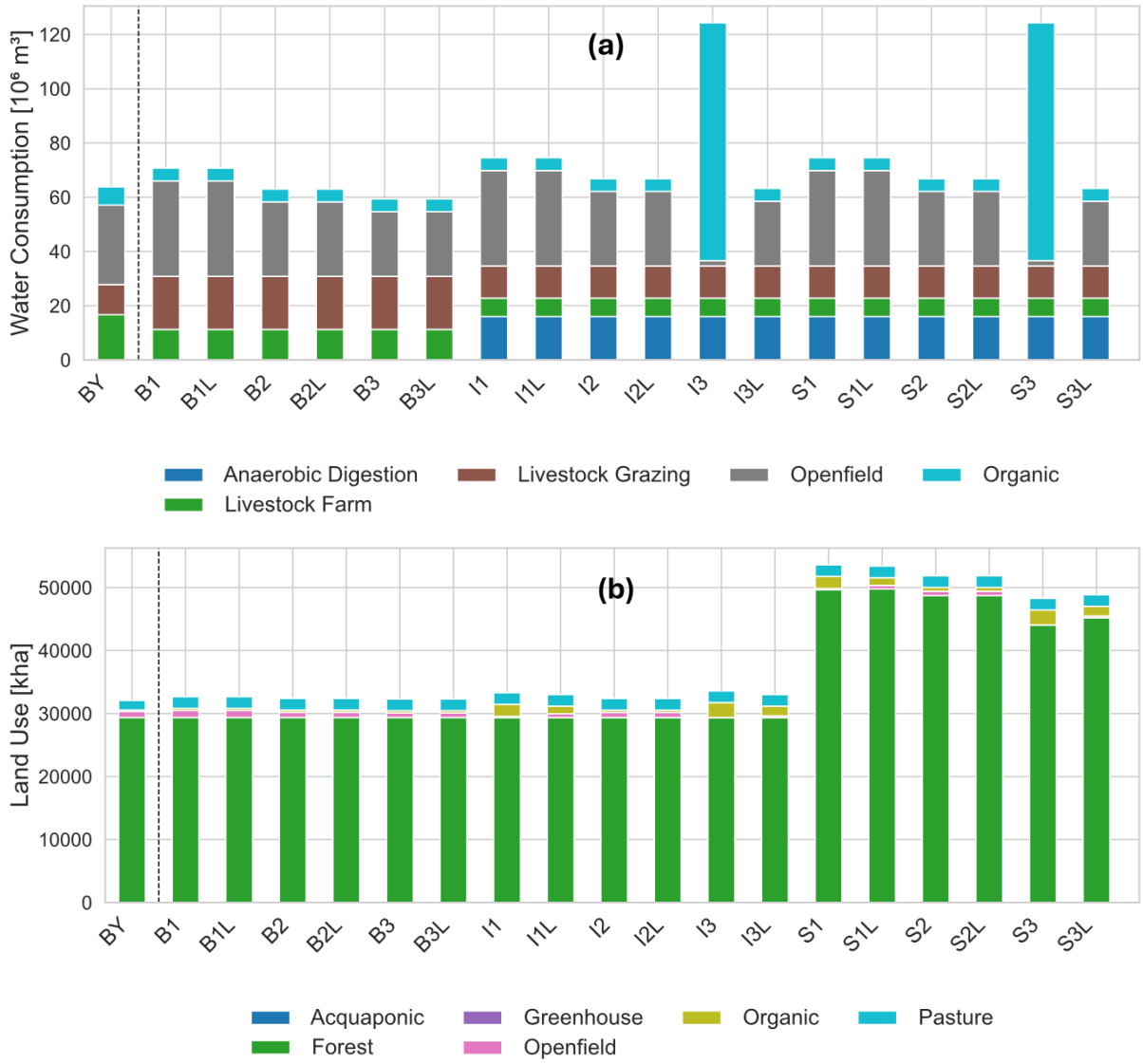

Figure 38. Water (a) and land (b) use by AFOLU sector at the base year (first column) and last year (2050) for the 18 analyzed scenarios.

3.3.3. Italian case study and scenario

The Italian case study represents a complex interplay of different stressors for the AFOLU sector, given its relatively high population with respect to the available surface, the mediterranean climate and expected effects of climate change, and the strong effort required to the AFOLU sector by the different stated policies. Indeed, Italy's National Energy and Climate Plan (PNIEC) [241] identifies a rapid expansion of renewable energy and bioenergy as cornerstones of its 2030 mitigation strategy, exerting new pressures on land and resource systems. At the same time, the National Climate Change Adaptation Plan (PNACC) [242] highlights vulnerabilities such as drought risk, desertification in southern regions, and the sensitivity of agricultural systems to extreme weather events and rising temperatures. Complementing these, the Farm to Fork Strategy [243] calls for systemic transformations in agriculture, promoting agroecological approaches, carbon sequestration, and sustainable land

use. In this landscape, the AFOLU sector emerges as both a driver and a bottleneck in the national transition [102]. However, most integrated assessments analysis of the Italian energy transition either neglect land-use interactions or rely on oversimplified assumptions that fail to capture the evolving role of AFOLU within broader energy system planning [244]. This is due, in part, to modelling limitations: land use and agriculture are often weakly represented in energy models, or are excluded altogether, despite their relevance in mitigation scenarios involving bioenergy, BECCS, or nature-based solutions [100]. The selected energy modelling framework is TEMOA – Italy, extensively detailed in Appendix A1.

Figure 39 presents an overview of Italy's greenhouse gas emissions in 2020 [245], with a particular focus on the AFOLU. Figure 39a displays a bar chart of total emissions by sector. The transport, energy, and industry sectors emerge as the highest contributors to national emissions, accounting together for around 60% of total emissions, followed by buildings and waste. While agriculture contributes a smaller share in relative terms, land use, land-use change, and forestry (LULUCF) sector exhibit net negative emissions, highlighting its role as a carbon sink. Figure 39b provides a detailed breakdown of emissions within the agricultural sector. Enteric fermentation from cattle is the largest source, contributing 33.4% of total agricultural emissions. This is followed by manure applied to soils (20.6%), emissions from inorganic fertilizers (13.9%), swine (9.9%), poultry (7.5%), and other animal-related sources (6.6%). Additional smaller sources include emissions from grazing animals (2.3%), organic fertilizers (5.6%), and field burning (0.1%).

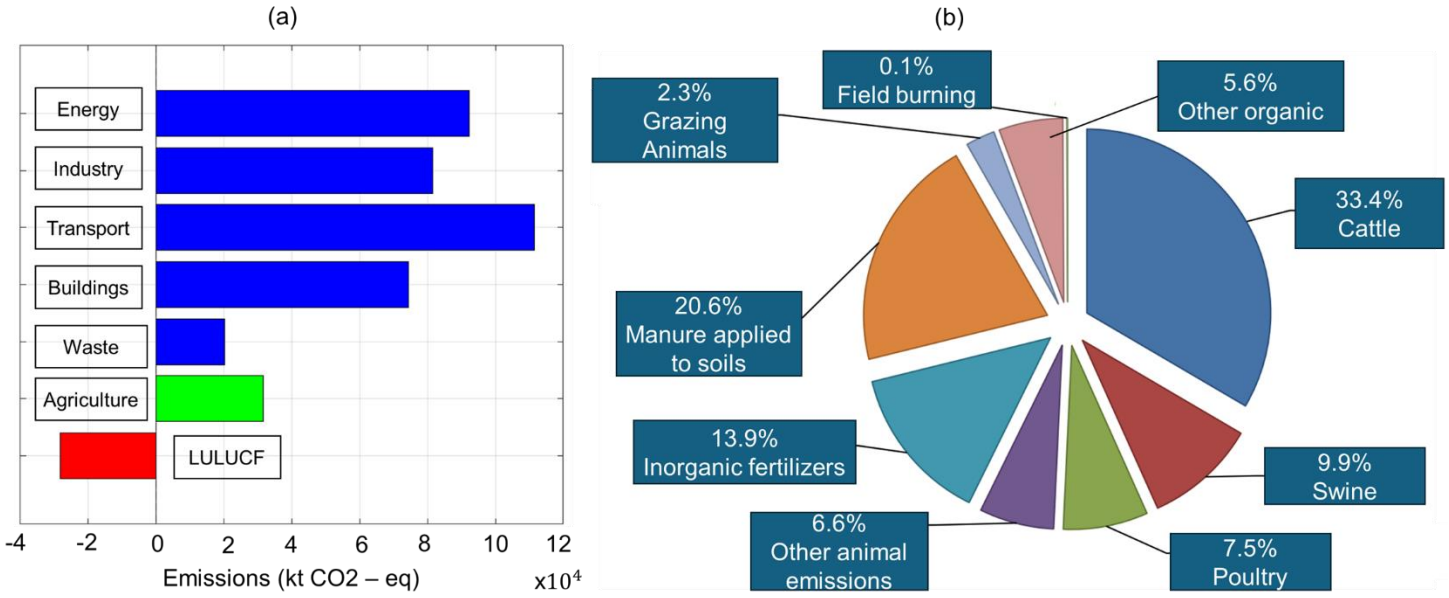

Figure 39. Italian GHG emissions by sector (a) and agriculture emissions by source (b) [245].

The modeled energy scenario impacts both the energy and the AFOLU domain. Concerning the future evolution of the energy system, TEMOA-Italy assumes the phase-out of coal-fired power plants no later than 2030, includes maximum capacity and activity constraints taken

from [246] for renewables and assumes import/export exchanges are nor higher than 2022 levels, taken from [247], for each energy commodity. Among those presented in Figure 40, scenarios involving an emission reduction pathway include a limit on the total CO_2^{EQ} emissions implementing the -55% emissions target stated by the "Fit for 55" EU package [248] for 2030 compared to 1990 and the net zero target set by the PNIEC, as well as by the Long-term Italian strategy for greenhouse gas emission reduction [249].

For the AFOLU sector, the analysis covers the challenges announced under the Farm to Fork strategy on biodiversity and food chain circularity, namely, reducing pesticides and fertilizers and increasing the share of organic farmland by 2030. Figure 40 summarizes the scenario features modelled in TEMOA-Italy to explore the effects of the Farm to Fork strategy. To limit the consumption of pesticides and fertilizers, in the two alternative scenarios (-PES and -FER), two external constraints are introduced respectively on the supply analysis focused on the assessment of the new Farm to Fork policy for 2023–2027, which is a key pillar of the European Green Deal [58]. As represented in Figure 40, eight scenarios are investigated to observe any changes in model behavior introduced by the new component and to better capture trade-offs and synergies resulting from the integration of this sector.

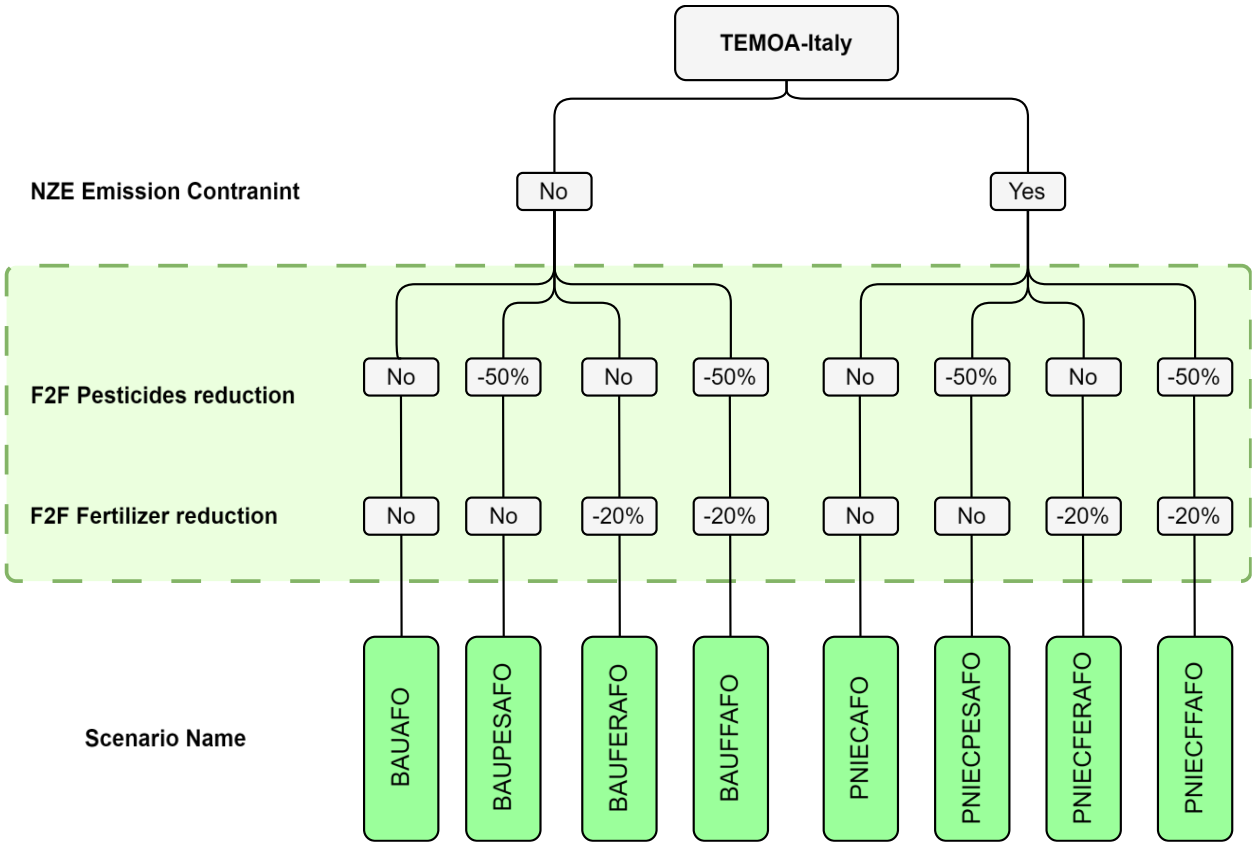

Figure 40. Scenario tree.

Intermediate scenarios involving the partial application of Farm-to-Fork constraints were omitted due to the absence of significant differences worth reporting, allowing the analysis to focus on the most relevant ones.

3.3.4. Italian results

This section starts with generic energy system results such as Total Primary Energy Supply (TPES), power production by source, and global emissions, to highlight the AFOLU role in the broader perspective. Then, provides a detailed analysis of AFOLU specific results, focusing on the technology, land use and emission dynamics internal to the sector. Since the analysis of the eight modeled scenarios revealed that two scenario clusters were effectively equivalent in their energy system characteristics, such that the application of AFOLU-specific constraints produced no discernible macro-scale effects on aggregated energy system variables. Consequently, for clarity and conciseness, only the BAU and PNIEC scenarios are presented in detail.

Across the two scenarios shown, the energy system undergoes a marked transition both in terms of GHG emissions and TPES.

a illustrates the sectoral breakdown of emissions in kilotons of CO_2-equivalent, while

b presents the corresponding TPES, categorized by fuel type and reported in petajoules (PJ). In the initial scenario. In both Figure 40 (a) and (b) BAU and PNIEC 2020, 2030 and 2050 behavior are reported. In 2020, for both scenarios, total emissions exceed 320,000 kt CO_2-eq, with the Transport and Electricity sectors accounting for the largest shares—approximately 100,000 and 70,000 kt CO_2-eq, respectively.

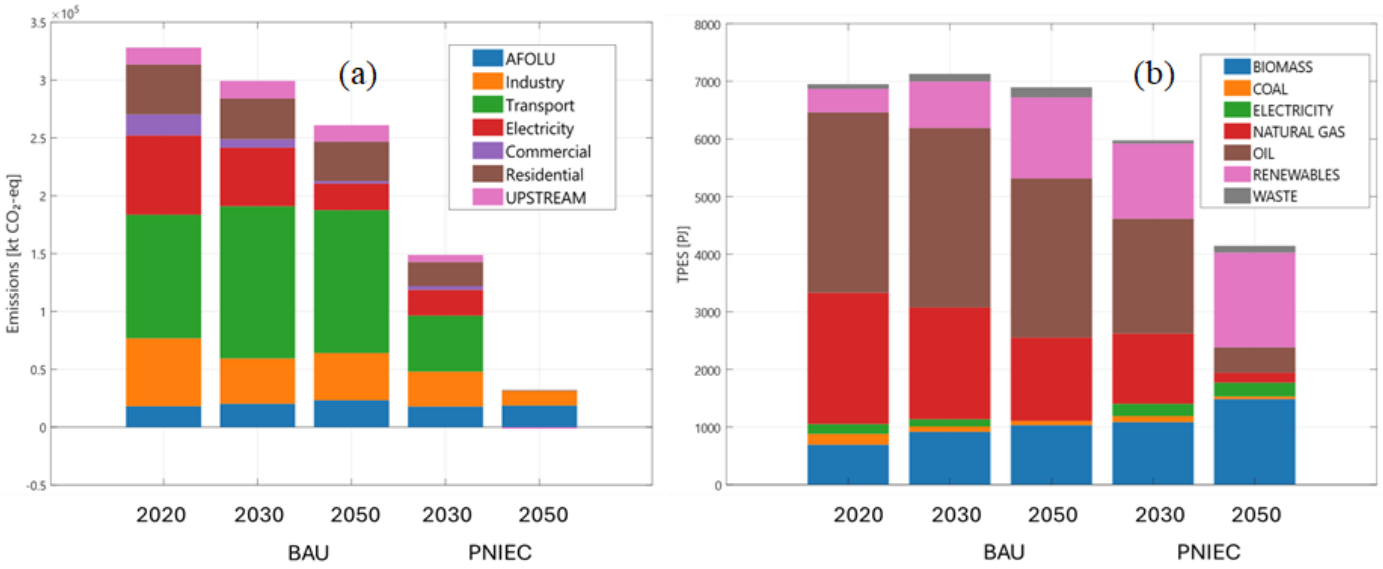

Figure 41. Sectoral greenhouse gas emissions (a) and total primary energy supply by source (b) across BAU and PNIEC scenario for TEMOA-Italy energy system.

The Industry and Residential sectors also contribute significantly, reflecting their high energy demand and fossil fuel reliance. Then, the difference in the two paths start arising. From 2030 BAU slightly reduces emissions, reaching approximately 260,000 kt CO_2-, with a 18% global reduction with respect to 2020. This transition is mainly driven by power sectors, which reach around one third of original emission, and commercial, shifting to carbon free inputs. In PNIEC, the scenarios progress, emissions decline sharply, reaching below 50,000 kt CO_2-eq in the final case. This reduction—more than 85%—is driven by near-complete decarbonization of the power sector, indicated by the disappearance of electricity-related emissions, as well as sharp reductions in Transport and Residential emissions. The Commercial and Upstream sectors also see modest but consistent declines. This decarbonization trend aligns with the transformation seen in TPES in Figure (b). In 2020, both scenarios are dominated by fossil fuels: oil and natural gas together make up the majority of most of the energy supply (~4500 PJ out of ~7000 PJ). BAU remains mostly the same, but with a significant substitution of renewable primary energy supply against oil and natural gas. Differently, in the PNIEC scenario, oil is nearly phased out and natural gas is reduced to a minor role. Renewables and biomass expand significantly, together comprising the largest share of supply (~3000 PJ out of ~4300 PJ). These patterns are also reflected in the power sector dynamics below in Figure 42. Indeed, the left plot (a) shows total installed capacity increasing steadily, from under 150 GW at 2020n to almost 300 GW in the PNIEC scenario at 2050. This rise is primarily driven by wind and solar, the capacity of which alone reach around 200 GW in the PNIEC at 2050, while for BAU in the same year, it remains limited to around 100 GW for both. In contrast, gas capacity remains relatively stable across scenarios moving from 2020 to 2050, reflecting its continued but limited role in flexible generation. Coal and oil capacities remain very low or phase out entirely due to PNIEC constraints. The electricity output (panel b) reflects these changes.

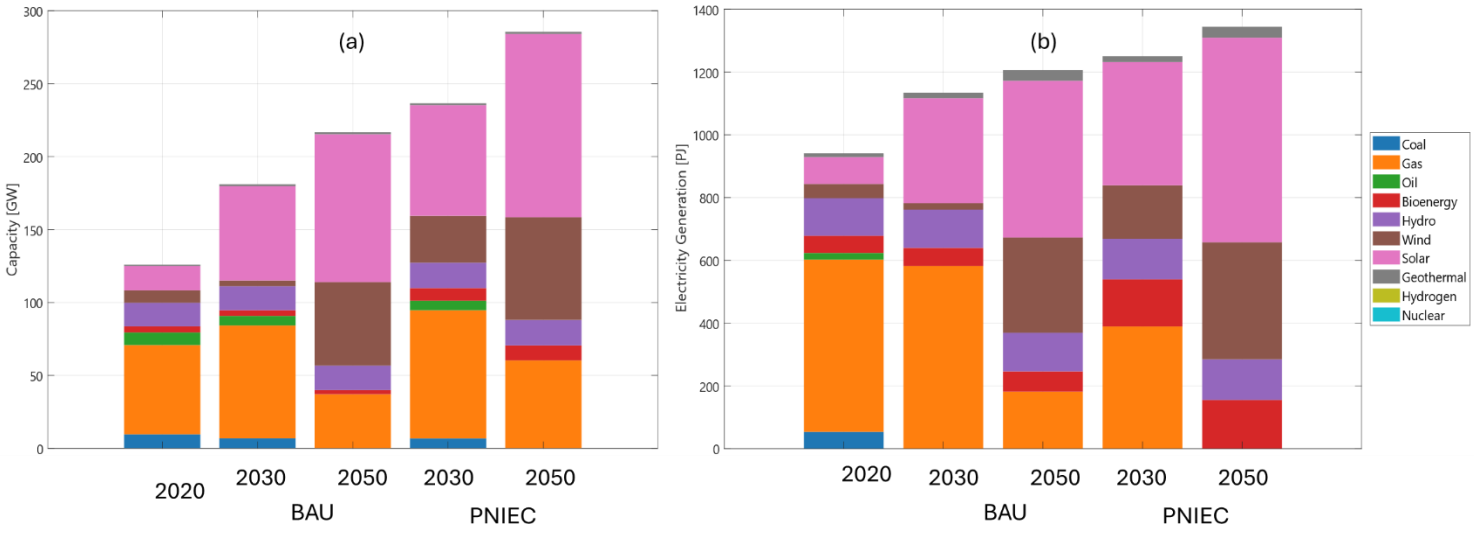

Figure 42. Evolution of electricity generation capacity (a) and actual generation output (b) across BAU and PNIEC scenario for TEMOA-Italy power sector.

Wind and solar represent most of the produced electricity, generating up to 75% of the total electricity supply in PNIEC. due to their lower capacity factors. Gas, stable in capacity, remains a stable contributor to generation - especially in mid-range scenarios - indicating its role as a

balancing or baseload technology. Hydro and nuclear remain steady in both panels, contributing to dispatchable low-carbon generation. Bioenergy makes a visible but modest contribution. After having discussed what happens to the energy system, it's necessary to dig down into the specific AFOLU subsectors, now referring to all the analyzed scenarios, as in Figure 43.

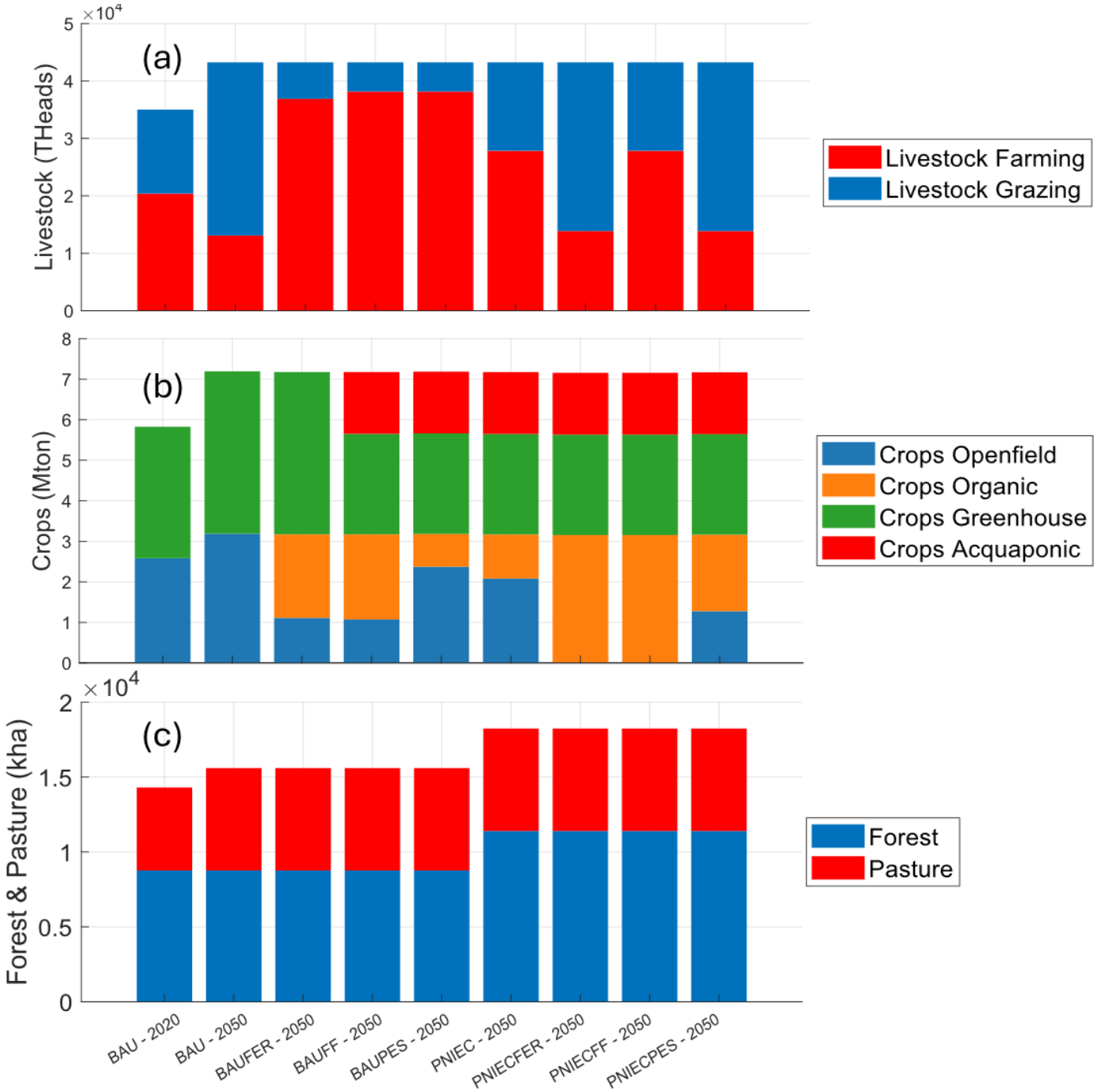

Figure 43. Changes in agricultural production, livestock systems, and land use under baseline and alternative scenarios to 2050. (a) Crop production is shown in million tons (Mt), disaggregated by cultivation system: open-field, organic, greenhouse, and aquaponic. (b) Livestock numbers are reported in thousand heads (k heads), distinguishing between farming-based and grazing-based systems.(c) Forest and pastureland areas are shown in thousand hectares (kha), highlighting shifts in land allocation between natural and managed ecosystems.

In Figure 43 (a) , total crop production increases from approximately 5.9 Mt in 2020 (BAU-2020) to around 7.5–7.8 Mt across 2050 scenarios. Open field systems decline from over 3.0 Mt in 2020 to under 1.5 Mt in PNIEC scenarios. Organic crops rise substantially, from near zero in 2020 to 2.0–2.5 Mt in 2050, becoming the second-largest contributor in all mitigation pathways. Greenhouse systems remain relatively stable, producing 2.2–2.5 Mt across scenarios. Aquaponic systems are absent in the base year but contribute consistently (~1.3 Mt) from BAUFER-2050 onward. In Figure 43 (b), total livestock increases from approximately 36,000 thousand heads in 2020 to just above 45,000 thousand heads in 2050. In the baseline year, grazing systems dominate, with over 20,000 thousand heads, while farming systems account for ~16,000. By 2050, the distribution reverses. Farming-based systems expand to ~30,000 thousand heads in all scenarios, while grazing systems shrink to ~14,000 thousand heads, indicating a structural shift in animal production systems. In Figure 43 (c), land use for forest and pasture increases from ~14,000 kha in 2020 to over 18,000 kha in PNIEC scenarios. Forest area grows from ~9,000 kha to 11,000–12,000 kha by 2050, reflecting large-scale afforestation. Pasture area increases moderately from ~5,000 kha to 6,000–6,500 kha, maintaining a stable share of total land use. Together, forest and pastureland expand to nearly 18% of national territory by 2050, up from ~14% in 2020.

A significant attention must be paid to the emissions. Indeed, AFOLU has been proved contributing to one-quarter of global mitigation pledges for 2030 [250]. Therefore, both the positive and negative role of emissions is detailed below. In particular, the issue is explained by keeping the positive and negative contribution separated, in order to differentiate between what is a source and what is a sink. The emission trend for the different scenarios and the difference in total emissions from 2020 to 2050 are shown in Figure 44.

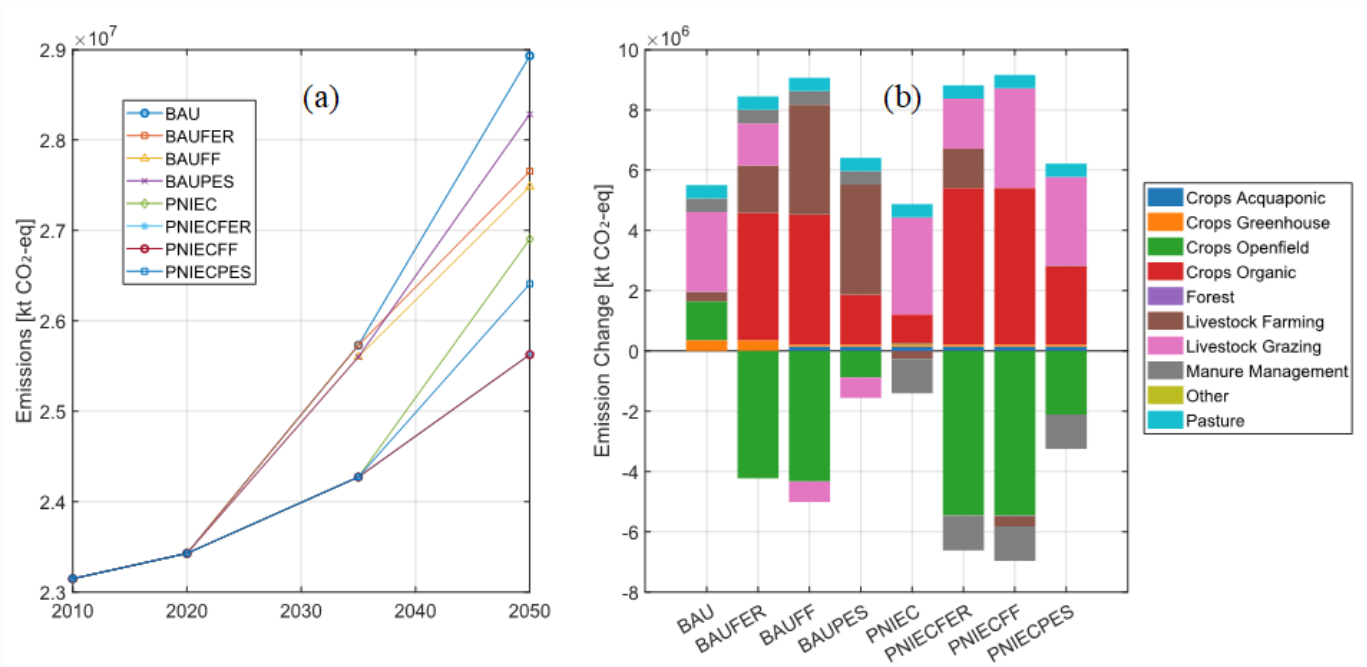

Figure 44. Positive AFOLU emission trend (a) and 2020-2050 positive emission change by source (b).

Panel (a) shows a nearly flat trajectory from 2010 to 2020—rising from ≈2.31×10⁷ to ≈2.35×10⁷ kt CO_2-eq—followed by divergence after 2030. By 2035 most scenarios cluster between 2.45–2.55×10⁷ kt, while by 2050 the spread widens markedly: BAU attains ≈2.90×10⁷ kt, BAUPES ≈2.85×10⁷ kt, BAUFER and BAUFF ≈2.72–2.75×10⁷ kt, PNIEC ≈2.70×10⁷ kt, PNIECPES ≈2.67×10⁷ kt, and PNIECF/PNIECFER the lowest at ≈2.60–2.65×10⁷ kt. Relative to 2020, 2050 increments therefore range from ~+2.5×10⁶ kt (PNIECF variants) to ~+5.5×10⁶ kt (BAU), implying a scenario spread of roughly 3×10⁶ kt by mid-century. Panel (b) decomposes the 2020→2050 change (units 10⁶ kt CO_2-eq) and reveals common structural features across scenarios. The largest negative contribution stems from Crops Openfield (typically −4 to −6), partly offset by a smaller negative from Manure Management (≈−0.5 to

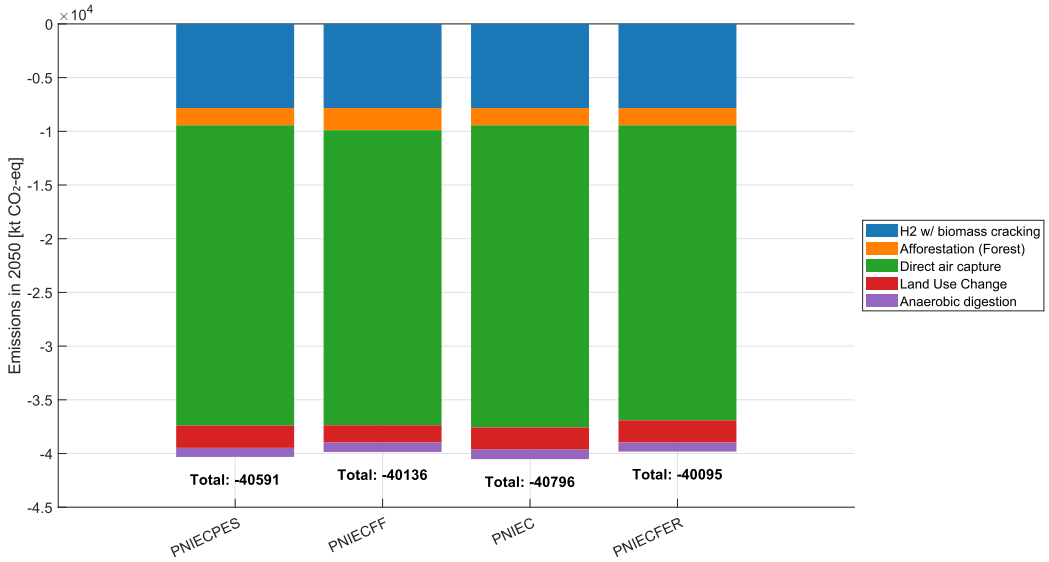

Figure 45. Negative emission technologies contribution in 2050 for net zero emission scenarios.

−1.5). Positive contributions dominate elsewhere: Crops Organic provides the single largest increase (≈+3–5), Livestock Grazing adds ≈+2–3, and Livestock Farming ≈+1.5–2.5. Forest is consistently positive (≈+0.8–1.8), Pasture small but positive (≈+0.4–0.8), while Crops Greenhouse and Aquaponic contribute modest gains (≈+0.3–0.6 and +0.1–0.3, respectively); "Other" sources are minor (≈+0.1–0.3). Summing segments yields net changes of about +5–6 (BAU), +8–9 (BAUFER), ~+9 (BAUFF), +6–7 (BAUPES), ~+5 (PNIEC), +8–9 (PNIECFER), ~+9–9.5 (PNIECF), and +6–6.5 (PNIECPES) ×10⁶ kt CO_2-eq. Thus, although the open-field reduction is substantial, increases from organic cropping and livestock-related sources dominate the balance, producing positive net changes in every case; the PNIEC-family trajectories moderate absolute 2050 levels by ≈0.2–0.3×10⁷ kt relative to BAU, with residual differences governed by the relative strength of open-field reductions versus organic and livestock increases. The same attention must be devoted to negative emissions in Figure 45.Figure 45 shows stacked negative emissions in 2050 for four scenarios (PNIECPES, PNIECFF, PNIEC, PNIECFER), with each bar summing contributions from six technologies. Total removals cluster tightly around 40 Mt CO_2-eq. In all cases, Direct Air Capture dominates the stack, providing about two-thirds of total removals (27.5–28.1 Mt CO_2-eq; 68–70%). Bio-hydrogen with geological storage is the second-largest wedge at ~7.8 Mt CO_2-eq (19–20%). Forest components appear as two distinct slices: capture by forest and land use change, and

together contribute ~3.7–4.1 Mt CO_2-eq (≈10% combined). Anaerobic digestion finally adds a small but visible segment of ~0.84–0.88 Mt CO_2-eq . It is also noteworthy to show the land us.e of AFOLU technology, especially in comparison with renewable soil occupation, to understand possible competition with the agricultural sector. Indeed, Figure illustrates projected land use in Italy's AFOLU + Energy related land use for 2020 and 2050 across multiple scenarios, with a disaggregation by type (Crops Open field, Crops Organic, PV, Wind) and an overlay of total agricultural land consumption as a share of national territory.

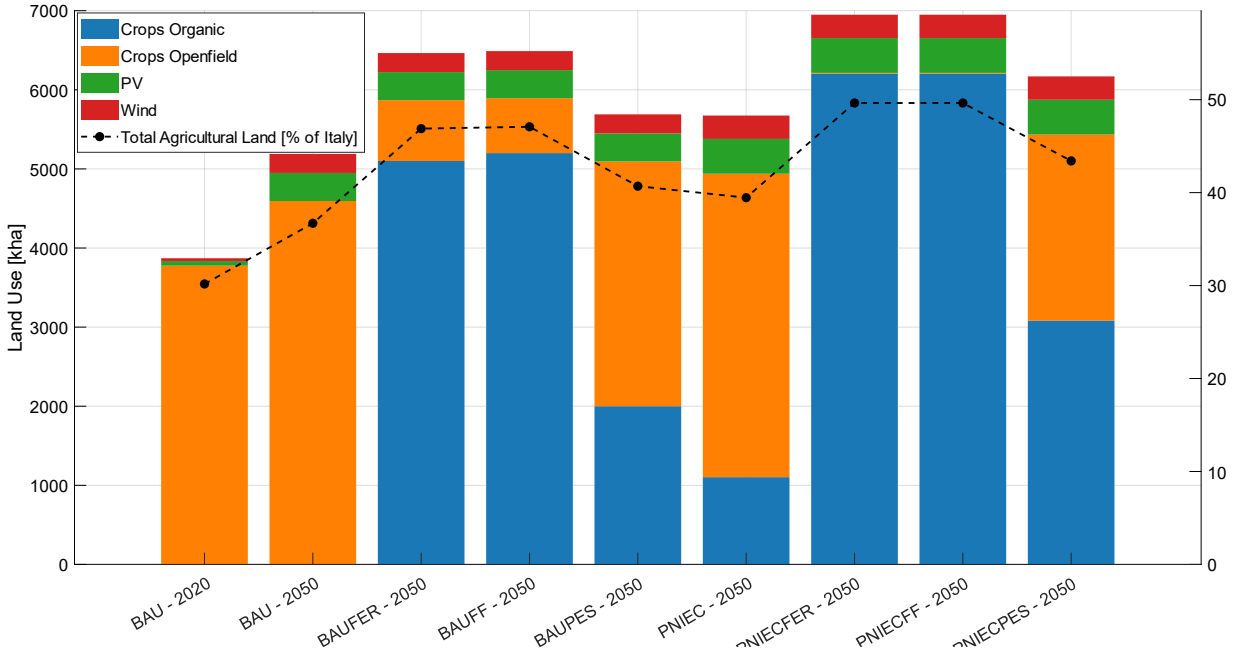

Figure 46. Land Use by cropping and renewable deployment in 2020 and 2050 for different mitigation scenarios

In 2020, total land use under the BAU scenario is approximately 3,800 kha, with nearly all of it accounted for by conventional open-field crops (~3,700 kha), and negligible contribution from PV and wind (<150 kha combined). By 2050, under baseline and BAU-derived, land use expands to ~5,200–5,700 kha, driven primarily by increased organic cropping, which reaches ~2,200 kha. In contrast, PNIEC-aligned mitigation scenarios project further land expansion to ~6,700 kha, with organic crops alone covering ~6,000 kha—nearly 90% of the total—indicating a complete replacement of conventional cropping systems. Contributions from photovoltaics and wind remain modest but non-negligible across all scenarios, reaching ~300 kha in the most technology-intensive cases. The secondary y-axis shows that land use as a percentage of Italy's total agricultural area increases from ~36% in 2020 to over 50% in all PNIEC scenarios by 2050, highlighting the significant land footprint of widespread organic agriculture adoption and renewable energy deployment under decarbonization pathways. Still, a big portion of the total Italian agricultural land remain unused, but this has more to do with economic reason on the agricultural market, that remain out of the scope for this work.

Chapter 3

Discussion, Conclusion and Perspectives

A necessary part of this manuscript must be devoted to analyzing what has been done and reflecting on the scientifically relevant aspects of all this work, both from a methodological point of view and from the point of view of empirical evidence, on the limitations that have characterized each of the individual works and on prospects for moving forward. Sustainability assessment

3.1. Ex-post sustainability assessment

In this section, each phase of the sustainability metric for the evaluation of the evolution of the power sector technology through energy scenarios is examined, highlighting potential challenges and opportunities for improvements within the context of these four critical areas: data uncertainties, assumptions, limitations, and reproducibility of the study. It starts with a recap of the main achievement of the study, following limitations and perspectives.

An analysis has been performed to cope with the necessity to produce insights that traditional energy system optimization models are not able to deal with, attempting to answer to a crucial question in the actual energy modeling field: how much can we exploit carbon emissions as an indicator of sustainability? The comprehensive and hierarchical framework for evaluating sustainability developed in this work allowed for the incorporation of preferred dimensions of sustainability while accounting for their relative importance. Since different stakeholders may rank sustainability aspects differently according to their preference, the role of the weight has been assessed through a post-mining analysis, to understand which weights mostly affect the SI profile trend and magnitude. These considerations have led to the development of a novel tool (the comprehensive Sustainability Index) for decision-making in energy planning, especially crucial for identifying and addressing potential negative impacts within the decarbonization strategies. The innovative aspect of the post-mining analysis has been used to identify the most challenging features of a decarbonization strategy, as this approach is capable to directly extract information on the role of individual indicators, without imposing limitations on the potential indicators that can be included or the number of weight combinations that can be tested. The utilization of the SI methodology in the context of the Italian decarbonization strategy has served as an illustrative example of the proper interpretation of results. Specifically, it has been demonstrated a significant impact of factors like Import Dependence, Environmental Production, and Quality of Labor on the magnitude of sustainability in the power sector, especially under the Reference scenario. The Decarbonization scenario shifts the focus towards Reliability due to increased renewable

energy penetration, with additional emphasis on issues such as Eutrophication from solar panel construction and Import Dependence. The analysis also reveals that Reliability and Land Use are key aspects for the Sustainability Index trend, indicating their high impact over time. In answering the question which originated the study, this analysis confirms the limitation of carbon emission as the only indicator of sustainable energy policy. Indeed, GWP does not turn out to be the most influencing indicator in predicting sustainability, highlighting the necessity of going deeply in exploring energy transition impact, and providing a tool for it.

Concerning the limitations, both are present in terms of source uncertainty of the data and in the hypothesis made in the calculation. Data essentially falls into two categories: Model-derived data and data obtained from external sources. The former can be categorized into two types pertaining to the techno-economic characterization of technologies and energy commodities: those that remain consistent across scenarios, namely the data for the reference energy system (RES), and those who varies (scenario-specific data). Uncertainty regarding these data has been addressed in the case-study presented here by using national data for both technical and economic parameters. As a rule, data precision tends to increase as the geographic scale decreases [88]. From a reproducibility perspective, the study ensures internal consistency by explicitly documenting the techno-economic assumptions, the sustainability indicators, the weighting structure, and the post-mining procedure adopted. All equations defining the Sustainability Index, as well as the clustering and AI-based analyses, are deterministic and can be replicated provided the same input data are used. The use of officially published national scenarios further strengthens reproducibility within the Italian context, as the underlying energy pathways are transparent, and policy aligned. Therefore, the reproducibility of the study is primarily linked to data availability rather than to methodological opacity. The set of technologies considered is extensive, and the technological discretization aligns as closely as possible with data from official sources and existing models. Concerning data that vary among the scenarios, a first limitation is encountered, namely the use of only two scenarios. The generalizability of the results discussed in the previous section is as robust as the number of scenarios confirming those results: however, exact (published) data were only available for the two analyzed scenarios, as per Italy's long-term strategy. Therefore, any other scenario would have been a modeler's hypothesis without a basis to be found in stated policies. The latter consideration generally holds true for the entire model, which has been extensively discussed, and for which all relevant data have been presented. The main limitation of the model, which will be discussed later, is the absence of data on import by country for energy commodities and critical materials used in the scenario. This required the use of external sources, assumptions, and simplifying hypotheses, significantly increasing the uncertainty of this study. As a first suggestion for future research direction, modelling frameworks providing a better representation of the different supply options will be beneficial for the scientific community. Regarding data from external sources, they primarily pertain to the sustainability indicator calculations. The foremost source of uncertainty undoubtedly lies in the selection of the entity that should encapsulate the sustainability phenomenon. This uncertainty is less pronounced concerning environmental indicators, as they are quantifiable through physical quantities (e.g., GHG emissions for global warming). However, for safety and social indicators, it was necessary to assume a quantitative measure to represent a qualitative phenomenon (e.g., the

Human Development Index for labor quality): these assumptions thus constitute a significant source of uncertainty. Nevertheless, by employing well-referenced data sources, logical assumptions in alignment with the scientific literature, we ensure comparability with existing studies.

Delving into the individual indicator definition, they can be categorized into three distinct groups: environmental ones, social ones, and energy security ones. All environmental indicators are derived from LCA frameworks, a scientifically validated and reproducible procedure. A potential issue concerns to the geographical extension of these data, which is not always available for the Italian territory and, sometimes, even for the European region. Furthermore, the technological discretization of the LCA database in comparison to the TEMOA-Italy technological database is significantly limited, necessitating associative assumptions. These assumptions, especially in the case of biomass, but generally applicable to all technologies, further exacerbate data uncertainty. Lastly, the LCA database undergoes a harmonization process to estimate values for future years. Although the assumption of keeping data as constant is incorrect from a technological point of view (technologies typically improved as time goes by), projecting future data accounts for the key impact driver\s for various technologies (e.g., lifetime and capacity factor for renewables, lifetime, and efficiency for fossil fuels). However, introducing such an assumption of variation infuses uncertainty concerning the actual extent of change, which remains unknown a priori. Regarding security data, several aspects need to be discussed, with the most critical aspect being simplifying assumptions. In the technologies data gathering phase, simplifications were introduced also during the metric calculation. Linking security to individual technologies introduces significant uncertainties. As energy systems are complex, their behavior cannot be explained solely by understanding their individual components. Thus, system security is not a function of individual components but rather their dynamic interactions [119]. The technology-centric approach of this paper has two main limitations. First, security indicators for power plants (e.g., PV) and energy carriers (natural gas) are underestimated in this study, even though the consequences of an import disruption differ significantly. Sustainability scores are assigned to each technology, and the overall score is weighted proportionally to activity. Theoretically, the renewable supply chain aspect should be evaluated in proportion to the new capacity installed, while commodity imports should relate to upstream sector activity. This approach was not adopted because the goal is to derive a single score rather than one for each model layer. Future research directions should focus on implementing more comprehensive metrics capable of accounting for these intricacies.

Delving into the mathematical aspects of the sustainability metric, the most intricate aspect arises when technology sustainability scores are multiplied by their respective activity shares to yield the final sustainability score. The underlying hypothesis is that all the indicators included in the sustainability score are proportional to the activity even if, as discussed above, this involves limitations particularly for the security indicators. Future research must address this issue by improving the mathematical formulation of the metric and the way it accounts upstream import, capacity installed, and overall electricity production (and not only its production share). Concerning the result section, a major observation must be done regarding

the power sector focus of this analysis. The sustainability comparison of the two scenarios is based solely on the shares of the different technologies in the electricity generation mix. If the sustainability comparison had been carried out based on the absolute values of power generation per technology instead of based on the shares, the impacts of the decarbonisation scenario would be significantly higher than those of the reference scenario. Regarding the post-mining phase, this analysis allows trend and magnitude analysis to be conducted independently. Where no trend is observed, this process provides an opportunity to identify a pattern and explain it. Where profiles with a marked upward or downward trend with different magnitudes are present, it is possible to understand both the factors driving the change and the ones influencing the magnitude value. That provides the possibility of maintaining a neutral approach. In similar situations, with stable profiles over time, both low-magnitude and high-magnitude effects occur, but s considerations can still be made (Reliability in cluster 4 of the Decarbonization trend). Concerning the use of AI, ML techniques allow the evaluation of many iterations identifying typological group inside them. In this regard, a very accurate model was developed, from which the analyses between input and output were subsequently extracted. This allows to extract general pattern able to explain the situation rather than developing knowledge from case-specific results.

Finally, despite the methodological, numerical and data limitations, there is a major aspect to be highlighted that is also the one who justified the following analysis. The inability of metrics to capture dynamics and to give an objective evaluation for the severity of a situation regarding a particular indicator. Let's take the water use intensity as an indicator. If the water in a certain region is very scarce a solution that appear high from a sustainability score point of view, but that do not have the physical water commodities to work, may be selected as the optimal one and implemented. This limitation stems from the use of LCA which average the data for an entire region and do not differentiate between region internal resource use and region external one. Leading to biased evaluation. Indeed, concerning LCA, a common approach is to adjust weights to better reflect the specificity of the case study. However, the resulting score may still lack a proper consistency check with respect to local-scale constraints and dynamic resource availability. It is important to clarify that this work already adopts a lifecycle sustainability perspective, as multiple environmental, social, and security-related indicators are evaluated at the technology level. Therefore, the limitation does not lie in the absence of a Life Cycle Sustainability Assessment (LCSA) approach per se, but rather in the level of precision, spatial representativeness, and informational content of the adopted indicators.

Future developments should focus on refining the environmental indicators to better capture local energy-system constraints and region-specific impacts. This includes the integration of more spatially explicit LCA datasets, context-dependent impact categories (e.g., site-specific water scarcity, land occupation intensity differentiated by ecosystem type, local critical material supply risks), and indicators directly linked to energy-system operational characteristics. Enhancing the model with geographically resolved and energy-relevant lifecycle indicators would improve the consistency between sustainability scores and actual system feasibility, particularly in constrained contexts such as small islands or resource-scarce regions.

These considerations reinforce the need to (i) endogenize the dynamics of resource use within the model and (ii) adopt the most local scale possible to avoid excessive data generalization. These limitations have guided the future perspective of this work, enabling the integration of land-use dynamics—identified as a critical factor—into the energy model of a small-island context.

3.2. Integration of land-use in ESOMs

The initial goal of this research was to quantify how much spatial information or consideration of spatial characteristics, when integrated within an energy system optimization modeling framework, can improve planning solutions fostering a more sustainable energy system development. One of these improvements was to obtain a modeling instance able to optimally allocate the new installation of renewable energy plants, accounting for local conditions and being able to suggest siting considerations, to minimize the use of land. In this context, the analysis has been divided in the *assessment phase* and in the *integration phase*. In general, this research effectively demonstrates the feasibility and benefits of incorporating spatially explicit considerations into ESOMs using open-source packages, highlighting the practicality and value of this approach. This integration not only enhances the realism and applicability of these models but also aligns with the pressing global shift toward sustainable and renewable energy sources. Also, by comparing traditional and spatially enhanced models, the study quantifies the added value brought by spatial planning and the influence of the new variable introduced in the model. A comparison between the traditional and land-explicit model configurations reveals the significant role of land pricing in shaping the energy system's technological mix and overall performance. The traditional and low land price scenarios produce nearly identical results, as expected, whereas the high land price configuration introduces substantial differences. This behavior indicates the presence of a cost threshold beyond which land price materially affects model outcomes. By 2050, the installed capacity in the low land price scenario reaches approximately 7 MW, compared to 5.8 MW in the high land price case—a reduction of about 17%. Similarly, electricity generation decreases from roughly 23 GWh to 20.8 GWh (a ~10% drop) under high land cost conditions. This difference is primarily due to a shift in technology preference: with low land prices, the model favors land-intensive photovoltaic systems (PV1_N), while under high land prices, it prioritizes wind technologies (WIN1_N) that offer higher energy yield per unit of land area. Despite these shifts, the land use constraint itself does not become binding in any scenario. No land cluster reaches full capacity, although usage patterns differ. Land cluster LC_3 is the most utilized in absolute terms, reaching around 10% occupation in 2040 under the low land price scenario and about 6% under the high price scenario. LC_2, while smaller in size, reaches the highest relative occupation—26% in both configurations due to wind installations. Cost differences between scenarios are also notable. In the high land price case, land-related costs increase from 0.026 M€ in 2025 to approximately 0.07 M€ annually from 2040 onward. In contrast, in the low land price instance, these costs remain significantly lower, peaking at around 0.014 M€ in 2040. These

findings demonstrate how spatial cost factors, even when not strictly limiting in terms of land availability, can drive substantial changes in the energy mix and system costs.

Despite its exploratory nature, the proposed framework allows several methodological insights to be generalized beyond the specific case study. The following discussion addresses data-related uncertainties, integration challenges, and, importantly, the transferability of both the methodological approach and the obtained results.

Concerning the assessment phase, referring to the practice of gathering data about renewable energy potential of a region (both in terms of physical and administrative availability), this can be further divided in two subtopics: data gathering and elaboration. In terms of data gathering, it is evident the need for a unified tool to perform this kind of analysis. Actual literature still relies on many incompatible packages for this analysis, even if some exceptions are arising. For example, the GLAES framework for LE analysis [147] has found recent application in different studies [251]. In terms of renewable energy potential assessment phase, there exists many valuable attempts([164] [150]), but a uniformly adopted methodology across studies is missing. In general, an interface to integrate spatial and temporal explicit data about VRES is needed. Even if, as confirmed by Aryanpur et.al., [252], the optimal choice of resolution is still dependent on model scope. The uncertainties inherent in the assessment phase stem from the analysis of land eligibility, complicated by ambiguous energy legislation. Notably, our approach did not consider buffer zones around any protected areas, a decision that potentially leads to an overestimation of available land. Further analysis (not detailed here) reveals that implementing buffer zones ranging from 25 to 200 meters around these areas drastically affects land availability. In some clusters, this results in the complete unavailability of land, while in the most favorable scenarios it causes a reduction of approximately 25%. Specifically, in the context of wind technology, the application of buffer zones rendered certain land clusters unsuitable, significantly altering the potential energy mix. This outcome underscores the necessity for more transparent and comprehensible landscape regulations. The challenge in setting fixed buffer values, as indicated by [158] , further complicates this issue, necessitating a nuanced approach to landscape management in the context of renewable energy development.

From a transferability perspective, the methodological structure adopted for the assessment phase is generalizable at least at the national level. Land eligibility constraints are largely determined by national regulatory frameworks, and although regional implementations may differ, the cartographic logic used to define exclusion and suitability criteria can be replicated wherever clear legislative specifications are available. Therefore, the main barrier to transferability does not lie in the GIS-based methodology itself, but rather in the clarity and consistency of national spatial regulations. In contexts where standardized geospatial datasets and transparent regulatory definitions exist, the approach can be directly reproduced. Concerning renewable resource variability, another transferable insight emerges regarding spatial resolution. Increasing spatial granularity beyond the intrinsic resolution of available climatic datasets—often around 10 km for solar radiation and wind speed reanalysis products—does not necessarily improve model accuracy. Over-disaggregation may instead introduce artificial precision without additional

informational value. Therefore, the optimal spatial resolution should remain consistent with the underlying climatic data quality and with the scope of the energy system model.

Diving in the integration phase, the first and primary challenge in implementing the land-use in an ESOM is the proliferation of energy technologies. This challenge arises due to the necessity of introducing, for each implemented technology, a multitude of technologies equivalent to the number of clusters employed. For example, to effectively model each photovoltaic technology, the model must encompass an N number of PV technologies, where N corresponds to the number of clusters identified where the technology can be installed. While this approach may find some applicability in constrained environments like the island of Pantelleria, its feasibility diminishes significantly in more expansive scenarios, such as national or European contexts. In this context, there is the need to find a trade-off between model accuracy and computational effort. Stolten et.al [164] highlight how this practice is strongly dependent on both spatial and temporal resolution and should be faced case-by-case. Despite the methodological issues, there is general knowledge that can be extracted from results. Results clearly indicate how the cost of land has a strong influence in limiting the land use intensive renewable energy sources, such as photovoltaic. The sensitivity analysis conducted according to Eurostat [194] suggests that economic factors, such as land prices, significantly influence technology selection and deployment strategies, leading to regional differentiation in the energy mix. According to this point, another remarkable limitation of this study is not considering the trade-offs and synergies with respect to other land-use intensive sectors. Indeed, the land-use one is a stand-alone sector related to agriculture, forestry and other land uses which cannot be hidden by a simple “land price” applied to the space. Therefore, a hard-linking or soft-linking with a more detailed AFOLU representation is recommended, and this has dictated the final part of this work.

A different consideration applies to the transferability of numerical results. The quantitative outcomes presented in this work are strongly influenced by the small scale of the case study and by its specific geographical and economic characteristics. As such, the magnitude of land-use impacts and the identified cost thresholds should not be interpreted as directly generalizable to larger territorial systems. In particular, the limited size of the analyzed system constrains the diversity of spatial trade-offs observable in the results. A national-scale application within the Italian context would likely reveal stronger differentiation effects and more complex interactions between land price, technology allocation, and spatial constraints. Therefore, while the methodological conclusions are broadly transferable, the numerical findings should be interpreted as case-specific and illustrative rather than universally representative.

3.3. AFOLU

A technology explicit module for AFOLU sectors has been integrated into two different ESOMs. The development of the AFOLU module led to significant evidence both from a methodological and from an empirical perspective. In Sweden, six scenarios were developed along three alternative storylines to test decarbonization policies within the AFOLU sector, incorporating varying assumptions related to organic cropping, crop yields, and land use. Results indicate that the integration of the AFOLU module does not distort the outcomes of the ESOM framework; instead, it enhances the model's capacity to capture emissions typically overlooked in traditional approaches, adding approximately 10% more emissions on the positive side while enabling the representation of forest-based negative emissions that can offset up to 60% of the total. A focused assessment of Sweden reveals the potential for a 48% reduction in AFOLU-related emissions by 2050 relative to the baseline, with 32% attributed to the crop sector—mainly due to the adoption of organic farming—and the remaining 16% from the livestock sector, where mitigation is supported by anaerobic digestion despite its limited economic competitiveness. Acidification emerges as the most cost-effective livestock-related measure. In Italy, the AFOLU-enhanced version of the TEMOA-Italy model increases base-year (2020) GHG emissions by 26–29 $MtCO_2eq$ compared to the non-AFOLU configuration, primarily due to livestock and cropland activities. The integration enables land-based mitigation measures such as afforestation, anaerobic digestion, and manure management, contributing up to ~10 $MtCO_2eq$ of removals by 2050 in scenarios aligned with the PNIEC, although most of the negative emissions are driven by DAC and CCS technologies. The inclusion of AFOLU processes does not alter broader energy system trends or cost-optimal technology pathways, but it clarifies the agricultural sector's influence on mitigation outcomes: crop yields and farming practices affect both emissions and land use, while livestock emissions—remaining above 5 $MtCO_2eq$ in 2050 across all scenarios—continue to pose a structural challenge, despite the availability of economically viable manure treatment and biogas solutions.

The integration of AFOLU systems into energy system models inevitably involves several methodological limitations that, in turn, originates empirical limitations in the result phase. These constraints arise from the complexity of the AFOLU sector, the scarcity of reliable global datasets, and the need for simplifying assumptions to ensure model tractability. Table 38 highlight the key limitations identified in this work, together with their expected effects on model outputs. These limitations are originated by the trade-offs between accuracy and usability that are characteristic of AFOLU modelling. Other limitations originate from the modelling choices required to embed AFOLU into energy system optimisation frameworks. The disaggregation of emissions into technology-specific factors through proxies, while necessary, introduces uncertainty where proxies are only loosely correlated with actual emissions. A notable example concerns crop emission factors. These are calculated by dividing total crop emissions by the total cultivated area, resulting in an average emission per hectare that is not specific to individual crop types. Different crops generate different emissions; however, to maintain a consistent global approach compatible with Tier 1 methodology, this aggregation was adopted. For livestock, the situation is more precise, as FAO provides emission factors already differentiated by species. Moreover, if the

production of all commodities—crops, livestock, or wood products—follows internal GDP growth as a proxy overlooks policy influences, export dynamics, and variations in consumption patterns, which ideally should be explored through sensitivity analyses. Similarly, the omission of fertilizer manufacturing emissions, despite its pragmatic rationale, can distort the evaluation of open-field systems relative to alternative cropping methods by neglecting a critical upstream source of greenhouse gases. Structural assumptions also play a significant role. By neglecting competition between agricultural land and energy technologies (e.g., solar, wind, bioenergy), but just accounting for them, the model is implicitly biased toward land-expansive agricultural scenarios. Moreover, the absence of transition costs for establishing new livestock or farming systems may overstate the economic feasibility of radical structural shifts. These simplifications reduce the capacity of the framework to represent real-world adoption barriers. Finally, the incomplete representation of mitigation options represents one of the most significant shortcomings. Key measures identified in the literature, such as soil carbon sequestration, agroforestry, biochar application, and advanced nutrient management, are not yet included in the current version of the model. As a result, the framework likely underestimates the technical and economic mitigation potential of the AFOLU sector. In addition, low-TRL innovations such as methane inhibitors or CH_4 vaccines for ruminants remain outside the scope of the modelling exercise, constraining the exploration of long-term innovation pathways. Taken together, these limitations introduce both conservative biases (underestimating AFOLU's mitigation potential) and optimistic biases (underestimating land competition and transition costs). Addressing them will require targeted efforts to improve global datasets, enhance the representation of upstream supply chains (e.g., fertilizers), and expand the mitigation portfolio to reflect the diversity of AFOLU strategies documented in the scientific literature.

From a reproducibility perspective, the AFOLU module is fully embedded within the structure of the underlying ESOMs, preserving their deterministic optimization logic. All technology definitions, emission factors, and land-use constraints are explicitly parameterized, allowing replication provided equivalent national datasets are available. The modular architecture adopted in both the Swedish and Italian implementations ensures that the AFOLU component can be activated or deactivated without altering the structural consistency of the core energy model. Regarding methodological transferability, the AFOLU module is structurally generalizable across national contexts, provided that country-specific agricultural statistics, emission inventories, and land-use data are accessible. The technology-explicit representation of crops, livestock, manure management, and forestry processes is not country-dependent per se, but requires recalibration of emission factors and productivity parameters to reflect local conditions. The dual implementation in Sweden and Italy already demonstrates the adaptability of the framework to structurally different systems—one characterized by a strong forestry sink and the other by land scarcity and livestock-related emissions. Thus, the methodological contribution lies in the modular integration strategy rather than in country-specific parameterization.

Beyond the methodological limitations previously discussed, it remains essential to provide a critical interpretation of the results obtained for both the Swedish and Italian case studies. These analyses yield not only context-specific empirical insights but also generalizable knowledge that aligns with and reinforces findings from existing literature.The first point to be addressed concerns

the role of the AFOLU sector in national decarbonization strategies. It is essential to recall that the AFOLU sector is both a source and a potential sink of GHG. Nevertheless, current policy frameworks and academic literature often emphasize its mitigation potential while neglecting the magnitude of its own emissions [253]. In some contexts, the sector's capacity to offset even its own emissions is limited, raising concerns over overestimated mitigation expectations [253].

This over-reliance is particularly evident in the Italian case study, where PNIEC reports an ambitious carbon sink potential from land use (28 Mt) that far exceeds the sector's own emission levels and plausible transformation trajectories (around 11 Mt). The model developed in this work confirms the hard to realize nature of those projections, revealing that the AFOLU sector's self-mitigation is already challenging, let alone its ability to compensate for other sectors' emissions. From this, a first general insight emerges: overestimating the AFOLU sector's mitigation potential can compromise the credibility and feasibility of national climate strategies. It is worth noting that most studies to date have focused on developed countries with stagnating or declining agricultural sectors[254]. However, many developing regions are expected to experience substantial population and agricultural growth, assuming of AFOLU as a net sink even more questionable in those contexts.

The Swedish case study presents a contrasting scenario. Here, the AFOLU sector already acts as a net carbon sink and integrating it into the energy system model allows for significant reductions in mitigation pressure on other sectors. In particular, the exploitation of forests as a source of negative emissions emerges as a cost-effective pathway. However, this finding must be treated with caution. Recent studies have questioned the long-term reliability of forest-based carbon sinks, due to climate risks, saturation effects, and uncertainties in permanence [255]. Although the Swedish case does not highlight major constraints in terms of land availability or biogas potential from manure, it should be emphasized that further sectoral integration and sensitivity analysis on forest dynamics would be necessary to validate these findings.

The Italian case is more complex and marked by multiple stressors. Key limitations include:

- Limited availability of land for agriculture and bioenergy, due to competition with food production, urban expansion, and environmental constraints.
- Lower relevance of forest-based carbon sinks compared to Sweden.
- Potential yield reductions under climate change, which are not yet accounted for in the model but are highly likely according to recent projections [256].

One particularly critical insight from the Italian case is that only half of the total agricultural land is currently utilized. While this may appear to be a positive signal for energy transition opportunities—since it implies land availability for renewables—it also reveals economic and structural weaknesses in the agricultural sector, which the model does not capture. A complete Nexus analysis would need to include agricultural economics, rural development, and land tenure systems to fully explain this under-utilization.

A distinction must be made between methodological transferability and the transferability of empirical findings. While the structural role of AFOLU as both emission source and potential sink is broadly applicable across countries, the magnitude of mitigation potential, the balance between positive and negative emissions, and the economic attractiveness of specific measures are highly context dependent. Factors such as forest coverage, livestock intensity, dietary patterns, land availability, and national climate policies substantially influence model outcomes. Therefore, the Swedish and Italian results should be interpreted as illustrative case studies rather than directly generalizable benchmarks. The comparative application nevertheless provides transferable insights regarding structural dynamics—for instance, the risk of overestimating AFOLU mitigation potential in countries with limited forest sinks, and the sensitivity of agricultural emissions to yield and management assumptions.

Despite the above challenges, the developed AFOLU module and its integration into the energy system model demonstrate significant analytical value. Rather than providing granular projections, the tool serves as an effective fact-checking instrument and a strategic lens to assess the realism of climate targets. In this regard, the module should be seen as an enabler of critical policy analysis and an originator of new scenario-based insights. It emphasizes the need for stronger alignment between national climate policies and bottom-up modelling tools, exposing gaps between declared ambitions and feasible implementation paths. Nevertheless, to fully capture the multi-sectoral trade-offs, future research should evolve toward a comprehensive Nexus-based modelling approach, ideally through hard-linked frameworks that integrate energy, water, and land-use systems into a unified optimization environment [98] coupled with metrics.

Table 38. Limitation and potential impacts of simplifying assumptions for the AFOLU module.

Stage	Limitation	Potential Impact
Data	Heavy reliance on FAOSTAT/UNFCCC datasets; limited national detail for non-OECD countries	Introduces structural uncertainty, reduces representativeness of country-specific practices
	Emissions allocated proportionally to land area or livestock heads	Over- or under-estimation of emissions for species/crop-specific systems
	Irrigation data fixed at 2010 levels	Underestimation of future water demand in irrigation-intensive regions
	Emission factors derived from proxies instead of NGHGIs	Potential mismatch with official inventories and reduced policy relevance
	Fertilizer manufacturing emissions excluded from AFOLU	Possible underestimation of emissions from high-input systems; bias toward open-field systems.
	NGHGI indirect emissions treated in aggregate	Divergence from inventory methodology; loss of sector-specific resolution may bias crop–livestock balance.
Model structure	Land represented as "capacity" rather than as a traded commodity	Simplifies optimisation but neglects explicit land competition between sectors
	Feed demand from crops to livestock not explicitly modelled	Limits capacity to analyse food-feed competition and land allocation trade-offs
	No cost assigned to new livestock/farming systems	May distort economic signals, overestimating feasibility of structural shifts in production.
	Negative emissions from forests/HWP based on simplified area→volume conversions	Risk of misrepresenting carbon sequestration dynamics
Mitigation options	Enteric fermentation excluded (low TRL, data scarcity)	Underestimates livestock mitigation potential

	Mitigation measures applied individually, not in combinations	Cannot capture synergies or overlaps (e.g. manure covers + acidification)
	Abatement costs drawn from regional case studies	High heterogeneity, limited transferability across contexts
	Limited mitigation portfolio (exclusion of soil carbon management, agroforestry, improved nutrient management, biochar, etc.)	Underrepresentation of AFOLU mitigation potential; constrains robustness of decarbonisation scenarios.
	Organic crop emissions calculated by subtracting fertilizer/pesticide use	Risk of masking feedback loops and underestimating emissions in organic systems.
Scenario applications	AFOLU integration raises baseline emissions by +26–29 $MtCO_2eq$ but leaves trends unchanged	Potential undervaluation of systemic feedback between land use and energy
	No explicit land competition with renewable energy technologies	Misses trade-offs between food, forestry and energy crops
	Upstream emissions (e.g. fertiliser production) excluded	Underestimates full life-cycle agricultural emissions
	Land use competition with energy technologies not modelled	Bias toward land-expansive agricultural scenarios, neglecting food–energy–land competition.
General	Framework intended for exploratory analysis, not to replace NGHGIs or detailed sectoral models	Limits direct use in compliance or official reporting

3.4. General discussion

This research examined the extent to which the analytical capacity of ESOMs can be enhanced through three complementary extensions: the introduction of a comprehensive sustainability metric, the integration of spatially explicit land-use constraints, and the endogenization of AFOLU processes. The methodological developments were substantial; however, their primary contribution lies in the interpretative insights that emerge when these extensions are evaluated jointly.

First, the ex-post sustainability assessment demonstrates the structural limitation of relying exclusively on carbon emissions as a proxy for sustainability. While greenhouse gas mitigation remains a necessary objective, the results show that other dimensions—such as reliability, land use, import dependence, and selected social indicators—can exert comparable or even greater influence on sustainability trajectories. This finding indicates that carbon-optimized pathways may conceal trade-offs that become visible only when multi-dimensional indicators are systematically assessed. Consequently, decarbonization pathways should be interpreted within a broader evaluative framework that explicitly accounts for environmental, social, and security-related dimensions.

Second, the spatial integration of land-use constraints highlights the non-neutrality of geographical abstraction in conventional ESOMs. Even when land availability does not become a binding constraint, the introduction of land pricing and eligibility criteria modifies technology allocation and investment patterns. The results show the existence of cost thresholds beyond which spatial factors materially affect system configuration. At the same time, increasing spatial resolution beyond the intrinsic granularity of climatic and regulatory datasets does not necessarily improve model robustness. This suggests that spatial explicitness enhances realism only when aligned with the informational content of the underlying data and with the scope of the modeling exercise.

Third, the AFOLU integration provides evidence that land-based sectors cannot be treated as externally defined carbon sinks without risking structural misinterpretation. The comparative application to Sweden and Italy illustrates that the mitigation role of AFOLU is highly context dependent. In systems characterized by extensive forest resources, AFOLU may alleviate mitigation pressure on other sectors, although uncertainties related to permanence and climate risks remain significant. In land-constrained systems with structurally high livestock emissions, the sector faces difficulties in offsetting its own emissions, let alone compensating for residual emissions elsewhere. These findings underscore the risk of overestimating land-based mitigation potential in national decarbonization strategies. At the same time, the modeling exercise reveals

how data aggregation, proxy emission factors, and incomplete mitigation portfolios introduce both conservative and optimistic biases, reinforcing the need for cautious interpretation.

Across the three research strands, a common pattern emerges: increasing model scope improves the capacity to identify structural trade-offs, but simultaneously amplifies uncertainty. Sustainability metrics require normative weighting assumptions; spatial modeling depends on regulatory clarity and geospatial consistency; AFOLU representation is constrained by data availability and biological complexity. The expansion of model boundaries therefore enhances interpretative depth, but it does not eliminate structural simplifications. The analytical value of these extensions lies less in predictive precision and more in their ability to expose sensitivities, trade-offs, and potential policy inconsistencies.

A further distinction must be made between methodological transferability and empirical generalizability. The developed architectures—the post-mining sustainability framework, the GIS-based land eligibility assessment, and the modular AFOLU integration—are structurally transferable across contexts, provided that adequate datasets are available. However, the magnitude of sustainability impacts, land-use thresholds, and AFOLU mitigation potentials remains highly dependent on local structural characteristics. Numerical results should therefore be interpreted as context-specific rather than universally representative.

Overall, the principal contribution of this work resides in demonstrating that extending ESOMs beyond carbon-centric optimization substantially improves their capacity to function as exploratory policy assessment tools. The integration of sustainability indicators, spatial constraints, and land-based sector dynamics transforms the model from a cost-minimization instrument into a framework capable of critically evaluating the realism and internal coherence of decarbonization strategies. Future research should advance toward more integrated Nexus-oriented modeling approaches, while maintaining transparency in assumptions and explicit recognition of structural uncertainties as central components of model-based analysis.

References

[1] K. Calvin *et al.*, "IPCC, 2023: Climate Change 2023: Synthesis Report. Contribution of Working Groups I, II and III to the Sixth Assessment Report of the Intergovernmental Panel on Climate Change [Core Writing Team, H. Lee and J. Romero (eds.)]. IPCC, Geneva, Switzerland.," Jul. 2023. doi: 10.59327/IPCC/AR6-9789291691647.

[2] T. S. Stephenson and J. J. Jones, "Impacts of Climate Change on Extreme Events in the Coastal and Marine Environments of Caribbean Small Island Developing States (SIDS)," *Science Review*, pp. 10–22, 2017, Accessed: Nov. 17, 2023. [Online]. Available: https://www.researchgate.net/publication/315719894

[3] C. Cirelli and I. La Jeunesse, "Adaptation of Water Management to Face Drought and Water Scarcity," *Facing Hydrometeorological Extreme Events: A Governance Issue*, pp. 245–259, Sep. 2019, doi: 10.1002/9781119383567.CH17.

[4] O. Lhotka, J. Kyselý, and A. Farda, "Climate change scenarios of heat waves in Central Europe and their uncertainties," *Theor. Appl. Climatol.*, vol. 131, no. 3–4, pp. 1043–1054, Feb. 2018, doi: 10.1007/S00704-016-2031-3/FIGURES/9.

[5] UNFCCC, "Paris Agreement," Paris, 2015. Accessed: Dec. 22, 2022. [Online]. Available: https://unfccc.int/sites/default/files/english_paris_agreement.pdf

[6] N. Stern and A. Valero, "Innovation, growth and the transition to net-zero emissions," *Res. Policy*, vol. 50, no. 9, p. 104293, Nov. 2021, doi: 10.1016/J.RESPOL.2021.104293.

[7] E. Bompard *et al.*, "An electricity triangle for energy transition: Application to Italy," *Appl. Energy*, vol. 277, p. 115525, Nov. 2020, doi: 10.1016/J.APENERGY.2020.115525.

[8] "Emissions Gap Report 2024 | UNEP - UN Environment Programme." Accessed: Sep. 14, 2025. [Online]. Available: https://www.unep.org/resources/emissions-gap-report-2024

[9] M. Bellanca, "What, how and where: an assessment of multi-level European climate mitigation policies," *npj Climate Action 2024 3:1*, vol. 3, no. 1, pp. 1–13, Dec. 2024, doi: 10.1038/S44168-024-00200-7.

[10] European Council and Council of the European Union, "European Green Deal." Accessed: Mar. 13, 2024. [Online]. Available: https://www.consilium.europa.eu/en/policies/green-deal/

[11] European Council, "Fit for 55 package." Accessed: Jan. 30, 2023. [Online]. Available: https://www.consilium.europa.eu/en/policies/green-deal/fit-for-55-the-eu-plan-for-a-green-transition/

[12] European Commission, "REPowerEU Plan," 2022. Accessed: May 24, 2024. [Online]. Available: https://energy.ec.europa.eu/system/files/2022-05/COM_2022_230_1_EN_ACT_part1_v5.pdf

[13] J. Moreno *et al.*, "The impacts of decarbonization pathways on Sustainable Development Goals in the European Union," *Commun. Earth Environ.*, vol. 5, no. 1, pp. 1–14, Dec. 2024, doi: 10.1038/S43247-024-01309-7;SUBJMETA.

[14] P. Glavič and R. Lukman, "Review of sustainability terms and their definitions," *J. Clean. Prod.*, vol. 15, no. 18, pp. 1875–1885, Dec. 2007, doi: 10.1016/J.JCLEPRO.2006.12.006.

[15] M. Nicoli *et al.*, "Enabling Coherence Between Energy Policies and SDGs Through Open Energy Models: The TEMOA-Italy Example," in *Aligning the Energy Transition with the Sustainable Development Goals: Key Insights from Energy System Modelling*, M. Labriet, K. Espegren, G. Giannakidis, and B. O'Gallachoir, Eds., Springer, 2024, pp. 97–118. doi: 10.1007/978-3-031-58897-6_5.

[16] United Nations (UN), "Sustainable Development Goals." Accessed: Jun. 03, 2022. [Online]. Available: https://www.un.org/sustainabledevelopment/sustainable-development-goals/

[17] "World Energy Trilemma Index | 2021 | World Energy Council." Accessed: Jan. 12, 2023. [Online]. Available: https://www.worldenergy.org/publications/entry/world-energy-trilemma-index-2021

[18] Y. Kaya, K. Yokobori, and by Yoichi Kaya, "This document represents the proceedings of the Tokyo Conference on 'Global Environment, Energy, and Economic Development' held at the United Nations University Headquarters in Tokyo," pp. 25–27, 1993, Accessed: Jan. 31, 2026. [Online]. Available: http://www.unu.edu/unupress/unupbooks/uu17ee/uu17ee00.htmseepages279,280

[19] G. Liu, "Development of a general sustainability indicator for renewable energy systems: A review," *Renewable and Sustainable Energy Reviews*, vol. 31, pp. 611–621, Mar. 2014, doi: 10.1016/J.RSER.2013.12.038.

[20] C. Feng, J. Yang, and H. Kang, "An Analysis of the Relationship between Energy Trilemma and Economic Growth," *Sustainability 2022, Vol. 14, Page 3863*, vol. 14, no. 7, p. 3863, Mar. 2022, doi: 10.3390/SU14073863.

[21] W. F. Programme. W. G. on Governance, "The blue paper :: work in progress / Executive Board, Working Group on Governance," 1999, *World Food Programme,*. Accessed: Oct. 20, 2023. [Online]. Available: https://digitallibrary.un.org/record/407762

[22] D. S. Armeanu, C. C. Joldes, S. C. Gherghina, and J. V. Andrei, "Understanding the multidimensional linkages among renewable energy, pollution, economic growth and urbanization in contemporary economies: quantitative assessments across different income countries' groups," *Renew Sustain Energy Rev*, vol. 142, p. 110818, May 2021, doi: 10.1016/j.rser.2021.110818.

[23] D. Gayen, R. Chatterjee, and S. Roy, "A review on environmental impacts of renewable energy for sustainable development," *International Journal of Environmental Science and Technology*, pp. 1–26, Dec. 2023, doi: 10.1007/S13762-023-05380-Z/FIGURES/1.

[24] International Energy Agency (IEA), “World Energy Investment 2022 – Analysis – IEA.” Accessed: Sep. 14, 2023. [Online]. Available: https://www.iea.org/reports/world-energy-investment-2022

[25] United Nations (UN), “Sustainable Development Goal 7 - Affordable and Clean Energy.” Accessed: May 15, 2023. [Online]. Available: https://www.un.org/sustainabledevelopment/energy/

[26] K. Debnath and L. Goel, “Power system planning - a reliability perspective,” *Electric Power Systems Research*, vol. 34, no. 3, pp. 179–185, 1995, doi: 10.1016/0378-7796(95)00976-X.

[27] E. Bompard, A. Carpignano, M. Erriquez, D. Grosso, M. Pession, and F. Profumo, “National energy security assessment in a geopolitical perspective,” *Energy*, vol. 130, pp. 144–154, 2017, doi: 10.1016/J.ENERGY.2017.04.108.

[28] I. M. Algunaibet, C. Pozo, Á. Galán-Martín, and G. Guillén-Gosálbez, “Quantifying the cost of leaving the Paris Agreement via the integration of life cycle assessment, energy systems modeling and monetization,” 2019, doi: 10.1016/j.apenergy.2019.03.081.

[29] R. Wüstenhagen, M. Wolsink, and M. J. Bürer, “Social acceptance of renewable energy innovation: An introduction to the concept,” *Energy Policy*, vol. 35, no. 5, pp. 2683–2691, May 2007, doi: 10.1016/J.ENPOL.2006.12.001.

[30] D. Nock and E. Baker, “Holistic multi-criteria decision analysis evaluation of sustainable electric generation portfolios: New England case study,” *Appl. Energy*, vol. 242, pp. 655–673, May 2019, doi: 10.1016/J.APENERGY.2019.03.019.

[31] A. Buchmayr, E. Verhofstadt, L. Van Ootegem, D. Sanjuan Delmás, G. Thomassen, and J. Dewulf, “The path to sustainable energy supply systems: Proposal of an integrative sustainability assessment framework,” *Renewable and Sustainable Energy Reviews*, vol. 138, p. 110666, Mar. 2021, doi: 10.1016/J.RSER.2020.110666.

[32] X. Y. Zhou *et al.*, “Influence of Russia-Ukraine War on the Global Energy and Food Security,” *Resour. Conserv. Recycl.*, vol. 188, p. 106657, Jan. 2023, doi: 10.1016/J.RESCONREC.2022.106657.

[33] C. Helbig, M. Bruckler, A. Thorenz, and A. Tuma, “An overview of indicator choice and normalization in raw material supply risk assessments,” *Resources*, vol. 10, no. 8, p. 79, Aug. 2021, doi: 10.3390/RESOURCES10080079/S1.

[34] M. C. Rulli, D. Bellomi, A. Cazzoli, G. De Carolis, and P. D’Odorico, “The water-land-food nexus of first-generation biofuels,” *Sci. Rep.*, vol. 6, no. 1, pp. 1–10, Mar. 2016, doi: 10.1038/SREP22521;SUBJMETA.

[35] “THE RELATIONSHIP BETWEEN LAND-USE CHANGE AND CLIMATE CHANGE - Dale - 1997 - Ecological Applications - Wiley Online Library.” Accessed: Jan. 31, 2026. [Online]. Available: https://esajournals.onlinelibrary.wiley.com/doi/abs/10.1890/1051-0761(1997)007[0753:TRBLUC]2.0.CO;2

[36] T. Searchinger *et al.*, “Use of U.S. Croplands for Biofuels Increases Greenhouse Gases Through Emissions from Land-Use Change,” *Science (1979).*, vol. 319, no. 5867, pp. 1238–1240, Feb. 2008, doi: 10.1126/SCIENCE.1151861.

[37] J. Fairhead, M. Leach, and I. Scoones, “Green Grabbing: a new appropriation of nature?,” *Journal of Peasant Studies*, vol. 39, no. 2, pp. 237–261, Apr. 2012, doi: 10.1080/03066150.2012.671770.

[38] A. M. Omer, “Energy, environment and sustainable development,” *Renewable and Sustainable Energy Reviews*, vol. 12, no. 9, pp. 2265–2300, Dec. 2008, doi: 10.1016/J.RSER.2007.05.001.

[39] N. Healy and J. Barry, “Politicizing energy justice and energy system transitions: Fossil fuel divestment and a ‘just transition,’” *Energy Policy*, vol. 108, pp. 451–459, 2017, doi: 10.1016/j.enpol.2017.06.014.

[40] J. Rockström, O. Gaffney, J. Rogelj, M. Meinshausen, N. Nakicenovic, and H. J. Schellnhuber, “A roadmap for rapid decarbonization,” *Science (1979).*, vol. 355, no. 6331, pp. 1269–1271, Mar. 2017, doi: 10.1126/SCIENCE.AAH3443.

[41] M. Nilsson, D. Griggs, and M. Visbeck, “Policy: Map the interactions between Sustainable Development Goals,” *Nature*, vol. 534, no. 7607, pp. 320–322, Jun. 2016, doi: 10.1038/534320A;SUBJMETA.

[42] D. Klenert *et al.*, “Making carbon pricing work for citizens,” *Nat. Clim. Chang.*, vol. 8, no. 8, pp. 669–677, Aug. 2018, doi: 10.1038/S41558-018-0201-2;SUBJMETA.

[43] Siddharth. Kara, “Cobalt red : how the blood of the Congo powers our lives,” p. 274, 2024, Accessed: Sep. 14, 2025. [Online]. Available: https://books.google.com/books/about/Cobalt_Red.html?hl=it&id=m2HPEAAAQBAJ

[44] A. Vai, G. Colucci, M. Nicoli, and L. Savoldi, “A Comprehensive Metric to Assess the Security of Future Energy Systems Through Energy System Optimization Models,” *Energy Proceedings*, vol. 47, 2024, doi: 10.46855/energy-proceedings-11292.

[45] P. Alstone, D. Gershenson, and D. M. Kammen, “Decentralized energy systems for clean electricity access,” *Nat. Clim. Chang.*, vol. 5, no. 4, pp. 305–314, Mar. 2015, doi: 10.1038/NCLIMATE2512;TECHMETA.

[46] F. Lanati, M. Gaeta, A. Gelmini, A. Gatti, and L. Mazzocchi, “Studi a supporto della Governance del sistema elettrico ed energetico nazionale,” 2018. Accessed: Aug. 18, 2023. [Online]. Available: https://www.rse-web.it/rapporti/18007604/

[47] “Enhancing effective implementation of sustainable energy action plans in European islands through reinforcement of smart multilevel governance Final Publishing Report”, Accessed: Oct. 20, 2023. [Online]. Available: www.sustainableislands.eu

[48] S. Abram *et al.*, “Just Transition: A whole-systems approach to decarbonisation,” *Climate Policy*, vol. 22, no. 8, pp. 1033–1049, Sep. 2022, doi: 10.1080/14693062.2022.2108365.

[49] C. Corson, K. I. MacDonald, and B. Neimark, “Grabbing ‘Green’: Markets, Environmental Governance and the Materialization of Natural Capital,” *Human*

Geography(United Kingdom), vol. 6, no. 1, pp. 1–15, Mar. 2013, doi: 10.1177/1942778613006001O1.

[50] C. R. Warren and M. McFadyen, "Does community ownership affect public attitudes to wind energy? A case study from south-west Scotland," *Land use policy*, vol. 27, no. 2, pp. 204–213, Apr. 2010, doi: 10.1016/J.LANDUSEPOL.2008.12.010.

[51] "A review of macroeconomic models for the WEFE nexus assessment - Fondazione Eni Enrico Mattei." Accessed: Nov. 06, 2023. [Online]. Available: https://www.feem.it/publications/a-review-of-macroeconomic-models-for-the-wefe-nexus-assessment/

[52] P. Suding, "Energy and Sustainable Development in Latin America and the Caribbean," 1995.

[53] D. Streimikiene, R. Ciegis, and D. Grundey, "Energy indicators for sustainable development in Baltic States," *Renewable and Sustainable Energy Reviews*, vol. 11, no. 5, pp. 877–893, Jun. 2007, doi: 10.1016/J.RSER.2005.06.004.

[54] A. Evans, V. Strezov, and T. J. Evans, "Assessment of sustainability indicators for renewable energy technologies," *Renewable and Sustainable Energy Reviews*, vol. 13, no. 5, pp. 1082–1088, Jun. 2009, doi: 10.1016/J.RSER.2008.03.008.

[55] I. Iddrisu and S. C. Bhattacharyya, "Sustainable Energy Development Index: A multi-dimensional indicator for measuring sustainable energy development," 2015, doi: 10.1016/j.rser.2015.05.032.

[56] ESMAP and World Bank Group, "RISE." Accessed: Jan. 08, 2024. [Online]. Available: https://rise.esmap.org/reports

[57] Ş. Kılkış, "Benchmarking South East European Cities with the Sustainable Development of Energy, Water and Environment Systems Index," *[Journal of Sustainable Development of Energy, Water and Environment Systems]*, vol. [6], no. [1], p. [162]-[209], Mar. 2018, doi: 10.13044/J.SDEWES.D5.0179.

[58] M. Teresa García-Álvarez, B. Moreno, and I. Soares, "Analyzing the sustainable energy development in the EU-15 by an aggregated synthetic index," *Ecol. Indic.*, vol. 60, pp. 996–1007, 2016, doi: 10.1016/j.ecolind.2015.07.006.

[59] M. Martín-Gamboa, D. Iribarren, D. García-Gusano, and J. Dufour, "A review of life-cycle approaches coupled with data envelopment analysis within multi-criteria decision analysis for sustainability assessment of energy systems," *J. Clean. Prod.*, vol. 150, pp. 164–174, May 2017, doi: 10.1016/J.JCLEPRO.2017.03.017.

[60] V. Campos-Guzmán, M. S. García-Cáscales, N. Espinosa, and A. Urbina, "Life Cycle Analysis with Multi-Criteria Decision Making: A review of approaches for the sustainability evaluation of renewable energy technologies," *Renewable and Sustainable Energy Reviews*, vol. 104, pp. 343–366, Apr. 2019, doi: 10.1016/J.RSER.2019.01.031.

[61] M. Ranjbari *et al.*, "Three pillars of sustainability in the wake of COVID-19: A systematic review and future research agenda for sustainable development," *J. Clean. Prod.*, vol. 297, p. 126660, May 2021, doi: 10.1016/J.JCLEPRO.2021.126660.

[62] R. Madurai Elavarasan, R. Pugazhendhi, M. Irfan, L. Mihet-Popa, P. E. Campana, and I. A. Khan, "A novel Sustainable Development Goal 7 composite index as the paradigm for energy sustainability assessment: A case study from Europe," *Appl. Energy*, vol. 307, p. 118173, Feb. 2022, doi: 10.1016/J.APENERGY.2021.118173.

[63] I. Gunnarsdottir, B. Davidsdottir, E. Worrell, and S. Sigurgeirsdottir, "Indicators for sustainable energy development: An Icelandic case study," *Energy Policy*, vol. 164, p. 112926, May 2022, doi: 10.1016/J.ENPOL.2022.112926.

[64] M. Saeid Atabaki, M. Mohammadi, and V. Aryanpur, "An integrated simulation-optimization modelling approach for sustainability assessment of electricity generation system," *Sustainable Energy Technologies and Assessments*, vol. 52, p. 102010, Aug. 2022, doi: 10.1016/J.SETA.2022.102010.

[65] F. Zanobetti, G. Pio, S. Jafarzadeh, M. Muñoz Ortiz, and V. Cozzani, "Decarbonization of maritime transport: Sustainability assessment of alternative power systems," *J. Clean. Prod.*, vol. 417, p. 137989, Sep. 2023, doi: 10.1016/J.JCLEPRO.2023.137989.

[66] M. Sadiq, P. Kokchang, and S. Kittipongvises, "Sustainability assessment of renewable power generation systems for scale enactment in off-grid communities," *Renewable Energy Focus*, vol. 46, pp. 323–337, Sep. 2023, doi: 10.1016/J.REF.2023.07.006.

[67] E. Rozzi, P. Marocco, and M. Gandiglio, "Life cycle inventory dataset for energy production and storage technologies: Standardized metrics for environmental modeling," *Data Brief*, vol. 60, p. 111666, Jun. 2025, doi: 10.1016/J.DIB.2025.111666.

[68] D. McCauley and R. Heffron, "Just transition: Integrating climate, energy and environmental justice," *Energy Policy*, vol. 119, pp. 1–7, Aug. 2018, doi: 10.1016/J.ENPOL.2018.04.014.

[69] R. R. Hernandez *et al.*, "Environmental impacts of utility-scale solar energy," *Renewable and Sustainable Energy Reviews*, vol. 29, pp. 766–779, Jan. 2014, doi: 10.1016/J.RSER.2013.08.041.

[70] B. W. Griscom *et al.*, "Natural climate solutions," *Proceedings of the National Academy of Sciences*, vol. 114, no. 44, pp. 11645–11650, Oct. 2017, doi: 10.1073/PNAS.1710465114.

[71] J. Gehl, "Cities for People (Google eBook)," p. 288, 2010, Accessed: Sep. 14, 2025. [Online]. Available: https://books.google.com/books/about/Cities_for_People.html?hl=it&id=lBNJoNILqQcC

[72] P. Alves Dias, S. Bobba, S. Carrara, and B. Plazzotta, "The role of rare earth elements in wind energy and electric mobility," 2020, doi: 10.2760/303258.

[73] Tsiropoulos I, Tarvydas D, and Lebedeva N, "Li-ion batteries for mobility and stationary storage applications Scenarios for costs and market growth," 2018. doi: 10.2760/87175.

[74] A. Vai, "How may the availability of critical raw materials affect the deployment of material-intensive technologies and the security of energy systems?,"

Politecnico di Torino, Turin, 2024. Accessed: Aug. 13, 2024. [Online]. Available: https://webthesis.biblio.polito.it/31959/

[75] D. Lerede, "Development of an open-source and open-data energy system optimization model for the analysis of the European energy mix," pp. 1–178, Mar. 2023, Accessed: May 05, 2023. [Online]. Available: https://iris.polito.it/handle/11583/2978154

[76] P. Rafaj and S. Kypreos, "Internalisation of external cost in the power generation sector: Analysis with Global Multi-regional MARKAL model," *Energy Policy*, vol. 35, no. 2, pp. 828–843, Feb. 2007, doi: 10.1016/J.ENPOL.2006.03.003.

[77] S. Jebaraj and S. Iniyan, "A review of energy models," *Renewable and Sustainable Energy Reviews*, vol. 10, pp. 281–311, 2006, doi: 10.1016/j.rser.2004.09.004.

[78] S. C. Bhattacharyya and G. R. Timilsina, "A review of energy system models," *International Journal of Energy Sector Management*, vol. 4, no. 4, pp. 494–518, Nov. 2010, doi: 10.1108/17506221011092742.

[79] Loulou R, Goldstein G, Kanudia A, Lettila A, and Remme U, *Documentation for the TIMES Model: Part I*. 2016. Accessed: Oct. 17, 2022. [Online]. Available: https://iea-etsap.org/docs/Documentation_for_the_TIMES_Model-Part-I_July-2016.pdf

[80] D. Mosso, G. Colucci, D. Lerede, M. Nicoli, M. S. Piscitelli, and L. Savoldi, "How much do carbon emission reduction strategies comply with a sustainable development of the power sector?," *Energy Reports*, vol. 11, pp. 3064–3087, Jun. 2024, doi: 10.1016/J.EGYR.2024.02.056.

[81] R. Loulou, G. Goldstein, A. Kanudia, A. Lehtilä, and U. Remme, *Documentation for the TIMES model: Part I*. 2016.

[82] R. Loulou, A. Lehtilä, A. Kanudia, U. Remme, and G. Goldstein, "Documentation for the TIMES Model Part II," 2016.

[83] North Carolina State University, "TEMOA Database Construction." Accessed: Oct. 24, 2022. [Online]. Available: https://temoacloud.com/temoaproject/Documentation.html#database-construction

[84] M. Gargiulo, K. Vailancourt, and R. De Miglio, *Documentation for the TIMES Model Part IV*. 2016.

[85] IPCC, *Climate Change 2021: The Physical Science Basis. Contribution of Working Group I to the Sixth Assessment Report of the Intergovernmental Panel on Climate Change*. Cambridge University Press. In Press, 2021.

[86] H. Blanco, V. Codina, A. Laurent, W. Nijs, F. Maréchal, and A. Faaij, "Life cycle assessment integration into energy system models: An application for Power-to-Methane in the EU," *Appl. Energy*, vol. 259, p. 114160, Feb. 2020, doi: 10.1016/J.APENERGY.2019.114160.

[87] "New Energy Externalities Development for Sustainability | NEEDS Project | Fact Sheet | FP6 | CORDIS | European Commission." Accessed: Jun. 06, 2022. [Online]. Available: https://cordis.europa.eu/project/id/502687

[88] L. Kotzur *et al.*, “A modeler’s guide to handle complexity in energy systems optimization,” *Advances in Applied Energy*, vol. 4, p. 100063, Nov. 2021, doi: 10.1016/J.ADAPEN.2021.100063.

[89] T. Junne, K. K. Cao, K. K. Miskiw, H. Hottenroth, and T. Naegler, “Considering Life Cycle Greenhouse Gas Emissions in Power System Expansion Planning for Europe and North Africa Using Multi-Objective Optimization,” *Energies 2021, Vol. 14, Page 1301*, vol. 14, no. 5, p. 1301, Feb. 2021, doi: 10.3390/EN14051301.

[90] M. Saeid Atabaki, M. Mohammadi, and V. Aryanpur, “An integrated simulation-optimization modelling approach for sustainability assessment of electricity generation system,” *Sustainable Energy Technologies and Assessments*, vol. 52, p. 102010, Aug. 2022, doi: 10.1016/J.SETA.2022.102010.

[91] J. V Spadaro and A. Rabl, “EXTERNAL COSTS OF ENERGY: APPLICATION OF THE EXTERNE METHODOLOGY IN FRANCE Final Report for Contract JOS3-CT95-0010,” 1998.

[92] D. García-Gusano, D. Iribarren, M. Martín-Gamboa, J. Dufour, K. Espegren, and A. Lind, “Integration of life-cycle indicators into energy optimisation models: the case study of power generation in Norway,” *J. Clean. Prod.*, vol. 112, pp. 2693–2696, Jan. 2016, doi: 10.1016/J.JCLEPRO.2015.10.075.

[93] T. R. Albrecht, A. Crootof, and C. A. Scott, “The Water-Energy-Food Nexus: A systematic review of methods for nexus assessment,” *Environ. Res. Lett*, vol. 13, p. 43002, 2018, doi: 10.1088/1748-9326/aaa9c6.

[94] J. Liu *et al.*, “Nexus approaches to global sustainable development,” *Nature Sustainability 2018 1:9*, vol. 1, no. 9, pp. 466–476, Sep. 2018, doi: 10.1038/s41893-018-0135-8.

[95] Z. Khan *et al.*, “Emerging Themes and Future Directions of Multi-Sector Nexus Research and Implementation,” *Front. Environ. Sci.*, vol. 10, p. 1025, Aug. 2022, doi: 10.3389/FENVS.2022.918085/BIBTEX.

[96] Sofia. Simoes *et al.*, “The JRC-EU-TIMES model - Assessing the long-term role of the SET Plan Energy technologies,” p. 376, 2013, doi: 10.2790/97799.

[97] G. Luderer *et al.*, “Environmental co-benefits and adverse side-effects of alternative power sector decarbonization strategies,” *Nature Communications 2019 10:1*, vol. 10, no. 1, pp. 1–13, Nov. 2019, doi: 10.1038/s41467-019-13067-8.

[98] A. Vinca *et al.*, “The NExus Solutions Tool (NEST) v1.0: An open platform for optimizing multi-scale energy-water-land system transformations,” *Geosci. Model Dev.*, vol. 13, no. 3, pp. 1095–1121, Mar. 2020, doi: 10.5194/GMD-13-1095-2020.

[99] R. Payet-Burin, M. Kromann, S. Pereira-Cardenal, K. Marc Strzepek, and P. Bauer-Gottwein, “WHAT-IF: An open-source decision support tool for water infrastructure investment planning within the water-energy-food-climate nexus,” *Hydrol. Earth Syst. Sci.*, vol. 23, no. 10, pp. 4129–4152, Oct. 2019, doi: 10.5194/HESS-23-4129-2019.

[100] K. Calvin *et al.*, “GCAM v5.1: Representing the linkages between energy, water, land, climate, and economic systems,” *Geosci. Model Dev.*, vol. 12, no. 2, pp. 677–698, Feb. 2019, doi: 10.5194/GMD-12-677-2019.
[101] M. Howells *et al.*, “Integrated analysis of climate change, land-use, energy and water strategies,” *Nat. Clim. Chang.*, vol. 3, 2013, doi: 10.1038/NCLIMATE1789.
[102] D. Mosso, L. Savoldi, and M. Nicoli, “From Crops to Carbon Sequestration: A Technology-Explicit AFOLU Module for Energy Models,” *EGU25*, Mar. 2025, doi: 10.5194/EGUSPHERE-EGU25-20520.
[103] J. Leah Jones-Crank *et al.*, “A review of water-energy-food-ecosystems Nexus research in the Mediterranean: evolution, gaps and applications,” *Environmental Research Letters*, vol. 18, no. 8, p. 083001, Jul. 2023, doi: 10.1088/1748-9326/ACE375.
[104] S. Namany *et al.*, “An Energy-Water-Food Nexus-based Decision-making Framework to Guide National Priorities in Qatar,” *Sustain. Cities Soc.*, vol. 75, p. 103342, Dec. 2021, doi: 10.1016/J.SCS.2021.103342.
[105] R. L. Moss *et al.*, “Critical Metals in Strategic Energy Technologies - Assessing Rare Metals as Supply-Chain Bottlenecks in Low-Carbon Energy Technologies,” Publications Office, 2011. doi: 10.2790/35600.
[106] A. Evans, V. Strezov, and T. J. Evans, “Assessment of sustainability indicators for renewable energy technologies,” *Renewable and Sustainable Energy Reviews*, vol. 13, no. 5, pp. 1082–1088, Jun. 2009, doi: 10.1016/J.RSER.2008.03.008.
[107] M. Martín-Gamboa, D. Iribarren, D. García-Gusano, and J. Dufour, “A review of life-cycle approaches coupled with data envelopment analysis within multi-criteria decision analysis for sustainability assessment of energy systems,” *J. Clean. Prod.*, vol. 150, pp. 164–174, May 2017, doi: 10.1016/J.JCLEPRO.2017.03.017.
[108] J. J. Wang, Y. Y. Jing, C. F. Zhang, and J. H. Zhao, “Review on multi-criteria decision analysis aid in sustainable energy decision-making,” *Renewable and Sustainable Energy Reviews*, vol. 13, no. 9, pp. 2263–2278, Dec. 2009, doi: 10.1016/J.RSER.2009.06.021.
[109] R. Lahdelma, J. Hokkanen, and P. Salminen, “SMAA - Stochastic multiobjective acceptability analysis,” *Eur. J. Oper. Res.*, vol. 106, no. 1, pp. 137–143, Apr. 1998, doi: 10.1016/S0377-2217(97)00163-X.
[110] M. Michetti, *Modelling Land Use, Land-Use Change, and Forestry in Climate Change: A Review of Major Approaches*. Elsevier BV, 2012. doi: 10.2139/SSRN.2122298.
[111] OECD, “Handbook on Constructing Composite Indicators: Methodology and UserGuide,” 2008.
[112] “ISO 14005:2019 - Environmental management systems — Guidelines for a flexible approach to phased implementation.” Accessed: Sep. 04, 2023. [Online]. Available: https://www.iso.org/standard/72333.html
[113] International Organization for Standardization (ISO), “ISO 14040:2006 - Environmental management - Life cycle assessment - Principles and framework.”

Accessed: Aug. 18, 2023. [Online]. Available: https://www.iso.org/standard/37456.html
[114] United Nations Economic Commission for Europe (UNECE), "Carbon Neutrality in the UNECE Region: Integrated Life-cycle Assessment of Electricity Sources," 2021.
[115] "ReCiPe 2016 v1.1 A harmonized life cycle impact assessment method at midpoint and endpoint level Report I: Characterization," 2017, Accessed: Jun. 07, 2022. [Online]. Available: www.rivm.nl/en
[116] "openLCA Nexus: The source for LCA data sets." Accessed: Jun. 07, 2022. [Online]. Available: https://nexus.openlca.org/database/NEEDS
[117] F. Gracceva and P. Zeniewski, "A systemic approach to assessing energy security in a low-carbon EU energy system," *Appl. Energy*, vol. 123, pp. 335–348, Jun. 2014, doi: 10.1016/J.APENERGY.2013.12.018.
[118] B. W. Ang, W. L. Choong, and T. S. Ng, "Energy security: Definitions, dimensions and indexes," *Renewable and Sustainable Energy Reviews*, vol. 42, pp. 1077–1093, Feb. 2015, doi: 10.1016/J.RSER.2014.10.064.
[119] J. P. Deane, F. Gracceva, A. Chiodi, M. Gargiulo, and B. P. Ó. Gallachóir, "Assessing power system security. A framework and a multi model approach," *International Journal of Electrical Power & Energy Systems*, vol. 73, pp. 283–297, Dec. 2015, doi: 10.1016/J.IJEPES.2015.04.020.
[120] E. Hache, "Do renewable energies improve energy security in the long run?," *International Economics*, vol. 156, pp. 127–135, Dec. 2018, doi: 10.1016/J.INTECO.2018.01.005.
[121] IEA, "Energy Technology Perspectives 2023 – Analysis - IEA," 2023. Accessed: Aug. 02, 2023. [Online]. Available: https://www.iea.org/reports/energy-technology-perspectives-2023
[122] JRC, "Critical Raw Materials for Strategic Technologies and Sectors in the EU," 2020. doi: 10.2873/865242.
[123] JRC, "Study on the critical raw materials for the EU 2023," 2023. Accessed: Aug. 02, 2023. [Online]. Available: https://op.europa.eu/en/publication-detail/-/publication/57318397-fdd4-11ed-a05c-01aa75ed71a1
[124] Ministry of Environment and Energy Security, "Bollettino petrolifero - Statistiche energetiche e minerarie." Accessed: Sep. 04, 2023. [Online]. Available: https://dgsaie.mise.gov.it/bollettino-petrolifero
[125] Ministry of Environment and Energy Security, "Bollettino del carbone - Statistiche energetiche e minerarie." Accessed: Sep. 04, 2023. [Online]. Available: https://dgsaie.mise.gov.it/bollettino-carbone
[126] European Commission, *Critical Raw Materials Act*. European Parliament and European Council, 2024. Accessed: May 08, 2024. [Online]. Available: http://data.europa.eu/eli/reg/2024/1252/oj
[127] D. Carrión, J. Palacios, M. Espinel, and J. W. González, "Transmission Expansion Planning Considering Grid Topology Changes and N-1 Contingencies Criteria," *Lecture Notes in Electrical Engineering*, vol. 762 LNEE, pp. 266–279, 2021, doi: 10.1007/978-3-030-72208-1_20/COVER.

[128] C. Helbig, M. Bruckler, A. Thorenz, and A. Tuma, “An overview of indicator choice and normalization in raw material supply risk assessments,” *Resources*, vol. 10, no. 8, p. 79, Aug. 2021, doi: 10.3390/RESOURCES10080079/S1.

[129] D. Kaufmann, A. Kraay, M. M. The, and W. Bank, “The Worldwide Governance Indicators : Methodology and Analytical Issues,” Sep. 2010, doi: 10.1596/1813-9450-5430.

[130] E. D. Gemechu, C. Helbig, G. Sonnemann, A. Thorenz, and A. Tuma, “Import-based Indicator for the Geopolitical Supply Risk of Raw Materials in Life Cycle Sustainability Assessments,” *J. Ind. Ecol.*, vol. 20, no. 1, pp. 154–165, Feb. 2016, doi: 10.1111/JIEC.12279.

[131] U. Nations, “Human Development Report 2021-22,” *Human Development Reports*, 2022.

[132] J. A. Salomon, “Disability-Adjusted Life Years,” *Encyclopedia of Health Economics*, pp. 200–203, Jan. 2014, doi: 10.1016/B978-0-12-375678-7.00511-3.

[133] S. J. W. Klein and S. Whalley, “Comparing the sustainability of U.S. electricity options through multi-criteria decision analysis,” *Energy Policy*, vol. 79, pp. 127–149, Apr. 2015, doi: 10.1016/J.ENPOL.2015.01.007.

[134] R. Pichs Madruga *et al.*, “Renewable Energy Sources and Climate Change Mitigation Special Report of the Intergovernmental Panel on Climate Change Edited by Ottmar Edenhofer Youba Sokona,” 2012, Accessed: Oct. 10, 2023. [Online]. Available: www.cambridge.org

[135] A. Capozzoli, M. S. Piscitelli, and S. Brandi, “Mining typical load profiles in buildings to support energy management in the smart city context,” *Energy Procedia*, vol. 134, pp. 865–874, Oct. 2017, doi: 10.1016/J.EGYPRO.2017.09.545.

[136] D. L. Davies and D. W. Bouldin, “A Cluster Separation Measure,” *IEEE Trans. Pattern Anal. Mach. Intell.*, vol. PAMI-1, no. 2, pp. 224–227, 1979, doi: 10.1109/TPAMI.1979.4766909.

[137] P. J. Rousseeuw, “Silhouettes: A graphical aid to the interpretation and validation of cluster analysis,” *J. Comput. Appl. Math.*, vol. 20, no. C, pp. 53–65, Nov. 1987, doi: 10.1016/0377-0427(87)90125-7.

[138] P. Law Biecek, “DALEX: Explainers for Complex Predictive Models in R,” *Journal of Machine Learning Research*, vol. 19, pp. 1–5, 2018, Accessed: Apr. 04, 2023. [Online]. Available: https://pbiecek.github.io/DALEX.

[139] D. M. W. Powers and Ailab, “Evaluation: from precision, recall and F-measure to ROC, informedness, markedness and correlation,” Oct. 2020, Accessed: Apr. 18, 2023. [Online]. Available: https://arxiv.org/abs/2010.16061v1

[140] Y. Lechón, C. De La Rúa, and H. Cabal, “Impacts of Decarbonisation on the Water-Energy-Land (WEL) Nexus: A Case Study of the Spanish Electricity Sector,” *Energies 2018, Vol. 11, Page 1203*, vol. 11, no. 5, p. 1203, May 2018, doi: 10.3390/EN11051203.

[141] M. Child, O. Koskinen, L. Linnanen, and C. Breyer, “Sustainability guardrails for energy scenarios of the global energy transition,” *Renewable and Sustainable*

Energy Reviews, vol. 91, pp. 321–334, Aug. 2018, doi: 10.1016/J.RSER.2018.03.079.

[142] M. Nicoli, F. Gracceva, D. Lerede, and L. Savoldi, "Can We Rely on Open-Source Energy System Optimization Models? The TEMOA-Italy Case Study," *Energies (Basel).*, vol. 15, no. 18, p. 6505, Sep. 2022, doi: 10.3390/en15186505.

[143] M. Yousuf Ansari, A. Ahmad, S. S. Khan, and G. Bhushan, "Spatiotemporal clustering: a review," *Artif. Intell. Rev.*, vol. 53, pp. 2381–2423, 2020, doi: 10.1007/s10462-019-09736-1.

[144] J. Balkovič *et al.*, "Pan-European crop modelling with EPIC: Implementation, up-scaling and regional crop yield validation," *Agric. Syst.*, vol. 120, pp. 61–75, Sep. 2013, doi: 10.1016/J.AGSY.2013.05.008.

[145] Joint Research Center (JRC), "European Meteorological derived High Resolution RES generation time series for present and future scenarios (EMHIRES)," 2021. Accessed: Jul. 12, 2023. [Online]. Available: https://data.jrc.ec.europa.eu/collection/id-0055

[146] R. Mckenna, S. Hollnaicher, and W. Fichtner, "Cost-potential curves for onshore wind energy: A high-resolution analysis for Germany," 2013, doi: 10.1016/j.apenergy.2013.10.030.

[147] D. S. Ryberg, M. Robinius, and D. Stolten, "Evaluating land eligibility constraints of renewable energy sources in Europe," *Energies (Basel).*, vol. 11, no. 5, 2018, doi: 10.3390/EN11051246.

[148] N. Wang, R. A. Verzijlbergh, P. W. Heijnen, and P. M. Herder, "A spatially explicit planning approach for power systems with a high share of renewable energy sources," 2019, doi: 10.1016/j.apenergy.2019.114233.

[149] D. S. Ryberg, Z. Tulemat, D. Stolten, and M. Robinius, "Uniformly constrained land eligibility for onshore European wind power," *Renew. Energy*, vol. 146, pp. 921–931, Feb. 2020, doi: 10.1016/J.RENENE.2019.06.127.

[150] F. Hofmann, J. Hampp, F. Neumann, T. Brown, and J. Hörsch, "atlite: A Lightweight Python Package for Calculating Renewable Power Potentials and Time Series," *J. Open Source Softw.*, vol. 6, no. 62, p. 3294, Jun. 2021, doi: 10.21105/JOSS.03294.

[151] C. Moscoloni *et al.*, "Wind Turbines and Rooftop Photovoltaic Technical Potential Assessment: Application to Sicilian Minor Islands," *Energies 2022, Vol. 15, Page 5548*, vol. 15, no. 15, p. 5548, Jul. 2022, doi: 10.3390/EN15155548.

[152] R. Mckenna *et al.*, "High-resolution large-scale onshore wind energy assessments: A review of potential definitions, methodologies and future research needs," 2021, doi: 10.1016/j.renene.2021.10.027.

[153] C. W. Klok, A. F. Kirkels, and F. Alkemade, "Impacts, procedural processes, and local context: Rethinking the social acceptance of wind energy projects in the Netherlands A R T I C L E I N F O," *Energy Res. Soc. Sci.*, vol. 99, pp. 2214–6296, 2023, doi: 10.1016/j.erss.2023.103044.

[154] "Rete Natura 2000 – S.I.T.R – Sistema Informativo Territoriale Regionale." Accessed: Feb. 01, 2023. [Online]. Available: https://www.sitr.regione.sicilia.it/download/tematismi/rete-natura-2000/

[155] “Explore the World’s Protected Areas.” Accessed: Nov. 09, 2023. [Online]. Available: https://www.protectedplanet.net/en/thematic-areas/wdpa?tab=WDPA
[156] “OpenStreetMap.” Accessed: Nov. 09, 2023. [Online]. Available: https://www.openstreetmap.org/#map=7/42.727/12.371
[157] A. Sousa, “The thematic accuracy of Corine land cover 2000 Assessment using LUCAS (land use/cover area frame statistical survey)”.
[158] “Comune di Pantelleria PIANO D’AZIONE PER L’ENERGIA SOSTENIBILE,” 2015, Accessed: Oct. 30, 2023. [Online]. Available: www.ambienteitalia.it
[159] “Aeolian.” Accessed: Nov. 08, 2023. [Online]. Available: https://atlanteeolico.rse-web.it/
[160] F. Lindberg *et al.*, “Urban Multi-scale Environmental Predictor (UMEP): An integrated tool for city-based climate services,” *Environmental Modelling & Software*, vol. 99, pp. 70–87, Jan. 2018, doi: 10.1016/J.ENVSOFT.2017.09.020.
[161] S. Tarquini, S. Vinci, M. Favalli, F. Doumaz, A. Fornaciai, and L. Nannipieri, “Release of a 10-m-resolution DEM for the Italian territory: Comparison with global-coverage DEMs and anaglyph-mode exploration via the web,” *Comput. Geosci.*, vol. 38, no. 1, pp. 168–170, Jan. 2012, doi: 10.1016/J.CAGEO.2011.04.018.
[162] “Rete Natura 2000 | Ministero dell’Ambiente e della Sicurezza Energetica.” Accessed: Nov. 09, 2023. [Online]. Available: https://www.mase.gov.it/pagina/rete-natura-2000
[163] M. R. Elkadeem *et al.*, “Geospatial-assisted multi-criterion analysis of solar and wind power geographical-technical-economic potential assessment,” 2022, doi: 10.1016/j.apenergy.2022.119532.
[164] J. Krzywanski *et al.*, “Advanced Spatial and Technological Aggregation Scheme for Energy System Models,” *Energies 2022, Vol. 15, Page 9517*, vol. 15, no. 24, p. 9517, Dec. 2022, doi: 10.3390/EN15249517.
[165] R. J. H. Dunn *et al.*, “HadISD: A quality-controlled global synoptic report database for selected variables at long-term stations from 1973-2011,” *Climate of the Past*, vol. 8, no. 5, pp. 1649–1679, 2012, doi: 10.5194/CP-8-1649-2012.
[166] J. Ramon, L. Lledó, N. Pérez-Zanón, A. Soret, and F. J. Doblas-Reyes, “The tall tower dataset: A unique initiative to boost wind energy research,” *Earth Syst. Sci. Data*, vol. 12, no. 1, pp. 429–439, Feb. 2020, doi: 10.5194/ESSD-12-429-2020.
[167] “MERRA-2.” Accessed: Nov. 09, 2023. [Online]. Available: https://gmao.gsfc.nasa.gov/reanalysis/MERRA-2/
[168] B. Bell *et al.*, “The ERA5 global reanalysis: Preliminary extension to 1950,” *Quarterly Journal of the Royal Meteorological Society*, vol. 147, no. 741, pp. 4186–4227, Oct. 2021, doi: 10.1002/QJ.4174.
[169] “CMIP5 - Home | ESGF-CoG.” Accessed: Nov. 09, 2023. [Online]. Available: https://esgf-node.llnl.gov/projects/cmip5/
[170] “EURO-CORDEX.” Accessed: Nov. 09, 2023. [Online]. Available: https://www.euro-cordex.net/
[171] “Global Solar Atlas.” Accessed: Nov. 09, 2023. [Online]. Available: https://globalsolaratlas.info/map

[172] “Solar irradiance data | Solargis.” Accessed: Nov. 09, 2023. [Online]. Available: https://solargis.com/
[173] “HelioClim-3 Monthly Irradiation GHI - Data Europa EU.” Accessed: Nov. 09, 2023. [Online]. Available: https://data.europa.eu/data/datasets/7237e78b-b12b-4fdb-85fb-33e9fe0c6994?locale=it
[174] “NEW EUROPEAN WIND ATLAS -.” Accessed: Nov. 09, 2023. [Online]. Available: https://www.neweuropeanwindatlas.eu/
[175] “Home | Dutch Offshore Wind Atlas.” Accessed: Nov. 09, 2023. [Online]. Available: https://www.dutchoffshorewindatlas.nl/
[176] “Aeolian.” Accessed: Nov. 09, 2023. [Online]. Available: https://atlanteeolico.rse-web.it/
[177] “Global Wind Atlas.” Accessed: Nov. 09, 2023. [Online]. Available: https://globalwindatlas.info/en
[178] “Windographer | Wind Data Analytics and Visualization Solution | UL Solutions.” Accessed: Nov. 09, 2023. [Online]. Available: https://www.ul.com/software/windographer-wind-data-analytics-and-visualization-solution
[179] “Home | Mesonet.” Accessed: Nov. 09, 2023. [Online]. Available: https://mesonet.org/
[180] M. H. McCutchan, D. G. Fox, M. H. McCutchan, and D. G. Fox, “Effect of Elevation and Aspect on Wind, Temperatme and Humidity.,” *JApMe*, vol. 25, no. 12, pp. 1996–2013, 1986, doi: 10.1175/1520-0450(1986)025.
[181] N. Chen, “Scale problem: Influence of grid spacing of digital elevation model on computed slope and shielded extra-terrestrial solar radiation”, doi: 10.1007/s11707-019-0770-z.
[182] M. Ŝúri and J. Hofierka, “A New GIS-based Solar Radiation Model and Its Application to Photovoltaic Assessments,” *Transactions in GIS*, vol. 8, no. 2, pp. 175–190, Apr. 2004, doi: 10.1111/J.1467-9671.2004.00174.X.
[183] “Accesso di accesso - ArcGIS Online.” Accessed: Nov. 09, 2023. [Online]. Available: https://www.arcgis.com/index.html
[184] “An overview of the Solar Radiation toolset—ArcGIS Pro | Documentation.” Accessed: Nov. 09, 2023. [Online]. Available: https://pro.arcgis.com/en/pro-app/latest/tool-reference/spatial-analyst/an-overview-of-the-solar-radiation-tools.htm
[185] B. B. Kausika and W. G. J. H. M. van Sark, “Calibration and Validation of ArcGIS Solar Radiation Tool for Photovoltaic Potential Determination in the Netherlands,” *Energies 2021, Vol. 14, Page 1865*, vol. 14, no. 7, p. 1865, Mar. 2021, doi: 10.3390/EN14071865.
[186] B. Hur Pintor *et al.*, “Solar Energy Resource Assessment Using R.SUN In GRASS GIS And Site Suitability Analysis Using AHP For Groundmounted Solar Photovoltaic (PV) Farm In The Central Luzon Region (Region 3), Philippines,” *Free and Open Source Software for Geospatial (FOSS4G) Conference Proceedings*, vol. 15, no. 1, p. 3, Feb. 2018, doi: https://doi.org/10.7275/R5N58JKF.

[187] I. Gašparović, M. Gašparović, and D. Medak, “Determining and analysing solar irradiation based on freely available data: A case study from Croatia,” *Environ. Dev.*, vol. 26, pp. 55–67, Jun. 2018, doi: 10.1016/J.ENVDEV.2018.04.001.

[188] L. El Chaar, L. A. Lamont, and N. El Zein, “Review of photovoltaic technologies,” *Renewable and Sustainable Energy Reviews*, vol. 15, pp. 2165–2175, 2011, doi: 10.1016/j.rser.2011.01.004.

[189] “Analysis of utility scale wind and solar plant performance in South Africa relative to daily electricity demand.” Accessed: Nov. 09, 2023. [Online]. Available: https://www.researchgate.net/publication/321192910_Analysis_of_utility_scale_wind_and_solar_plant_performance_in_South_Africa_relative_to_daily_electricity_demand

[190] “Benvenuti a wind-turbine-models.com.” Accessed: Nov. 10, 2023. [Online]. Available: https://it.wind-turbine-models.com/

[191] E. W. Peterson, J. P. , Jr. Hennessey, E. W. Peterson, and J. P. , Jr. Hennessey, “On the Use of Power Laws for Estimates of Wind Power Potential.,” *JApMe*, vol. 17, no. 3, pp. 390–394, 1978, doi: 10.1175/1520-0450(1978)017.

[192] International Renewable Energy Agency (IRENA), “Renewable Power Generation Costs in 2021,” *International Renewable Energy Agency*, p. 160, 2022, Accessed: Nov. 10, 2023. [Online]. Available: https://www.irena.org/-/media/Files/IRENA/Agency/Publication/2018/Jan/IRENA_2017_Power_Costs_2018.pdf

[193] B. Resch *et al.*, “GIS-Based Planning and Modeling for Renewable Energy: Challenges and Future Research Avenues,” *ISPRS International Journal of Geo-Information 2014, Vol. 3, Pages 662-692*, vol. 3, no. 2, pp. 662–692, May 2014, doi: 10.3390/IJGI3020662.

[194] Eurostat data browser, “Yearly Land rent price for a year.” Accessed: Nov. 30, 2023. [Online]. Available: https://ec.europa.eu/eurostat/databrowser/view/APRI_LRNT__custom_5264437/bookmark/table?lang=en&bookmarkId=0e5713d6-6cad-4033-b9ac-e09b5270c489

[195] “Econnextion: la mappa delle connessioni rinnovabili - Terna spa.” Accessed: Nov. 10, 2023. [Online]. Available: https://www.terna.it/it/sistema-elettrico/rete/econnextion

[196] TemoaProject, “Temoa Project Documentation - Objective Function.” Accessed: Mar. 22, 2023. [Online]. Available: https://temoacloud.com/temoaproject/Documentation.html#objective-function

[197] “Wind Costs.” Accessed: Nov. 10, 2023. [Online]. Available: https://www.irena.org/Data/View-data-by-topic/Costs/Wind-Costs

[198] TemoaProject, “Temoa Project Documentation.” Accessed: Jul. 12, 2023. [Online]. Available: https://temoacloud.com/temoaproject/index.html

[199] M. Hughes *et al.*, “System Integration with Multiscale Networks (Simon): A Modular Framework for Resource Management Models,” *Proceedings - Winter*

Simulation Conference, vol. 2020-December, pp. 656–667, Dec. 2020, doi: 10.1109/WSC48552.2020.9383983.

[200] R. J. G. B. Campello, D. Moulavi, and J. Sander, "Density-based clustering based on hierarchical density estimates," *Lecture Notes in Computer Science (including subseries Lecture Notes in Artificial Intelligence and Lecture Notes in Bioinformatics)*, vol. 7819 LNAI, no. PART 2, pp. 160–172, 2013, doi: 10.1007/978-3-642-37456-2_14/COVER.

[201] S. Mannor *et al.*, "K-Means Clustering," *Encyclopedia of Machine Learning*, pp. 563–564, 2011, doi: 10.1007/978-0-387-30164-8_425.

[202] M. Ester, H.-P. Kriegel, J. Sander, and X. Xu, "A Density-Based Algorithm for Discovering Clusters in Large Spatial Databases with Noise," 1996, Accessed: Nov. 13, 2023. [Online]. Available: www.aaai.org

[203] J.-F. Wang, A. Stein, B.-B. Gao, and Y. Ge, "A review of spatial sampling," *Spat. Stat.*, 2012, doi: 10.1016/j.spasta.2012.08.001.

[204] G. Guo, H. Wang, D. Bell, Y. Bi, and K. Greer, "KNN model-based approach in classification," *Lecture Notes in Computer Science (including subseries Lecture Notes in Artificial Intelligence and Lecture Notes in Bioinformatics)*, vol. 2888, pp. 986–996, 2003, doi: 10.1007/978-3-540-39964-3_62/COVER.

[205] P. J. Rousseeuw, "Silhouettes: a graphical aid to the interpretation and validation of cluster analysis," *J. Comput. Appl. Math.*, vol. 20, pp. 53–65, 1987.

[206] "Pantelleria | Clean energy for EU islands." Accessed: Jun. 14, 2023. [Online]. Available: https://energy.ec.europa.eu/topics/markets-and-consumers/clean-energy-eu-islands_en

[207] "Comune di Pantelleria." Accessed: Feb. 01, 2023. [Online]. Available: https://www.comunepantelleria.it/

[208] "Agriculture, Forestry and Other Land Uses (AFOLU)," *Climate Change 2022 - Mitigation of Climate Change*, pp. 747–860, Aug. 2023, doi: 10.1017/9781009157926.009.

[209] "Land Use, Land-Use Change and Forestry (LULUCF) | UNFCCC." Accessed: Mar. 06, 2023. [Online]. Available: https://unfccc.int/topics/land-use/workstreams/land-use--land-use-change-and-forestry-lulucf

[210] "FAOSTAT." Accessed: Sep. 08, 2023. [Online]. Available: https://www.fao.org/faostat/en/#data

[211] R. Loulou, A. Lehtilä, A. Kanudia, U. Remme, and G. Goldstein, "Documentation for the TIMES Model: Part II," 2016. Accessed: Nov. 20, 2023. [Online]. Available: http://www.iea-etsap.org/web/Documentation.asp

[212] IPCC, "Mitigation of Climate Change Climate Change 2022 Working Group III contribution to the Sixth Assessment Report of the Intergovernmental Panel on Climate Change," 2022. Accessed: Feb. 10, 2023. [Online]. Available: https://www.ipcc.ch/report/ar6/wg3/downloads/report/IPCC_AR6_WGIII_FullReport.pdf

[213] IPCC, "2019 Refinement to the 2006 IPCC Guidelines for National Greenhouse Gas Inventories," 2019. Accessed: Feb. 13, 2023. [Online]. Available: https://www.ipcc-nggip.iges.or.jp/public/2019rf/

[214] M. V. Chiriacò *et al.*, "A catalogue of land-based adaptation and mitigation solutions to tackle climate change," *Scientific Data* , vol. 12, no. 1, pp. 1–11, Dec. 2025, doi: 10.1038/S41597-025-04484-0;SUBJMETA.
[215] OECD and FAO, "OECD-FAO Agricultural Outlook 2021-2030." doi: 10.1787/19428846-en.
[216] D. I. Pomoni, M. K. Koukou, M. G. Vrachopoulos, and L. Vasiliadis, "A Review of Hydroponics and Conventional Agriculture Based on Energy and Water Consumption, Environmental Impact, and Land Use," *Energies 2023, Vol. 16, Page 1690*, vol. 16, no. 4, p. 1690, Feb. 2023, doi: 10.3390/EN16041690.
[217] B. Yep and Y. Zheng, "Aquaponic trends and challenges – A review," *J. Clean. Prod.*, vol. 228, pp. 1586–1599, Aug. 2019, doi: 10.1016/J.JCLEPRO.2019.04.290.
[218] J. Lobillo-Eguíbar, V. M. Fernández-Cabanás, L. A. Bermejo, and L. Pérez-Urrestarazu, "Economic Sustainability of Small-Scale Aquaponic Systems for Food Self-Production," *Agronomy 2020, Vol. 10, Page 1468*, vol. 10, no. 10, p. 1468, Sep. 2020, doi: 10.3390/AGRONOMY10101468.
[219] "Costs in large-scale forestry - Skogsstyrelsen." Accessed: Sep. 22, 2025. [Online]. Available: https://www.skogsstyrelsen.se/en/statistics/economy/costs-in-large-scale-forestry/
[220] "Agriculture, Forestry and Other Land Uses (AFOLU)," *Climate Change 2022 - Mitigation of Climate Change*, pp. 747–860, Aug. 2023, doi: 10.1017/9781009157926.009.
[221] G. J. Nabuurs *et al.*, "Agriculture, Forestry and Other Land Uses (AFOLU)," *Climate Change 2022 - Mitigation of Climate Change*, pp. 747–860, Aug. 2023, doi: 10.1017/9781009157926.009.
[222] "Pathways towards lower emissions," *Pathways towards lower emissions*, Dec. 2023, doi: 10.4060/CC9029EN.
[223] "Landbrug & Fødevarer." Accessed: Sep. 22, 2025. [Online]. Available: https://lf.dk/
[224] "Bioenergy – International Collaboration in Bioenergy." Accessed: Sep. 22, 2025. [Online]. Available: https://www.ieabioenergy.com/
[225] IEA-ETSAP, "TIMES." Accessed: Jun. 25, 2022. [Online]. Available: https://iea-etsap.org/index.php/etsap-tools/model-generators/times
[226] M. Nicoli, F. Gracceva, D. Lerede, and L. Savoldi, "Can We Rely on Open-Source Energy System Optimization Models? The TEMOA-Italy Case Study," *Energies (Basel).*, vol. 15, no. 18, p. 6505, Sep. 2022, doi: 10.3390/en15186505.
[227] "Sweden - Food, Agriculture, Biodiversity, Land-Use, and Energy (FABLE) Consortium." Accessed: Dec. 17, 2024. [Online]. Available: https://fableconsortium.org/sweden/
[228] S. Basnet, A. Wood, E. Röös, T. Jansson, I. Fetzer, and L. Gordon, "Organic agriculture in a low-emission world: exploring combined measures to deliver sustainable food system in Sweden," *Sustain. Sci.*, vol. 18, no. 1, pp. 501–519, Jan. 2023, doi: 10.1007/S11625-022-01279-9.

[229] E. Moberg, H. K. Potter, A. Wood, P. A. Hansson, and E. Röös, “Benchmarking the Swedish diet relative to global and national environmental targets-Identification of indicator limitations and data gaps,” *Sustainability (Switzerland)*, vol. 12, no. 4, Feb. 2020, doi: 10.3390/SU12041407.
[230] “FAOSTAT.” Accessed: Sep. 08, 2023. [Online]. Available: https://www.fao.org/faostat/en/#data
[231] “Area of approved regeneration unchanged in 2024 - Skogsstyrelsen.” Accessed: Dec. 17, 2024. [Online]. Available: https://www.skogsstyrelsen.se/en/news/area-of-approved-regeneration-unchanged-in-2024/
[232] “Swedish Forest Industries Federation.” Accessed: Dec. 17, 2024. [Online]. Available: https://www.forestindustries.se/news/latest-news/2024/
[233] F. N. Tubiello, M. Salvatore, S. Rossi, A. Ferrara, N. Fitton, and P. Smith, “The FAOSTAT database of greenhouse gas emissions from agriculture,” *Environmental Research Letters*, vol. 8, no. 1, p. 015009, Feb. 2013, doi: 10.1088/1748-9326/8/1/015009.
[234] “Energy Systems Modelling.” Accessed: Apr. 08, 2025. [Online]. Available: https://energymodellinglab.com/
[235] “Sustainable research and consultancy - IVL.se.” Accessed: Apr. 08, 2025. [Online]. Available: https://www.ivl.se/english/ivl.html
[236] “Implications of Low Carbon City Sustainability Strategies for 2050. - IVL.se.” Accessed: Apr. 08, 2025. [Online]. Available: https://www.ivl.se/english/ivl/publications/publications/implications-of-low-carbon-city-sustainability-strategies-for-2050..html
[237] Energy imports dependency, “Eurostat.” Accessed: Feb. 21, 2025. [Online]. Available: https://ec.europa.eu/eurostat/cache/metadata/en/nrg_ind_id_esmsip2.htm
[238] “MOF, Alm.del - 2020-21 - Bilag 395: Notat om, hvordan et virkemiddelkatalog kan bidrage til en omkostningseffektiv klimaregulering af landbruget.” Accessed: Mar. 06, 2025. [Online]. Available: https://www.ft.dk/samling/20201/almdel/MOF/bilag/395/2349911/index.htm
[239] “Costs in large-scale forestry - Skogsstyrelsen.” Accessed: Mar. 06, 2025. [Online]. Available: https://www.skogsstyrelsen.se/en/statistics/subject-areas/costs-in-large-scale-forestry/
[240] “Real GDP long-term forecast | OECD.” Accessed: Dec. 18, 2024. [Online]. Available: https://www.oecd.org/en/data/indicators/real-gdp-long-term-forecast.html
[241] Ministero dell’Ambiente e della Sicurezza Energetica (MASE) and Ministero dell’Ambiente e della Sicurezza Energetica, “PIANO NAZIONALE INTEGRATO PER L’ENERGIA E IL CLIMA,” 2024. Accessed: Jul. 23, 2024. [Online]. Available: https://www.mase.gov.it/portale/documents/d/guest/pniec_2024_revfin_01072024-pdf

[242] “Supporto tecnico-scientifico per il Ministero dell’Ambiente e della Tutela del Territorio e del Mare (MATTM) ai fini dell’Elaborazione del Piano Nazionale di Adattamento ai Cambiamenti Climatici (PNACC)”.
[243] “Farm to Fork Strategy - European Commission.” Accessed: Aug. 02, 2025. [Online]. Available: https://food.ec.europa.eu/horizontal-topics/farm-fork-strategy_en
[244] S. Di Leo *et al.*, “The TIMES Land-WEF model: An integrated analysis of the agricultural system of the Basilicata Region (Southern Italy),” *Energy Nexus*, vol. 15, p. 100315, Sep. 2024, doi: 10.1016/J.NEXUS.2024.100315.
[245] “Inventario Nazionale – EMISSIONI.” Accessed: Aug. 12, 2025. [Online]. Available: https://emissioni.sina.isprambiente.it/inventario-nazionale/
[246] P. Ruiz *et al.*, “ENSPRESO - an open, EU-28 wide, transparent and coherent database of wind, solar and biomass energy potentials,” *Energy Strategy Reviews*, vol. 26, p. 100379, Nov. 2019, doi: 10.1016/J.ESR.2019.100379.
[247] Eurostat, “Energy balances - Energy - Eurostat.” Accessed: Aug. 19, 2022. [Online]. Available: https://ec.europa.eu/eurostat/web/energy/data/energy-balances
[248] European Council, “Fit for 55 - The EU’s plan for a green transition.” Accessed: Jan. 29, 2023. [Online]. Available: https://www.consilium.europa.eu/en/policies/green-deal/fit-for-55-the-eu-plan-for-a-green-transition/
[249] Ministry of the Environment and Land and Sea Protection, Ministry of Economic Development, Ministry of Infrastructure and Transport, and F. and F. P. Ministry of Agricultural, “Italian long-term strategy of greenhouse gases emissions reduction,” 2021. Accessed: Aug. 30, 2023. [Online]. Available: https://www.mase.gov.it/sites/default/files/lts_gennaio_2021.pdf
[250] R. M. Roman-Cuesta *et al.*, “Land remains a blind spot in tracking progress under the Paris Agreement due to lack of data comparability,” *Communications Earth & Environment 2025 6:1*, vol. 6, no. 1, pp. 1–17, Jul. 2025, doi: 10.1038/s43247-025-02494-9.
[251] D. S. Ryberg, Z. Tulemat, D. Stolten, and M. Robinius, “Uniformly constrained land eligibility for onshore European wind power,” *Renew. Energy*, vol. 146, pp. 921–931, Feb. 2020, doi: 10.1016/J.RENENE.2019.06.127.
[252] V. Aryanpur, B. O’Gallachoir, H. Dai, W. Chen, and J. Glynn, “A review of spatial resolution and regionalisation in national-scale energy systems optimisation models,” *Energy Strategy Reviews*, vol. 37, p. 100702, Sep. 2021, doi: 10.1016/J.ESR.2021.100702.
[253] K. Dooley, K. L. Christiansen, J. F. Lund, W. Carton, and A. Self, “Over-reliance on land for carbon dioxide removal in net-zero climate pledges,” *Nature Communications* , vol. 15, no. 1, pp. 1–10, Dec. 2024, doi: 10.1038/S41467-024-53466-0;TECHMETA.
[254] G. Grassi *et al.*, “Critical adjustment of land mitigation pathways for assessing countries’ climate progress,” *Nat. Clim. Chang.*, vol. 11, no. 5, pp. 425–434, May 2021, doi: 10.1038/S41558-021-01033-6.

[255] M. Migliavacca *et al.*, “Securing the forest carbon sink for the European Union’s climate ambition,” *Nature*, vol. 643, no. 8074, pp. 1203–1213, Jul. 2025, doi: 10.1038/S41586-025-08967-3;TECHMETA.
[256] E. J. Molina Bacca *et al.*, “Uncertainty in land-use adaptation persists despite crop model projections showing lower impacts under high warming,” *Communications Earth & Environment 2023 4:1*, vol. 4, no. 1, pp. 1–13, Aug. 2023, doi: 10.1038/s43247-023-00941-z.
[257] Loulou R, Goldstein G, Kanudia A, Lettila A, and Remme U, “Documentation for the TIMES Model: Part I,” 2016. Accessed: Oct. 17, 2022. [Online]. Available: https://iea-etsap.org/docs/Documentation_for_the_TIMES_Model-Part-I_July-2016.pdf
[258] L. Gurobi Optimization, “Gurobi Optimizer Reference Manual.” Accessed: Feb. 06, 2025. [Online]. Available: https://www.gurobi.com
[259] MAHTEP Group, “MAHTEP/TEMOA-Italy - Release 3.0,” GitHub. Accessed: Oct. 28, 2023. [Online]. Available: https://github.com/MAHTEP/TEMOA-Italy/releases/tag/3.0
[260] M. Nicoli, F. Gracceva, D. Lerede, and L. Savoldi, “Can We Rely on Open-Source Energy System Optimization Models? The TEMOA-Italy Case Study,” *Energies (Basel).*, vol. 15, no. 18, p. 6505, Sep. 2022, doi: 10.3390/en15186505.
[261] MAHTEP Group, “MAHTEP/TEMOA,” GitHub. Accessed: Oct. 28, 2023. [Online]. Available: https://github.com/MAHTEP/TEMOA
[262] G. Colucci, D. Lerede, M. Nicoli, and L. Savoldi, “A dynamic accounting method for CO2 emissions to assess the penetration of low-carbon fuels: application to the TEMOA-Italy energy system optimization model,” *Appl. Energy*, vol. 352, no. 121951, Dec. 2023, doi: 10.1016/j.apenergy.2023.121951.
[263] World Bank, “Commodity Markets.” Accessed: Jul. 19, 2023. [Online]. Available: https://www.worldbank.org/en/research/commodity-markets
[264] IEA, “World Energy Outlook 2022,” 2022. Accessed: Dec. 22, 2022. [Online]. Available: www.iea.org/t&c/
[265] A. Oliva, F. Gracceva, D. Lerede, M. Nicoli, and L. Savoldi, “Projection of Post-Pandemic Italian Industrial Production through Vector AutoRegressive Models,” *Energies 2021, Vol. 14, Page 5458*, vol. 14, no. 17, p. 5458, Sep. 2021, doi: 10.3390/EN14175458.
[266] S. Laera, G. Colucci, V. Di Cosmo, D. Lerede, M. Nicoli, and L. Savoldi, “Technology-specific hurdle rates for Energy System Optimization Models,” *Energy Proceedings*, vol. 39, 2024, doi: 10.46855/energy-proceedings-10911.
[267] M. Nicoli, “A TIMES-like open-source model for the Italian energy system,” Politecnico di Torino, Turin, 2021. Accessed: Jul. 05, 2022. [Online]. Available: https://webthesis.biblio.polito.it/18850/
[268] Terna, “Electric System.” Accessed: Jul. 10, 2023. [Online]. Available: https://www.terna.it/en/electric-system
[269] Gestore Servizi Energetici (GSE), “Statistiche.” Accessed: Jul. 17, 2023. [Online]. Available: https://www.gse.it/dati-e-scenari/statistiche

[270] Ministry of Economic Development, Ministry of the Environment and Land and Sea Protection, and Ministry of Infrastructure and Transport, “Integrated National Energy and Climate Plan 2019,” 2019. Accessed: Aug. 19, 2022. [Online]. Available: https://commission.europa.eu/energy-climate-change-environment/implementation-eu-countries/energy-and-climate-governance-and-reporting/national-energy-and-climate-plans_en

[271] Ministry of Economic Development, “Long term Italian strategy for greenhouse gas emission reduction,” 2021. Accessed: Jun. 21, 2022. [Online]. Available: https://ec.europa.eu/clima/sites/lts/lts_it_it.pdf

[272] National Agency for New Technologies Energy and Sustainable Economic Development (ENEA), “The TIMES-Italy Energy Model Structure and Data 2010 Version,” Rome, 2011. Accessed: Sep. 02, 2022. [Online]. Available: https://biblioteca.bologna.enea.it/RT/2011/2011_9_ENEA.pdf

[273] National Renewable Energy Laboratory (NREL), “2022 Annual Technology Baseline (ATB) Cost and Performance Data for Electricity Generation Technologies,” Golden, CO: National Renewable Energy Laboratory. Accessed: Jul. 06, 2023. [Online]. Available: https://atb.nrel.gov/electricity/2022/about

[274] National Renewable Energy Laboratory (NREL), “Useful Life | Energy Analysis | NREL.” Accessed: Jul. 06, 2023. [Online]. Available: https://www.nrel.gov/analysis/tech-footprint.html

[275] Sofia. Simoes *et al.*, “The JRC-EU-TIMES model - Assessing the long-term role of the SET Plan Energy technologies,” p. 376, 2013, doi: 10.2790/97799.

[276] M. E. Alfano, “Modeling the Energy and the Water Systems in an open-access Energy System Optimization Model: the Pantelleria case study,” Politecnico di Torino, 2022. Accessed: Jan. 19, 2023. [Online]. Available: https://webthesis.biblio.polito.it/24982/

Appendix A: The TEMOA Modelling Framework

TEMOA is a tool for long-term energy planning and scenario analysis. TEMOA produces the cost-optimal evolution of the studied energy system and relies on a technology-rich database including the techno-economic characterization of technology options and commodity flows. The main sectors typically included in a TEMOA model structure are shown in Figure A1. The basic structure of the system required to comprehensively model the existing energy balance of a country includes three demand-side sectors (buildings, transport, and industry) and supply-side sectors (e.g., upstream and electricity generation). While the demand-side sectors consume energy to satisfy final energy service demands, the supply-side sectors produce energy carriers to feed the demand-side. A complete energy system should be structured to include the techno-economic description of the available technologies, drivers for demands projection, and technical and environmental constraints.

Figure A2 shows the essential items for the definition of the system structure: technologies and commodities. Technologies represent processes devoted to energy mining, transformation and final use. On the contrary, commodities may represent energy and material flows, final energy service demands, and emissions. Final energy service demands represent the final step of the technology chain and represent energy-intensive services to be satisfied by the energy system under analysis. They may include, for instance, space heating for residential buildings, production of industrial products in industry and transport services.

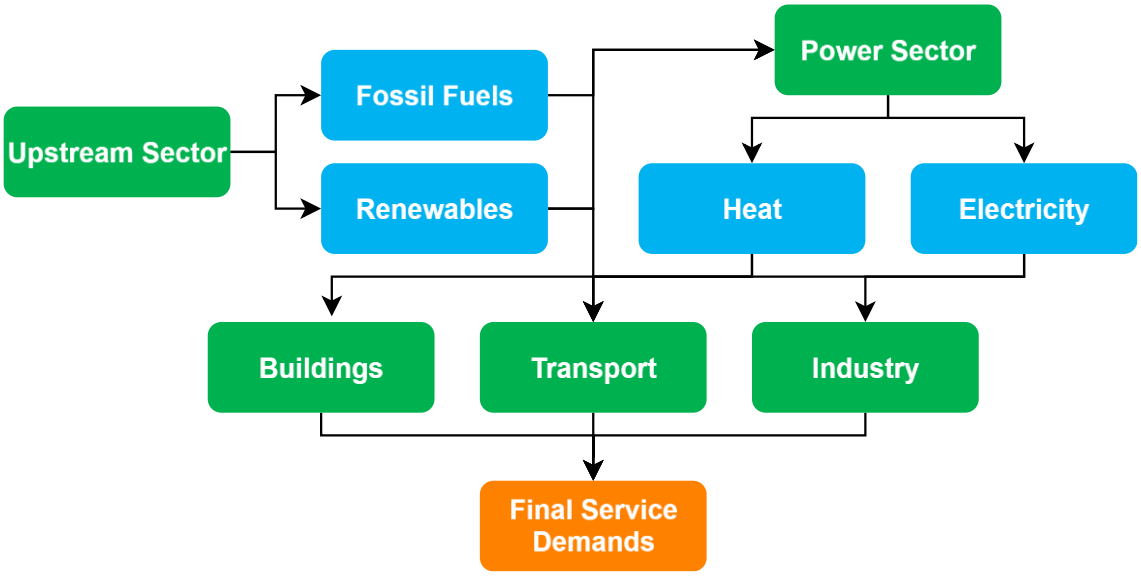

Figure A1. Simplified structure of an energy system as typically represented in energy system optimization models.

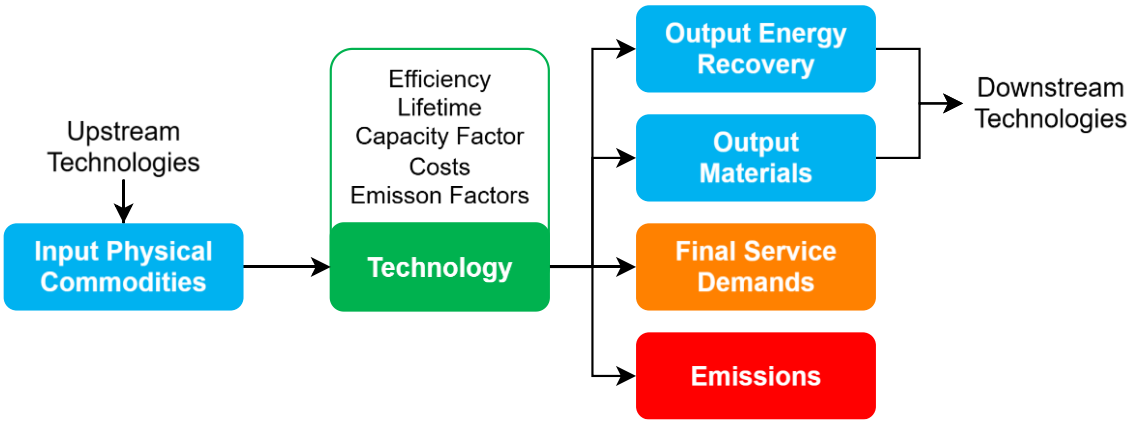

Figure A2. Schematic representation of the different commodity categories in the RES construction.

TEMOA tackles a linear optimization problem similar to most of the ESOMs [257]. The optimization is performed using Gurobi [258] as the solver for the analyses presented in this thesis. Gurobi employs by default the concurrent algorithm – running multiple optimization algorithms (such as primal and dual simplex) in parallel to determine the most efficient solution path. However, for more complex runs – such as those involving energy storage with high temporal resolution – the barrier algorithm was utilized. The barrier method, a type of interior-point algorithm, is particularly effective for large, sparse problems, offering faster convergence by navigating through the interior of the feasible region rather than along its edges [258].

The optimization problem involves minimizing the objective function, which represents the total cost of the energy system (denoted as C_{total} in Equation A1). depends on the discounting factor ($DiscountingFactor$, representing the discounted value to the beginning of the time horizon of a unitary payment) and the cost values of individual technologies chosen in the optimal technology mix. Three key parameters in technology modeling play a crucial role in computing the objective function: investment cost (C_{loans} [M€/cap.]), fixed operation and maintenance (O&M) cost (C_{fixed} [M€/cap.]), and variable O&M cost ($C_{variable}$ [M€/cap.]). Investment cost and fixed O&M cost are linked to a technology $Capacity$, variable O&M cost is tied to the $Activity$.

Several decision variables govern the optimal configuration and operation of the energy system in ESOMs. One of the most important is technology **capacity**, which determines the amount of new capacity to be installed for various technologies such as power generation units, storage systems, and infrastructure. The available technology capacity represents the maximum production potential assuming constant operation at full capacity and guides long-term investment decisions. In the example of a power generation plant, the capacity represents the available power (e.g., in GW).

Closely related is the **activity** level, which represents the amount of energy produced or consumed by each technology over time, ensuring that demand is met efficiently while accounting for factors like fuel availability and renewable generation variability. Energy flow variables capture the transfer of energy across sectors and regions, including the operation of transmission networks and cross-sectoral exchanges like electricity-to-hydrogen conversion.

Storage levels and charging/discharging rates are critical for modeling flexibility, particularly in systems with high shares of variable renewables, as they help balance supply

and demand over different timeframes. In multi-regional models, import and export variables define cross-border energy exchanges, influencing system reliability and market integration.

$$C_{total} = C_{loans} + C_{fixed} + C_{variable} =$$
$$= \sum_{r,t,v} \left(CostInvest_{r,t,v} \cdot DiscountingFactor_{r,t,v} \cdot Capacity_{r,t,v} \right) +$$
$$+ \sum_{r,p,t,v} \left(CostFixed_{r,p,t,v} \cdot DiscountingFactor_{r,t,v} \cdot Capacity_{r,t,v} \right) + \quad \text{(A1)}$$
$$+ \sum_{r,p,t,v} \left(CostVariable_{r,p,t,v} \cdot DiscountingFactor_{r,p,t,v} \cdot Activity_{r,p,t,v} \right)$$

A list of the main parameters involved in the energy system modeling within the TEMOA environment is provided in

Table . The mathematical formulation of constraints and the equations defining the features of processes in TEMOA is extensively described in the model documentation [198].

Table A1. Main items included in the TEMOA formulation.

Category	Description	Name in TEMOA
Labels used for internal database processing	Commodity category	commodity_labels
	Technology category	technology_labels
	Technology sector	sector_labels
	Time period labels	time_periods_labels
Sets	Region names	regions
	Commodity names	commodities
	Technology names	technologies
	Time periods	time_periods
	Seasons of the year	time_season
	Times of day	time_of_day
Parameters used to define processes	Capacity to activity	Capacity2Activity
	Capacity factors	CapacityFactor CapacityFactorTech CapacityFactorProcess
	Commodity emission factor	CommodityEmissionFactor
	Process emission factor	EmissionActivity
	Material Intensity	MaterialIntensity
	Investment Cost	CostInvest
	Fixed O&M Cost	CostFixed
	Variable O&M Cost	CostVariable
	Demands	Demand
	Efficiency	Efficiency
	Existing Capacity	ExistingCapacity
	Discount Rate	GlobalDiscountRate
	Hurdle Rate	DiscountRate
	Economic Lifetime	LifetimeLoanTech
	Technical Lifetime	LifetimeTech LifetimeProcess
Parameters used to define constraints	Maximum activity constraint	MaxActivity
	Minimum activity constraint	MinActivity
	Maximum capacity constraint	MaxCapacity
	Minimum capacity constraint	MinCapacity
	Maximum activity for technology groups	MaxActivityGroup
	Minimum activity for technology groups	MinActivityGroup
	Maximum capacity for technology groups	MaxCapacityGroup
	Minimum capacity for technology groups	MinCapacityGroup
	Minimum share of input commodity for single technologies	TechInputSplit
	Minimum share of output commodity for single technologies	TechOutputSplit
	Maximum share of input commodity for technology groups	MaxInputGroup
	Minimum share of input commodity for technology groups	MinInputGroup
	Maximum share of output commodity for technology groups	MaxOutputGroup
	Minimum share of output commodity for technology groups	MaxOutputGroup
	Maximum production across time periods	MaxResource
	Maximum materials production across time periods	MaxMaterialReserve

Appendix A.1: The TEMOA-Italy

Here, the model TEMOA-Italy is presented (Release 3.0, [259]), developed within the previously described TEMOA modelling framework [260], [261] . Since a specific methodology for emissions accounting was recently implemented in TEMOA-Italy and the model behaviour was precisely tested in a reference [260] and in a low emissions scenario [262], this works aims to extend the analysis to evaluate the overall sustainability level for the evolution of the power sector computed throughout the two scenarios. The TEMOA-Italy RES represents the Italian energy system with a single spatial region and across a time horizon that spans from 2006 (base year) to 2050. Energy imports/exports are modelled in TEMOA-Italy with a single technology per each imported/exported commodity, representing the average import/export price according to World Bank historical data [263] and the World Energy Outlook 2022 future projections [264]. Constraints for imported and exported commodities are from Eurostat [247] for the historical period 2006-2020 and progressively relaxed for future years. The demand projection for future years is presented in [265]. The set of hurdle rates is from [266]. Focusing on the power sector (the object of this study), Figure shows the main technology groups and their input/output commodities, also highlighting the connections with the other sectors of the model and, namely, the hydrogen and CCUS modules and the demand sectors (including electricity and heat consumption options). A major distinction in the power sector is present for existing and new technologies, since the same technology (e.g., natural gas combined cycle power plant) may present different parameters value (e.g., efficiency, capacity factor) according to its existing or new version.

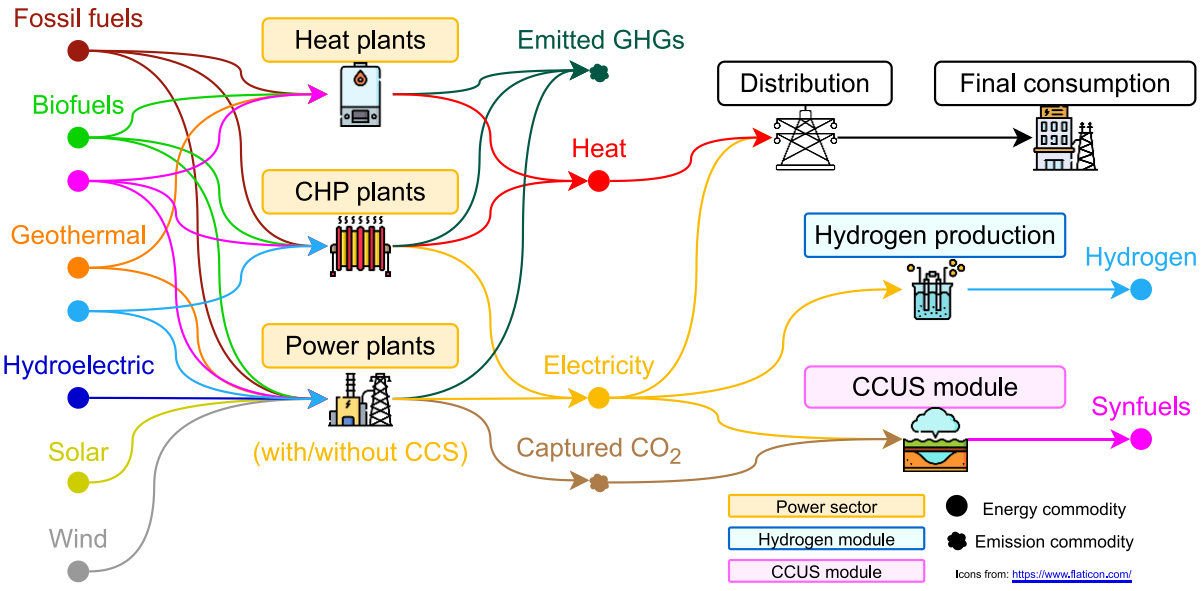

Figure A3. The power sector as represented in TEMOA-Italy.

Table A2 shows a summary of the main parameters used for the existing technology modeling (as discussed in [267]), aggregated by plant category (power, CHP, and heat production plants) and input resource (more than one technology is associated to each resource). The capacity of existing technologies lead to a total gross capacity in 2006 equal to 91.80 GW (including heat plants), correspondent to statistics by TERNA [8].

Table A2. Techno-economic characterization of existing technologies in the TEMOA-Italy power sector [259].

Category	Resource	Efficiency (%)	Existing Capacity (GW)	End of Life	Fixed O&M Cost (M€$_{2009}$/GW)	Variable O&M Cost (M€$_{2009}$/PJ)	Capacity Factor (%)
Power Plants	Coal	32	7.73	≈ 2030	31	0.46	≈ 40
	Oil Products	35	9.28	≈ 2030	32	0.47	
	Natural Gas	46	28.03	≈ 2050	18	0.49	
	Biofuels	27	0.76	≈ 2030	13	0.36	
	Geothermal	10	0.79	≈ 2030	94	3.48	
	Hydroelectric		21.38		25	0.08	
	Solar		0.02	≈ 2025	31	13.89	
	Wind		2.12	≈ 2020	34		
CHP Plants	Coal	37	0.91	≈ 2030	221	0.83	≈ 60
	Oil Products	35	3.23	≈ 2020	32	0.47	
	Natural Gas	48	14.83	≈ 2050	29	0.61	
	Biofuels	39	0.82	≈ 2050	221	0.83	
Heat Plants	Natural Gas	80	0.77	≈ 2035			50
	Geothermal	80	1.13	≈ 2035			

The complete techno-economic characterization of new technologies is available in Table A3. While the overall technology categories are power plants (devoted to electricity production), CHP and micro-CHP plants (devoted to combined electricity and heat production) and heat plants (devoted to heat production), several technology options are available. More specifically, the possible energy inputs for the TEMOA-Italy power sector are fossil fuels, biofuels, renewables, and hydrogen. No nuclear options are currently included in the model database, neither fission nor future fusion facilities. The main sources of data for the applied set of constraints are:

- TERNA Statistics [268], Eurostat Energy Balances [247] and GSE Statistics [269] for the calibration on the historical period 2006-2020.
- National Integrated Plan for Energy and Climate (PNIEC) [270], Long term Italian strategy for greenhouse gas emission reduction (LTS) [271], Fit for 55 [248] with respect to stated future policies implemented in the model. This includes the phase-out of coal power plants no later than 2030.
- Elaboration from ENSPRESO Database [246], for renewable future potentials.

To apply the presented methodology to the Italian long-term strategy on emission reduction [249] two alternative scenarios were developed within TEMOA-Italy, spanning on a time horizon from 2020 to 2050. The Reference scenarios was developed including a projection up to 2050 of the PNIEC 2019 [270] minimum targets for renewables development, while the

Decarbonization scenario reflects the net zero emission target in 2050 [259]. For the 2025-2030 period, the PNIEC targets concerning renewable production (Figure) are implemented as constraints for the model. In the Reference scenario, the PNIEC policies are imposed as five constraints, forcing the model to exactly reproduce them. Differently, in the Decarbonization scenario, they are implemented as a set of minimum targets, allowing for higher values in the final electricity production mix. This approach, in synergy with the 2025-2050 carbon emission constraint reported in Figure (b) allows to reach a configuration that should lead close to carbon neutrality by 2050 (around 29 $MtCO_{2\ eq}$ residual).

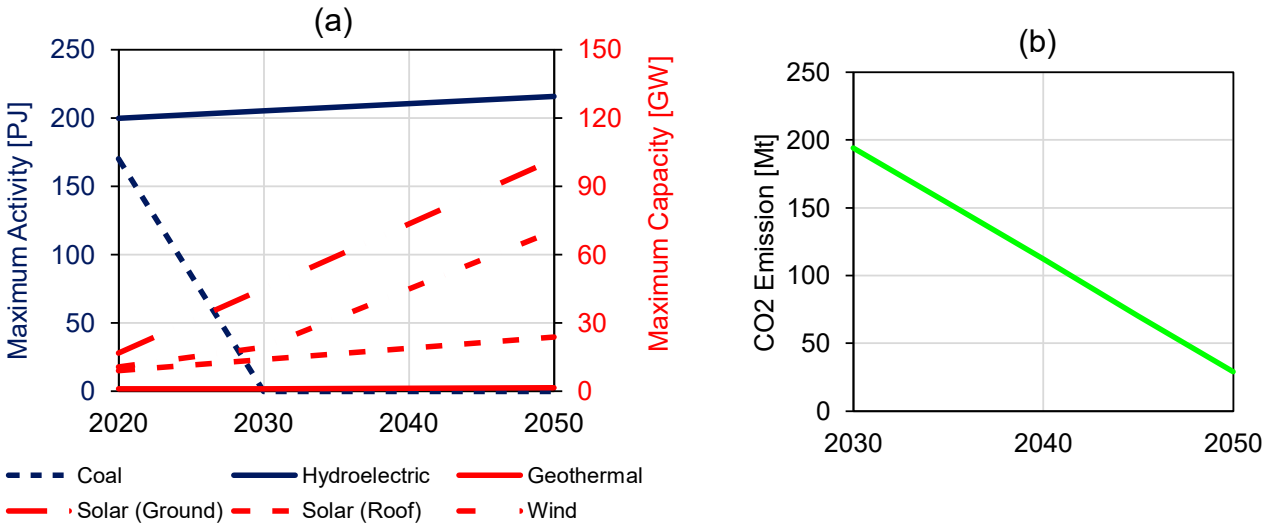

Figure A4. Targets for renewables development of the (a) Reference scenario (PNIEC targets projected up to 2050). (b) Overall gross emissions constraints implemented in the Decarbonization scenario.

Table A3. Techno-economic characterization of new technologies in the TEMOA-Italy power sector (Release 3.0 [259])..

Category	Resource	Technology	Efficiency (%)	Lifetime	Investment Cost		Fixed O&M Cost		Variable O&M Cost		Discount Rate (%)	Capacity to Activity	Capacity Factor (%)	Capacity Credit (%)	CHPR	Source
Power Plants	Natural Gas	Gas Cycle	35 ~ 49	30	703 ~ 922	M$2020/GW	21	M$2020/GW	1.39	M$2020/PJ	10	31.536 PJ/GW	95	100		[272] [273] [274]
		Combined Cycle	54 ~ 59	30	838 ~ 1038	M$2020/GW	28	M$2020/GW	0.56	M$2020/PJ			90			
		95% CCS	55	30	1330	M€2010/GW	38	M€2010/GW	0.34	M€2010/PJ			90			
	Coal	Steam Cycle	40 ~ 44	30	2240 ~ 3075	M$2020/GW	74	M$2020/GW	2.22	M$2020/PJ			76			
		79 ~ 84 % CCS	41 ~ 48	15 ~ 30	2757 ~ 3758	M€2010/GW	69 ~ 88	M€2010/GW	0.64 ~ 1.62	M€2010/PJ			90			
	Oil Products	Steam Cycle	40 ~ 44	30	2240 ~ 3075	M$2020/GW	74	M$2020/GW	2.22	M$2020/PJ			85			
	Biofuels	Biodiesel Plant	35 ~ 39	15	3626 ~ 4416	M$2020/GW	151	M$2020/GW	1.61	M$2020/PJ			70			
		Biomass Plant	25 ~ 28	15	3626 ~ 4416	M$2020/GW	151	M$2020/GW	1.61	M$2020/PJ			57			
		Agriculture and Farming Biogas Plant	32 ~ 40	9	2025 ~ 3500	M€2009/GW							58 ~ 65	70		[272]
		Landfill Biogas Plant			900 ~ 1100	M€2009/GW	40 ~ 75	M€2009/GW	1.61	M€2009/PJ			49 ~ 60	50		
	Hydroelectric	Micro-hydroelectric		30	4500	M€2009/GW	78	M€2009/GW					≈ 0.23	30		[272]
		Mini-hydroelectric			2250	M€2009/GW	33	M€2009/GW						30		
	Geothermal	High Enthalpy Plant	10	15	3200 ~ 4000	M€2009/GW	60 ~ 86	M€2009/GW					86	100		[272]
		Low Enthalpy Plant			4480 ~ 6000	M€2009/GW							88 ~ 90	100		
	Solar	Ground Photovoltaic		30	620 ~ 6000	M$2020/GW	13 ~ 43	M$2020/GW			5		≈ 0.14	20		[272] [273] [274]
		Rooftop Photovoltaic			751 ~ 8000	M$2020/GW	10 ~ 48	M$2020/GW						15		
		Thermodynamic Plant			3928 ~ 5429	M$2020/GW			0.81	M$2020/PJ				70		
	Wind	Onshore		20	765 ~ 2532	M$2020/GW	33 ~ 49	M$2020/GW					≈ 0.17	25		[272] [273] [274]
		Offshore (Fixed)			2343 ~ 5000	M$2020/GW	70 ~ 111	M$2020/GW						30		
		Offshore (Floating)			3467 ~ 4049	M$2020/GW	57 ~ 69	M$2020/GW						35		
	Hydrogen	PEM Fuel Cell	45 ~ 47	15	1000 ~ 3000	M€2013/GW	56 ~ 61	M€2013/GW	8.33 ~ 29.17	M€2013/PJ			90	100		[275]
CHP Plants	Natural Gas	Gas Cycle	77 ~ 86	25	960	M€2009/GW			1.11 ~ 1.67	M€2009/PJ	10	31.536 PJ/GW	57	70	≈ 1.3	[272]
		Combined Cycle	90	30	720	M€2009/GW			0.33 ~ 0.50	M€2009/PJ			34		≈ 0.6	
		Cycle in Counter Pressure	84	35	702	M€2009/GW			1.39	M€2009/PJ			74		≈ 4.0	
		Cycle with Steam Tapping	82	35											≈ 2.5	
	Municipal Waste	Municipal Waste Cycle	38	20	2059 ~ 4000	M€2009/GW			9.50 ~ 12.50	M€2009/PJ			70 ~ 80		≈ 0.5	
Micro-CHP Plants	Natural Gas	Internal Combustion Engine (Commercial)	80 ~ 88	15	900 ~ 1100	M€2009/GW			4.17	M€2009/PJ	10	31.536 PJ/GW	34	20	≈ 1.1	[272]
		Microturbine (Commercial)	80 ~ 88	12 ~ 20	1000 ~ 1500	M€2009/GW			2.78	M€2009/PJ			34		≈ 0.4	
		Combined Cycle (Commercial)	80	15 ~ 20	1300	M€2009/GW			5.00	M€2009/PJ			34		≈ 0.4	
		Solid Oxide Fuel Cell (Commercial)	90 ~ 96	20	2250 ~ 10000	M€2020/GW			4.86 ~ 30.56	M€2020/PJ			90		≈ 0.4	[275]

	Biofuels	Internal Combustion Engine (Commercial)	80	15	1350 ~ 1870	M€$_{2009}$/GW			4.17	M€$_{2009}$/PJ			34		≈ 0.4	[272]
	Hydrogen	PEM Fuel Cell (Commercial)	94 ~ 96	20	1050 ~ 1500	M€$_{2020}$/GW			6.94 ~ 13.89	M€$_{2020}$/PJ			90		≈ 0.8	[275]
	Natural Gas	Internal Combustion Engine (Residential)	80 ~ 88	15	900 ~ 1100	M€$_{2009}$/GW			2.78 ~ 4.17	M€$_{2009}$/PJ			34	20	≈ 1.1	[272]
		Microturbine (Residential)	80 ~ 92	12 ~ 20	1000 ~ 1500	M€$_{2009}$/GW			1.67 ~ 2.78	M€$_{2009}$/PJ			34		≈ 1.5	
		Combined Cycle (Residential)	80	15 ~ 20	1300	M€$_{2009}$/GW			0.42 ~ 0.50	M€$_{2009}$/PJ			34		≈ 0.4	
		Stirling Engine (Residential)	80 ~ 90	15	2100 ~ 2180	M€$_{2009}$/GW			2.78 ~ 5.00	M€$_{2009}$/PJ			34		≈ 0.2	
		Solid Oxide Fuel Cell (Residential)	90	20	3500 ~ 10000	M€$_{2020}$/GW			6.97 ~ 27.78	M€$_{2020}$/PJ			90		≈ 0.5	[275]
	Hydrogen	PEM Fuel Cell (Residential)	92 ~ 96	20	4000 ~ 6000	M€$_{2020}$/GW			6.94 ~ 20.89	M€$_{2020}$/PJ			90		≈ 0.5	
	Natural Gas	Internal Combustion Engine (Industry)	80 ~ 91	15	1030 ~ 1100	M€$_{2009}$/GW			2.78 ~ 4.17	M€$_{2009}$/PJ			57	100	≈ 1.1	[272]
		Gas Turbine (Industry)	74 ~ 80	20 ~ 25	800	M€$_{2009}$/GW			1.39 ~ 1.67	M€$_{2009}$/PJ			74		≈ 1.2	
		Steam Turbine (Industry)	75 ~ 79	30	1500	M€$_{2009}$/GW							63		≈ 0.3	
	Biofuels	Internal Combustion Engine (Industry)	85 ~ 93	15	1800 ~ 2100	M€$_{2009}$/GW			2.50 ~ 3.75	M€$_{2009}$/PJ			57		≈ 0.2	
Heat Plants	Natural Gas	Natural Gas Plant	80	60	4	M€$_{2009}$/PJ	2.4	M€$_{2009}$/PJ			10	1.00 PJ/PJ	60	100		[272]
	Coal	Coal Plant			6	M€$_{2009}$/PJ	2.8	M€$_{2009}$/PJ								
	Oil Products	Oil Products Plant			5	M€$_{2009}$/PJ	2.5	M€$_{2009}$/PJ								
	Biofuels	Biofuels Plant			6	M€$_{2009}$/PJ	2.8	M€$_{2009}$/PJ								
	Geothermal	High Enthalpy Plant	10		12	M€$_{2009}$/PJ	2.5	M€$_{2009}$/PJ								
		Low Enthalpy Plant			12	M€$_{2009}$/PJ	2.5	M€$_{2009}$/PJ								

Appendix A.2: The TEMOA-Pantelleria

The Reference Energy System (RES) for the island of Pantelleria had already been modelled within the TEMOA-Pantelleria model developed by the MATHEP group at the Politecnico di Torino. For a detailed description of the model, please refer to [276] . In this section, an overview of the main components of the RES will be provided to offer a comprehensive understanding of the context in which the land-use sector will be developed. As shown in Figure , the Reference Energy System consists of the following parts:

- Upstream sector
- Intermediate commodities
- Power sector
- Demand side sector
- Demand side services

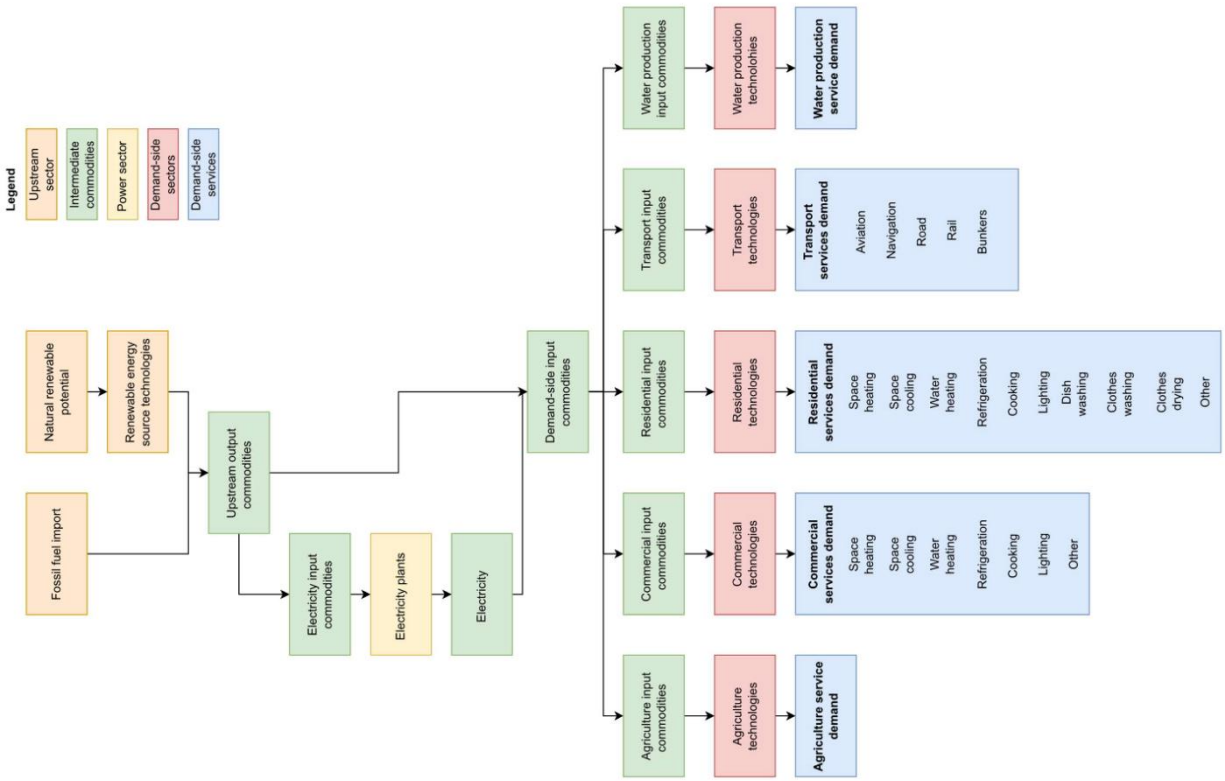

Figure A5 – Reference energy system of Pantelleria [276]

Upstream sector

The upstream sector is composed of fossil fuels and renewable resources. Since Pantelleria imports fossil fuels from the mainland rather than extracting them locally, they are entirely modelled as imported resources, representing an external input to the energy system. Fictitious technologies are used to model the import of fossil fuels giving them a price (Table A4)and constrains.

Table A4 - Fuel importation price for Pantelleria Island [276]

Fuel category	**Fuel**	**Pantelleria importation price [M€/MWh]**
Oil products	Diesel	1.21E-04
	Gasoline	1.21E-04
	LPG	1.21E-04

The capacity of renewable energy sources has been modelled through technologies designed to represent them. These technologies are defined with a cost, it is also possible to set constraints in the base year and for future scenarios.

Power sector

Since the heat is produced from the demand side technologies absorbing electricity the power sector, in this model, produces only electricity. The electricity is produced by two technologies in the base year: the diesel plant (producing almost the overall electricity needed by the island) and the solar photovoltaic panels. Table A5 summarizes the characterization parameter of the two technologies and their values in the base year.

Table A5 - Power sector technologies characterization [276]

Technology description	Input commodity	Output commodity	Efficiency	Installed power [MW]	Fixed operation and maintenance cost [M€/MWh]	Variable operation and maintenance cost [M€/MWh]
Diesel plant	Diesel	Electricity	3.9E-1	22	22	1.8E-6
Solar plant	Solar	Electricity	1.00	1.4E-1	3.1E-2	5E-5